CRESOL NOVOLAC/EPOXY NETWORKS: SYNTHESIS, PROPERTIES, AND PROCESSABILITY

by
Sheng Lin-Gibson

Dissertation submitted to the faculty of the Virginia Polytechnic Institute and State University in partial fulfillment of the requirements for the degree of

Doctor of Philosophy
in
Chemistry

Judy S. Riffle, Chair
John J. Lesko
James E. McGrath
Allan R. Shultz
Thomas C. Ward

12 April 2001
Blacksburg, Virginia

Keywords: Cresol novolac, controlled molecular weight, phenolic, epoxy, structure-property relationships, flame retardance, composite, latent catalyst

Cresol Novolac/Epoxy Networks: Synthesis, Properties and Processability

Sheng Lin-Gibson

Abstract

Void-free phenolic networks have been prepared by the reaction of phenolic novolac resins with various diepoxides. The stoichiometric ratio can be adjusted to achieve networks with good mechanical properties while maintaining excellent flame retardance. A series of linear, controlled molecular weight, 2,6-dimethylphenol endcapped cresol novolac resins have been synthesized and characterized. The molecular weight control was achieved by adjusting the stoichiometric ratio of cresol to 2,6-dimethylphenol and using an excess of formaldehyde. A dynamic equilibrium reaction was proposed to occur which allowed the targeted molecular weight to be obtained.

A 2000 g/mol *ortho*-cresol novolac resin was crosslinked by a diepoxide oligomer and by an epoxidized phenolic oligomer in defined weight ratios and the structure-property relationships were investigated. The networks comprised of 60 or 70 weight percent cresol novolac exhibited improved fracture toughness, high glass transition temperatures, low water uptake, and good flame retardance. The molecular weights between crosslinks were also determined for these networks. The stress relaxation moduli were measured as a function of temperature near the glass transition temperatures. Crosslink densities as well as the ability to hydrogen bond affect the glassy moduli of these networks. Rheological measurements indicated that cresol novolac/epoxy mixtures have an increased processing window compared to phenolic novolac/epoxy mixtures.

Maleimide functionalities were incorporated into cresol novolac oligomers, and these were crosslinked with bisphenol-A epoxy. The processability of oligomers containing thermally labile maleimides were limited to lower temperatures. However, sufficiently high molecular weight oligomers were necessary to obtain good network

mechanical properties. Networks prepared from 1250 g/mol cresol novolac containing maleimide functionilities and epoxy exhibited good network properties and could be processed easily.

Latent triphenylphosphine catalysts which are inert at processing temperatures (~140°C) but possess significant catalytic activity at cure temperatures 180-220°C were necessary for efficient composite fabrication using phenolic novolac/epoxy matrix resins. Both sequestered catalyst particles and sizings were investigated for this purpose. Phenolic novolac/epoxy mixtures containing sequestered catalysts exhibited significantly longer processing time windows than those containing free catalysts. The resins also showed accelerated reaction rates in the presence of sequestered catalysts at cure temperatures. Trihexylamine salt of a poly(amic acid) was sized onto reinforcing carbon fibers and the composite properties indicated that fast phenolic novolac/epoxy cure could be achieved in its presence.

Acknowledgements

I would like to dedicate this dissertation to my family; especially my loving husband Ben, who gave me constant love, support, and encouragement, and my parents Yin-Nian and Qin who instilled in me the important value of continued education and a strong work ethic. I am truly blessed to have such wonderful parents who dedicated their lives to bettering the lives of my brother, Dave, and I.

I am grateful and fortunate to have an incredible committee with a great wealth of knowledge in polymer science and an undying devotion to the field. I express sincere gratitude to, and the utter most respect for, my adviser and mentor, Dr. Judy S. Riffle who opened my eyes to the world of polymer science. She is truly an inspiration to all of her students as well as a role model for women in science. She has provided me with both technical and personal guidance throughout my undergraduate and graduate studies. I am also deeply indebted to Dr. James E. McGrath who constantly provided insight on various aspects of polymer chemistry, Dr. Allan R. Shultz for his invaluable suggestions and comments related to my research, Dr. John J. Lesko for his guidance on composite properties, and Dr. Thomas C. Ward for his suggestions on the physical chemistry aspect of my research. I would also like to thank the other CASS faculty and staff members, especially Dr. John Dillard and Dr. Jim Wightman, who gave me the opportunity for undergraduate research here at Virginia Tech.

I would like to thank my fellow graduate students in the "McGrath" group, the "Lesko" group, and the "Poly-P-Chem" group, and especially the "Riffle" group, for their advice and critical suggestions. I am grateful to the "Riffle girls" and Brian Starr with whom I developed valuable friendships throughout my years at Virginia Tech. I would particularly like to thank Angie and Mark Flynn for their invaluable assistance. Lastly, I would like to acknowledge the summer undergraduate students who assisted me in my research, Michael "Shane" Thompson and Vince Baranauskas.

Contents

List of Figures

List of Tables

1. Introduction

Fiber reinforced polymer matrix composites for structural applications, generally comprised of continuous fiber embedded in a polymer matrix, have high strength to weight ratios. Such composites also have superior oxidative resistance relative to steel and better freeze-thaw durability relative to concrete. However, the high combustibility of organic matrix materials limits their use in construction or transportation applications.

Phenolics are widely used as adhesives, coatings, and in various electric, structural, and aerospace applications. The main advantages of phenolic resins, both novolacs and resoles, and their networks are excellent flame retardance and low cost. A significant amount of academic research, therefore, has been devoted to understanding phenolic resin synthesis and network formation both mechanistically and kinetically. The thermal and thermo-oxidative degradation pathways have also been extensively investigated. A survey on phenolic resin syntheses, network formations, and degradation pathways is included in a phenolic chemistry literature review (chapter 2). One major shortcoming of typical phenolic networks is their large void contents due to released volatiles in the cure reactions. This, and the lack of control over network crosslink density, gives rise to brittle networks. Therefore, we and others have investigated phenolic or phenolic network modifications in order to improve these mechanical properties while retaining high thermal stability and flame retardance.

Previous work in our group focused on developing novolac/epoxy networks as composite matrix materials for structural applications.[1] A relatively high molecular weight novolac (7 hydroxyl groups per chain) was reacted with various diepoxides where the phenolic was the major component. The network density was controlled by adjusting the ratio of phenol to epoxy. Fracture toughness of the networks having 3 to 5 phenols per epoxy exceeded that of an untoughened epoxy control (bisphenol-A stoichiometrically cured with 4,4'-DDS) and far exceeded that of phenolic resoles. The flame retardance of the phenolic novolac/epoxy networks was significantly improved relative to the epoxy control.

[1] C. S. Tyberg, "Void-Free Flame Retardant Phenolic Networks: Properties and Processability," Dissertation, Virginia Tech, March 22, 2000.

Latent catalysts were subsequently developed to allow melt processing of the phenolic novolac/bisphenol-A epoxy mixtures. Catalysts were encapsulated onto the fiber, which eliminated resin/catalyst contact, and therefore prevented premature curing during processing. Results indicated that a poly(amic acid) salt of tris-(trimethoxy-phenylphosphine) was effective in catalyzing the phenolic novolac/epoxy reaction.

The ultimate goal of this research was to develop tough, flame retardant matrix resins which can be processed easily using typical composite fabrication methods. Attempts were also made to improve the specific drawbacks on existing phenolic novolac/epoxy systems such as high water uptake, and relatively short processing windows even in the absence of added catalysts. Following a literature review, the specific work of this dissertation is presented. This work has four major sections.

1) The first section focuses on the synthesis and characterization of controlled molecular weight cresol novolac resins. Specific reaction conditions and means to achieve molecular weight control are described.
2) The second section discusses in detail the network properties of a 2000 g/mol cresol novolac resin crosslinked with various epoxies at defined compositions. It investigates the network structure-property relationships, which allowed for understanding of the parameters that affect the network mechanical properties, flame retardance and processability. It also examines the molecular relaxation behaviors (cooperativity) and its relationships with network crosslink density and chemical structures.
3) The third section extends the results obtained in section 2 and assesses the effects of incorporating maleimide functionalities into cresol novolac/epoxy networks. The balance between network properties and processability is addressed.
4) The last section considers various approaches to sequester and encapsulate tertiary amines or phosphine catalysts which can be added directly to novolac/epoxy mixtures at melt processing temperatures. It also presents poly(amic acid)/trihexylamine as a more cost effective latent catalyst sizing for phenolic novolac/epoxy reactions.

2. Literature Review

Chemistry and Properties of Phenolic Resins and Networks

2.1. Introduction

Phenolic resins comprise a large family of oligomers and polymers (Table 2. 1), which are various products of phenols, reacted with formaldehyde. They are versatile synthetic materials with a large range of commercial applications. Plywood adhesives account for nearly half of all phenolic applications while wood binding and insulation materials also make up a significant portion.[2] Other uses for phenolics include coatings, adhesives, binders for abrasives, automotive and electrical components, electronic packaging and as matrices for composites.

Table 2. 1. U.S. Phenolic production (in millions of pounds on a gross weight basis)[3]

1998	1997	% Change
3940	3734	5.5

Phenolic oligomers are prepared by reacting phenol or substituted phenols with formaldehyde or other aldehydes. Depending on the reaction conditions (e.g., pH) and the ratio of phenol to formaldehyde, two types of phenolic resins are obtained. Novolacs are derived from an excess of phenol under neutral to acidic conditions, while reactions under basic conditions using an excess of formaldehyde result in resoles.

Phenolic resins were discovered by Baeyer in 1872 through acid catalyzed reactions of phenols and acetaldehyde. Kleeberg found in 1891 that resinous products could also be formed by reacting phenol with formaldehyde. But it was Baekeland who was granted patents in 1909 describing both base catalyzed resoles (known as Bakelite resins) and acid catalyzed novolac products.[4]

This chapter emphasizes the recent mechanistic and kinetic findings on both phenolic oligomer syntheses and network formation. The synthesis and characterization

[2] Society of Plastic Industries Facts and Figures, SPI, Washington, D.C. (1994).

[3] Society of Plastic Industries Facts and Figures, SPI, Washington D.C. (1999).

of both novolac and resole type phenolic resins and their resulting networks are described. Three types of networks, novolac/hexamethylene tetramine (HMTA), novolac/epoxies, and thermally cured resoles will be primarily discussed. Other phenolic based networks include benzoxazines and cyanate esters. Since phenolic materials possess excellent flame retardance, a discussion of the thermal and thermo-oxidative degradation pathways will be included. Detailed information on the chemistry, applications, and processing of phenolic materials can be found in a number of references.[4,5,6,7,8]

2.2. Materials for the synthesis of novolac and resole phenolic oligomers

2.2.1. Phenols

The most common precursor to phenolic resins is phenol. More than 95% of phenol is produced via the cumene process developed by Hock and Lang (Figure 2. 1). Cumene is obtained from the reaction of propylene and benzene through acid catalyzed alkylation. Oxidation of cumene in air gives rise to cumene hydroperoxide, which decomposes rapidly at elevated temperatures under acidic conditions to form phenol and acetone. A small amount of phenol is also derived from coal.

---

[4] A. Knop and L. A. Pilato, *Phenolic Resins--Chemistry, Applications and Performance*, Springer-Verlag, Berlin, 1985.

[5] A. Knop, W and W. Scheib, *Chemistry and Application of Phenolic Resins*, Springer-Verlag, New York, 1979.

[6] S. R Sandler and W. Karo, *Polymer Synthesis,* 2nd editions, Academic Press, Boston, Vol. 2*,* 1992.

[7] P. W. Kopf in J. I. Kroschulitz, ed., *Encyclopedia of Chemical Technology,* 4th Ed., Vol 18, John Wiley & Sons, 1996, pp 603-644.

[8] R.T. Conley, *Thermal Stability of Polymers*, Marcel Dekker, Inc., New York, 1970, pp. 459-496.

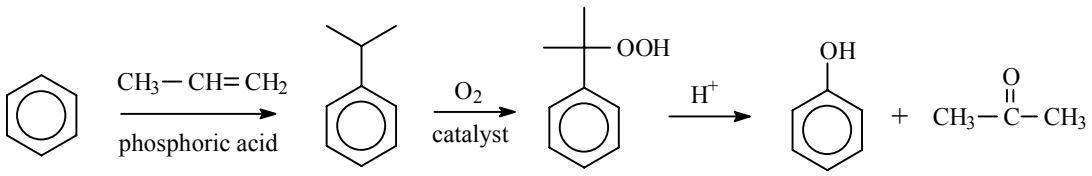

Figure 2. 1. Preparation of phenol monomer

Substituted phenols such as cresols, *p*-*tert*-butylphenol, *p*-phenylphenol, resorcinol, and cardanol (derived from cashew nut shells) have also been used as precursors for phenolic resins. Alkylphenols with at least three carbons in the substituent lead to more hydrophobic phenolic resins which are compatible with many oils, natural resins and rubbers.[9] Such alkylphenolic resins are used as modifying and crosslinking agents for oil varnishes, as coatings and printing inks, and as antioxidants and stabilizers. Bisphenol-A (2,2-*p*-hydroxyphenylpropane), a precursor to a number of phenolic resins, is the reaction product of phenol and acetone under acidic conditions.

An additional activating hydroxyl group on the phenolic ring allows resorcinol to react rapidly with formaldehyde even in the absence of catalysts.[10] This provides a method for room temperature cure of resorcinol-formaldehyde resins or mixed phenol-formaldehyde/resorcinol-formaldehyde resins. Trihydric phenols have not achieved commercial importance, probably due to their higher costs.

2.2.2. Formaldehyde and formaldehyde sources

Formaldehyde, produced by dehydrogenation of methanol, is used almost exclusively in the synthesis of phenolic resins (Figure 2. 2). Iron oxide, molybdenum oxide or silver catalysts are typically used for preparing formaldehyde. Air is a safe source of oxygen for this oxidation process.

---

[9] K. Hultzsch "Recent Chemical and Technical Aspects on Alkylphenolic Resins," *American Chemical Society, Division of Organic Coating & Plastic Chemistyr, Pap*. **26**(1), 121-128 (1966)

[10] U.S. Patents 2,385,370 (1947) A. J. Norton; U.S Patents 2,385,372 (1946) P. H. Phodes.

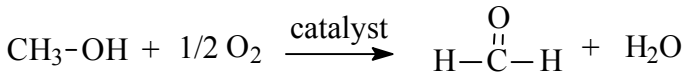

Figure 2. 2. Synthesis of formaldehyde

Since formaldehyde is a colorless pungent irritating gas, it is generally marketed as a mixture of oligomers of polymethylene glycols either in aqueous solutions (formalin) or in more concentrated solid forms (paraformaldehyde). The concentration of formalin ranges between about 37 and 50 wt %. A 40 wt % aqueous formalin solution at 35°C typically consists of methylene glycols with 1 to 10 repeat units. The molar concentration of methylene glycol with one repeat unit (HO-CH_2-OH) is highest and the concentrations decrease with increasing numbers of repeat units.[11] Paraformaldehyde, a white solid, contains mostly polymethylene glycols with 10 to 100 repeat units. It is prepared by distilling aqueous formaldehyde solutions and generally contains 1-7 wt % water.

Methanol, the starting reagent for producing formaldehyde, stabilizes the formalin solution by forming acetal endgroups and is usually present in at least small amounts (Figure 2. 3). Methanol may also be formed by disproportionation during storage. The presence of methanol reduces the rate of phenol/formaldehyde reactions but does not affect the activation energies.[12] It is generally removed by stripping at the end of the reaction.

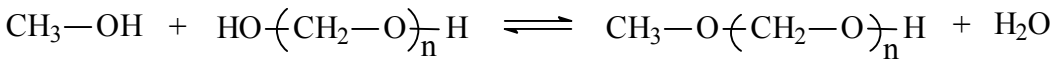

Figure 2. 3. Formation of hemiformals

Water is necessary for decomposing paraformaldehyde to formaldehyde (Figure 2. 4). However, water can serve as an ion sink and water-phenol mixtures phase separate

---

[11] H Diehm and A. Hit, "Formaldehyde" *Ullmanns Encyclopadie der Techn. Chem.*, *4th ed,* Verlag Chemie, Weinheim, Vol.11, 1976.

[12] C. M. Chen and S. L. Chen, "Effects of Methanol on the Reactions of the Phenol-Formaldehyde System," *Forest Products Journal* **38**(5), 49-52 (1988).

as the water concentration increases. Therefore, large amounts of water reduce the rate of reaction between phenol and formaldehyde.[13]

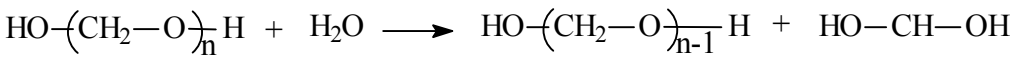

Figure 2. 4. Depolymerization of aqueous polyoxymethylene glycol

Hexamethylenetetramine (HMTA) used for crosslinking novolacs or catalyzing resole syntheses is prepared by reacting formaldehyde with ammonia (Figure 2. 5). The reaction is reversible at high temperatures, especially above 250°C. HMTA can also be hydrolyzed in the presence of water.

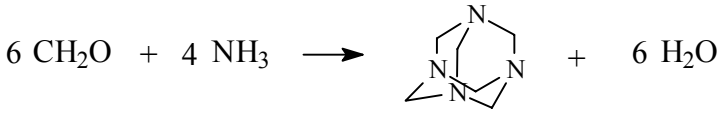

Figure 2. 5. Synthesis of hexamethylenetetramine

2.3. Novolac resins

The most common precursors for preparing novolac oligomers and resins are phenol, formaldehyde sources and to a lesser extent, cresols. Three reactive sites for electrophilic aromatic substitution are available on phenol which give rise to three types of linkages between aromatic rings, i.e. *ortho-ortho*, *ortho-para*, and *para-para*. The complexity of the isomers leads to amorphous materials. For a novolac chain with ten phenol groups, 13,203 isomers[14] can statistically form, making the separation of pure phenolic compounds from novolacs nearly impossible.

---

[13] A. J. Rojas and R. J. J. Williams, "Novolacs From Paraformaldehyde," *Journal of Applied Polymer Science* **23**, 2083-2088 (1979).

[14] N. J. L. Megson, "Unsolved Problems in Phenol Resin Chemistry," *Chem.-Ztg.,* **96**(1-2), 15-19 (1972).

2.3.1. Synthesis of novolac resins

Novolacs are prepared with an excess of phenol over formaldehyde under acidic conditions (Figure 2. 6). A methylene glycol is protonated by an acid from the reaction medium, which then releases water to form a hydroxymethylene cation (step 1 in Figure 2. 6). This ion hydroxyalkylates a phenol via electrophilic aromatic substitution. The rate determining step of the sequence occurs in step 2 where a pair of electrons from the phenol ring attacks the electrophile forming a carbocation intermediate. The methylol group of the hydroxymethylated phenol is unstable in the presence of acid and loses water readily to form a benzylic carbonium ion (step 3). This ion then reacts with another phenol to form a methylene bridge in another electrophilic aromatic substitution. This major process repeats until the formaldehyde is exhausted.

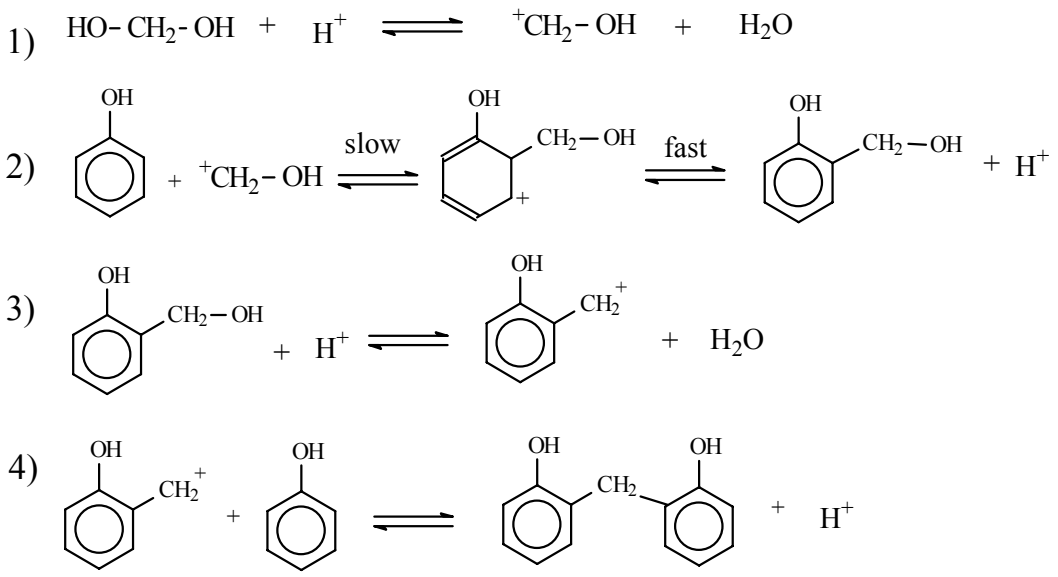

Figure 2. 6. Mechanism of novolac synthesis via electrophilic aromatic substitution

The reaction between phenol and formaldehyde is exothermic. Therefore the temperature must be controlled to prevent the build-up of heat, particularly during the early stages of reaction.[6] When formalin is used, water provides a medium for heat dissipation.

Typical formaldehyde to phenol ratios in novolac syntheses range from about 0.7 to 0.85 to maintain oligomers with sufficiently low molecular weights and reasonable

melt viscosities. This is especially important since phenol is trifunctional and a gel fraction begins to form as conversion increases. As a result, the number average molecular weights of novolac resins are generally below 1000g/mol.

The acidic catalysts used for these reactions include formic acid, HX (X=F, Cl, Br), oxalic acid, phosphoric acid, sulfuric acid, sulfamic acid, and *p*-toluenesulfonic acid.[6] Oxalic acid is preferred since resins with low color can be obtained. Oxalic acid also decomposes at high temperatures (>180°C) to CO_2, CO and water, which facilitates the removal of this catalyst thermally. Typically, 1-6 wt % catalyst is used. Hydrochloric acid results in corrosive materials and reportedly releases carcinogenic chloromethyl ether by-products during resin synthesis.[4]

Approximately 4-6 wt % phenol can typically be recovered following novolac reactions. Free phenol can be removed by washing with water repeatedly. The recovered phenolic components may contain 1,3-benzodioxane, probably derived from benzyl hemiformals (Figure 2. 7).[4]

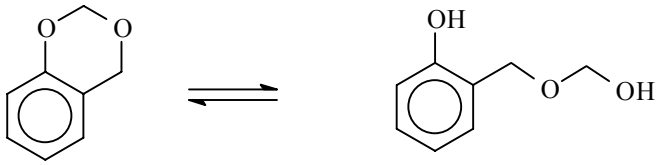

1,3-benzodioxane benzyl hemiformal

Figure 2. 7. Byproducts of novolac synthesis

2.3.2. "High *ortho*" novolac resins

High *ortho*-novolacs (Figure 2. 8) are sometimes more desirable since they cure more rapidly with HMTA. A number of oxides, hydroxide or organic salts of electropositive metals increase the reactivity of the *ortho* position during oligomer formation.[15] These high *ortho*-novolacs are typically formed at pHs of 4 to 6 as opposed to the more common strongly acidic conditions.

[15] U.S. Patents 2,464,207 and U.S. Patent 2,475,587 (1949) H. L. Bender, A.G Farnham and J. W. Guyer.

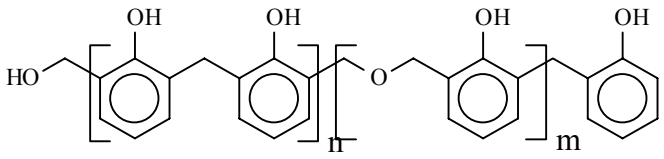

Figure 2. 8. High *ortho* novolacs

Metal hydroxides of first and second group elements can enhance *ortho* substitution, the degree of which depends on the strength of metal chelating effects linking the phenolic oxygen with the formaldehyde as it approaches the *ortho* position. Transition metal ions of elements such as Fe, Cu, Cr, Ni, Co, Mn and Zn as well as boric acid also direct *ortho* substitutions via chelating effects (Figure 2. 9).

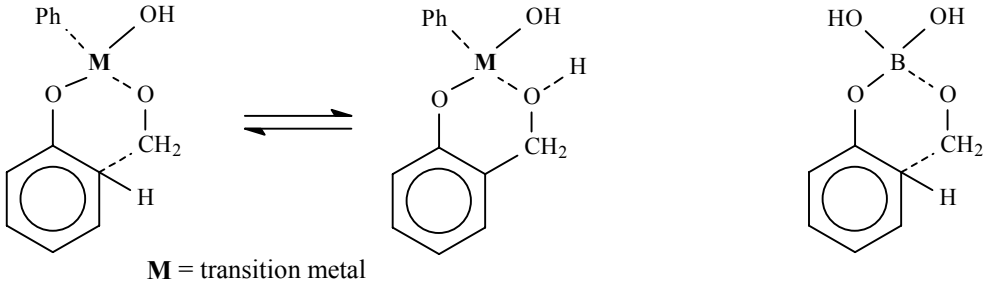

Figure 2. 9. Proposed chelate structures in the synthesis of high *ortho* novolac oligomers

Phenol-formaldehyde reactions catalyzed by zinc acetate as opposed to strong acids have been investigated, but this results in lower yields and requires longer reaction times. The reported *ortho-ortho* content yield was as high as 97%. Several divalent metal species such as calcium, barium, strontium, magnesium, zinc, cobalt and lead combined with an organic acid (such as sulfonic and/or fluoroboric acid) improved the reaction efficiencies.[16] The importance of an acid catalyst was attributed to facilitated decomposition of any dibenzyl ether groups formed in the process. It was also found the reaction rates could be accelerated with continuous azeotropic removal of water.

An interesting aspect of high *ortho* novolac oligomers is their so-called "hyperacidity". The enhanced acidity of high *ortho* novolac resins, intermediate between

[16] U.S. Pat. 4,113,700 (Sept. 12, 1978), W. Aubertson (to Monsanto Co.).

phenols and carboxylic acids, has been attributed to increased dissociation of the phenol protons due to strong intramolecular hydrogen bonding (Figure 2. 10). These materials are also reported to form strong complexes with di- and tri-valent metals and nonmetals.[4]

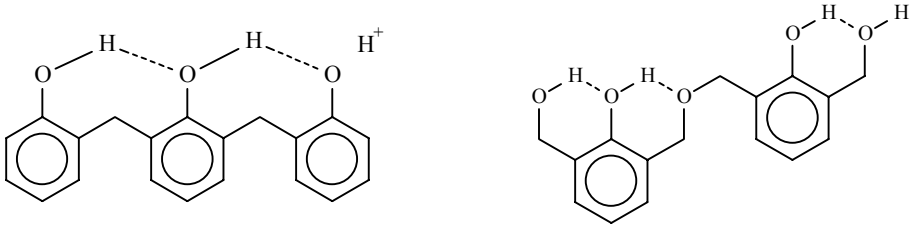

Figure 2. 10. Intramolecular hydrogen bonding of high *ortho* novolacs

2.3.3. Model phenolic oligomer synthesis

Linear novolac oligomers containing only *ortho* linkages were prepared using bromomagnesium salts under dry conditions.[17] The bromomagnesium salt of phenol coordinates with the incoming formaldehyde (Figure 2. 11A) or quinone methide (Figure 2. 11B) directing the reaction onto only *ortho* positions.

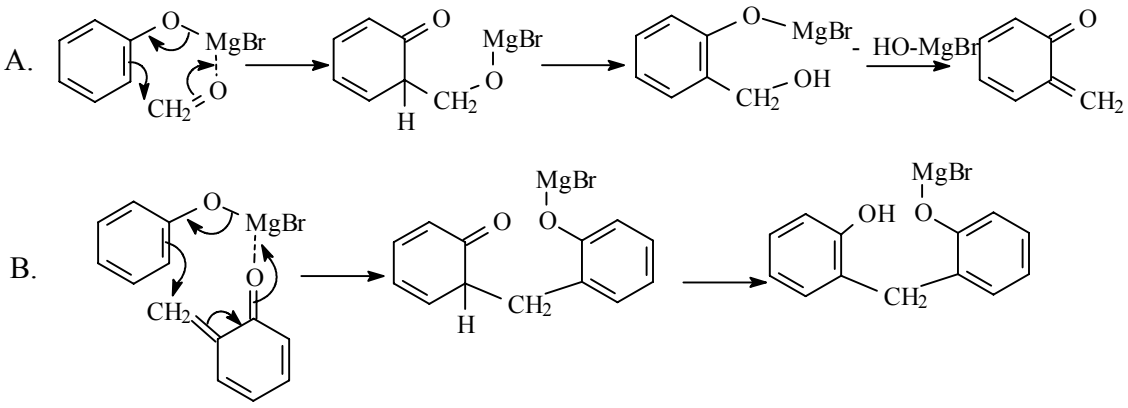

Figure 2. 11. Selective *ortho* coupling reaction using bromomagnesium salts

[17] G. Casnati. A. Pochini, G. Sartori, and R. Ungaro, "Template Catalysis via Non-Transition Metal Complexes-New Highly Selective Synthesis on Phenol Systems," *Pure and Applied Chemistry* **55**(11), 1677-1688 (1983).

Solomon et al.[18] prepared low molecular weight model novolac compounds containing 4 to 8 phenolic units utilizing the bromomagnesium salt methodology (Figure 2. 12). A *para-para* linked dimer was used as the starting material where *tert*-butyldimethylsilyl chloride was reacted with one phenol on a dimer to deactivate its ring against electrophilic reaction with formaldehyde. Selective *ortho* coupling formed bridges between the remaining phenol rings; then the *tert*-butyldimethylsilyl protecting groups were removed with fluoride ion. These compounds and all *ortho* linked model compounds prepared using bromomagnesium salts were subsequently used as molecular weight standards for calibrating gel permeation chromatography and to study model reactions with HMTA (see section 3.8).

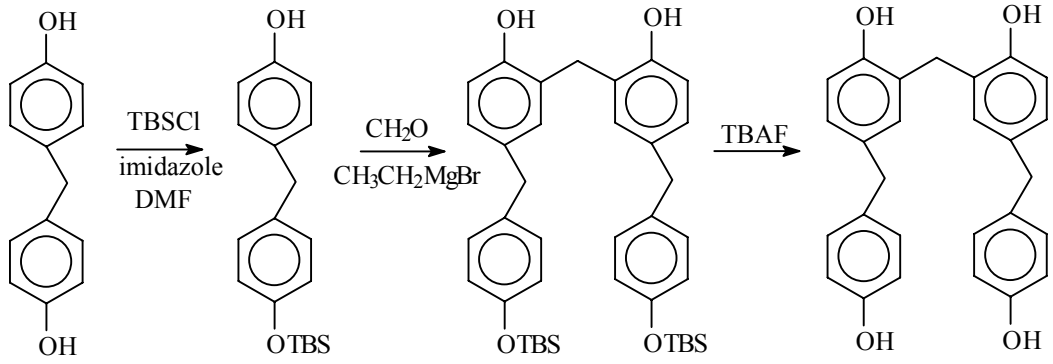

Figure 2. 12. Synthesis of model phenolic compound

2.3.4. Reaction conditions and copolymer effects

Alkyl substituted phenols have different reactivities than phenol toward reaction with formaldehyde. Relative reactivities determined by monitoring the disappearance of formaldehyde in phenol/paraformaldehyde reactions (Table 2. 2) show that under basic conditions, *meta*-cresol reacts with formaldehyde approximately 3 times faster than phenol while *ortho*- and *para*-cresols react at approximately 1/3 the rate of phenol.[19]

---

[18] P. J. de Bruyn, A. S. L. Lim, M. G. Looney, and D. H. Solomon, "Strategic Synthesis of Model Novolac Resins," *Tetrahedron Letters* **35**(26), 4627-4630 (1994).

[19] M. M. Sprung, "Reactivity of Phenol Toward Formaldehyde," *Journal of Applied Polymer Science* **63**(2), 334-343 (1941).

Similar trends were observed for the reactivities of acid catalyzed phenolic monomers with formaldehyde.

One comparison study of oxalic acid catalyzed reactions involving *ortho*- and *meta*-cresol mixtures demonstrated that *meta*-cresol was preferentially incorporated into the oligomers during the early stages of reaction.[20] Given the same reaction conditions and time, higher *ortho*-cresol compositions (of the mixtures) resulted in decreased overall yields since there was insufficient time for *ortho*-cresol to fully react. Consequently, the molecular weights and T_gs were also lower in these partially reacted materials. As expected, the molecular weight increased if a larger amount of catalyst was used or if more time was allowed for reaction. Increased catalyst concentrations also broadened molecular weight distributions.

Table 2. 2. Relative reaction rates of various phenols with formaldehyde under basic conditions[5]

Compound	Relative reactivity
2,6-xylenol	0.16
ortho-cresol	0.26
para-cresol	0.35
2,5-xylenol	0.71
3,4-xylenol	0.83
phenol	1.00
2,3,5-trimethylphenol	1.49
meta-cresol	2.88
3,5-xylenol	7.75

Bogan conducted similar studies in which *meta*- and/or *para*-cresols were reacted with formaldehyde at 99°C for 3 hours using oxalic acid dihydrate as the catalyst to form

[20] St. Miloshev, P. Novakov, Vl. Dimitrov, and I. Gitsov, "Synthesis of Novolac Resins. I. Influence of the Chemical Structure of the Monomers and Reaction Conditions on Some Properties of Novolac Oligomers," *Chemtronics* **4**, 251-253 (1989).

novolac type structures.[21] Using a relative reactivity of 0.09±0.03 for *para*-cresol with formaldehyde versus. *meta*-cresol with formaldehyde, a statistical model was employed to predict the amounts of unreacted cresols during the reactions, branching density, and *m/p*-cresol copolymer compositions. Good agreement was found between the predictions and experimental results. Since *para*-cresol reacted much slower that *meta*-cresol, it was to a first approximation considered an unreactive diluent. When *meta*- and *para*-cresol mixtures were reacted, oligomers consisting of mostly *meta*-cresol formed first, then when the *meta*-cresol content was depleted, *para*-cresol incorporation was observed (mostly at the chain ends). Full conversions were not achieved in these investigations, probably due to insufficient reaction times for *para*-cresol to react completely.

Linear novolac resins prepared by reacting *para*-alkylphenols with paraformaldehyde are of interest for adhesive tackifiers. As expected for step-growth polymerization, the molecular weights and viscosities of such oligomers prepared in one exemplary study increased as the ratio of formaldehyde to *para*-nonylphenol was increased from 0.32 to 1.00.[22] As is usually the case, however, these reactions were not carried out to full conversion and the measured M_n of an oligomer prepared with an equimolar phenol to formaldehyde ratio was 1400 g/mol. Plots of apparent shear viscosity vs. shear rate of these *p*-nonylphenol novolac resins showed non-Newtonian rheological behavior.

Reaction media play an important role in *meta*-cresol/paraformaldehyde reactions.[23] Higher molecular weight resins, especially those formed from near

---

[21] L. E. Bogan, Jr., in P. N. Prasad, ed., "Understanding the Novolac Synthesis Reaction," *Frontiers of Polymers and Advanced Materials*, Plenum Press, New York, 1994, 311-318.

[22] C. N. Cascaval, D. Rosu, and F. Mustata, "Synthesis and Characterization of Some *para*-Nonylphenol Formaldehyde Resins," *European Polymer Journal* **30**(3), 329-333 (1994).

[23] St. Miloshev, P. Novakov, Vl. Dimitrov, and I. Gitsov, "Synthesis of Novolac Resins: 2. Influence of the Reaction Medium on the Properties of the Novolac Oligomers," *Polymer* **32**(16), 3067-3070 (1991).

equimolar *meta*-cresol to formaldehyde ratios, can be obtained by introducing a water miscible solvent such as ethanol, methanol, or dioxane to the reaction. Small amounts of solvent (0.5 moles solvent per mole cresol) increased reaction rates by reducing the viscosity and improving homogeneity. Further increases in solvent, however, diluted the reagent concentrations to an extent that decreased the rates of reaction.

2.3.5. Molecular weight and molecular weight distribution calculations

The molecular weights and molecular weight distributions of phenolic oligomers have been evaluated using gel permeation chromatography (GPC),[24,25] NMR spectroscopy,[26] vapor-pressure osmometry,[27] intrinsic viscosity,[28] and more recently by matrix assisted laser desorption/ionization time of flight mass spectrometry (MALDI – TOFMS).[29]

---

[24] T. Yoshikawa, K. Kimura and S. Fujimura, "The Gel Permeation Chromatography of Phenolic Compound," *Journal of Applied Polymer Science* **15**, 2513-2520 (1971).

[25] T. A. Yamagishi, M. Nomoto, S. Ito, S. Ishida, and Y. Nakamoto, "Preparation and Characterization of High Molecular Weight Novolac Resins," *Polymer Bulletin* **32**, 501-507 (1994).

[26] L. E. Bogan, Jr., "Determination of Cresol Novolac Copolymer and Branch Density Using C-13 NMR Spectroscopy," *Macromolecules* **24**, 4807-4812 (1991).

[27] M. G. Kim, W. L. Nieh, T. Sellers, Jr., W. W. Wilson, and J. W. Mays, "Polymer Solution Properties of a Phenol-Formaldehyde Resol Resin by Gel Permeation Chromatography, Intrinsic-Viscosity, Static Light-Scattering, and Vapor Pressure Osmometric Methods," *Industrial & Engineering Chemistry Research* **31**(3), 973-979 (1992).

[28] F. L. Tobiason, C. Chandler, and F. E. Schwarz, "Molecular Weight-Intrinsic Viscosity Relationships for Phenol-Formaldehyde Novolak Resins," *Macromolecules* **5**(3), 321-325 (1972).

[29] H. Mandal and A. S. Hay, "M.A.L.D.I.-T.O.F. Mass Spectrometry Characterization of 4-Alkyl Substituted Phenol-Formaldehyde Novolac Type Resins," *Polymer* **38**(26), 6267-6271 (1997).

The most widely used molecular weight characterization method has been GPC which separates compounds based on hydrodynamic volume. State-of-the-art GPC instruments are equipped with a concentration detector (e.g., differential refractometer, UV and/or IR) in combination with viscosity or light scattering. A viscosity detector provides in-line solution viscosity data at each elution volume, which in combination with a concentration measurement, can be converted to specific viscosity. Since the polymer concentration at each elution volume is quite dilute, the specific viscosity is considered a reasonable approximation for the dilute solution intrinsic viscosity. The plot of $\log[\eta]M$ vs. elution volume (where $[\eta]$ is the intrinsic viscosity) provides a universal calibration curve where absolute molecular weights of a variety of polymers can be obtained. Unfortunately, many reported analyses for phenolic oligomers and resins are simply based on polystyrene standards and only provide relative molecular weights instead of absolute numbers.

Dargaville et al.[30] and Yoshikawa et al.[24] recognized the difficulties in obtaining accurate GPC molecular weights of phenolic resins due to large amounts of isomers and their associated differences in hydrodynamic sizes. These workers generated GPC calibration curves using a series of low molecular weight model novolac compounds: (1) linear compounds with only *ortho-ortho* methylene linkages, (2) compounds with *ortho-ortho* methylene linked backbones and where each unit had a pendent *para-para* methylene linked unit, and (3) compounds with *ortho-ortho* methylene linked backbones and where each unit had a pendent *para-ortho* methylene linked unit.[30] For a given molecular weight, the hydrodynamic volume of oligomers with only the *ortho-ortho* methylene links was smaller than the others. It was reasoned that the reduced hydrodynamic volume was caused by "extra" intramolecular hydrogen bonding in high-*ortho* novolacs, which was a similar argument to that suggested previously by Yoshikawa et al.[24] Based on the GPC calibration curves of the model compounds and their known

[30] T. R. Dargaville, F. N. Guerzoni, M. G. Looney, D. A. Shipp, D. H. Solomon, and X. Zhang, "Determination of Molecular Weight Distribution of Novolac Resins by Gel Permeation Chromatography," *Journal of Polymer Science. Part A: Polymer Chemistry* **35**(8), 1399-1407 (1997).

chemical structures, simulated calibration curves were generated for idealized 100% *ortho-para* methylene linked oligomers and for 100% *para-para* linked oligomers.

GPC chromatograms for a series of commercial novolacs, including resins with statistical distributions of *ortho* and *para* linkages and high *ortho* novolac resins were measured. Carbon-13 NMR provided the relative compositions of *o,o, o,p,* and *p,p* linked methylene groups. Molecular weights from GPC were calculated by considering the fractions of each type of linkage multiplied by the MW calculated from each of the 3 *o,o* (experimental), *o,p* (simulated), and *o,o* (simulated) GPC calibration curves. Good agreement was found between the resin molecular weights measured from ^{1}H NMR and the interpolated GPC numbers for oligomers up to an average of 4-5 units per chain, whereas more deviation was observed for higher molecular weights. This was attributed to complicated intramolecular hydrogen bonding in the higher molecular weight materials. Another factor may be that branching becomes significant in the higher molecular weight materials and the hydrodynamic volume effects of architecture are also complicated.

^{1}H NMR integrations of methylene and aromatic regions can be used to calculate the number average molecular weights of novolac resins.[30]

$$[CH_2]/[Ar] = (2n-2)/(3n+2) \qquad \textbf{(2. 1)}$$

where $[CH_2]/[Ar]$ is the ratio of methylene protons to aromatic protons and n is the number of phenolic units. The method is quite accurate for novolacs with less than 8 repeat units.

Solution ^{13}C NMR has been used extensively to examine the chemical structures of phenolic resins.[26,31] By ratioing the integration of peaks, degree of polymerization, number average molecular weights, degrees of branching, numbers of free *ortho* and *para* positions, and isomer distributions have been evaluated. A typical ^{13}C NMR spectrum of a novolac resin shows three regions (Table 2. 3): the methylene linkages resonate between 30 and 40 ppm; the peaks between 146-157 ppm are due to hydroxyl substituted

[31] R. A. Pethrick and B. Thomson, "^{13}C Nuclear Magnetic Resonance Studies of Phenol-Formaldehyde Resins 1-Model Compounds," *British Polymer Journal* **18**(3), 171-180 (1986).

aromatic carbons; and peaks between 113 and 135 ppm represent the remainder of the aromatic carbons.

Table 2. 3. Peak assignments for ^{13}C NMR chemical shifts of phenolic resins [32,42]

Chemical Shift Region (ppm)	Assignment
150-156	Hydroxyl-substituted phenolic carbons
127-135	Other phenolic carbons
121	*Para*-unsubstituted phenolic carbons
116	*Ortho*- unsubstituted phenolic carbons
85.9	HO-CH_2-O-CH_2-OH
81.4	HO-CH_2-OH
71.1	*Para*-linked dimethylene ether
68.2	*Ortho*- linked dimethylene ether
40.8	*Para-para* methylene linkages
35.5	*Para-ortho* methylene linkages
31.5	*Ortho-ortho* methylene linkages

The number of remaining *ortho* reactive sites versus the number of *para* reactive sites can also be calculated using ^{13}C NMR (Table 2. 3). Since the rates of novolac cure reactions differ with the amount of *ortho* versus *para* reactive sites available, it is of great interest to calculate these parameters.

Degrees of polymerization can be calculated from quantitative ^{13}C NMR data by considering the number of substituted (reacted) relative to unsubstituted (not yet reacted) *ortho* and *para* phenolic carbons where ([S]) is the sum of substituted *ortho* and *para* carbons and ([S]+[U]) is the total *ortho* and *para* carbons. The fraction of reacted *ortho* and *para* sites is denoted by f_s (equation 2). Thus, the number average number of phenol units per chain (n) can be calculated using equation 3. This leads to a simple calculation of M_n = (n) 106 –14.

$$f_s = [S]/([S] + [U]) \quad \textbf{(2. 2)}$$

$$n = 1/(1-1.5\, f_s) \quad \textbf{(2. 3)}$$

FTIR and FT Raman spectroscopy have been used to characterize phenolic compounds. The lack of hydroxyl interference is a major advantage of using FT Raman spectroscopy as opposed to FTIR to characterize phenolic compounds. Two regions of interest in Raman spectra are between 2800 and 4000 cm^{-1} where phenyl C-H stretching and methylene bridges are observed and between 400 and 1800 cm^{-1}.[32] For a high *ortho* novolac resin, the phenyl C-H stretch and methylene bridge appear at 3060 and 2940 cm^{-1} respectively. In the fingerprint region, the main bands are 1430-1470 cm^{-1} representative of methylene linkages, and 600-950 cm^{-1} for out-of-plane phenyl C-H bonds. Phenol, mono-*ortho*, di- and tri-substituted phenolic rings can be monitored between 814-831 cm^{-1}, 753-794 cm^{-1}, 820-855 cm^{-1} and 912-917 cm^{-1} respectively. *Para* substituted phenolic rings also absorb in the 820-855 cm^{-1} region.

Hay et al.[29] used MALDI–TOF mass spectrometry to determine the absolute molecular masses and endgroups of 4-phenylphenol novolac resins prepared in xylene or chlorobenzene. Peaks with a mass difference of 44 (the molecular weight of a xylene endgroup) suggested that reactions conducted in xylene included some incorporation of xylene onto the chain ends when a strong acid such as sulfuric acid was used to catalyze the reaction. By contrast, no xylene was reacted into the chain when a milder acid catalyst such as oxalic acid was used. No chlorobenzene was incorporated regardless of the catalyst used.

2.3.6. Hydrogen bonding

The abundant hydroxyl groups on phenolic resins causes these materials to form strong intra- and intermolecular hydrogen bonds. Intramolecular hydrogen bonding of phenolic resins gives rise to their hyperacidity while intermolecular hydrogen bonding facilitates miscibility with a number of materials containing electron donors such as carbonyl, amide, hydroxyl, ether and ester groups. Miscible polymer blends of novolac

---

[32] B. Ottenbourgs, P. Adriaensens, R. Carleer, D. Vanderzande, and J. Gelan, "Quantitative Carbon-13 Solid-State n.m.r. And FT-Raman Spectroscopy in Novolac Resins," *Polymer* **39**(22), 5293-5300 (1998).

resins include those with some polyamides,[33] poly(ethylene oxide),[34] poly(hydroxyether)s,[35] poly(vinyl alcohol),[36] and poly(decamethylene adipate) and other poly(adipate ester)s[37]. The specific strength of hydrogen bonding is a function of the groups involved, e.g. hydroxyl-hydroxyl interactions are stronger than hydroxyl-ether interactions.[38]

The effects of intermolecular hydrogen bonding on neat novolac resins with compounds containing hydrogen acceptors, e.g., 1,4-diazabicyclo[2,2,2]octane (DABCO) and hexamethylene tetramine, were also investigated.[39] Glass transition temperatures of neat resins and blends were measured using differential scanning calorimetry to assess

---

[33] F. Y. Wang, C. C. M. Ma, and H. D. Wu, "Hydrogen Bonding in Polyamide Toughened Novolac Type Phenolic Resin," *Journal of Applied Polymer Science* **74**, 2283-2289 (1999).

[34] P.P. Chu, H. D. Wu, and C. T. Lee, "Thermodynamic Properties of Novolac-Type Phenolic Resin Blended with Poly(ethylene oxide)," *Journal of Polymer Science, Part B: Polymer Physics* **36**(10), 1647-1655 (1998).

[35] H. D. Wu, C. C. M. Ma, and P. P. Chu, "Hydrogen Bonding in the Novolac Type Phenolic Resin Blended with Phenoxy Resin," *Polymer* 38(21), 5419-5429 (1997).

[36] H. D. Wu, P. P. Chu, C.C. M. Ma, and F. C. Chang, "Effects of Molecular Structure of Modifiers on the Thermodynamics of Phenolic Blends: An Entropic Factor Complementing PCAM," *Macromolecules* **32**(9), 3097-3105 (1999).

[37] H. D. Wu, C. C. M. Ma, P.P. Chu, H. T. Tseng, and C. T. Lee, "The Phase Behaviour of Novolac Type Phenolic Resin Blended with Poly(adipic ester)," *Polymer* **39**(13), 2856-2865 (1998).

[38] C. C. M. Ma, H. D. Wu, and C. T. Lee, "Strength of Hydrogen Bonding in the Novolac-Type Phenolic Resin Blends," *Journal of Polymer Science. Part B: Polymer Physics* **36**(10), 1721-1729 (1998).

[39] Z. Katovic and M. Stefanic, "Intermolecular Hydrogen Bonding in Novolacs," *Industrial & Engineering Chemistry Product Research And Development* **24**, 179-185 (1985).

the degrees of hydrogen bonding. Hydrogen-bonding interactions of novolac resins with electron donor sites such as oxygen, nitrogen, or chlorine atoms resulted in increased T_gs.

The propensity for dry novolac resins to absorb water at room temperature under 100% humidity is another indication that strong hydrogen bonds form. Approximately 15 wt% water is absorbed after 4 days which corresponds to one water molecule per hydroxyl group.[39]

Holland et al.[40] conducted dielectric measurements on novolac resins to evaluate the degrees of inter- and intramolecular hydrogen bonding. The frequency dependence of complex permittivity (ε^*) within a relaxation region can be described with a Havriliak and Negami function (HN function, equation 4)

$$\varepsilon^* = \varepsilon_\infty + \frac{\varepsilon_S - \varepsilon_\infty}{(1 + (i\omega\tau_o)^\beta)^\gamma} \qquad \textbf{(2. 4)}$$

where ε_S and ε_∞ are the relaxed and unrelaxed dielectric constants, □ is the angular frequency, τ_o is the relaxation time, and β and γ are fitting parameters. The complex permittivity is comprised of permittivity (ε') and dielectric loss (ε"). Fitting parameters in the HN function are related to shape parameters, m and n, which describe the limiting behavior of dielectric loss (ε") at low and high frequencies respectively. Intermolecular (characterized by "m") and intramolecular (characterized by 'n') hydrogen bonding can be correlated with m and n values which range from 0 to 1 (where lower values correspond to stronger hydrogen bonding). For one novolac resin examined (M_n = 1526 determined via GPC using polystyrene standards, MWD = 2.6, T_g = 57°C), m was 0.52 and n was 0.2. These results were considered indicative of strong intramolecular hydrogen bonding within the novolac structures.

2.3.7. Novolac crosslinking with Hexamethylene Tetramine (HMTA)

The most common crosslinking agent for novolac resins is HMTA which provides a source of formaldehyde. Novolac resins prepared from a P/F ratio of 1/0.8 can be cured

[40] C. Holland, W. Stark, and G. Hinrichsen, "Dielectric Investigations on Novolac Phenol-Formaldehyde Resins," *Acta Polymer* **46**, 64-67 (1995).

with 8-15 wt % HMTA, although it has been reported that 9-10 wt % results in networks with the best overall performance.[5]

2.3.7.1. Initial reactions of novolacs with HMTA

The initial cure reactions of a novolac with HMTA were studied by heating reactants at 90°C for 6 hours, then raising the temperature incrementally to a maximum of 205°C. This leads to mostly hydroxybenzylamine and benzoxazine intermediates (Figure 2. 13).[41,42] Hydroxybenzylamines form via repeated electrophilic aromatic substitutions of the active phenolic ring carbons on the methylenes of the HMTA (and derivatives of HMTA). Since novolac resins form strong intermolecular hydrogen bonds with electron donors, a plausible mechanism for the initial reaction between novolac and HMTA involves hydrogen bonding between phenolic hydroxyl groups and an HMTA nitrogen. Such hydrogen bonding can lead to proton transfer where a phenolate ion is generated. A negatively charged *ortho* or *para* carbon can attack the methylene carbon next to the positively charged nitrogen on HTMA which results in cleavage of a C-N bond. Benzoxazines form by nucleophilic attack of the phenolic oxygen on HMTA-phenolic intermediates. Upon further reaction, methylene linkages form as the major product of both types of intermediates through various thermal decomposition pathways.

---

[41] P. W. Kopf and E. R. Wagner, "Formation and Cure of Novolacs-NMR Study of Transient Molecules," *Journal of Polymer Science: Polymer Chemistry Edition* **11**(5), 939-960 (1973).

[42] S. A. Sojka, R. A. Wolfe, and G. D. Guenther, "Formation of Phenolic Resins: Mechanism and Time Dependence of the Reaction of Phenol and Hexamethylene-tetramine as Studied by Carbon-13 Nuclear Magnetic Resonance and Fourier Transform Infrared Spectroscopy," *Macromolecules* **14**,1539-1543 (1981).

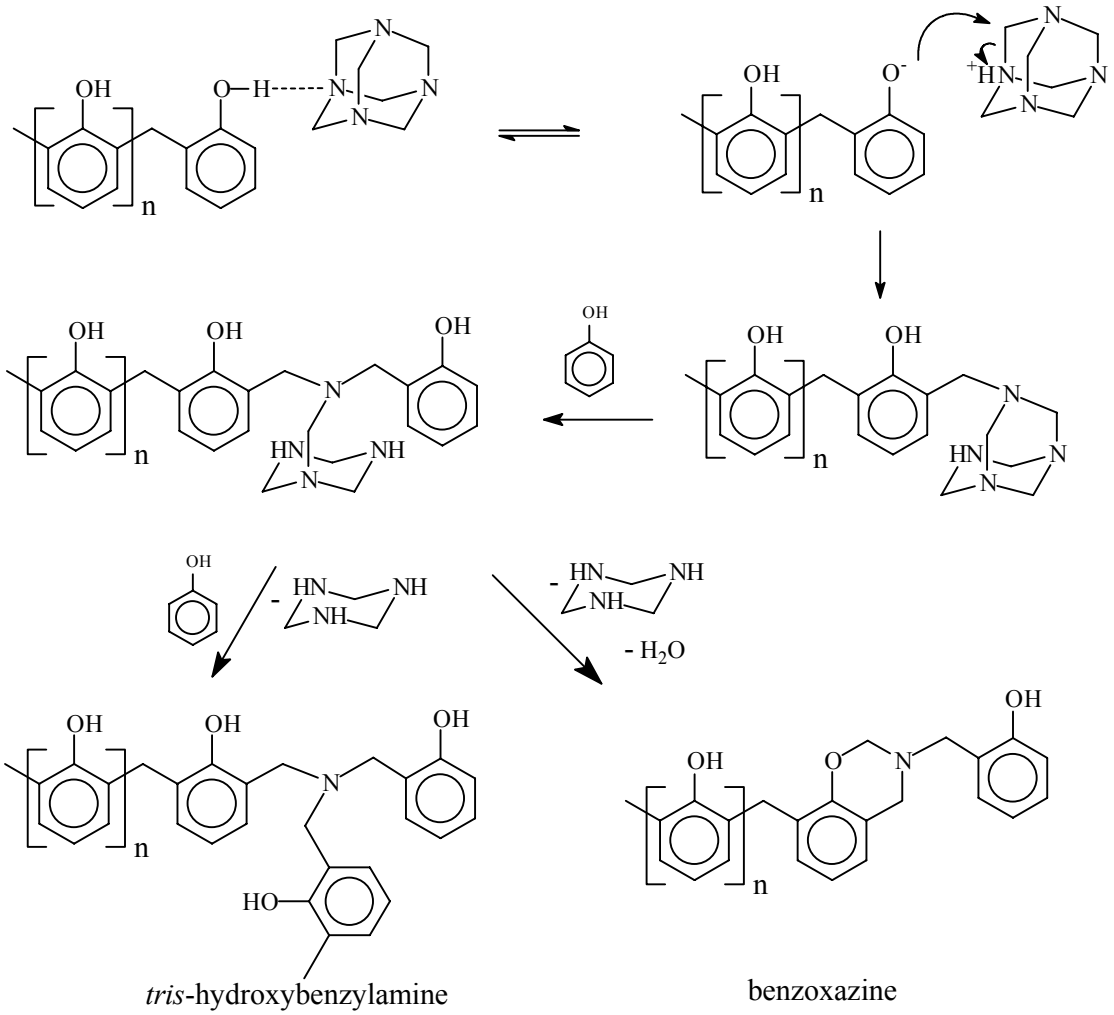

Figure 2. 13. Initial reaction of novolac and HMTA via a hydrogen bonding mechanism

Since a small amount of water is always present in novolac resins, it has also been suggested that some decomposition of HMTA proceeds by hydrolysis, leading to the elimination of formaldehyde and amino-methylol compounds (Figure 2. 14).[43] Phenols can react with the formaldehyde elimination product to extend the novolac chain or form methylene bridged crosslinks. Alternatively, phenol can react with amino-methylol

[43] Y. Ogata and A. Kawasaki in J. Zabicky ed., "Equilibrium Additions to Carbonyl Compounds," *The Chemistry of the Carbonyl Group*, Interscience, London, Vol. 2. 1970.

intermediates in combination with formaldehyde to produce *ortho*- or *para*-hydroxybenzylamines (i.e., Mannich type reactions).

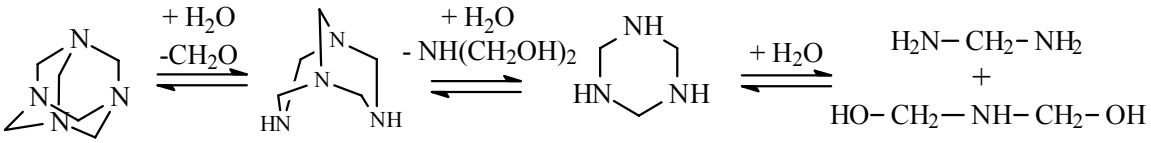

Figure 2. 14. Decomposition of HMTA

Reaction pathways involved in the curing of novolacs with HMTA have been extensively investigated by Solomon and coworkers.[44,45,46,47,48,49,50,51] In a series of model

---

[44] T. R. Dargaville, P. J. De Bruyn, A. S. C. Lim, M. G. Looney, A. C. Potter, and D. H. Solomon, "Chemistry of Novolac Resins. II, Reaction of Model Phenols with Hexamethylenetetramine," *Journal of Polymer Science. Part A*. **35**, 1389-1398 (1997).

[45] X. Zhang, M. G. Looney, D. H. Solomon, and A. K. Whittaker, "The Chemistry of Novolac Resins: 3. ^{13}C and ^{15}N n.m.r. Studies of Curing with Hexamethylenetetramine," *Polymer* **38**(23), 5835-5948 (1997).

[46] X. Zhang, A. C. Potter, and D. H. Solomon, "The Chemistry of Novolac Resins-V. Reactions of Benzoxazine Intermediates," *Polymer* **39**(2), 399-404 (1998).

[47] X. Zhang and D. H. Solomon, "The Chemistry of Novolac Resins-VI. Reactions Between Benzoxazine Intermediates and Model Phenols," *Polymer* **39**(2), 405-412 (1998).

[48] X. Zhang, A. C. Potter, and D. H. Solomon, "The Chemistry of Novolac Resins: Part 7. Reactions of *para*-Hydroxybenzylamine Intermediates," *Polymer* **39**(10), 1957-1966 (1998).

[49] X. Zhang, A. C. Potter, and D. H. Solomon, "The Chemistry of Novolac Resins: Part 8. Reaction of *para*-Hydroxybenzylamines with Model Compounds," *Polymer* **39**(10), 1967-1975 (1998).

[50] X. Zhang and D. H. Solomon, "The Chemistry of Novolac Resins: 9. Reaction Pathways Studied via Model Systems of *ortho*-Hydroxybenzylamine Intermediates and Phenols," *Polymer* **39**(24), 6153-6162 (1998).

studies where 2,6-xylenol and/or 2,4-xylenol were reacted with HMTA, these workers found that the types of linkages formed were affected by the initial chemical structure of the novolac, i.e. amount of *ortho* vs. *para* reactive positions, the amount of HMTA, and the pH. Reaction intermediates for the cure were identified, mostly via FTIR, ^{13}C NMR and ^{15}N NMR.

As previously described, the main intermediates generated from the initial reaction between *ortho* reactive sites on novolac resins and HMTA are hydroxybenzylamines and benzoxazines.[45] Triazines, diamines, and in the presence of trace amounts of water, benzyl alcohols and ethers also form (Figure 2. 15). Similar intermediates, with the exception of benzoxazines, are also observed when *para* sites react with HMTA.

The thermolysis rates to form methylene linkages depend on the stabilities of hydroxybenzylamine and benzoxazine intermediates. Comparatively, *ortho*-linked hydroxybenzylamine intermediates are more stable than *para*-linked structures because six-membered rings can form between the nitrogen and phenolic hydroxyl groups via intramolecular hydrogen bonding. For the same reason, benzoxazines are the most stable intermediates and decompose only at higher temperatures (185°C).[46] If a high *ortho*-novolac resin is cured with HMTA, the reaction occurs at lower temperatures due to formation of relatively unstable intermediates and the amount of side products is low. If, however, a typical novolac is used, the reaction temperature must be higher to decompose the more thermally stable *ortho* intermediates, and the amount of nitrogen containing side products is significantly higher.[47,48]

---

[51] A. S. C. Lim, D. H. Solomon, and X. Zhang, "Chemistry of Novolac Resins. X. Polymerization Studies of HMTA and Strategically Synthesized Model Compounds," *Journal of Polymer Science Part A: Polymer Chemistry* **37**, 1347-1355 (1999).

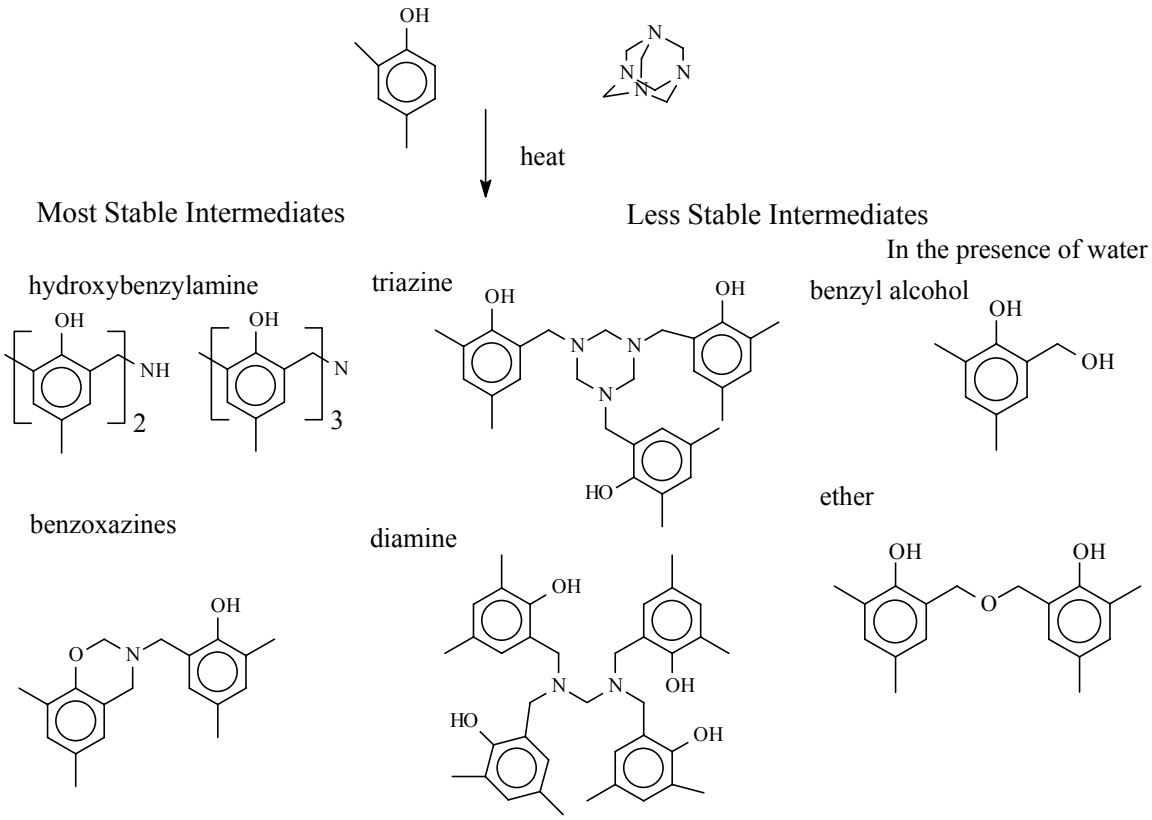

Figure 2. 15. Possible reaction intermediates for reaction of 2,4-xylenol with HTMA

If only *ortho* sites are available for reaction, the amount of hydroxybenzylamine vs. benzoxazine generated is largely dependent on the novolac/HMTA ratio. Hydroxybenzylamine is favored when the HMTA content is low whereas more benzoxazine is formed at higher HMTA concentrations. This is expected since only one HMTA carbon is needed per reactive *ortho* position in the formation of hydroxybenzylamine, but the formation of benzoxazine requires three HMTA carbons per two reactive *ortho* positions. The HMTA concentration therefore is one key in determining the structure of the resulting networks. Lower HMTA contents leading to more hydroxybenzylamine intermediates means that lower temperatures can be used for decomposition into methylene bridges and correspondingly lower levels of side products form under such conditions.

2.3.7.2. Hydroxybenzylamine and Benzoxazine decompositions in novolac/HMTA cures

*Thermal Decomposition of Hydroxybenzylamines***.** Depending on the concentration of HMTA and mobility of the system, hydroxybenzylamine and benzoxazine intermediates react by a number of pathways to form crosslinked novolac networks. Tris-hydroxybenzylamines eliminate benzoquinone methide between 90-120°C to form bis-hydroxybenzylamines, which decompose to methylene linkages with elimination of CH_2=NH at higher temperatures (Figure 2. 16).[47]

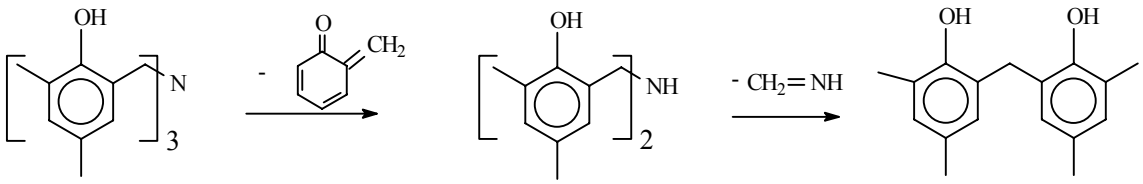

Figure 2. 16. Thermal decomposition of hydroxybenzylamine

Thermal Decomposition of Benzoxazines. Thermal decomposition of benzoxazines does not occur substantially until the temperature reaches ~160°C. This begins with proton transfer from a phenolic hydroxyl group to a nitrogen. Cleavage of the C-O bond with water generates a tertiary hydroxymethylamine which can eliminate formaldehyde, then CH_2=NH, to form methylene linkages (Figure 2. 17A). Alternatively, C-N bond cleavage in the benzoxazine leads to elimination of a benzoquinone methide, which can react with phenols to primarily yield the product methylene bridged species (Figure 2. 17B).[46] Further decomposition of benzoxazines can also lead to a variety of side products in small amounts.

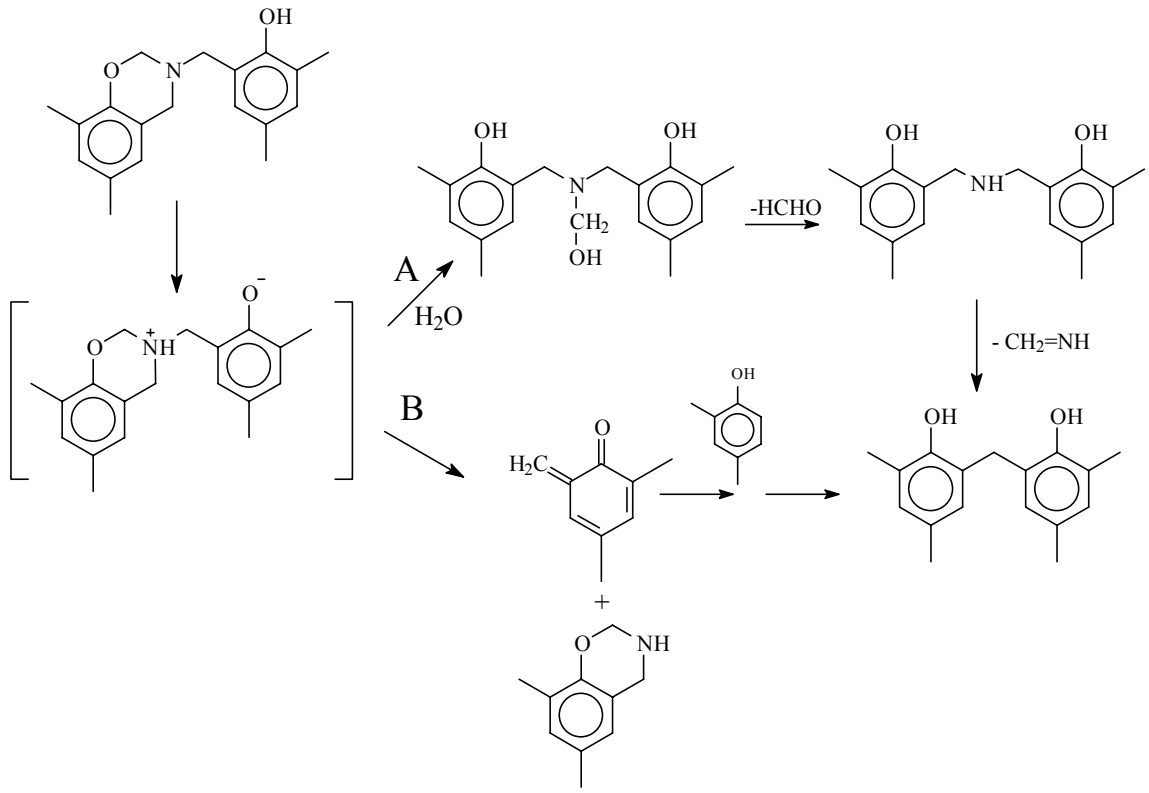

Figure 2. 17. Thermal decomposition of benzoxazine

Reactions of Benzoxazines with Phenols. In the presence of 2,4-xylenol, benzoxazine intermediates react at lower temperatures (~90°C) to form hydroxybenzylamines (Figure 2. 18), which can then decompose to *ortho-ortho* methylene linkages (as described in Figure 2. 16).[47] The reaction between benzoxazine and free *ortho* reactive positions on 2,4-xylenol occurs via electrophilic aromatic substitution facilitated by hydrogen bonding between benzoxazine oxygen and phenolic hydroxyl groups (Figure 2. 18).

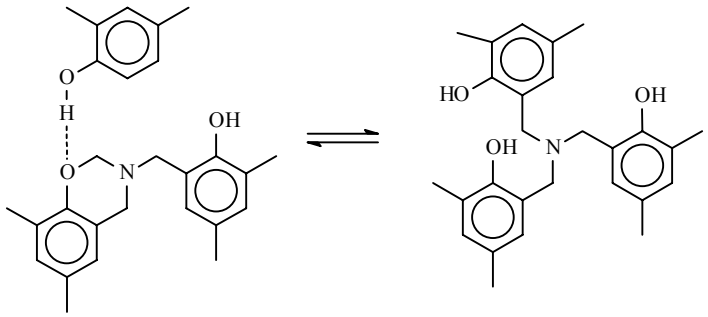

Figure 2. 18. Reaction of benzoxazines and 2,4-xylenol

The reaction of benzoxazine in the presence of 2,6-xylenol does not occur until ~135°C, presumably because the hydrogen bonded intermediate depicted for the 2,4-xylenol reaction (Figure 2. 18) cannot occur. All three types of linkages are obtained in this case. *Para-para* methylene linked 2,6-xylenol dimers, obtained from reaction of 2,6-xylenol with formaldehyde, formed in decomposition of the benzoxazine, (or with other by-products of that process) dominate. Possible side products from benzoxazine decomposition include formaldehyde and CH_2=NH, either of which may provide the source of methylene linkages. The amount of *ortho-para* linkages, formed by reaction of 2,6-xylenol with benzoxazine is low. *Ortho-ortho* methylene linked products presumably form by a decomposition pathway from benzoxazine (as in Figure 2. 17).

HMTA Crosslinking Reactions of Novolacs Containing Both Ortho and Para Reactive Sites. When both *ortho* and *para* positions on novolac materials are available for reaction with HMTA, *ortho-ortho*, *ortho-para*, and *para-para* methylene linkages form through several pathways. This section will address crosslinking reaction pathways where components which have been eliminated as "by-products" re-enter the reactions. In particular, reactions of quinone methides, formaldehyde and imine will be discussed. We will also describe exchange reactions between hydroxybenzylamine intermediates with phenolic methylol derivatives which lead to methylene bridged final products. Exchange reactions between two different hydroxybenzylamine intermediates, which lead to primarily *ortho-ortho* linked products, are also important.

In one model reaction where tris(*para*-hydroxybenzyl)amine was heated to 205°C in the presence of 2,4-xylenol (1:1 ratio), the *ortho-ortho*, *ortho-para*, and *para-para* methylene bridge ratio in the products was found to be 44%, 14%, and 38% respectively (Figure 2. 19).[49] This model study demonstrated the importance of benzoquinone methide intermediates in the formation of various products in the novolac/HMTA curing reaction. Formaldehyde, CH_2=NH, and water liberated during the cure reaction also affect the reaction pathways (pathways 3, 4 and 5). Approximately 4% of 1,2-bis(*para*-hydroxyphenyl)ethane was also observed, presumably formed through dimerization of two quinone methides.

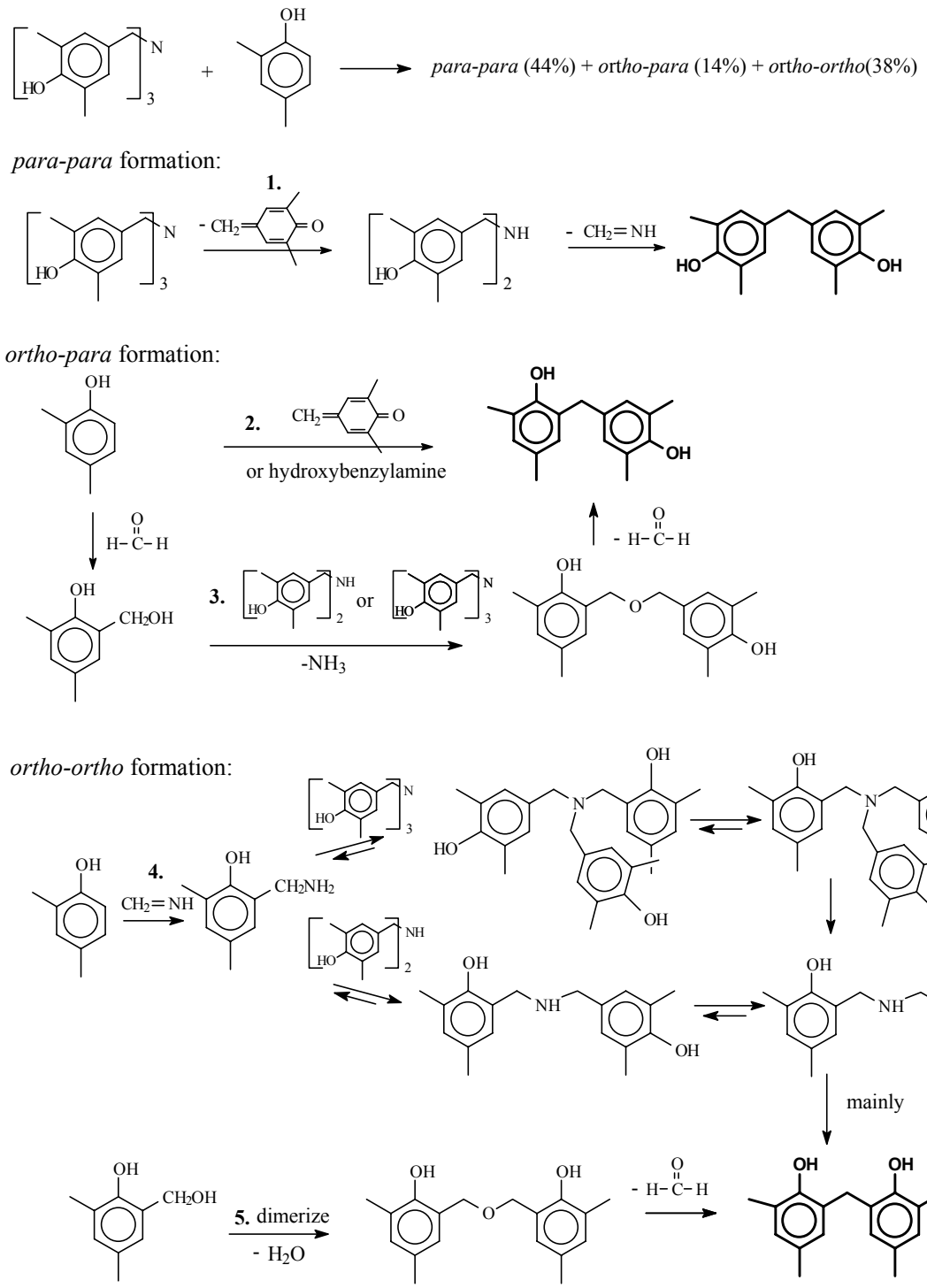

Figure 2. 19. Reaction pathways for formation of *ortho-ortho*, *ortho-para*, and *para-para* through the reaction of *para*-trishydroxybenzylamine and 2,4-xylenol

Para-para methylene linkages appeared first via hydroxybenzylamine decomposition at lower temperatures (pathway 1 in Figure 20). *Ortho-para* methylene linkages also formed at the lower reaction temperatures (pathway 2). Since the only source of an *ortho*- methylene linked phenol product was the 2,4-xylenol starting material, these mixed products must have formed by reaction of 2,4-xylenol with either a *para*-hydroxybenzylamine or with a quinone methide eliminated in pathway 1. *Ortho-para* methylene linkages also formed at higher reaction temperatures, which were attributed to exchange reactions between a methylol derivative of 2,4-xylenol and a hydroxybenzylamine (pathway 3). *Ortho-ortho* methylene linkages formed only at higher temperatures via hydroxybenzylamine exchange and methylol dimerization reactions described in pathways 4 and 5. The reactions depicted in pathway 4 involved sequential exchanges between *para*- and *ortho*- substituted intermediates through nucleophilic substitutions on hydroxybenzylamines. Since the amount of *ortho-para* linked products was low, it was suggested that the major product of pathway 4 was the *ortho-ortho* linkage. This is reasonable since the equilibrium of these exchange reactions lies toward *ortho*-hydroxybenzylamines where hydrogen bonding provides stability. These more thermally stable hydroxybenzylamines then decompose at higher temperatures to form *ortho-ortho* linkages.

Small amounts of various phenolic side products incorporating groups such as imines, amides, ethers and ethanes into the networks also form. A number of these side products undergo further reactions which eventually lead to methylene linkages. Some side products generally remain in the networks even after heating at 205°C.

Solomon et al. also investigated HMTA-phenolic reactions with somewhat larger model compounds (e.g., 2 and 4 ring compounds), and established that similar reaction pathways to those described previously occurred.[51] For these model compounds (as opposed to 1-ring model compounds) that are more representative of typical oligomeric systems, increased molecular weight favored the formation of hydroxybenzylamines, but not benzoxazines. This was suggested to be a steric effect.

Other crosslinking agents that provide sources of formaldehyde for methylene linkages include paraformaldehyde and trioxane, but these have only achieved limited importance. Quantitative ^{13}C solid-state NMR and FT-Raman spectroscopy were used to

monitor the cure reactions of a high *ortho*-novolac resin using paraformaldehyde under different conditions.[32] The weight percent paraformaldehyde needed to achieve the maximum crosslinking (1.5 moles formaldehyde per mole phenol) for the particular novolac examined (M_n=430 g/mol determined via ^{13}C NMR) was calculated to be 17.76 wt %. Eleven weight percent formaldehyde (1.18 moles formaldehyde relative to phenol) was used in these studies so that phenol sites were in excess. The degree of conversion was assessed by comparing the formaldehyde to phenol ratio in the polymer to 1.18. As expected, higher temperatures and/or pressures lead to higher reaction conversions. However, none of these reaction conversions reached 100%, and this was attributed to a lack of mobility.

2.4. Resole resins and networks

2.4.1. Resole resin syntheses

Resoles are prepared under alkaline conditions using an excess of formaldehyde over phenol (1:1 to 3:1) at typical temperatures of 60-80°C. The basic catalysts commonly used are NaOH, Na_2CO_3, KOH, K_2CO_3, $Ba(OH)_2$, R_4NOH, NH_3, RNH_2 and R_2NH.[6] In aqueous solutions, ammonia and HMTA are easily hydrolyzed to amines and also catalyze resole syntheses. Typical resole resins comprise a mixture of monomers, dimers, trimers, and small amounts of higher molecular weight oligomers with multiple methylol functional groups.

Resole syntheses entail substitution of formaldehyde (or formaldehyde derivatives) on phenolic *ortho* and *para* positions (Figure 2. 20) followed by methylol condensation reactions which form dimers and oligomers (Figure 2. 22). Under basic conditions, phenolate rings are the reactive species for electrophilic aromatic substitution reactions. A simplified mechanism is generally used to depict the formaldehyde substitution on the phenol rings (Figure 2. 20). It should be noted that this mechanism does not account for pH effects, the type of catalyst, or the formation of hemiformals. Mixtures of mono-, di-, and tri-hydroxymethyl substituted phenols are produced.

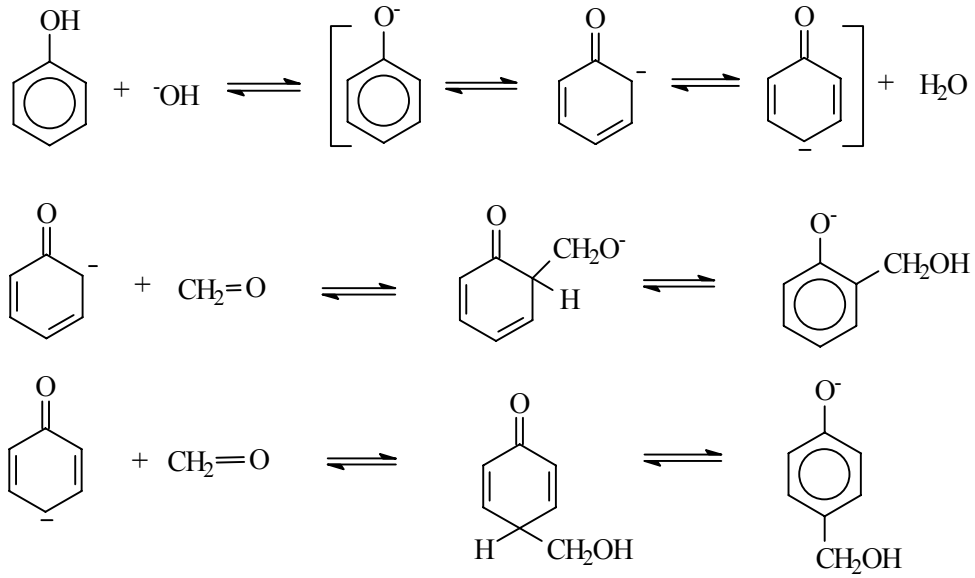

Figure 2. 20. Mechanism of resole synthesis

Phenol reacts with formaldehyde in either the *ortho* or the *para* position to form mono-hydroxymethyl substituted phenols, which further react with formaldehyde to form di- and tri-hydroxymethyl substituted phenols (Figure 2. 21).

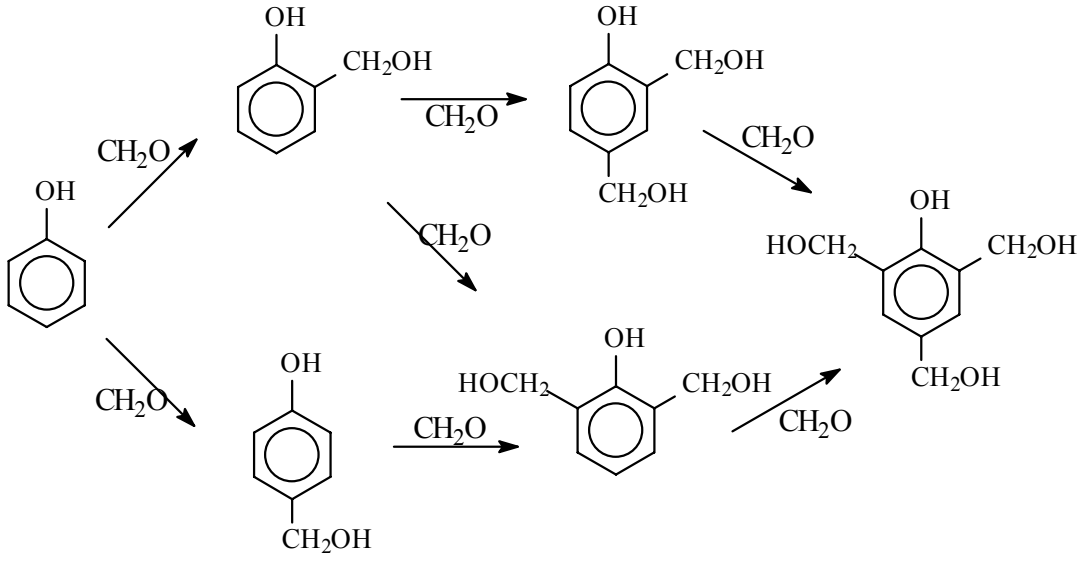

Figure 2. 21. Reaction pathways for phenol/formaldehyde reactions under alkaline conditions

Condensation reactions between two hydroxymethyl substituents eliminate water to form ether linkages (Figure 2. 22A) or eliminate both water and formaldehyde to form methylene linkages (Figure 2. 22B). Ether formation is favored under neutral or acidic conditions and up to ~130°C above which formaldehyde departs and methylene linkages are generated. The methylene linkage formation reaction, which eliminates water and formaldehyde, is more prevalent under basic conditions. Condensation reactions between hydroxymethyl groups and reactive *ortho* or *para* ring positions also lead to methylene bridges between phenolic rings (Figure 2. 22C). Relative reactivities of hydroxymethyl substituted phenols with formaldehyde and with other hydroxymethyl substituted phenols appear to be strongly dependent on interactions between *ortho*-methylol groups and the phenolic hydroxyl position. Hydroxymethyl condensation reactions under basic conditions strongly favor the formation of *para-para* and *ortho-para* methylene linkages.

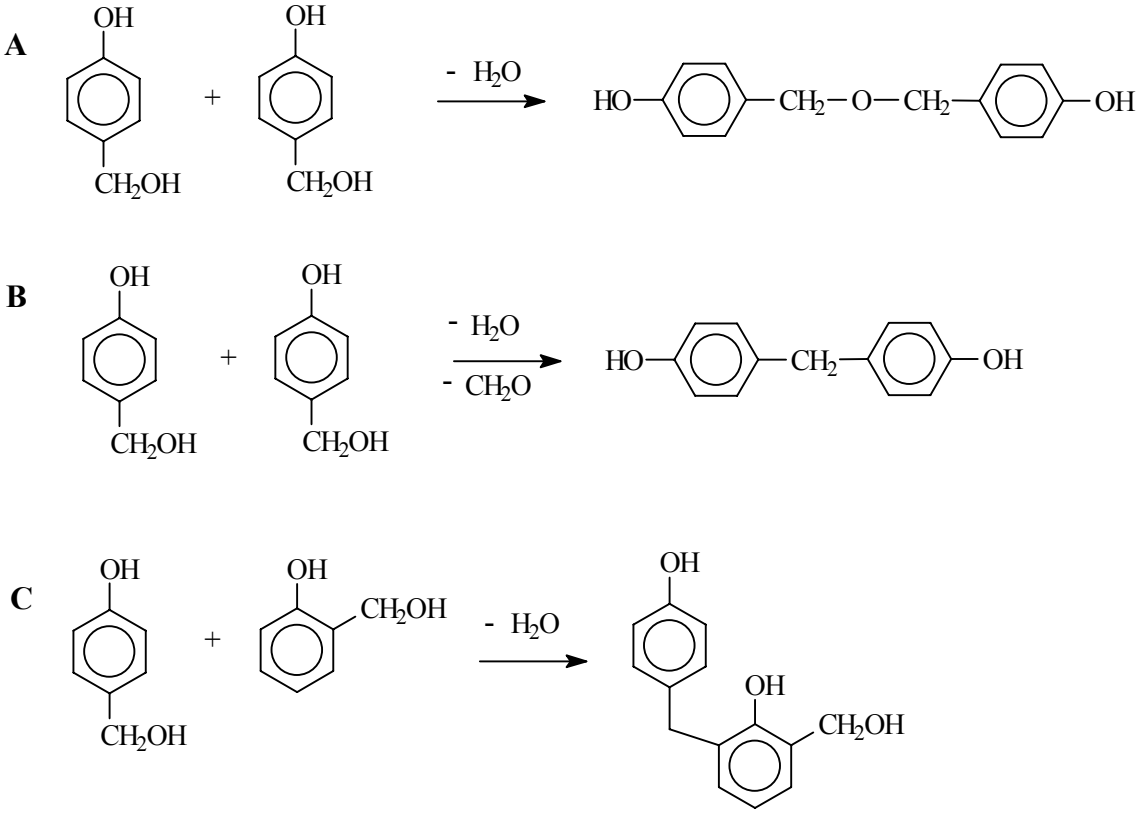

Figure 2. 22. Condensation of hydroxymethyl groups

Quinone methides are the key intermediates in both resole resin syntheses and crosslinking reactions. They form by dehydration of hydroxymethylphenols or dimethylether linkages (Figure 2. 23).

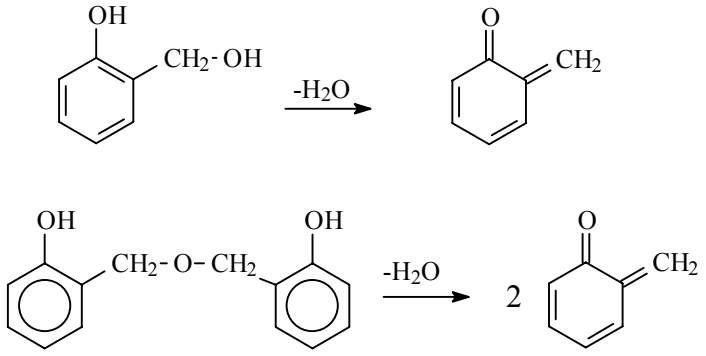

Figure 2. 23. Dehydration of methylols or benzylic ethers to form quinone methides

Resonance forms for quinone methides include both quinoid and benzoid structures (Figure 2. 24). The oligomerization or crosslinking reaction proceeds by nucleophilic attack on the quinone methide carbon.

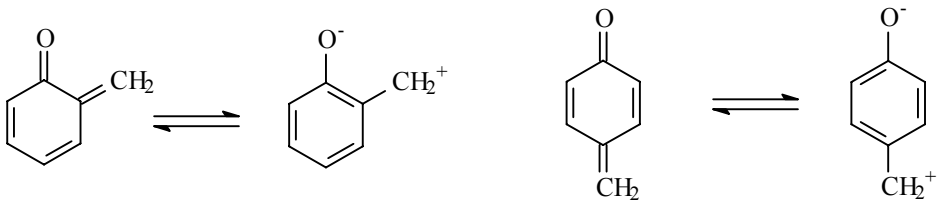

Figure 2. 24. Resonance of quinone methides

Ortho-quinone methides are difficult to isolate due to their high reactivity which leads to rapid Diels-Alder dimerization or trimerization (Figure 2. 25). At 150°C, a partial retro-Diels-Alder reaction of the trimer can occur to form *ortho*-quinone methide and bis(2-hydroxy-3,5-dimethylphenyl) ethane (dimer).[52]

[52] K. Lenghaus, G. G. Qiao, and D. H. Solomon, "Model Studies of the Curing of Resole Phenol-Formaldehyde Resins Part 1. The Behavior of *ortho* Quinone Methide in a Curing Resin," *Polymer* **41**, 1973-1979 (2000).

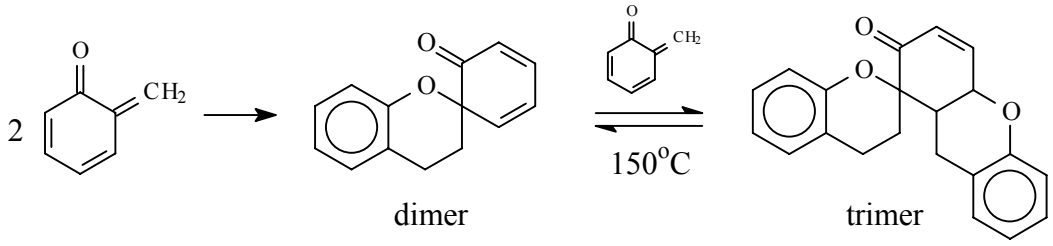

Figure 2. 25. Dimer and trimer structures of *ortho* quinone methides

Base catalyzed phenol-formaldehyde reactions exhibit second order kinetics (equation 2.5). Several alkylphenols such as cresols also follow this rate equation.

$$\text{rate} = k[\text{phenolate}][\text{formaldehyde}] \qquad \textbf{(2. 5)}$$

The rate constants for various hydroxymethylation steps (Figure 2. 21) have been evaluated by several groups (Table 2. 4)[53,54,55] and more recently by Grenier-Loustalot et al.[57]

[53] J. H. Freemann and C. W. Lewis, "Alkaline Catalyzed Reaction of Formaldehyde and the Methylol of Phenol-A Kinetic Study," *Journal of American Chemical Society* **76**(8), 2080-2087 (1954).

[54] A. A. Zsavitsas and R. D. Beaulieu, "Base Catalyzed Hydroxymethylation of Phenol by Aqueous Formaldehyde: Kinetic and Mechanism," *Journal of Polymer Science AI* **6**, 2451 (1969).

[55] K. C. Eapen and L. M. Yeddanapalli, "Kinetics and Mechanism of Alkaline Catalyzed Addition of Formaldehyde to Phenol and Substituted Phenol," *Makromolekulare Chemie* **119**, 4 (1968).

Table 2. 4. Relative positional reaction rates in base catalyzed phenol-formaldehyde reaction

	Relative reaction rates		
	Freeman et al.[53]	Zsavitsas et al.[54]	Eapen et al.[55]
phenol → 2-hydroxymethylphenol	1.00	1.00	1.00
phenol → 4-hydroxymethylphenol	1.18	1.09	1.46
2-hydroxymethylphenol → 2,6-dihydroxymethylphenol	1.66	1.98	1.75
2-hydroxymethylphenol → 2,4-dihydroxymethylphenol	1.39	1.80	3.05
4-hydroxymethylphenol → 2,4-dihydroxymethylphenol	0.71	0.79	0.85
2,4-dihydroxymethylphenol→2,4,6-trihydroxymethylphenol	1.73	1.67	2.04
2,6-dihydroxymethylphenol→2,4,6-trihydroxymethylphenol	7.94	3.33	4.36

Some consensus observations for reactions conducted at 30°C indicate that the *para* reactive site on phenol is slightly more reactive than *ortho* reactive sites due to higher electron density on the *para* position. In addition, *ortho* hydroxymethyl substituents significantly activate the rings toward further electrophilic addition of formaldehyde. This is especially pronounced for 2,6-dihydroxymethylphenols. *Ortho*-hydroxymethyl substituents are proposed to stabilize the quinoid resonance form via hydrogen bonding between the phenolic hydroxyl and *ortho*-hydroxymethyl groups in basic aqueous media (Figure 2. 26). This intramolecular stabilization activates the *para* position by intensifying electron density on the *para* carbon. This reasoning, however, does not explain the reduced reactivity reported for 2,4-dihydroxymethylphenol.

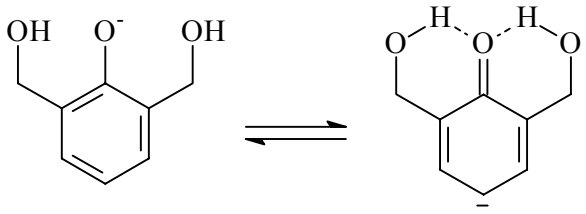

Figure 2. 26. Quinoid resonance forms activating the *para* ring position

More recently, the reaction advancement of resole syntheses (pH=8 and 60°C) was monitored using high performance liquid chromatography, ^{13}C NMR, and chemical

assays.[56,57] The disappearance of phenol and the appearances of various hydroxymethyl substituted phenolic monomers and dimers has been measured. By assessing residual monomer as a function of reaction time, this work also demonstrated the unusually high reactivity of 2,6-dihydroxymethylphenol. The rate constants for phenolic monomers towards formaldehyde substitution have been measured (Table 2. 5).

Table 2. 5. Second order rate constants for reaction of phenolic monomers with formaldehyde[57]

Compound	k ($mol^{-1}h^{-1}$)x10^2
phenol	5.1
2-hydroxymethylphenol	9.9
4-hydroxymethylphenol	10.7
2,4-dihydroxymethylphenol	8.6
2,6-dihydroxymethylphenol	13.0

As the reactions proceed, the disappearance of phenol is delayed due to competitions for reaction with formaldehyde between phenol and faster-reacting hydroxymethyl substituted phenols. Since the limiting step for phenolic reactions is formaldehyde substitution on phenol, particularly on the *ortho* positions, reaction conditions should be oriented toward fast phenol/formaldehyde reaction during the initial stages of reaction. Competition also exists between formaldehyde substitution reactions and condensation reactions between rings. Condensation reactions between two *ortho*-hydroxymethyl substituents are the least favorable condensation pathway. Depending on the reaction conditions, substitutions occur predominately in the earlier stages of reaction and condensations become the major reactions in later stages.[56]

---

[56] M. F. Grenier-Loustalot, S Larroque, P. Grenier, J. Leca, and K. Bedel, "Phenolic Resins: 1. Mechanisms and Kinetics of Phenol and of the First Polycondensations Towards Formaldehyde in Solution," *Polymer* **35**(14), 3046-3054 (1994).

[57] M. F. Grenier-Loustalot, S. Larroque, P. Grenier, and D. Bedel, "Phenolic Resins: 3. Study of the Reactivity of the Initial Monomers Towards Formaldehyde at Constant pH, Temperature and Catalyst type," *Polymer* **37**(6), 939-953 (1996).

As described previously, condensation reactions of hydroxymethyl substituents strongly favor the formation of *para-para* and *ortho-para* linkages.[58,59,60] Various hydroxymethyl substituted phenolic monomers were heated in the absence of formaldehyde (60°C, pH=8.0) to investigate condensation reactions under typical resole synthesis conditions but without formaldehyde substitution.[59] Only methylene linkages were observed under the particular experimental conditions. Highly substituted dimers were predominant in the product mixture since monomers with more hydroxymethyl substituents had higher probabilities for condensation. *Ortho*-hydroxymethyl groups only condensed with substituents in the *para* position, and therefore no *ortho-ortho* methylene linkages were observed. *Para*-hydroxymethyl substituents, on the other hand, reacted with either *ortho* or *para* hydroxymethyl substituents or reactive ring positions, but preferentially with *para*-hydroxymethyl groups. ^{13}C and ^{1}H NMR monitoring condensation reactions of resole resins comprised of two to five phenolic units showed that, with the exception of one trimer containing a dimethylene ether linkage, only *para-para* and *ortho-para* methylene linkages formed.

Upon further reaction, especially at higher temperatures (70-100°C), hydroxymethylated compounds reacted to form almost exclusively *para-para* and *ortho-para* methylene linkages. Since the key intermediates for the condensation of hydroxymethylphenols are quinone methides, the formation of *para-para* and *ortho-para* methylene linkages is attributed to exclusive formation of a *para*-quinone methide intermediate (Figure 2. 27).[7] This is attributed to intramolecular hydrogen bonding

---

[58] B. Mechin, D. Hanton, J. Le Goff and J. P. Tanneur, "HPLC and NMR Identification of the Main Polynuclear Constituents of Resol-Type Phenol-Formaldehyde Resins," *European Polymer Journal* **22**(2), 115-124 (1986).

[59] M. F. Grenier-Loustalot, S. Larroque, P. Grenier, and D. Bedel, "Phenolic Resins: 4. Self-Condensation of Methylolphenols in Formaldehyde-Free Media," *Polymer* **37**(6), 955-964 (1996).

[60] L. Prokai, "Separation and Identification of Phenol-Formaldehyde Condensates by Gas Chromatography-Mass Spectrometry. II. Base-Catalyzed Condensation Products," *Journal of Chromatography* **333**(1), 91-98 (1985).

between both *ortho* hydroxymethyl substituents with quinone methide oxygen, which lead to stable *para*-quinone methide structures. The *para*-quinone methide intermediates then react with *ortho* or *para* reactive positions to form *ortho-para* and *para-para* methylene linkages; or the quinone methide reacts with hydroxymethyl groups to form ethers which further advance to methylene linkages.

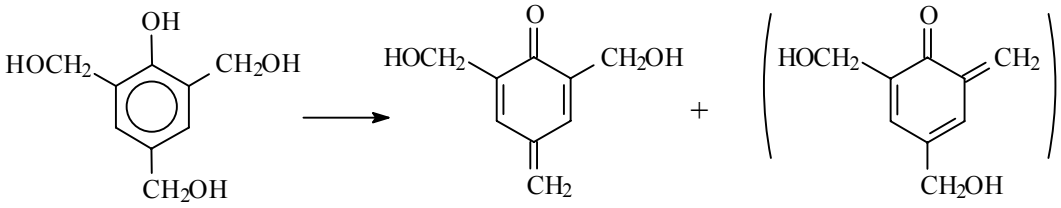

Figure 2. 27. Preferential formation of *para* quinone methides

The mechanisms for model condensation reactions of *para*-hydroxymethyl substituted phenol (and therefore *para*-quinone methide) with reactive *ortho* positions are described in Figure 2. 28. The phenolate derivatives react with *para*-quinone methide via a Michael type addition to form methylene linkages (Figure 2. 28 A). Hydroxyl groups on methylol can also attack methide carbons to form dibenzyl ether linkages which subsequently eliminate formaldehyde to form methylene links (Figure 2. 28 B). An *ipso* substitution where a nucleophilic ring carbon having a hydroxymethyl substituent attacks a quinone methide has also been postulated to generate methylene linkages (Figure 2. 28 C).

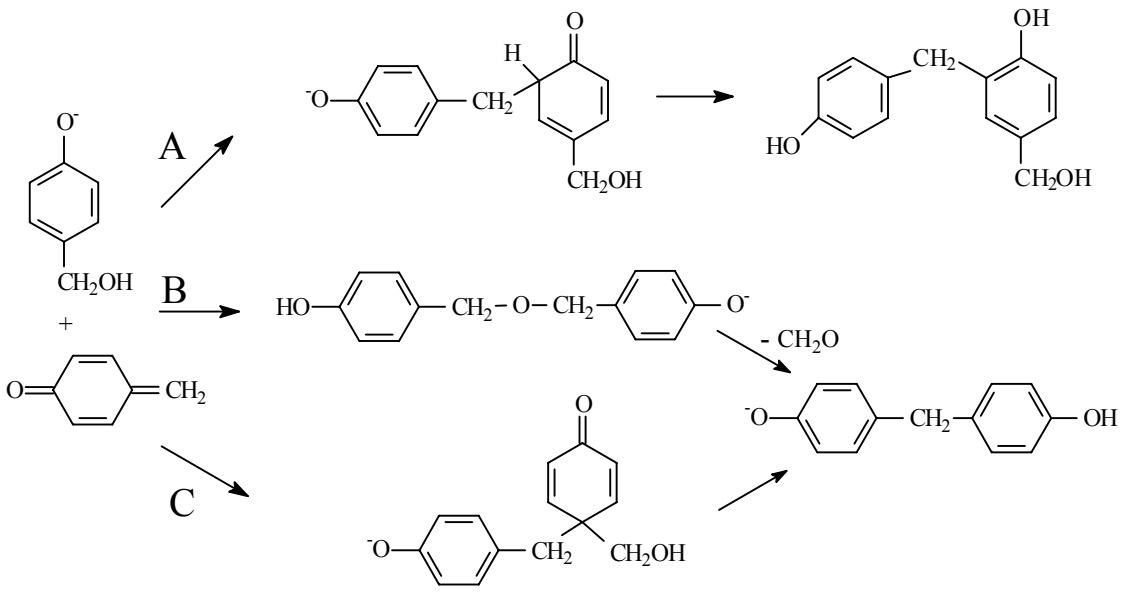

Figure 2. 28. Reactions of a quinone methide with a hydroxymethyl substituted phenolate

The reaction conditions, formaldehyde to phenol ratio, and the concentration and type of catalyst govern the mechanisms and the kinetics of resole syntheses. Higher formaldehyde to phenol ratios accelerate the reaction rates. This is to be expected since phenol/formaldehyde reactions follow second order kinetics. Increased hydroxymethyl substitution on phenols due to higher formaldehyde compositions also leads to more condensation products.[56]

The amount of catalyst and the pH of reaction determine the extent of phenolate formation. Phenol/formaldehyde mixtures (F/P=1.5, 60°C) did not react at pH=5.5 and reaction rate increased as the pH was increased to about 9.25.[56] There was a linear relationship between the rate constant and the [NaOH]/[phenol] ratio (between pHs 5.5 and 9.25). It was suggested that a limiting pH of approximately 9 exists, above which an increase in pH does not enhance the rate of reaction due to saturation of phenolate anions. Considerable Canizarro side reactions occurred on formaldehyde at pH>10.[56,61]

The type of catalyst influences the rate and the mechanism of reactions. Reactions catalyzed with both monovalent and divalent metal hydroxides, KOH, NaOH, LiOH, and $Ba(OH)_2$, $Ca(OH)_2$ and $Mg(OH)_2$, showed that both valence and ionic radius

[61] R. A Haupt and T. Sellers, "Characterization of Phenol-Formaldehyde Resol Resins," *Industrial & Engineering Chemistry Research* **33**(3), 693-697 (1994).

of hydrated cations affect the formation rate and final concentrations of various reaction intermediates and products.[62] For the same valence, a linear relationship was observed between formaldehyde disappearance rate and ionic radius of hydrated cations where larger cation radii gave rise to higher rate constants. In addition, irrespective of the ionic radii, divalent cations lead to faster formaldehyde disappearance rates than monovalent cations. For the proposed mechanism where an intermediate chelate participates in the reaction (Figure 2. 29), an increase in positive charge density in smaller cations was suggested to improve the stability of the chelate complex, and therefore, decrease the rate of the reaction. The radii and valence also affect the formation and disappearance of various hydroxymethylated phenolic compounds which dictate the composition of final products.

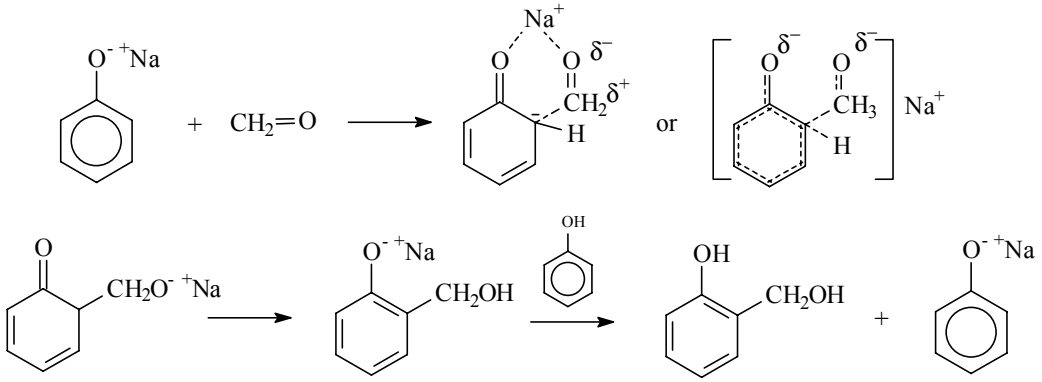

Figure 2. 29. Reaction mechanism of phenol and formaldehyde using base catalyst involving the formation of chelate

Tetraalkylammonium hydroxides have slightly lower catalytic activities than NaOH in resole syntheses. Increased alkyl length on tetraalkylammonium ions (larger ionic radii) decreased the catalytic activity. Contrary to the chelating effect, the reduced activity observed with tetraalkylammonium hydroxides was attributed to screening effects of alkyl groups. Water solubility was limited to resole resins prepared with

[62] M. F. Grenier-Loustalot, S. Larroque, D. Grande, P. Grenier, and D. Bedel, "Phenolic Resins: 2. Influence of Catalyst Type on Reaction Mechanisms and Kinetics," *Polymer* **37**(8), 1363-1369 (1996).

tetramethylammonium hydroxide and tetraethylammonium hydroxide. These catalysts also give rise to resins with longer gelation times.

Resole syntheses catalyzed with various amounts of triethylamine (pH adjusted to 8 using NaOH) and various pHs (pH = 8.0, 8.23 and 8.36) were monitored.[63] As expected, shorter condensation times, faster reaction rates, and higher advancement in polymerizations were reached with increased catalyst concentrations. The pH, on the other hand, did not affect these parameters significantly. The reaction mechanisms differed when NaOH was used to adjust the pH since the hydroxide formed phenolate ions which favored *para* addition reactions. In the absence of NaOH, free phenolic hydroxyl groups formed complexes with triethylamine to promote *ortho* substitution.

2.4.2. Crosslinking reactions of resole resins

Resole resins are generally crosslinked under neutral conditions between 130 and 200°C or in the presence of an acid catalyst such as hydrochloric acid, phosphoric acid, *p*-toluenesulfonic acid, and phenolsulfonic acid under ambient conditions.[5] The mechanisms for crosslinking under acidic conditions are similar to acid catalyzed novolac formation. Quinone methides are the key reaction intermediates. Further condensation reactions in resole resin syntheses under basic conditions at elevated temperatures also lead to crosslinking.

The self-condensation of *ortho*-hydroxymethyl substituents and the condensation between this substituent with *ortho* or *para* reactive sites were investigated under neutral conditions.[52] 2-Hydroxymethyl-4,6-dimethylphenol was reacted 1) alone, 2) in the presence of 2,4-xylenol, and 3) in the presence of 2,6-xylenol. The rates of methylene versus dimethylether formation between rings at 120°C were monitored as a function of time and the percent yields after 5 hours were recorded (Table 2. 6). The ether linkage was more prevalent in the self-condensation of 2-hydroxymethyl-4,6-dimethylphenol. Possibly the 5% methylene bridged product formed via *ipso* substitution of an *ortho*

[63] G. Astarloa-Aierbe, J.M. Echeverria, A. Vazquez, and I. Mondragon, "Influence of the Amount of Catalyst and Initial pH on the Phenolic Resole Resin Formation," *Polymer* **41**, 3311-3315 (2000).

quinone methide electrophile onto the methylene position of another ring. Essentially no differences in product composition were observed between the 2-hydroxymethyl-4,6-dimethylphenol self-condensation and reaction of this compound in the presence of 2,6-xylenol. The formation of methylene linkages proceeded much more favorably in the presence of 2,4-xylenol. Moreover, increases in 2,4-xylenol concentrations further increased the methylene linkage yield. This suggests vacant *ortho* positions are significantly more reactive than *para* reactive sites in reactions with *ortho*-quinone methide. These model reactions provide further evidence supporting quinone methides as the key reactive intermediates.

Table 2. 6. % yield of methylene and ether linkages of 2-hydroxylmethyl-4,6-dimethylphenol self-reaction, 1:1 with 2,4-xylenol, and 1:1 with 2,6-xylenol.

	Methylene % yield	Ether % yield
Self-reaction	5	80
with 2,4-xylenol	38	65
with 2,6-xylenol	5	80

In addition to methylene and dimethylether linkages, cured networks contain ethane and ethene linkages (Figure 2. 30). These side products are proposed to form through quinone methide intermediates.

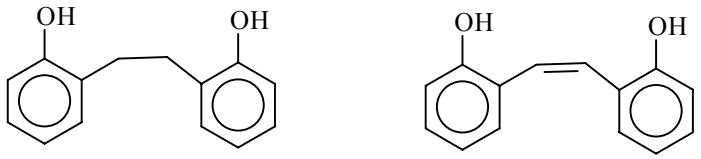

Figure 2. 30. Ethane and ethene linkages derived from quinone methide structures

Crosslinking resoles in the presence of sodium carbonate or potassium carbonate lead to preferential formation of *ortho-ortho* methylene linkages.[64] Resole networks crosslinked under basic conditions showed that crosslink density depends on the degree of hydroxymethyl substitution, which is affected by the formaldehyde to phenol ratio and the reaction time, the type and concentration of catalyst (uncatalyzed, with 2% NaOH, with 5% NaOH).[65] As expected, NaOH accelerated the rates of both hydroxymethyl substitution and methylene ether formation. Significant rate increases were observed for *ortho* substitutions as the amount of NaOH increased. The *para* substitution, which does not occur in the absence of the catalyst, formed only in small amounts in the presence of NaOH.

.

2.4.3. Resole characterization

A number of analytical techniques such as Fourier transform infrared spectroscopy (FTIR),[66,67] ^{13}C NMR,[68,69] solid-state ^{13}C NMR,[70] gel permeation

---

[64] B. D. Park and B. Riedl, "C-13-NMR Study of Cure-Accelerated Phenol-Formaldehyde Resins with Carbonates," *Journal of Applied Polymer Science* **77**(6), 1284-1293 (2000).

[65] M. Grenier-Loustalot, S. Larroque and P. Grenier, "Phenolic Resins: 5. Solid-State Physicochemical Study of Resoles with Variable F/P Ratios," *Polymer* **37**(4), 639-650 (1996).

[66] T. Holopainen, L. Alvila, J. Rainio, and T. T. Pakkanen, "IR Analysis of Phenol-Formaldehyde Resole Resins," *Journal of Applied Polymer Science* **69**(11), 2175-2185 (1998).

[67] G. Carotenuto and L. Nicolais, "Kinetic Study of Phenolic Resin Cured by IR Spectroscopy," *Journal of Applied Polymer Science* **74**(11), 2703-2715 (1999).

[68] T. Holopainen, L. Alvila, J. Rainio, and T. T. Pakkanen, "Phenol-Formaldehyde Resol Resins Studied by C-13-NMR Spectroscopy, Gel Permeation Chromatography, and Differential Scanning Calorimetry," *Journal of Applied Polymer Science* **66**(6), 1183-1193 (1997).

chromatography or size exclusion chromatography (GPC),[68,69,71,72,73] high performance liquid chromatography (HPLC),[74] mass spectrometric analysis,[75] differential scanning calorimetry (DSC),[68,76,77] and dynamic mechanical analysis (DMA)[78,79] have been utilized

---

[69] M. G. Kim, L.W. Amos, and E. E. Barnes, "Study of the Reaction Rates and Structures of a Phenol Formaldehyde Resol Resin by C-13 NMR and Gel-Permeation Chromatography," *Industrial & Engineering Chemistry Research* **29**(10), 2032-2037 (1990).

[70] P. Luukko, L. Alvila, T. Holopainen, J. Rainio, and T. T. Pakkanen, "Optimizing the Conditions of Quantitative ^{13}C NMR Spectroscopy Analysis for Phenol-Formaldehyde Resole Resins," *Journal of Applied Polymer Science* **69**, 1805-1812 (1998).

[71] T. Sellers and M. L. Prewitt "Applications of Gel-Filtration Chromatography for Resole Phenolic Resins using Aqueous Sodium-Hydroxide and Solvent," *Journal of Chromatography* **513**, 271-278 (1990).

[72] G. Gobec, M. Dunky, T. Zich, and K. Lederer, "Gel Permeation Chromatography and Calibration of Resolic Phenol-Formaldehyde Condensates," *Angewandte Makromolekulare Chemie* **251**, 171-179 (1997).

[73] M.G. Kim, W. L. Nieh, T. Sellers, W.W. Wilson, and J. W. Mays, "Polymer-Solution Properties of a Phenol Formaldehyde Resol Resin by Gel-Permeation Chromatography, Intrinsic-Viscosity, Static Light Scattering, and Vapor-Pressure Osmometric Methods," *Industrial & Engineering Chemistry Research* **31**(3), 973-979 (1992).

[74] G. Astarloa-Aierbe, J. M. Echeverria, J. L. Egiburu, M, Ormaetxea, and I. Mondradon, "Kinetics of Phenolic Resol Resin Formation by HPLC," *Polymer* **39**(14), 3147-3153 (1998).

[75] L. Prokai and W. J. Simonsick, "Direct Mass-Spectrometric Analysis of Phenol Formaldehyde Oligocondensates- A Comparative Desorption Ionization Study," *Macromolecules* **25**(24), 6532-6539 (1992).

[76] J. M. Kenny, G. Pisaniello, F. Farina, and S. Puzziello, "Calorimetric Analysis of the Polymerization Reaction of a Phenolic Resin," *Thermochimica Acta* **269**, 201-211(1995).

to characterize resole syntheses and crosslinking reactions. Packed-column supercritical fluid chromatography with a negative-ion atmospheric-pressure chemical ionization mass spectrometric detector has also been used to separate and characterize resole resins.[80] This section provides some examples of how these techniques are used in practical applications.

Using FTIR spectroscopy, resole resin formation and cure reactions can be examined (Table 2. 7). FTIR can be used to monitor the appearance and disappearance of hydroxymethyl groups and/or methylene ether linkages, *ortho* reactive groups, and *para* reactive groups for resole resin syntheses. Other useful information deduced from FTIR are the type of hydrogen bonding, i.e. intra- vs. inter-molecular, the amount of free phenol present in the product, and the formaldehyde/phenol molar ratio. FTIR bands and patterns for various mono-, di-, and tri-substituted phenols have been identified using a series of model compounds.

The kinetics of resole cure reactions via FTIR indicates that a diffusion mechanism dominates below 140°C. The cure above 140°C exhibits a homogeneous first order reaction rate. The activation energy of the cure reaction was ~ 49.6 KJ/mol.[67]

---

[77] W. W. Focke, M. S. Smit, A. T. Tolmay, L. S. Vandervalt, and W. L. Vanwyk, "Differential Scanning Calorimetry Analysis of Thermoset Cure Kinetics- Phenolic Resol Resin," *Polymer Engineering and Science* **31**(23), 1665-1669 (1991).

[78] M. G. Kim, W. L. S. Nieh, and R. M. Meacham, "Study of the Curing of Phenol-Formaldehyde Resol Resins by Dynamic Mechanical Analysis," *Industrial & Engineering Chemistry Research* **30**(4), 798-803 (1991).

[79] R. A. Follensbee, J. A. Koutsky, A.W. Christiansen, G.E. Myers, and R. L. Geimer, "Development of Dynamic Mechanical Methods to Characterize the Cure State of Phenolic Resole Resins," *Journal of Applied Polymer Science* **47**(8), 1481-1496 (1993).

[80] M. J. Carrott and G. Davidson, "Separation of Characterization of Phenol-Formaldehyde (Resole) Prepolymers using Packed-Column Supercritical Fluid Chromatography with APCI Mass Spectrometric Detection," *Analyst* **124**(7), 993-997 (1999).

^{13}C NMR has proven to be an extremely powerful technique for both monitoring the phenolic resin synthesis and determining the product compositions and structures. Insoluble resole networks can be examined using solid state ^{13}C NMR which characterizes substitutions on *ortho* and *para* positions, the formation and disappearance of hydroxymethyl groups, and the formation of *para-para* methylene linkages. Analyses using ^{13}C NMR have shown good agreement with those obtained from FTIR.[65]

Table 2. 7. FTIR absorption band assignment of resole resins[66]

Wave No. (cm^{-1})	Assignment*	Nature
3350	v(CH)	Phenolic and methylol
3060	v (CH)	Aromatic
3020	v (CH)	Aromatic
2930	v_{ip}(CH2)	Aliphatic
2860	v_{op} (CH2)	Aliphatic
1610	v (C=C)	Benzene ring
1500	v (C=C)	Benzene ring
1470	d(CH2)	Aliphatic
1450	v (C=C)	Benzene ring
1370	d_{ip} (OH)	Phenolic
1240	v_{ip} (C-O)	Phenolic
1160	d_{ip} (CH)	Aromatic
1100	d_{ip} (CH)	Aromatic
1010	v (C-O)	Methylol
880	d_{op} (CH)	Isolated H
820	d_{op} (CH)	Adjacent 2H, *para* substituted
790	d_{op} (CH)	Adjacent 3H
760	d_{op} (CH)	Adjacent 4H, *ortho* substituted
690	d_{op} (CH)	Adjacent 5H, phenol

*v=stretching, d=deformation, ip=in plane, op=out of plane

Various ionization methods were used to bombard phenol/formaldehyde oligomers in mass spectroscopic analysis. The molecular weights of resole resins were

calculated using field desorption mass spectroscopy of acetyl-derivatized samples.[75] Peracetylation was used to enable quantitative characterization of all molecular fractions by increasing the molecular weight in increments of 42.

Dynamic DSC scans of resole resins show two distinguishable reaction peaks, which correspond to formaldehyde addition and formation of ether and methylene bridges characterized by different activation energies. Kinetic parameters calculated using a regression analysis show good agreement with experimental values.[76]

DMA was used to determine the cure times and the onset of vitrification in resole cure reactions.[78] The time at which two tangents to the storage modulus curve intersect (near the final storage modulus plateau) was suggested to correspond to the cure times. In addition, the time to reach the peak of the tan delta curve was suggested to correspond to the vitrification point. As expected, higher cure temperatures reduced the cure times. DMA was also used to measure the degree of cure achieved by resole resins subsequent to their exposure to combinations of reaction time, temperature and humidity.[78] The ultimate moduli increased with longer reaction times and lower initial moisture contents. The area under the tan delta curve during isothermal experiments was suggested to be inversely proportional to the degree of cure developed in samples prior to the measurement.

A NaOH catalyzed resole resin, acetylated or treated with an ion exchange resin (neutralized and free of sodium), was analyzed using GPC in THF solvent. [81] The molecular weight of the ion exchange treated resin, calculated by GPC using polystyrene standards, was significantly lower than that estimated for the acetylated resin. The molecular weight for the ion exchange treated resin calculated by ^{1}H NMR and VPO agreed with the results from GPC. The higher molecular weight observed for the acetylated resin was attributed to higher hydrodynamic volume and/or intermolecular association in acetylated samples.

[81] Y. Yazaki, P. J. Collins, M. J. Reilly, S. D. Terrill and T. Nikpour, "Fast-Curing Phenol-Formaldehyde (PF) Resins," *Holzforschung* **48**(1), 41-48 (1994).

2.4.4. Resole network properties

Voids in resole networks detract from the mechanical properties. Irrespective of the curing conditions, all resole networks contain a significant amount of voids due to volatiles released during the cure reactions. The catalyst concentration in resole crosslinking reactions can lead to different pore microstructures, which influence the mechanical properties.[82] Resole networks cured using *p*-toluenesulfonic acid between 40 and 80°C showed that increased catalyst concentrations led to reduced average void diameters. Higher cure temperatures also resulted in reduced void diameters although the effect was not as substantial. The same study showed that while the catalyst concentration did not affect the network T_gs, higher cure and post-cure temperatures increased T_gs and reduced fracture strains.

In another exemplary study, optical microscopy revealed that the void content of resole networks ranged from 0.13 to 0.21.[83] Resole networks prepared from different F/P molar ratios showed comparable void distributions. A bimodal distribution was observed for all networks, which was attributed to thermodynamic phase separations of reaction volatile (free phenol, formaldehyde and water) and reaction kinetics.

The glass transition temperatures were determined from the peaks of tan delta curves measured using dynamic mechanical analysis for a series of resole networks (prepared with F/P molar ratios ranging from 1 to 2.5).[83] Networks obtained from resoles with high F/P molar ratios (>1.2) had fairly consistent T_gs (between 240 and 260°C). The lowest T_g (190°C) was observed for networks prepared with low hydroxymethyl substituted resoles (F/P=1) and this was attributed to the low network crosslink densities at this ratio. The highest T_g occurred at F/P=1.2 (~280°C), but it superimposed the degradation temperatures. The width of the tan delta curves was used to assess the

---

[82] J. Wolfrum and G. W. Ehrenstein, "Interdependence Between the Curing, Structure, and the Mechanical Properties of Phenolic Resins," *Journal of Applied Polymer Science* **74**, 3173-3185 (1999).

[83] L. B. Manfredi, O. de la Osa, N. Galego Fernandez, and A. Vazquez, "Structure-Properties Relationship for Resoles with Different Formaldehyde/Phenol Molar Ratio," *Polymer* **40**, 3867-3875 (1999).

distributions of chain length as well as the crosslink densities. Networks cured with resole (F/P=1.3 and 1.4) exhibited the highest T_gs and therefore the highest crosslink densities.

2.4.5. Modified phenol-formaldehyde resins

Phenol, formaldehyde and urea have been copolymerized to achieve resins and subsequent networks with improved flame retardance and lower cost relative to phenol/formaldehyde analogues. The condensation of a phenolic methylol group with urea (Figure 2. 31) is believed to be the primary reaction under the weakly acidic conditions normally used.

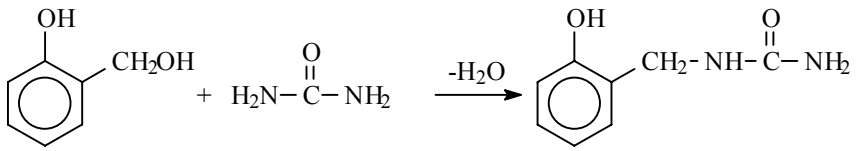

Figure 2. 31. Reaction of hydroxymethylphenol and urea

Resins were prepared by co-condensing low molecular weight hydroxymethyl substituted resoles with urea. The rate of the urea-methylol reaction was greatly enhanced by increased acidity in the reaction medium.[84] *Para*-methylol groups reacted faster than *ortho* methylol groups. The extent of urea incorporation depended on the F/P ratio and the resole/urea composition. Increased urea incorporation ensued at higher urea concentrations and/or in the presence of highly hydroxymethylated resole resins (prepared from larger F/P ratios). Since reactions were conducted under acidic conditions, the condensation of methylol and urea competes with methylol self condensation. Increased urea concentrations suppress the self-condensation reactions.

[84] B. Tomita and C. Hse, "Synthesis and Structual Analysis of Cocondensed Resins from Urea and Methylolphenols," *Mokuzai Gakkaishi* **39**(11), 1276-1284 (1993).

The curing process of tri-hydroxymethylphenol reacted with urea was monitored using torsional braid analysis.[85] Curing proceeded in two stages where the first stage occurred at lower temperatures and was attributed to the reaction of *para*-hydroxymethyl and urea groups. The second stage was due to the higher temperature reaction of *ortho*-hydroxymethyl and urea groups.

Condensation reactions of hydroxymethyl groups on phenolic resoles and amines on melamine take place between pHs 5 and 6 (Figure 2. 32). Only self-condensations of hydroxymethyl substituents occur under strongly acidic or basic conditions.

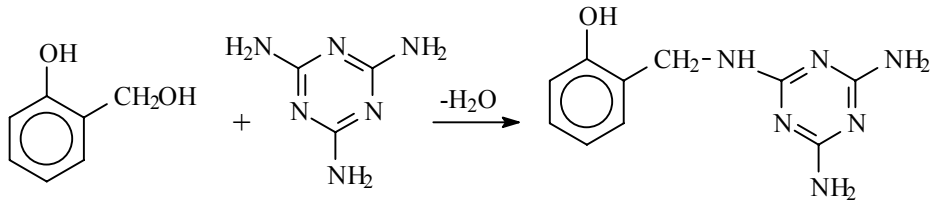

Figure 2. 32. Reaction of hydroxymethylphenol and melamine

2.5. Epoxy/phenol networks

Void free phenolic networks can be prepared by crosslinking novolacs with epoxies instead of HMTA. A variety of difunctional and multifunctional epoxy reagents can be used to generate networks with excellent dielectric properties.[4] One example of epoxy reagents used in this manner is the epoxidized novolac (Figure 2. 33) derived from the reaction of novolac oligomers with an excess of epichlorohydrin.

[85] B. Tomita, M. Ohyama, A. Itoh, K. Doi, and C. Hse "Analysis of Curing Process and Thermal Properties of Phenol-Urea-Formaldehyde Cocondensation Resins," *Mokuzai Gakkaishi* **40**(2), 170-175 (1994).

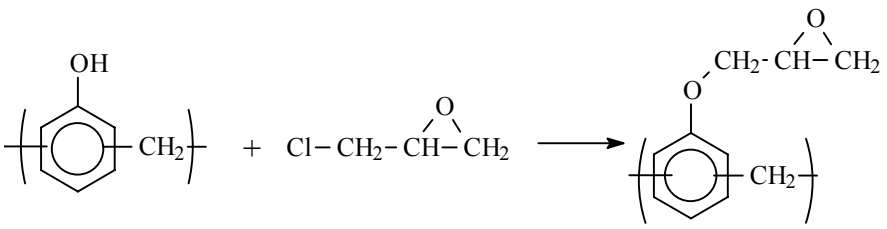

Figure 2. 33. Reaction of phenol and epichlorohydrin to form epoxidized novolacs

2.5.1. Mechanism of the epoxy/phenolic reaction

The reactions between phenolic hydroxyl groups and epoxides have been catalyzed by a variety of acid and base catalysts, group 5a compounds, and quaternary ammonium complexes,[86] although they are typically catalyzed by tertiary amines or phosphines, with triphenylphosphine being the most commonly used reagent. The reaction mechanism (Figure 2. 34) involves triphenylphosphine attacking an epoxide which results in ring opening and produces a zwitterion. Rapid proton transfer occurs from the phenolic hydroxyl group to the zwitterions to form phenoxide anions and secondary alcohols. The phenoxide anion subsequently reacts with either an electrophilic carbon next to the phosphorus regenerating the triphenylphosphine (Figure 2. 34 A)[87] or it can ring open an epoxy followed by proton transfer from another phenol to regenerate the phenoxide anion (Figure 2. 34 B). The phenolate anion is the reactive species for the crosslinking reaction.

---

[86] R. W. Biernath and D. S. Soane in J. S. Salamone and J. S. Riffle, Ed., "Cure Kinetics of Epoxy Cresol Novolac Encapsulant for Microelectronic Packaging," *Contemporary Topic in Polymer Science, Advances in New Material,* Plenum Press, New York, Vol. 7, 1992, pp. 103-160.

[87] W. A. Romanchick, J. E. Sohn, and J. F. Geibel in R. S. Bauer, ed., "Synthesis, Morphology, and Thermal Stability of Elastomer-Modified Epoxy Resin," *ACS Symposium Series 221 - Epoxy Resin Chemistry II*, American Chemical Society: Washington D.C. 1982, pp. 85-118.

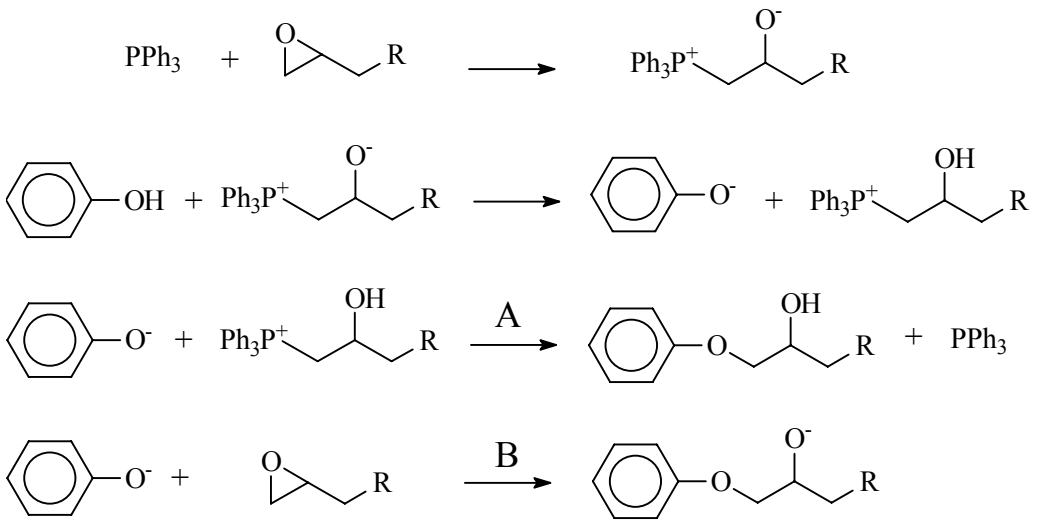

Figure 2. 34. Mechanism for the triphenylphosphine catalyzed phenol/epoxy reaction

Melt reaction mechanisms of tertiary aliphatic amine catalyzed phenolic/epoxy reactions was proposed to begin with a trialkylamine abstracting a phenolic hydroxyl proton to form an ion pair (Figure 2. 35).[88] The ion pair was suggested to complex with an epoxy ring which then dissociates to form a β-hydroxyether and regenerate the trialkylamine.

[88] D. Gagnebien, P. J. Madec, and E. Marechal, "Synthesis of Poly(Sulphone-b Siloxane)s 1- Model Study of the Epoxy-Phenol Reaction in the Melt," *European Polymer Journal* **21**(3), 273-283 (1985).

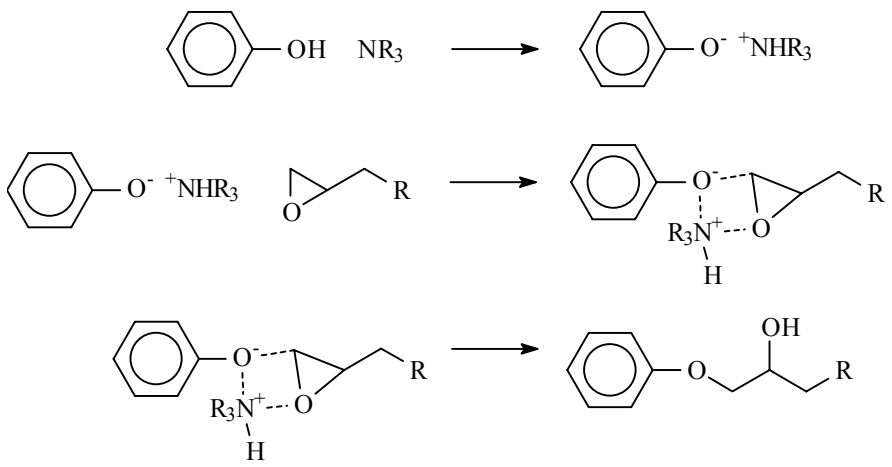

Figure 2. 35. Proposed mechanism for tertiary amine catalyzed phenol/epoxy reaction

Side reactions involving branching through a secondary hydroxyl group can also occur. The extent of these side reactions should decrease as the ratio of epoxy to phenol decreases since phenolate anions are significantly more nucleophilic than aliphatic hydroxyl groups.

2.5.2. Epoxy phenolic reaction kinetics

A review on epoxy/novolac reaction mechanisms and kinetics is provided by Soane.[86] Depending on the structures of novolac and epoxies, reactions may proceed through an *n*th order mechanism or an autocatalytic mechanism.[89] First order reaction kinetics where epoxy ring opening dictates the reaction rate has been found to fit well for a number of novolac/epoxy reactions. Reactions are autocatalytic if more catalyst is produced and the rate accelerates as the reaction proceeds. Autocatalytic kinetics appears to fit well if an active catalytic complex, C, must form initially to generate reaction products.

Soane concluded that phenolic novolac and epoxidized cresol novolac cure reactions using triphenylphosphine as catalyst showed a short initiation regime wherein

[89] W. G. Kim, J. Y. Lee and K. Y. Park, "Curing Reaction of o-Cresol Novolac Epoxy Resin According to Hardener Change," *Journal of Polymer Science, Part A: Polymer Chemistry* **31**, 633-639 (1993).

the concentration of phenolate ion increased followed by a (steady-state) propagation regime where the number of reactive phenolate species was constant.[86] The epoxy ring opening reaction was reportedly first-order in the "steady-state" regime.

$$\frac{d\alpha}{dt} = k_1 (\alpha_{max} - \alpha) \qquad \textbf{(2. 6)}$$

where α is the fraction of epoxy reacted, α_{max} is the maximum fraction of epoxy reacted at the given stoichiometry and temperature, and k_1 is the first order kinetic rate constant.

The isothermal reaction rate for autocatalytic cure kinetics is calculated using

$$\frac{d\alpha}{dt} = k'\alpha^m (1-\alpha)^n \qquad \textbf{(2. 7)}$$

where k' is the kinetic rate constant, and m and n are the reaction orders.

To describe the reaction rate where the initial rate is not zero, the following modification was made[90]

$$\frac{d\alpha}{dt} = (k_1 + k_2\alpha^m)(1-\alpha)^n \qquad \textbf{(2. 8)}$$

where k_1 and k_2 are kinetic rate constants.

The mechanism for the tertiary amine catalyzed reaction between phenol and epoxy was proposed by Sorokin and Shode[91]

$$\begin{aligned} &E + P + B \xrightarrow{k_1} I \\ &E + P + I \xrightarrow{k_2} Pr + I \end{aligned} \qquad \textbf{(2. 9)}$$

---

[90] M. R. Kamal, "Thermoset Characterization for Moldability Analysis," *Polymeric Engineering Sci*ence **14**(3), 231-239 (1974).

[91] M. F. Sorokin and L. G. Shode, "Reactions of □-Oxides with Proton Donor Compounds in the Presence of Tertiary Amines. 1. Reaction of Phenyl Glycidyl Ether with Phenol in the Presence of Teritary Amines" *Zhurnal Organicheskoi Khimii* **2**(8), 1463-1468 (1966).

where E represents epoxy groups, P the phenol, B the basic catalyst, I an intermediate complex, PR the product of the phenol and epoxide reaction, and k_1 and k_2 the kinetic constants. This mechanism suggests that the isothermal reaction rate is directly proportional to catalyst concentration. Thus, the catalyst concentration may be introduced into the rate expression.

A diffusion effect was incorporated into equation 7 to improve the conversion vs. time prediction fit above 90 % conversion.[92] The diffusion factor $f(\alpha)$ is based on free volume principles.[93]

$$\frac{d\alpha}{dt} = (k_1' + k_2'\alpha^m)(1-\alpha)^n [B] f(\alpha) \qquad \textbf{(2. 10)}$$

$$f(\alpha) = \frac{1}{1+\exp[C(\alpha-\alpha_c)]} \qquad \textbf{(2. 11)}$$

where C is the material constant, α_c is the critical conversion, and k_1' and k_2' are "normalized" kinetic rate constants. For $\alpha << \alpha_c$, in which the rate of diffusion is not reaction rate limiting, $f(\alpha)$ is essentially equal to unity. As α approaches α_c, the diffusion factor decreases. The measured reaction conversion for triphenylphosphine catalyzed biphenyl epoxy/phenol novolac cure plotted vs. reaction time fits extremely well the conversion values calculated via the above expression for all catalyst concentrations over the conversion range.

Ortho-cresol novolac epoxy oligomers were cured with a phenolic novolac or a phenolic novolac acetate resin catalyzed by 2-methylimidzole.[94] While the phenolic

---

[92] S. Han, H. G. Yoon, K. S. Suh, W. G. Kim and T. J. Moon, "Curing Kinetics of Biphenyl Epoxy-Phenol Novolac Resin System Using Triphenylphosphine as Catalyst," *Journal Polymeric Science, Part A: Polymeric Chemistry* **37**, 713-720 (1999).

[93] C. S. Chern and G.W. Poehlein, "A Kinetic Model for Curing Reaction of Epoxides with Amines," *Polymer Engineering & Science* **27**(11), 788-795 (1987).

[94] X. W. Luo, Z. H. Ping, J. P. Ding, Y. D. Ding, and S. J. Li, "Mechanism Studies on Water Sorption and Permeation in Epoxy Resin by Impedance Spectroscopy. II. Cure

novolac acetate system clearly followed nth order kinetics by showing a linear plot of log(dα/dt) vs. log(1-α), the phenolic novolac cured system was better fitted with autocatalytic reaction kinetics.

2.5.3. Epoxy/phenol network properties

Void-free phenolic/epoxy networks prepared from an excess of phenolic novolac resins to various diepoxides have been investigated by Riffle et al. (Figure 2. 36).[95,96] The novolacs and diepoxide were cured at approximately 200°C in the presence of triphenylphosphine and other phosphine derivatives. Network densities were controlled by stoichiometric offsets between phenol and epoxide groups. These networks contained high phenolic concentrations (up to ~80 wt %) to retain the high flame retardance of the phenolic materials while the mechanical properties were tailored by controlling the crosslink densities and molecular structures.

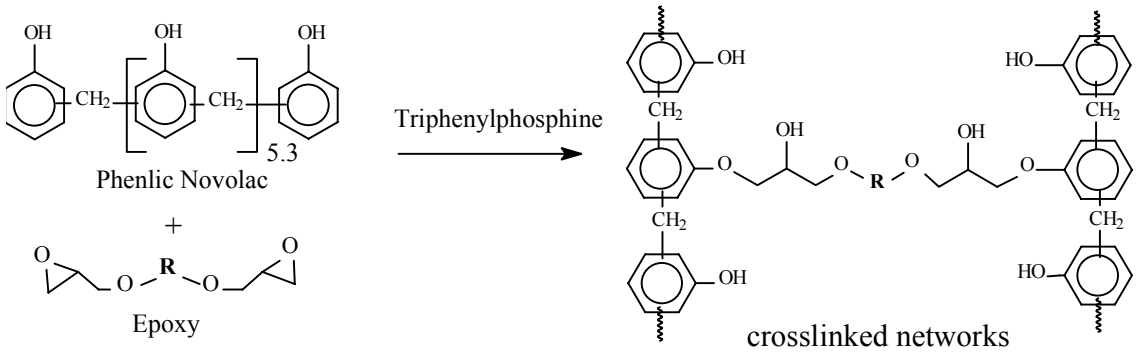

Figure 2. 36. Network formation of phenolic novolac and epoxy

---

Kinetics of o-Cresol Novolac Resin with Esterified Phenol Novolac Resin," *Pure Applied Chemistry* **A34**(11), 2279-2291 (1997).

[95] C. S. Tyberg, M. Sankarapandian, K. Bears, P. Shih, A. C. Loos, D. Dillard, J. E. McGrath, and J. S. Riffle, "Tough, Void-Free, Flame Retardant Phenolic Matrix Materials," *Construction and Building Materials* **13**, 343-353 (1999).

[96] C. S. Tyberg, K. Bergeron, M. Sankarapandian, P. Shih, A. C. Loos, D. A. Dillard, J. E. McGrath, and J. S. Riffle, "Structure Property Relationships of Void Free Phenolic Epoxy Matrix Materials," *Polymer* **41**(13), 5053-5062 (2000).

Several diepoxides were utilized to determine structure property relationships of the networks and flame properties (Figure 2. 37).

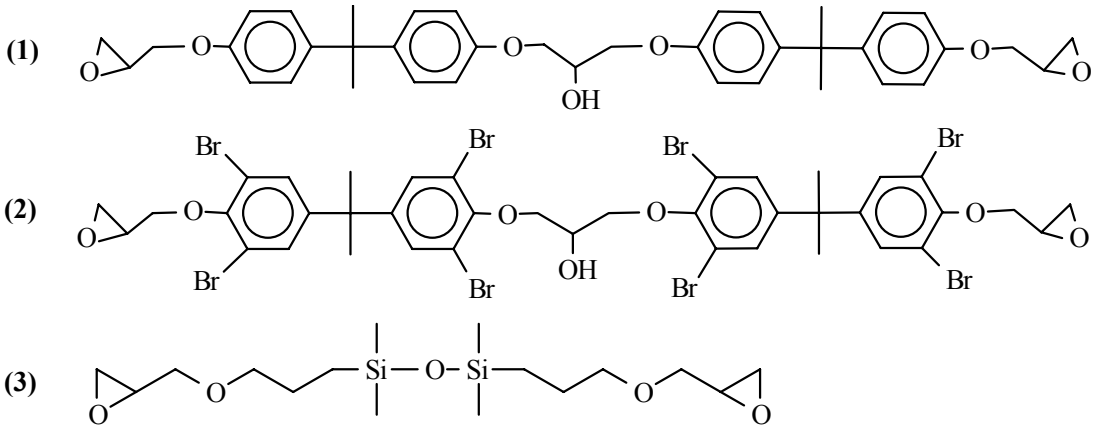

Figure 2. 37. Diepoxide structures: (1) bisphenol-A based diepoxide, (2) brominated bisphenol-A based diepoxide, and (3) siloxane diepoxide

Network structure property relationships and flame properties were determined for a novolac cured with various diepoxides at defined compositions. The fracture toughness of the networks, determined by the plane-strain stress intensity factors (K_{IC}), increased with increased stoichiometric offset to a maximum of approximately 1.0 MPa*$m^{1/2}$ for the 5 phenol/1 epoxy equivalence ratio (Table 2. 8). All novolac/epoxy networks were significantly tougher than a thermally cured resole network (0.16 MPa*$m^{1/2}$). Further stoichiometric offset (to 7/1) reduced the fracture toughness. This was undoubtedly related to the increase in dangling ends and unconnected phenolic chains at these very high phenol to epoxy ratios. Likewise, as expected, glass transition temperatures of fully cured networks decreased as the distances between crosslinks (M_x) increased. In general, network toughness increased with the average molecular weight between crosslinks up to some point beyond which the amount of unconnected phenolic chains began to detract from properties. Likewise, as expected, glass transition temperatures of fully cured networks decreased as the distances between crosslinks (M_x) increased.

Table 2. 8. T_g and K_{IC} of phenolic novolac/epoxy networks

Epoxy	Phenol/Epoxy (wt/wt)	Phenol/Epoxy (mol:mol)	T_g (C°)	K_{IC} (MPa*$m^{1/2}$)	M_x (g/mol)
Bisphenol-A Epoxy cured with 4,4'-DDS		--	127	0.62	
Phenolic control (thermally cured resole)		--	--	0.16	
Bisphenol-A	80/20	7:1	114	070	4539
	65/35	3:1	127	0.85	1413
	50/50	2:1	151	0.64	643
Brominated Bisphenol-A	65/35	5.8:1	130	0.74	3511
	50/50	3.1:1	148	0.84	1554
Disiloxane epoxy	80/20	7.2:1	96	0.62	4051
	65/35	3:1	87	0.77	1030

The flame retardance was measured using a cone calorimeter with a heat flux of 50 kW/m^2 and 20.95 mol % O_2 content (atmospheric oxygen). All phenolic novolac/epoxy networks with relatively high novolac compositions showed much lower peak heat release rates (PHRR) than a typical amine cured epoxy network (bisphenol-A epoxy stoichiometrically cured with *p,p'*-diaminodiphenylsulfone) (Table 2. 9). Brominated epoxy reagents were also investigated since halogenated materials are well known for their roles in promoting flame retardance. Networks cured with the brominated diepoxide showed the lowest peak heat release rates, but the char yields of these networks were lower and the smoke toxicity (CO yield /CO_2 yield) was increased. Incorporating siloxane moieties into networks reduced the peak heat release rates and smoke toxicities compared to the novolac networks cured with bisphenol-A diepoxides.

Table 2. 9. Flame retardance of networks prepared form a phenolic novolac crosslinked with various epoxies[97]

Epoxy	Phenolic/Epoxy (wt/wt)	PHRR (KW/m^2)	Char yield (%)	Smoke Toxicity* ($x10^{-3}$)
Bisphenol-A Epoxy cured with 4,4'-DDS		1230	5	44
Phenolic control (thermally cured resole)		116	63	
Bisphenol-A	80/20	260	33	27
Bisphenol-A	65/35	360	29	34
Bisphenol-A	50/50	380	23	36
Brominated bisphenol-A	65/35	165	8	189
Brominated bisphenol-A	50/50	158	9	175
Disiloxane epoxy	80/20	226	35	15
Disiloxane epoxy	65/35	325	24	27

*smoke toxicity: CO/CO_2 release

A biphenol diglycidyl ether based epoxy resin was crosslinked with amine curing agents (4,4'-diaminodiphenylmethane and aniline novolac) and phenol curing agents (phenol novolac and catechol novolac), and the thermo-mechanical properties were investigated.[98] Unlike bisphenol-A epoxy based networks, distinct T_gs were not observed with the amine cured biphenol epoxy networks. This was hypothesized to be caused by the mesogenic nature of the biphenol groups which allowed the chains to be more closely packed. Thus, it was reasoned that the mobility did not decrease significantly with the transition into the rubbery region. The presence of a distinct T_g when phenols were used to cure biphenol based diepoxide depended on the phenolic structure. Whereas a distinct T_g was evident in the phenolic novolac cured systems, no definite T_gs were observed when catechol novolac was used. The higher moduli shown by the catechol novolac

[97] Tests were conducted at Naval Surface Warfare Center, Carderock, Maryland.

[98] M. Ochi, N. Tsuyuno, K. Sakaga, Y. Nakanishi, and Y. Murata, "Effect of Network Structure on Thermal and Mechanical Properties of Biphenyl-Type Epoxy Resins Cured with Phenols," *Journal of Applied Polymer Science* **56**, 1161-1167 (1995).

cured networks were attributed to the orientation of mesogenic biphenyl groups which suppressed micro-Brownian chain motions.

Network properties and microscopic structures of various epoxy resins crosslinked by phenolic novolacs were investigated by Suzuki et al.[99] Positron annihilation spectroscopy (PAS) was utilized to characterize intermolecular-spacing of networks and the results were compared to bulk polymer properties. The lifetime (τ_3) and intensity (I_3) of the active species (positronium ions) correspond to volume and number of "holes" which constitute the free volume in the network. Networks cured with flexible epoxies had more "holes" throughout the temperature range, and were more affected by the temperature changes. Glass transition temperatures and thermal expansions (α) were calculated from plots of τ_3 (free volume) versus temperature. The T_gs and thermal expansion efficients obtained from PA were lower than these obtained from thermomechanical analysis. These differences were attributed to the micro-Brownian motions determined by PAS versus large-scale polymer properties determined by thermomechanical analysis. The differences in T_gs and thermal expansion efficients were more pronounced for the more highly crosslinked materials. The rate of moisture absorption is proportional to I_3 of the network, therefore networks with larger free volume absorbed water at a faster rate.

2.6. Benzoxazines

Benzoxazines are heterocyclic compounds obtained from Mannich reactions of phenols, primary amines, and formaldehyde (Figure 2. 38).[100,101] As described previously,

---

[99] T. Suzuki, Y. Oki, M. Numajiri, T. Miura, K. Kondo, Y. Shiomi, and Y. Ito, "Novolac Epoxy Resins and Positron Annihilation," *Journal of Applied Polymer Science* **49**, 1921-1929 (1993).

[100] W. J. Burke, E. L. M. Glennie, and C. Weatherbee, "Condensation of Halophenols with Formaldehyde and Primary Amines," *Journal Organic Chemistry* **29**, 909 (1964).

[101] X. Ning and H. Ishida, "Phenolic Materials via Ring-Opening Polymerization: Synthesis and Characterization of Bisphenol-A Based Benzoxazines and Their

they are key reaction intermediates in the hexamethylenetetramine (HMTA) novolac cure reaction.[41,44] Crosslinking benzoxazines at high temperatures give rise to void free networks with high T_gs, excellent heat resistance, good flame retardance, and low smoke toxicity.[102] As in HMTA cured novolac networks, further structural rearrangement may occur at higher temperatures.

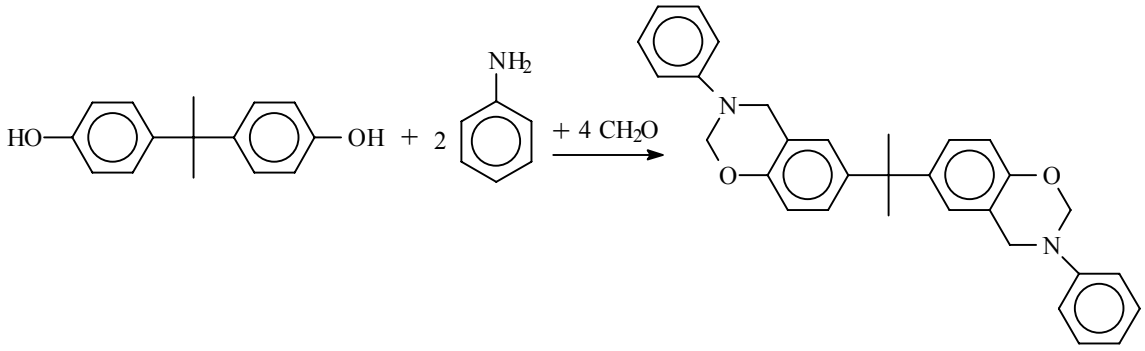

Figure 2. 38. Synthesis of bisphenol-A based benzoxazines

A difunctional bisphenol-A epoxy based benzoxazine has been synthesized and characterized by GPC and ^{1}H NMR.[101] A small of amount of dimers and oligomers also formed. Thermal crosslinking of bisphenol-A benzoxazine containing dimers and oligomers resulted in networks with relatively high T_gs. Dynamic mechanical analysis of the network showed a peak of tan delta at approximately 185°C.

The kinetics of bisphenol-A benzoxazine crosslinking reactions was studied using differential scanning calorimetry.[102] The activation energy, estimated from plots of conversion as a function of time for different isothermal cure temperatures, was between 102 and 116 KJ/mol. Phenolic compounds with free *ortho* positions were suggested to initiate the benzoxazine reaction (Figure 2. 39).[103] Fast reactions between benzoxazines

---

Polymers," *Journal of Polymer Science. Part A: Polymer Chemistry* **32**, 1121-1129 (1994).

[102] H. Ishida and Y. Rodriguez, "Cure Kinetics of a New Benzoxazine-Based Phenolic Resin by Differential Scanning Calorimetry," *Polymer* **36**(16), 3151-3158 (1995).

[103] G. Riess, J. M. Schwob, G. Guth, M. Roche, and B. Lande in B. M. Culbertson and J. E. McGrath, eds, "Ring Opening Polymerization of Benzoxazines-A New Route to

and free *ortho* phenolic positions, which formed hydroxybenzylamines, were facilitated by hydrogen bonding between the phenol hydroxyl and benzoxazine oxygen (as shown in Figure 2. 18). Subsequent thermal decompositions of these less stable hydroxybenzylamines lead to more rapid thermal crosslinking (as described for the HMTA/novolac cure).

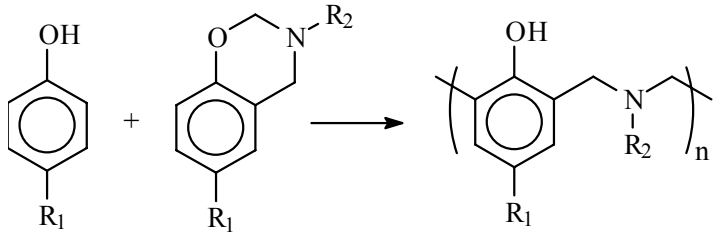

Figure 2. 39. Reaction of benzoxazines with free *ortho* positions on phenolic compounds

The reaction of bisphenol-A benzoxazine under strong and weak acidic conditions was also investigated.[104] The proposed mechanism for the benzoxazine ring opening reaction in the presence of a weak acid involves an initial tautomerization between the benzoxazine ring and chain forms. Electrophilic aromatic substitution reaction between a phenolic ring position and the chain tautomer, an iminium ion was suggested to follow. Strongly acidic conditions, high temperatures and the presence of water lead to various side reactions, including benzoxazine hydrolysis in a reverse Mannich reaction. Side reactions could also terminate reaction or lead to crosslinking.

The oxazine ring in benzoxazine assumes a distorted semi-chair conformation.[105] The ring strain and the strong basicity of the nitrogen and oxygen allow benzoxazines to

---

Phenolic Resins," in *Advances in Polymer Synthsis*,. Plenum Press, New York, 1985, pp 27-50.

[104] J. Dunkers and H. Ishida, "Reaction of Benzoxazine-Based Phenolic Resins with Strong and Weak Carboxylic Acids and Phenol as Catalysts," *Journal of Polymer Science. Part A: Polymer Chemistry* **37**(13), 1913-1921 (1999).

[105] H. Ishida and D. J. Allen, "Physical and Mechanical Characterization of Near Zero Shrinkage Polybenzoxazines," *Journal Polymer Science. Polymer Physical Ed*. **34**(6), 1019-1031 (1996).

undergo cationic ring opening reactions. A number of catalysts and/or initiators such as PCl_5, PCl_3, $POCl_3$, $TiCl_4$, $AlCl_3$ and MeOTf are effective in promoting benzoxazine polymerization at moderate temperatures (20-50°C).[106] Dynamic DSC studies revealed multiple exotherms in polymerization of benzoxazine, indicating a complex reaction mechanism.

2.7. Phenolic triazine (PT) resins

Novolac hydroxyl groups reacted with cyanogen bromide under basic conditions to produce cyanate ester resins (Figure 2. 40).[107,108] Cyanate esters can thermally crosslink to form void free networks, wherein at least some triazine rings form. The resultant networks possess high T_gs, high char yield at 900°C and high decomposition temperatures.[107]

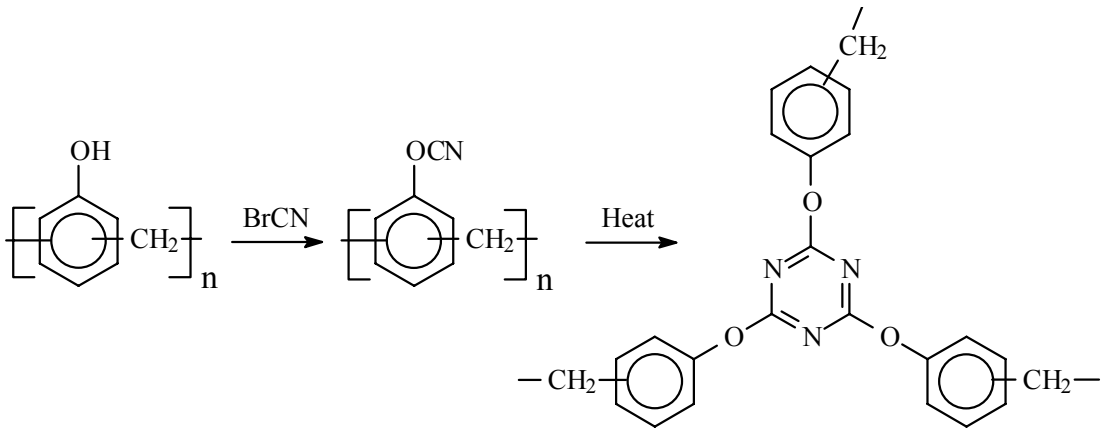

Figure 2. 40. Synthesis of phenolic triazine resins

---

[106] Y. X. Wang and H. Ishida, "Cationic Ring-Opening Polymerization of Benzoxazines," *Polymer* **40**(16), 4563-4570 (1999).

[107] U.S. Pat. 4,831,086 (May 16, 1989), S. Das and D. C. Prevorsek, "Cyanate group containing phenolic resins, phenolic triazines derived therefrom" (to Allied-Signal, Inc.).

[108] S. Das, "Phenolic-Triazine (PT) Resin-A New Family of High Performance Thermosets," *Abstracts of papers of the American Chemical Society-PMSE* **203**, 259 (1992).

Novolac resins containing cardanol moieties have also been converted to cyanate ester resins.[109] The thermal stability and char yield, however, was reduced when cardanol was incorporated into the networks.

2.8. Thermal and thermo-oxidative degradation

Phenolic networks are well known for their excellent thermal and thermo-oxidative stabilities. The mechanisms for high temperature phenolic degradation include dehydration, thermal crosslinking, and oxidation which eventually lead to char.

Thermal degradation below 300°C in inert atmospheres produces only small amounts of gaseous products. These are mostly unreacted monomers or water, which are by-products eliminated from condensation reactions between hydroxymethyl groups and reactive *ortho* or *para* positions on phenolic rings. A small amount of oxidation may occur in air as some carbonyl peaks have been observed using ^{13}C NMR.[110]

Degradation in inert atmospheres between 300 and 600°C results in porous materials. Little shrinkage has been observed in this temperature range. Water, carbon monoxide, carbon dioxide, formaldehyde, methane, phenol, cresols and xylenols are released. According to various thermogravimetric analyses, the weight loss rate reaches a maximum during this temperature range. The elimination of water at this stage may also be caused by the phenolic hydroxyl condensations which give rise to biphenyl ether linkages (Figure 2. 41).

---

[109] C. P. R. Nair, R. L. Bindu, and V. C. Joseph, "Cyanate Esters Based on Cardanol Modified-Phenol-Formaldehyde Resins-Synthesis and Thermal Characterizations," *Journal of Polymer Science. Part. A. Polymer Chemistry* **33**(4), 621-627 (1995).

[110] C. A. Fyfe, M. S. McKinnon, A. Rudin, and W. J. Tchir, "Investigation of the Mechanisms of the Thermal Decomposition of Cured Phenolic Resins by High Resolution ^{13}C CP/MAS Solid-State NMR Spectroscopy," *Macromolecules* **16**, 1216-1219 (1983).

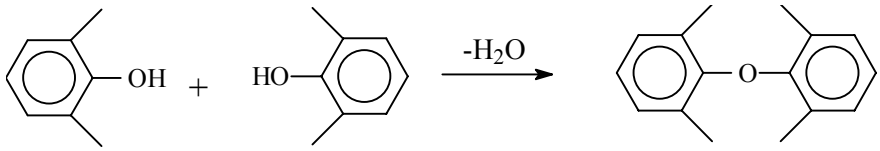

Figure 2. 41. Dehydration of hydroxyl groups

Morterra and Low[111,112] proposed that thermal crosslinking may occur between 300°C and 500°C where phenolic hydroxyl groups react with methylene linkages to eliminate water (Figure 2. 42). Evidence for this mechanism is provided by IR spectra which show decreased OH stretches and bending absorptions as well as increased complexity of the aliphatic CH stretch patterns in this temperature range.

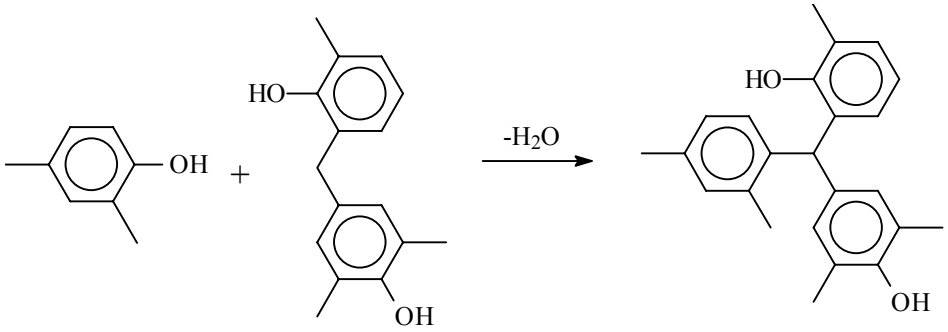

Figure 2. 42. Thermal crosslinking of phenolic hydroxyl and methylene linkages

At elevated temperatures, methylene carbons cleave from aromatic rings to form radicals (Figure 2. 43). Further fragmentation decomposes xylenol to cresols and methane (Figure 2. 43A). Alternatively, auto-oxidation occurs (Figure 2. 43B). Aldehydes and ketones are intermediates before decarboxylation or decarbonylation takes place to generate cresols and carbon dioxide. These oxidative reactions are possible even in inert atmospheres due to the presence of hydroxyl radicals and water.[7]

---

[111] C. Morterra and M. I. D. Low, "IR Studied of Carbons-VII. The Pyrolysis of a Phenol-Formaldehyde Resin," *Carbon* **23**(5), 525-530 (1985).

[112] C. Morterra and M. I. D. Low, "Infrared Studies of Carbon. 8. The Oxidation of Phenol-Formaldehyde Chars," *Langmuir* **1**, 320-326 (1985).

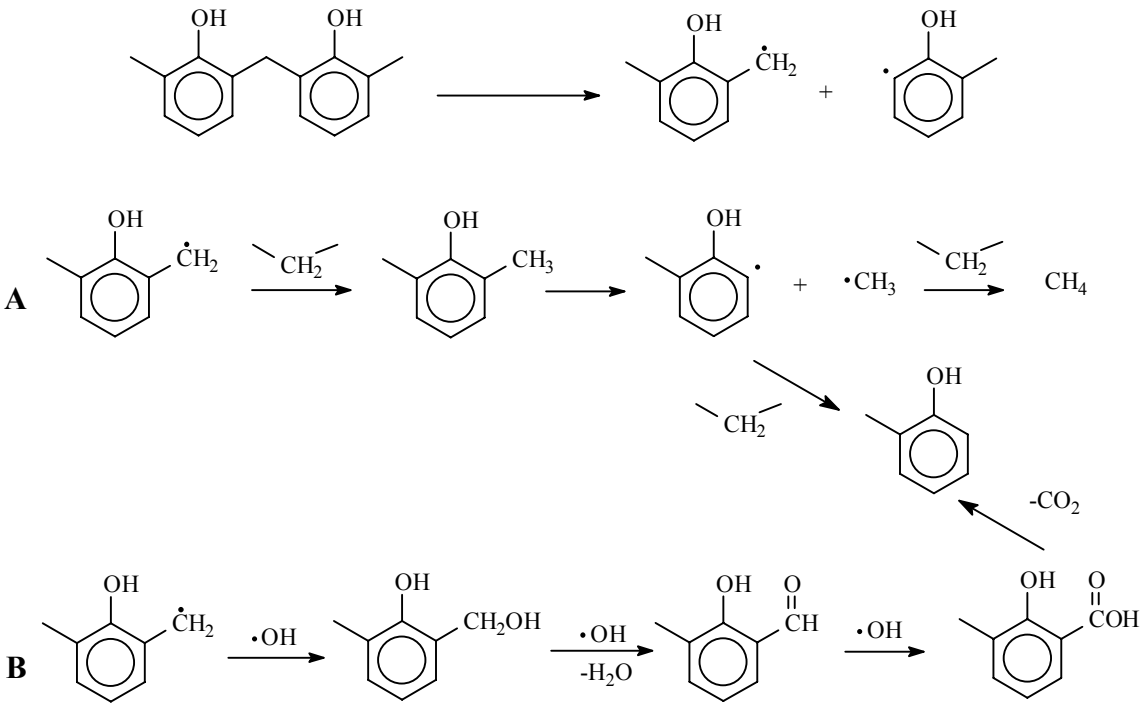

Figure 2. 43. Thermal bond rupture: a) fragmentation reaction b) oxidation degradation

Oxidative degradation begins at lower temperatures in air (<300 °C) and oxidation occurs most readily on benzylic methylene carbons since they are the most vulnerable sites. This leads to dihydroxybenzohydrole and dihydroxybenzophenone derivatives (Figure 2. 44). Dihydroxybenzophenone may cleave and further oxidize to carboxylic acid before decomposing to form cresols, xylenols, CO and CO_2.

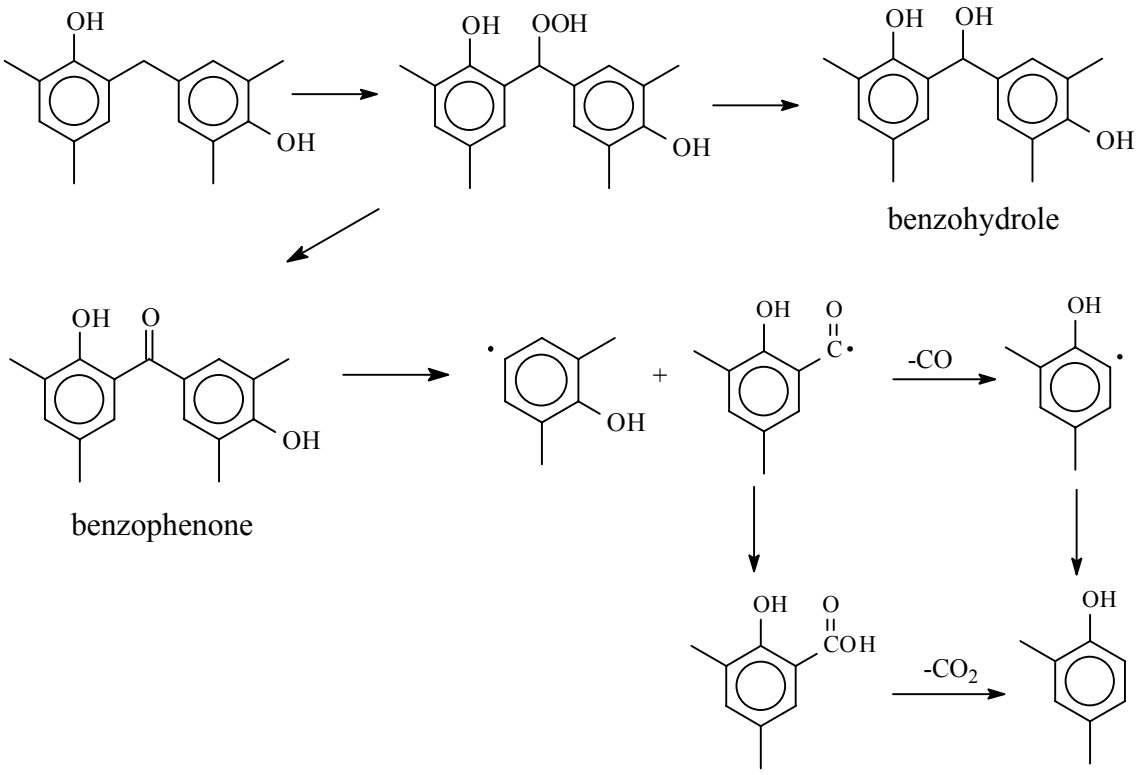

Figure 2. 44. Oxidation degradation on methylene carbon

Hydroxyl elimination is necessary for the formation of benzaldehyde and benzoic acid derivatives, and ultimately, benzene and toluene (Figure 2. 45).[4] It is proposed that a cleavage between the hydroxyl group and aromatic ring leads to benzonoid species which undergo further cleavage coupled with oxidation to give various decomposition products.

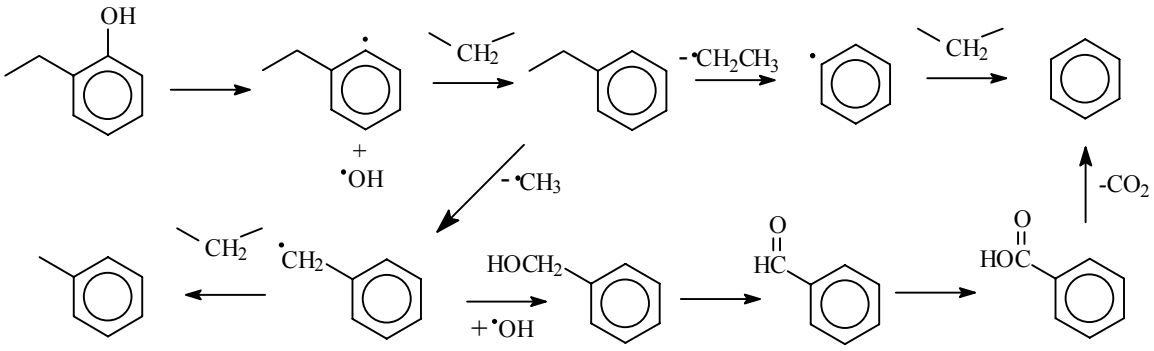

Figure 2. 45. Formation of benzenoid species

Oxidative branching and crosslinking are prevalent degradation pathways in air (Figure 2. 46). Phenoxy radicals are formed via hydrogen abstraction. These relatively stable intermediates can couple with each other, and, depending on carbon-carbon or carbon-oxygen coupling, form ether linkages or ketones. Diphenolquinones derived from carbon-carbon dimerization further oxidize.[4]

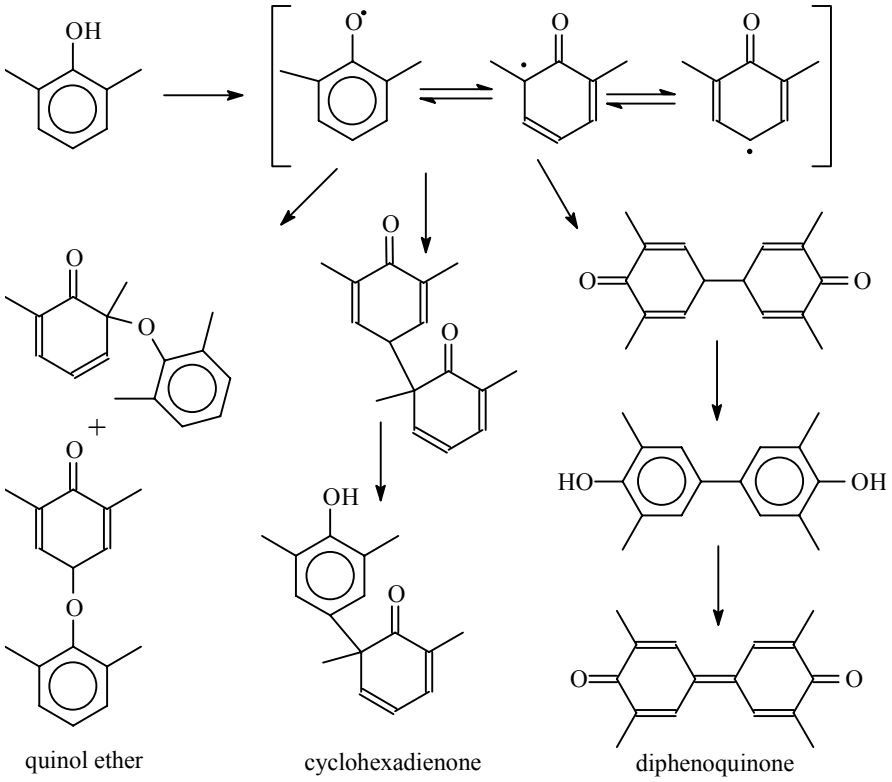

Figure 2. 46. Decomposition via phenoxy radical pathways

Upon further heating above 600°C, the density increases as shrinkage occurs at a high rate. High temperature degradation monitored via gas chromatography indicated that the formation of carbon char parallels carbon monoxide evolution. Along with the same by-products released at lower temperatures, pyrolysis-GC-MS identified the formation of other low volatility compounds including naphthalene, methylnaphthalenes, biphenyl, dibenzofuran, fluorene, phenanthrene, and anthracene. These products may

result from condensation of hydroxyl groups of adjacent *ortho-ortho* linked phenolic rings[113] (Figure 2. 47).

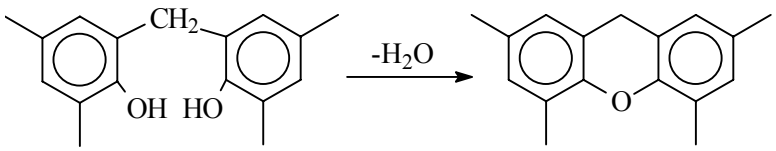

Figure 2. 47. Condensation of *ortho* hydroxyl groups

The reaction sequence for char formation was also proposed to occur through initial formation of quinone type linkages, which lead to polycyclic products[7] (Figure 2. 48). The quinone functionalities were confirmed through IR studies. NMR spectra showed that at 400°C almost all methylene linkages and carbonyl groups shift or disappear. Mostly aromatic species are present. This is consistent with the proposed char forming mechanism but is also compatible with the formation of biphenyls through direct elimination of CO.[110]

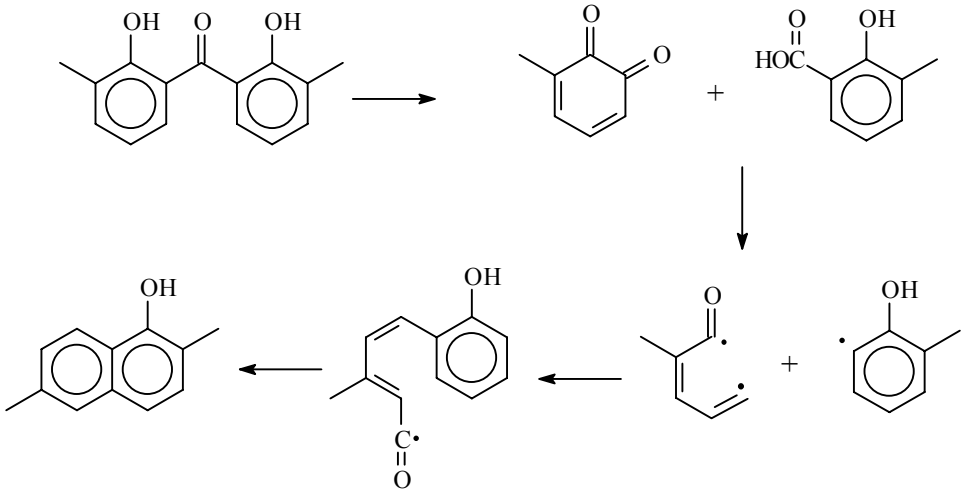

Figure 2. 48. Char formation

[113] J. Hetper and M. Sobera, "Thermal Degradation of Novolac Resins by Pyrolysis-Gas Chromatography with a Movable Reaction Zone," *Journal of Chromatography A* **833**, 277-281 (1999).

Conley showed that the primary degradation route for resole networks is oxidation regardless of the atmosphere.[8] By contrast, Morterra et al. found that auto-oxidation was not the major degradation pathway for novolac resins.[111] The degradation is proposed to occur in two stages depending on the temperature. Fragmentation of the polymer chain, beginning at approximately 350°C, does not affect the polymer integrity. Above 500°C the network collapses as polyaromatic domains form.

Novolac network degradation mechanisms vary from those of resole networks due to differences in crosslinking methods. Nitrogen containing linkages must also be considered when HMTA (or other crosslinking agent) was used to cure novolac networks. For example, tribenzylamines, formed in HMTA cured novolac networks, decompose to cresols and azomethines (Figure 2. 49).

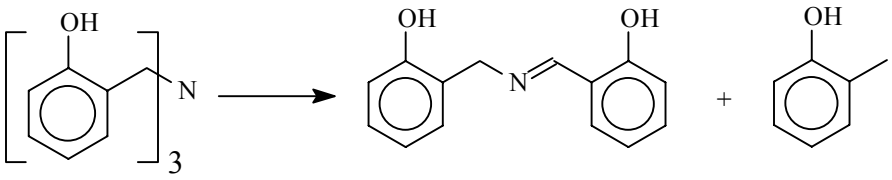

Figure 2. 49. Decomposition of tribenzylamine

Novolacs and networks which had been slowly heated in an inert atmosphere were studied. 1-2 wt. % of water and phenol evolved between 100 and 350°C.[114] Above that temperature, small quantities of CO, CO_2, CH_4, and low molecular weight aromatics evolved leaving behind 75–85% by weight of polymer. The degradation of these pre-exposed networks were then studied at temperatures up to ~700°C in both air and nitrogen. The rate of weight loss in air suggested that degradation under these conditions is a multistage process. Evidence suggested that this multistage thermo-oxidative process was due to two types of linking units present, which pyrolyzed at 375-400°C and 500-550°C respectively. By contrast, the degradation process in nitrogen was a single stage process. Both processes formed a char representing 90-95% by weight of the pre-

[114] V. Jha, A. Banthia, and A. Paul, "Thermal Analysis of Phenolic Resin Based Pyropolymers," *Journal of Thermal Analysis* **35**, 1229-1235 (1989).

exposed materials. As expected, lower weight loss occurred with increased levels of the HMTA crosslinking reagent introduced into the network.

Oxygen indices of a series of phenolic networks, i.e. heat cured resoles, novolacs cured with formaldehyde, trioxane, or terephthaloyl chloride were investigated.[115] It has been previously shown that oxygen indices (OI) correlate linearly with char yields at 800°C in nitrogen except for cases involving gas phase retarders such as halogenated aromatic materials (van Krevelen). *Meta*- and *para*-cresol formaldehyde networks exhibited slightly lower OI values than unsubstituted phenolics, presumably due to the presence of flammable methyl substituents. The halogenated phenolics showed higher OI values but lower char yields since halogenated materials undergo a gas phase retardation of burning and the heavy halogen substituents convert to gaseous products. The crosslinking agent also has an affect on OI. Networks with methylene linkages derived from formaldehyde crosslinking reagents give rise to higher OI values than these with ester linkages derived from terephthaloyl chloride. The formaldehyde cured novolacs also showed higher OI than trioxane cured materials since less stable ether linkages were formed in the trioxane crosslinked systems.

The effects of structures and the levels of crosslink densities on thermal stabilities of novolac resins were investigated.[116] Three types of novolacs were prepared by reacting phenol with formaldehyde, *meta*-cresol with formaldehyde, and *para*-cresol with formaldehyde in formaldehyde/phenol molar ratio of 0.95. Lightly crosslinked networks were obtained when the trifunctional phenol or *meta*-cresol was used. As expected, *para*-cresol novolac was linear. The thermal degradation behaviors for the lightly crosslinked networks, the *para*-cresol novolac as well as typical novolac resins were examined. Under inert atmosphere, TGA results revealed that the crosslinked samples had lower

---

[115] Y. Zaks, J. Lo, D. Raucher, and E.M. Pearce, "Some Structural Property Relationships in Polymer Flammability: Studies of Phenolic-Derived Polymers," *Journal Applied Polymer Science* **27,** 913-930 (1982).

[116] L. Costa, L. Rossi di Montelera, G. Camino, E. D. Weil, and E. M. Pearce, "Structure-Charring Relationship in Phenol-Formaldehyde Type Resins," *Polymer Degradation and Stability* **56**, 27-35 (1997).

decomposition temperatures but the char yields were significantly higher. The greater stabilities exhibited at higher temperatures (500°C+) for the crosslinked materials were attributed to lesser fragmentation, and therefore, lower volatiles. In air, the crosslinked materials were less stable throughout the whole temperature range with complete degradation occurring 50°C below the low molecular weight resins. It was suggested that the crosslinked materials may be less susceptible to oxidation, and therefore, unable to form more thermally stable intermediates. Comparatively, the phenol-formaldehyde resin showed the highest thermal and thermal oxidative stability, followed by the *meta*-cresol-formaldehyde resin. The *para*-cresol-formaldehyde showed the least stability. Since the reactivity of starting phenolic monomer was different, novolac oligomers prepared via the same approach resulted in different structures. The results obtained in this study therefore could not be compared quantitatively.

A low molecular weight *para*-cresol novolac resin (M_n~560) prepared by Belbachir et al.[117] showed high crystalline ratio according to X-ray diffraction. No weight loss was observed below 400°C. However, the morphology changes to a semicrystalline state after repeat thermal heating/cooling cycles.

[117] A. Hamou, C. Devallencourt, F. Burel, J. M. Saiter, and M. Belbachir, "Thermal Stability of a *para*-Cresol Novolac Resin," *Journal of Thermal Analysis* **52**, 697-703 (1998).

3. Controlled Molecular Weight Cresol-Formaldehyde Oligomers

3.1. Introduction

Phenolic resins are among the oldest known and highest volume thermosetting materials produced in the United States.[118] Among the numerous attractive properties of phenolic resins and their networks are low cost and excellent flame retardance.[119,120] Therefore, we and others are investigating this class of materials as possible matrix resins for flame retardant structural composites. The most common phenolic prepolymers are derived from reacting phenol with formaldehyde or with formaldehyde derivatives. This reaction occurs most rapidly under extremely acidic or basic conditions. The pH of the reactions and the stoichiometric ratio of the monomers give rise to two classes of phenolic prepolymers known as novolacs and resoles.

Novolac oligomers are prepared in acidic media using an excess of phenol over formaldehyde. The mechanism associated with this reaction has been described in four steps (Figure 3. 1). First a methylene glycol is protonated by an acid from the reaction medium, which then releases water to form a hydroxymethylene carbonium ion (step 1). This ion acts as a hydroxyalkylating agent by reacting with a phenol via electrophilic aromatic substitution. A pair of electrons from the benzene ring attacks the electrophile forming a carbocation intermediate followed by deprotonation and regain of aromaticity (step 2). The methylol group of the hydroxymethylated phenol is unstable under acidic conditions and loses water readily to form a benzylic carbonium ion (step 3). This ion

---

[118] A. Knopp and L. A. Pilato, Phenolic Resins: Chemistry, Application and Performance-Future Directions; Springer-Verlag, New York, 2000.

[119] F. Y. Hsieh and H. D. Beeson, "Flammability Testing of Flame Retarded Epoxy Composites and Phenolic Composites," *Fire and Materials* **21**, 41-49 (1997).

[120] C. J. Hilado, A M. Machado, and D. P. Brauer, "Effect of Char Yield and Chemical Structure on Toxicity of Pyrolysis Gases," *Proc. West. Pharmacol. Soc.* **22**, 201-4 (1979).

then reacts with another phenol to form a methylene bridge in another electrophilic aromatic substitution. This major process repeats until the formaldehyde is exhausted.[121]

Typically 0.75 to 0.85 moles of formaldehyde are used for each mole of phenol in the synthesis of low molecular weight novolacs,[118] and branched oligomers with phenol endgroups are formed since phenol is used in excess. These prepolymers are thermally stable and can be stored effectively. Novolac crosslinking is usually achieved by introducing a source of methylene groups to form additional methylene bridges between aromatic rings. Hexamethylenetetramine (HMTA) is the most widely used curing agent (source of formaldehyde) for these reactions. Other curing agents with limited importance include paraformaldehyde and trioxane.[118]

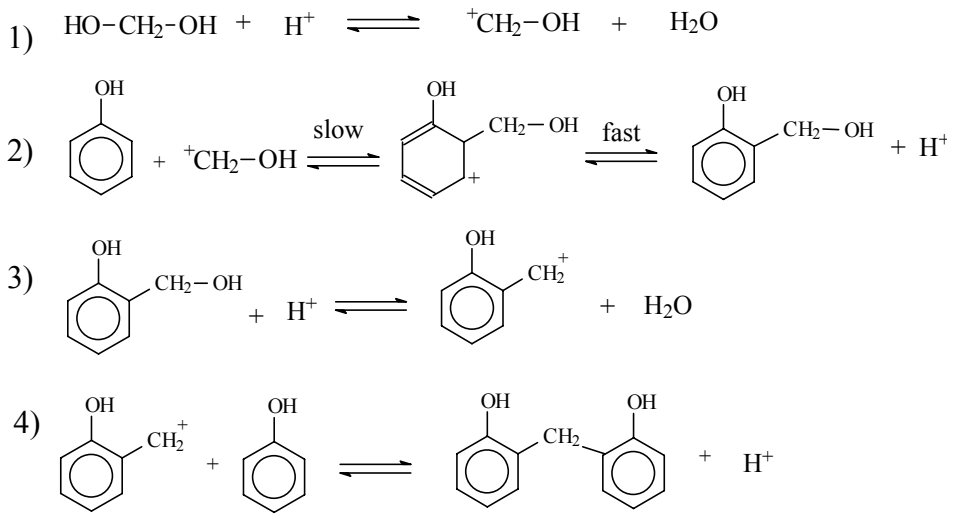

Figure 3. 1. Mechanism for the major process of phenolic novolac resin synthesis

Resoles are obtained by reacting an excess of formaldehyde with phenol under basic conditions. This produces resins with aromatic methylol groups derived from the excess of formaldehyde. Resoles are fairly stable at ambient temperatures, but react rapidly at elevated temperatures forming methylene linkages by eliminating water and

[121] A. Knopp and W. Scheib, *Chemistry and Application of Phenolic Resins*, Springer-Verlag, New York, 1979.

other by-products. Since these materials can be "self"-crosslinked thermally, long-term storage is more difficult.

Regardless of the curing method, either by introducing a crosslinking agent or by thermal self-condensation, the network forming process is accompanied by the generation of volatile by-products such as ammonia, water and formaldehyde. Volatiles often cause voids in the networks.[122,123,124] This, along with a lack of control over crosslink density, results in brittle networks.

Void-free networks can be prepared by reacting phenolic novolacs with epoxies in reactions where the phenolic hydroxyl groups react with the epoxy groups.[125,126,127,128] Workers in our laboratories have previously demonstrated that phenolic-epoxy networks with high phenolic compositions, and with a relatively high phenol functionality per chain (~7), exhibit significantly improved toughness while retaining most of the flame-

---

[122] C. M. Branco, J. M. Ferreira, and M. O. W. Richardson, "A Comparative Study of the Fatigue Behaviour of GRP Hand Lay-up and Pultruded Phenolic Composites," *Int. J. Fatigue* **18**(4), 255-2643 (1995).

[123] J. Wolfrum and G. W. Ehrenstein, "Interdependence Between the Curing, Structure, and the Mechanical Properties of Phenolic Resins," *Journal of Applied Polymer Science* **74**, 3173-3185 (1999).

[124] L. B. Manfredi, O. de la Osa, N. Galego Fernandez, and A. Vazquez, "Structure-Properties Relationship for Resoles with Different Formaldehyde/Phenol Molar Ratio," *Polymer* **40**, 3867-3875 (1999).

[125] Potter, W. G, *Epoxide Resins*, Springer-Verlag, New York, 1970.

[126] A. Hale, C. W. Macosko, and H. E. Bair, "DSC and C-13-NMR Studies of the Imidazole-Accelerated Reaction Between Epoxides and Phenols," *Journal of Applied Polymer Science* **38**(7), 1253-1269 (1989).

[127] M. Ogata, N. Kinjo, and T. Kawata, "Effects of Crosslinking on Physical Properties of Phenol-Formaldehyde Novolac Cured Epoxy Resins," *Journal of Applied Polymer Science* **48**, 583-601 (1993).

[128] A. K. Banthia and J. E. McGrath,."Catalysts for Bisphenol-Diglycidyl Ether Linear Step-Growth Polymerization," *ACS Polym. Prepr. Div. Polym. Chem*. ***20***(2), 629 (1979).

retardant properties.[129,130] These improved mechanical properties have been correlated with increased molecular weight between crosslinks achieved by leaving many phenolic hydroxyl groups unreacted.

Linear, cresol novolac oligomers, obtained by reacting difunctional *ortho*- or *para*-cresol with formaldehyde, are widely used as coatings, adhesives, electronic insulation materials, and for automotive applications.[118] Low molecular weight oligomers have also been reacted with epichlorohydrin to form epoxy resins.[125] A *para*-cresol novolac (M_n=580 g/mol) exhibited a semi-crystalline structure with good thermal stability.[131] *Ortho*- and *para*-cresol have also been copolymerized with *meta*-cresol for use in the electronic industry as photoresists. Since *ortho*- and *para*-cresol have slower reaction rates with formaldehyde than *meta*-cresol, oligomers with *meta*-cresol blocks were obtained having primarily *ortho*- or *para*-cresol endgroups.[132,133]

Ortho- or *para*-cresol novolac formation, which involves exclusively difunctional monomers, are linear condensation polymerizations. The molecular weights of these

---

[129] C. S. Tyberg, K. Bergeron, M. Sankarapandian, P. Shih, A. C. Loos, D. A. Dillard, J. E. McGrath, and J. S. Riffle; "Structure Property Relationshiips of Void Free Phenolic Epoxy Matrix Materials," *Polymer* **41**(13), 5053-5062 (2000).

[130] H. Ghassemi, H. K. Shoba, M. Sankarapandian, A. Shultz, C. L. Sensenich, J. S. Riffle, J. J. Lesko, and J. E. McGrath, "Volatile-Free Phenolic Networks for Infrastructure," in Fiber Composites in Infrastructure, H. Saasatamanesh, M. R. Ehsani, editors, **1**, 14-22 (1998).

[131] A. Hamou, C. Devallencourt, F. Burel, J. M. Saiter, and M. Belbachir, "Thermal Stability of a para-Cresol Novolac Resin," *Journal of Thermal Analysis and Calorimetry* **52**(3), 697-703 (1998).

[132] L. E. Bogan, Jr., in P. N. Prasad, ed., "Understanding the Novolac Synthesis Reaction," *Frontiers of Polymers and Advanced Materials*, Plenum Press, New York, 1994, 311-318.

[133] St. Miloshev, P. Novakov, Vl. Dimitrov, and I. Gitsov, "Synthesis of Novolac Resins. I. Influence of the Chemical Structure of the Monomers and Reaction Conditions on Some Properties of Novolac Oligomers," *Chemtronics* **4**, 251-253 (1989).

cresol novolacs, therefore, should depend on the monomer feed ratio. However, to date, cresol resin syntheses follow typical phenolic novolac synthesis procedures where reactions are terminated at a pre-determined viscosity or reaction time. The difficulty in molecular weight control arises from side reactions, which offset the stoichiometric ratio necessary to obtain target molecular weights. This paper describes the synthesis of linear controlled molecular weight cresol novolacs. The degree of molecular weight control achievable and properties such as glass transition temperatures, molecular weight distributions, and melt viscosities will be discussed. These cresol novolacs have also been crosslinked with epoxies. The network formation reactions and their properties will be addressed in a separate paper.

3.2. Experimental

3.2.1. Materials

Ortho-cresol (99+%), *para*-cresol (99%), 2,6-dimethylphenol (99%), paraformaldehyde (powder, 95%), formaldehyde (37 wt % solution in water), and oxalic acid dihydrate (99%) were obtained from Aldrich. A commercial phenolic resin was kindly provided by Georgia-Pacific (Product #GP-2073). All reagents were used as received.

3.2.2. Molecular Weight Calculations

The following method was used to calculate the stoichiometric ratio of monomers required to obtain specified number average molecular weights. The molecular weight of two endcapping molecules, 2,6-dimethylphenol, and one methylene linkage, $-CH_2-$, were subtracted from the total targeted molecular weight. The remaining weight was divided by the molecular weight of each repeat unit (120 g/mol) to obtain the number of repeat units within the chain (x). The stoichiometric ratio then consisted of two moles of 2,6-dimethylphenol, x moles of cresol, and x+1 moles of formaldehyde.

3.2.3. Synthesis of 2,6-Dimethylphenol Endcapped Cresol Novolac Resin

Ortho-cresol novolac and *para*-cresol novolac resins were prepared in the same manner. The following shows a sample reaction for preparing a 2000 g/mol *ortho*-cresol

novolac resin. In a resin kettle equipped with a stainless steel mechanical stirrer and a condenser connected to an outlet, *ortho*-cresol (303.5g, 2.81mol) and 2,6-dimethylphenol (47.2g, 0.39mol) and paraformaldehyde (94.9g, 3.0 mol) were added. This mixture, along with oxalic acid dihydrate (2.5 wt. % (2.14 mol %) based on the weight of cresol, 7.59g) was heated for approximately 6 hours at 100°C, then an ~10mol % excess of formaldehyde (37 wt. % formaldehyde in water, 27 ml) was added to the reaction. The reaction was continued for an additional 18 hours. It was washed twice with boiling deionized water, then stripped under mild vacuum while being slowly heated to 215°C.

3.2.4. Sample Preparation for Viscosity Measurements

All cresol novolac resins and the control commercial phenolic resin were vacuum stripped (30 Hg) for 2 hours at 165°C prior to any measurements.

3.2. Characterization

3.2.1. Nuclear Magnetic Resonance Spectroscopy

^{1}H NMR and ^{13}C NMR spectra were obtained on a Varian Unity 400 NMR spectrometer. For ^{1}H NMR, 5 mm diameter tubes containing approximately 20 mg samples dissolved in DMSO-d_6 were analyzed under ambient conditions. The experimental parameters included a 1.0 second relaxation delay, 23.6 degree pulse, and 6744.9 Hz spectral width. Thirty-two repetitions were performed for each sample. For ^{13}C NMR, samples of approximately 0.6 g were dissolved in ~ 2 ml acetone or DMSO. The samples were placed in 10 mm diameter tubes for analysis under ambient conditions. An inverse gated decoupling technique with a 90 degree pulse, a 6 second relaxation delay, a frequency of 100.578 MHz, and 1.2 seconds acquisition time were used to obtain quantitative ^{13}C NMR data. Approximately 1000 repetitions were used for each sample.

3.2.2. Gel Permeation Chromatography

GPC was conducted on a Waters GPC/ALC 150-C chromatograph equipped with a differential refractometer detector connected in parallel to a differential viscometer

detector Viscotek model 150R. The injection and column compartment, connecting line, and DV detector were individually controlled and maintained at the same temperature (60°C). The signals from the RI and DV detectors permitted the calculation of intrinsic viscosity for universal calibration purposes by using Viscotek software Unical 4.04 assuming that the polymer concentration at the outlet of the SEC columns approached infinite dilution due to separation and column dispersion. The mobile phase was NMP (dried over phosphorus pentoxide, then vacuum distilled) with a flow rate of one ml/min. The columns were Styragel HT with pore sizes of 10^3 and 10^4 angstroms. The injection volume was 100 µl.

3.2.3. Viscosity Determinations

Complex viscosities were obtained from a Bohlin VOR Rheometer operating in continuous oscillation mode at a frequency of 1 Hz. Temperature control was accomplished with a Bohlin HTC. The auto-strain was set to maintain the torque at 25% of the maximum torque allowed. The maximum strain for the instrument was 0.25. Approximately 0.7g of cresol novolac pellets were placed between the preheated 25 mm diameter parallel plates of the rheometer. The gap was closed to approximately 1mm and the sides were scraped to remove excess sample before the run was started.

The glass transition temperatures of neat resins were obtained with a Perkin-Elmer DSC-7 instrument. The DSC was calibrated with indium and zinc standards, and ice water was used as the coolant. Samples in aluminum pans were heated from 20°C to 180°C. The glass transition temperatures were calculated as the midpoints of the curves.

3.3. Results and Discussion

3.3.1. Introduction

A series of linear, controlled molecular weight, 2,6-dimethylphenol endcapped cresol novolac resins have been synthesized via electrophilic aromatic substitution (Figure 3. 2). The use of *ortho*- or *para*-cresol as a monomer allows for preparing linear oligomers since the cresol ring has only two activated positions for formaldehyde

substitution. By contrast, phenol has three reactive sites (i.e. both *ortho* and the *para* positions) and therefore, branching is inevitable as higher molecular weight develops. For example, branching has been shown to occur significantly once the molecular weight reached 900-1000 g/mol.[118] Addition of calculated amounts of 2,6-dimethylphenol endgroups to the linear *ortho*- or *para*-cresol-formaldehyde reactions allows for controlled molecular weight materials to be generated.

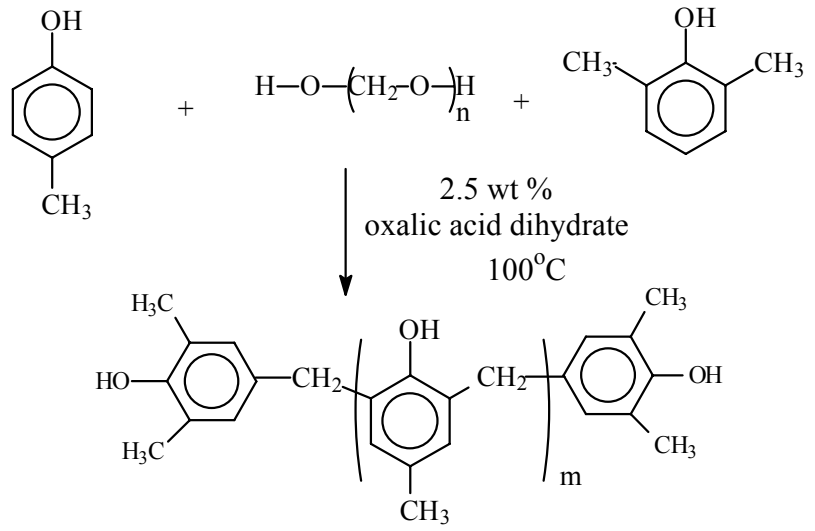

Figure 3. 2. Synthesis of 2,6-dimethylphenol endcapped *para*-cresol novolac resins

The reactivity rates for phenol versus cresol formaldehyde substitutions are different. Phenol reacts with formaldehyde approximately three times faster than *ortho*- or *para*-cresol.[134] Water reduces the rate of reaction between phenol and formaldehyde if used in large amounts.[121] In this work, cresol novolacs were prepared with paraformaldehyde, as opposed to aqueous formaldehyde, to achieve faster reaction rates. Paraformaldehyde contains only 1-9 wt. % water whereas the formaldehyde typically used in phenolic syntheses contains approximately 50 to 63 wt. % water.

Oxalic acid dihydrate was used as the catalyst since it is a relatively strong acid. Oxalic acid dihydrate is preferred over other catalysts because resins with less color can

[134] M. M. Sprung, "Reactivity of Phenol Toward Formaldehyde," *Journal of Applied Polymer Science* **63**(2), 334-343 (1941).

be obtained. Moreover, there is no need to remove the catalyst after the reaction since it can be thermally decomposed to CO, CO_2, and water above approximately 180°C.[118]

In these reactions, the initial viscosities were low and the solutions were miscible. However, as the reactions proceeded and molecular weights increased, the solutions phase separated. The low molecular weight oligomers formed a water-insoluble melt, while the acid catalyst and the formaldehyde probably remained predominantly in the aqueous phase. Slow reaction rates were observed which are probably attributable to the 2-phase nature. The formaldehyde added toward the end of the reactions was in an aqueous solution. Water was desirable in this stage to plasticize the reaction mixtures and lower the viscosities. This was particularly important in the syntheses of higher molecular weight cresol novolacs when the viscosities were high.

3.3.2. Molecular Weight Control and Calculations

Typical phenolic novolac syntheses lack molecular weight control. The reactions are generally terminated after a certain reaction time or once a specified viscosity is reached.[135] The molecular weights of the cresol novolac resins described herein were strategically controlled by the stoichiometric ratio of cresol to 2,6-dimethylphenol (Table 3. 1). The molecular weights of oligomers increased as the amount of endcapping reagent was decreased.

The number average molecular weights in these cresol novolac syntheses was controlled by the cresol to endgroup molar ratio. However, in contrast to usual practice, it was necessary to add formaldehyde in excess to achieve full conversions of phenolic reactive ring positions. When the calculated amounts of formaldehyde were used, the molecular weights of products were always lower than the targeted molecular weights, and it was evident from ^{13}C NMR spectra that unreacted ring positions on cresols remained under such conditions. Formaldehyde was added in two portions to couple all of the reactive sites on cresol. Initially, the stoichiometrically calculated amount of formaldehyde was charged to the reactions with cresol and 2,6-dimethylphenol at 100ºC.

---

[135] S. R Sandler and W. Karo, *Polymer Synthesis,* 2nd edition, Academic Press, Boston, Vol. 2*,* 1992, p49-86.

The early stages of reactions were exothermic and the reactions refluxed. After 6 hours, more formaldehyde (10 mol % of the calculated amount in the form of formalin) was added to ensure that sufficient formaldehyde was available to complete the reactions.

Targeted molecular weights were consistently achieved using the approach of adding excess formaldehyde as described above. This suggests a reversible reaction between cresol or its derivatives and formaldehyde whereby substitution and elimination of formaldehyde occurs. This would allow for coupling regenerated ring positions and methylols to form methylene linkages and achieve the targeted molecular weights. It is also possible that some gaseous formaldehyde, formed by depolymerization of polyoxymethylene, escaped from the reactions during the initial exothermic stages.

The required stoichiometries for controlling molecular weights were calculated using the Carother's approach. A step-growth polymerization was considered involving the reaction of monomers AWA, BYB, and AZ in which the functional groups A react with functional groups B. It was assumed that very high conversion was achieved and that stoichiometric amounts of A and B groups were in the reaction feed. This latter assumption can be expressed as

$$N(BB) = N(AA) + N(A)/2 \qquad \textbf{(3. 1)}$$

where N(BB) = moles of BYB
N(AA) = moles of AWA
N(A) = moles of AZ

The reaction of N(AA) with N(BB) yields a statistically determined size distribution of N(A)/2 moles of product molecules (oligomeric and polymeric) plus by-product molecules which can be represented schematically as follows:

$$N(AA) + N(BB) + N(A) \rightarrow \sum [ZA\text{-}BYB\text{-}(AWA\text{-}BYB\text{-})_x - AZ] + \text{by-products} \qquad \textbf{(3. 2)}$$

A "combined endgroup" is defined as ZA-BYB- plus –AZ and an "internal repeat unit" is defined as –AWA-BYB-. Each mole of a given product molecule therefore has one mole of combined endgroup and x moles of internal repeat units.

The number average molecular weight of the reaction product is then:

$$M_n = \frac{\text{total mass of product molecules}}{\text{moles of product molecules}}$$

$$M_n = \frac{\sum (m_e + x \cdot m_u)}{N(A)/2} \qquad \textbf{(3. 3)}$$

where m_e is the molar mass of the combined endgroup and m_u is the molar mass of an internal unit. The summation is over all N(A)/2 moles of product molecules and all x values. This leads to

$$M_n = m_e + X_n \cdot m_u \qquad \textbf{(3. 4)}$$

where X_n is the number average number of internal units in the product molecules.

By inspection of the schematic molecular structure (3.2) and equation (3.4), one sees that

$$x_n = \frac{N(AA)}{N(A)/2} = 2\,\frac{N(AA)}{N(A)} \qquad \textbf{(3. 5)}$$

Arbitrarily choosing the number of moles of AWA, then substituting equation (3.5) into equation (3.4) and rearranging, one now has a complete description of the feed composition required to achieve a target M_n:

moles of monomer AWA: $N(AA)$

moles of endcapper AZ: $N(A) = \left[\frac{2\,m_u}{M_n - m_e}\right] \cdot N(AA)$

moles of monomer BYB: $N(BB) = N(AA) + N(A)/2$ **(3. 6)**

In the present work AWA is cresol, AZ is 2,6-dimethylphenol, and BYB is formaldehyde.

Table 3. 1. Molecular weight of *ortho*- and *para*-cresol novolac resins calculated using ^{13}C NMR. The molecular weights were controlled by adjusting N_{AA}/N_{ZA}' ratio.

Target M_n (g/mol)	N_{AA} (cresol) (mole)	$N_{ZA'}$ (2,6-DMP*) (moles)	*Ortho* Series M_n (g/mol)	*Para* Series M_n (g/mol)
500	1	0.984	490	510
1000	1	0.323	930	1010
1500	1	0.193	1380	1460
2000	1	0.138	2250	2150

*2,6-DMP – 2,6-dimethylphenol

3.3.3. Structure of Reaction Intermediates and Products

^{13}C NMR has been used extensively to characterize phenolic resins and their synthesis and crosslinking reactions.[136,137,138,139,140] Carbon chemical shifts of typical

[136] X. Zhang and D. H. Solomon, "The Chemistry of Novolac Resins: 9. Reaction Pathways Studied via Model Systems of *ortho*-Hydroxybenzylamine Intermediates and Phenols," *Polymer* **39**(24), 6153-6162 (1998).

[137] X. Zhang, M. G. Looney, D. H. Solomon, and A. K. Whittaker, "The Chemistry of Novolac Resins: 3. ^{13}C and ^{15}N n.m.r. Studies of Curing with Hexamethylenetetramine," *Polymer* **38**(23), 5835-5948 (1997).

[138] P. Luukko, L. Alvila, T. Holopainen, J. Rainio, and T. T. Pakkanen, "Optimizing the Conditions of Quantitative ^{13}C NMR Spectroscopy Analysis for Phenol-Formaldehyde Resole Resins," *Journal of Applied Polymer Science* **69**, 1805-1812 (1998).

[139] M. G. Kim, L.W. Amos, and E. E. Barnes, "Study of the Reaction Rates and Structures of a Phenol Formaldehyde Resol Resin by C-13 NMR and Gel-Permeation Chromatography," *Industrial & Engineering Chemistry Research* **29**(10), 2032-2037 (1990).

[140] P. W. Kopf and E. R. Wagner, "Formation and Cure of Novolacs-NMR Study of Transient Molecules," *Journal of Polymer Science: Polymer Chemistry Edition* **11**(5), 939-960 (1973).

phenolic resins and some related reaction intermediates are provided in Table 3. 2. Quantitative ^{13}C NMR was used in this study to monitor reaction progress and to determine the molecular weights of the final products. Acetone was the preferred solvent for the *ortho*-cresol novolacs since its carbon peak did not overlap with the sample peaks but *para*-cresol novolacs were not soluble in acetone. DMSO, which was used to analyze the *para*-cresol novolacs, resonates at 40 ppm and overlapped with the *para-para* methylene linkages. There were no significant differences in the chemical shifts in these two solvents.

Table 3. 2. ^{13}C NMR assignments for novolac resins and related reaction intermediates[137]

Chemical Shift Region (ppm)	Assignment
150-156	Hydroxyl-substituted phenolic carbons
127-135	Other phenolic carbons
121	*Para*-unsubstituted phenolic carbons
116	*Ortho*-unsubstituted phenolic carbons
85.9	HO-CH_2-O-CH_2-OH
81.4	HO-CH_2-OH
71.1	*Para*-linked dimethylene ether
68.2	*Ortho*- linked dimethylene ether
40.8	*Para-para* methylene linkages
35.5	*Ortho-para* methylene linkages
31.5	*Ortho-ortho* methylene linkages

^{13}C NMR spectra provided an excellent means for structural characterization of the cresol novolac oligomers (Figure 3. 3**)**. The chemical shifts for cresol novolac resins matched well with those observed for phenolic novolacs. The peaks between 150-156 ppm represent hydroxyl substituted aromatic carbons. *Ortho*-unsubstituted aromatic carbons resonate at 118 ppm, and *para*-unsubstituted aromatic carbons are observed at 120 ppm. The rest of the aromatic carbon peaks resonate between 121 and 136 ppm. ^{13}C NMR spectra can define three distinct types of methylene linkages between aromatic

rings, *para-para* (41 ppm), *ortho-para* (36 ppm), and *ortho-ortho* (31.5 ppm). The peaks between 15 and 18 ppm represent the methyl carbons on the aromatic rings.

The formation of oligomers in bulk reactions at 100°C with 2.5 wt. % oxalic acid catalyst was monitored by ^{13}C NMR (Figure 3. 3). The first spectrum represents the reaction mixture immediately after becoming homogeneous (~20 minutes). The reaction had clearly begun at this stage. This was evidenced by the downfield shift of hydroxyl-substituted carbons, shifts in aromatic regions, the appearance of acetone soluble oxymethylene peaks (83-93 ppm), the formation of *para*-linked dimethylene ethers (67.5 ppm) and methylols (64 ppm), and the formation of *para-para* and *ortho-para* methylene linkages. It should be noted that paraformaldehyde was insoluble in the acetone NMR solvent, but its derivatives were soluble. As the reactions progressed, the amount of methylol intermediates and *ortho* and *para* unsubstituted aromatic carbons decreased, and the peaks for methylene linkages increased. ^{13}C NMR spectra showed no *ortho* or *para* unsubstituted carbon peaks in products indicating full conversion of reactive ring positions.

As shown in the literature,[134] *para* positions on phenolic compounds react faster than *ortho* positions. ^{13}C NMR spectra revealed that *para-para* methylene linkages formed most rapidly followed by *ortho-para* methylene linkages (Figure 3. 3). *Ortho-ortho* methylene linkages were observed in small amounts after 1 hour.

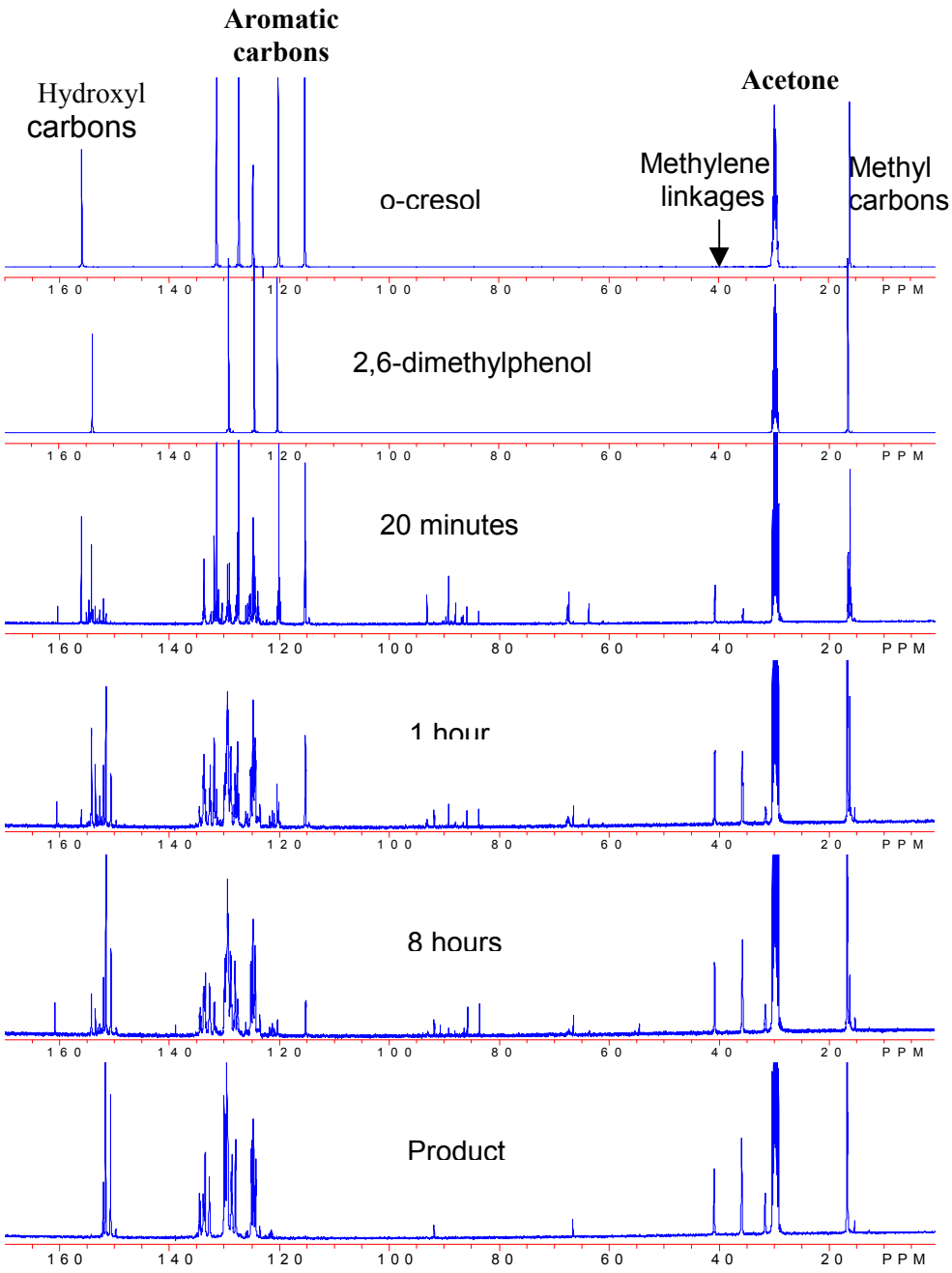

Figure 3. 3. **^{13}C NMR spectra monitoring a 2000g/mol *ortho*-cresol novolac resin synthesis as a function of reaction time. The product was reacted for 24 hours at 100°C, then heated to 200°C under mild vacuum to decompose the catalyst.**

Hydroxymethyl condensation reactions, which eliminate water to form dimethylene ether linkages, are prevalent under acidic conditions. It has been suggested that dimethylene ether linkages decompose at elevated temperatures to form methylene bridges between rings.[118] ^{13}C NMR monitoring the reaction progress of these cresol novolac reactions confirmed the formation of both *ortho* (66.5 ppm) and *para* linked dimethylene ethers (67.5 ppm). *Para*-dimethylene ether linkages formed early and decomposed as the reaction proceeded (Figure 3. 3). *Ortho*-linked dimethylene ethers formed later and remained in the oligomer chain even after heating to 200°C to decompose the catalyst. The high stability of *ortho*-linked dimethylene ethers was attributed to the formation of strong intramolecular hydrogen bonding (Figure 3. 4).

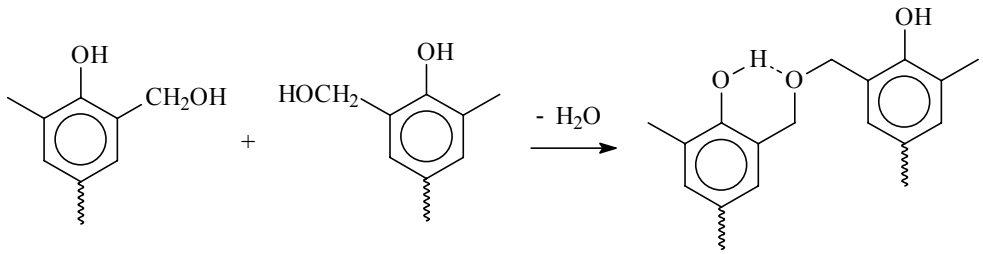

Figure 3. 4. Condensation of *ortho*-hydroxymethyl substituent forming stable *ortho*-linked dimethylene ethers

The residual dimethylene ether linkages can only account for a small fraction of the excess formaldehyde required in these reactions to achieve the targeted molecular weights (Table 3. 3). These dimethylene ether linkages do not change molecular weights significantly.

Table 3. 3. Mole percent ortho-dimethylene ether linkages

M_n (g/mol)	*Ortho* series	*Para* series
500	1.3	2.8
1000	1.5	3.1
1500	1.6	3.6
2000	1.7	3.5

^{13}C NMR peaks for methyl carbons were also used to monitor the cresol novolac reactions (Figure 3. 5).

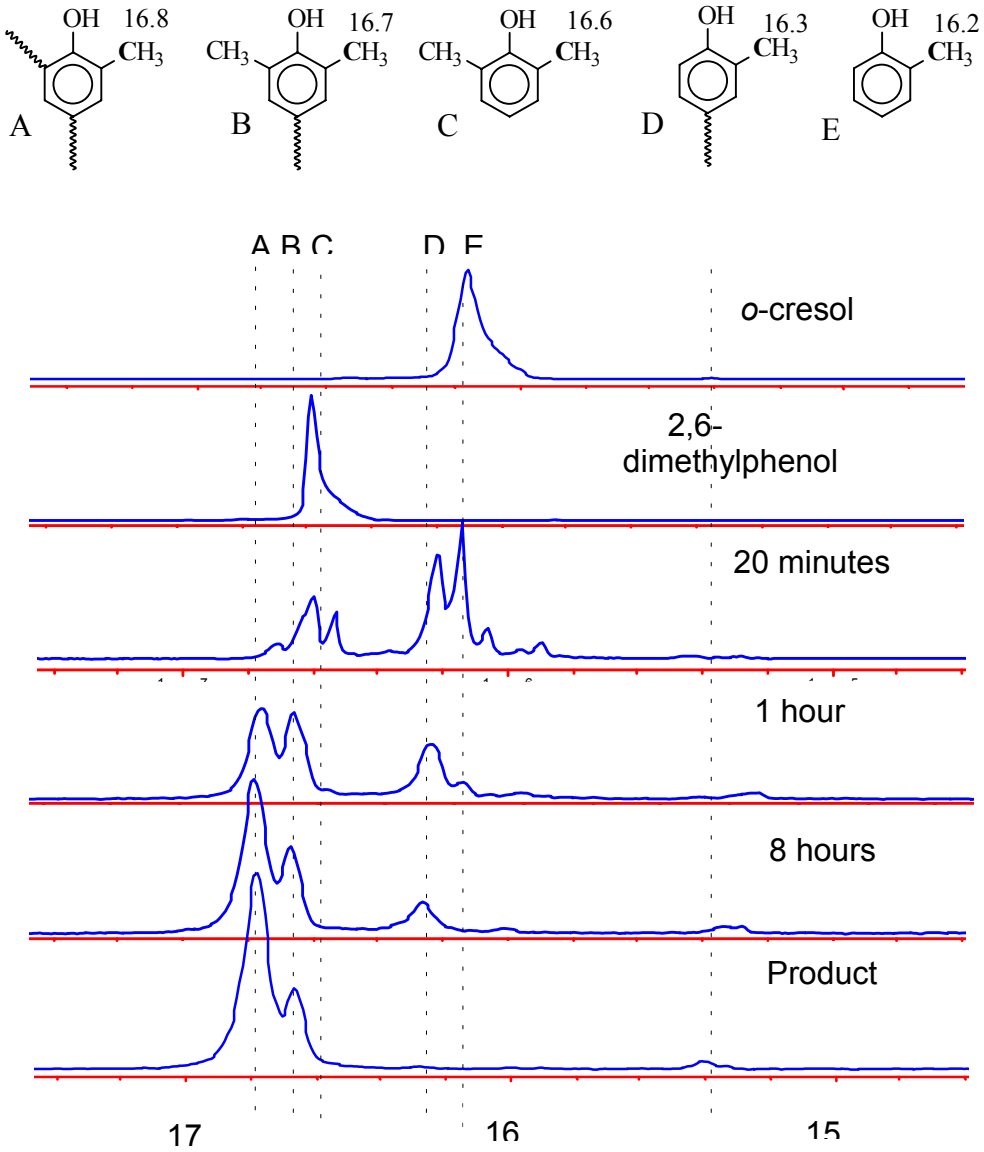

Figure 3. 5. Expanded ^{13}C NMR spectra monitoring a 2000 g/mol *ortho*-cresol novolac resin synthesis as a function of reaction time

The methyl groups on *ortho*-cresol (peak E) resonate at 16.13 ppm, and the methyl groups on 2,6-dimethylphenol (peak C) resonate at 16.60 ppm. The methyl carbon on both monomers shift downfield upon reaction of one site, then the cresol methyl shifts further downfield upon reaction of the second site. The endgroup methyls

are not well resolved with the methyl groups on internal units due to the similarities in their structures. A small peak at 15.4 ppm was attributed to methyl carbons on cresol units linked with dimethylene ethers. This corresponds well with *ortho* methyl carbon shift for 2-hydroxymethyl-4,6-dimethylphenol (15.53 ppm).[141] The ^{13}C NMR analysis showed that all the reactive positions on cresol and 2,6-dimethylphenol were reacted in the product, further confirming quantitative conversion.

The molecular weights of cresol novolac oligomers were calculated by comparing the peak intensities corresponding to methyl carbons on the endgroups versus the internal methyl carbons. Since the two peaks are not well resolved, a deconvolution technique was used to determine the peak integrations (Figure 3. 6). The peak area corresponding to the 2,6-dimethylphenol endgroups accounted for four methyl carbons per chain. The relative number of methyl groups within the repeat units was determined by ratioing the peak integrations of the interior methyl carbons versus the endgroup carbons, then multiplying by 4.

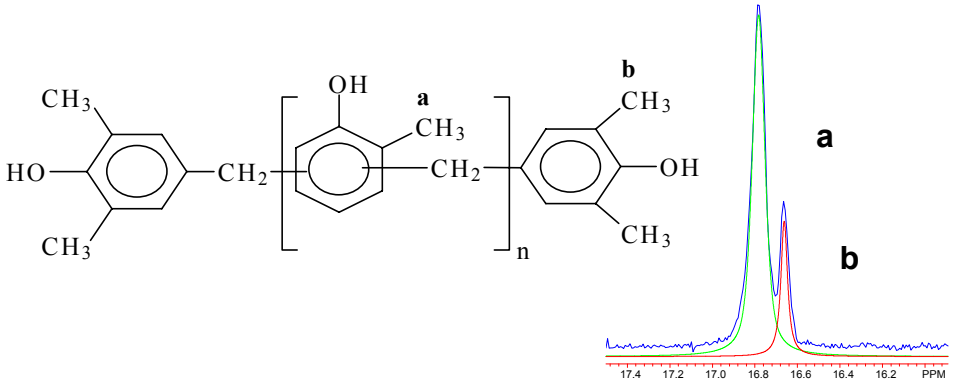

Figure 3. 6. Deconvolution of methyl carbon peaks

The methyl regions of ^{13}C NMR spectra for a series of *ortho*-cresol novolac oligomers with different molecular weights were compared (Figure 3. 7). The peak integration ratio of internal methyl carbons to those on the endgroups (peak a to b)

[141] K. Lenghaus, G. G. Qiao, and D. H. Solomon, "Model Studies of the Curing of Resole Phenol-Formaldehyde Resins Part 1. The Behavior of *ortho* Quinone Methide in a Curing Resin," *Polymer* **41**, 1973-1979 (2000).

increased as the molecular weight increased. This was expected since more repeat units, relative to endgroups, were incorporated as higher molecular weights developed.

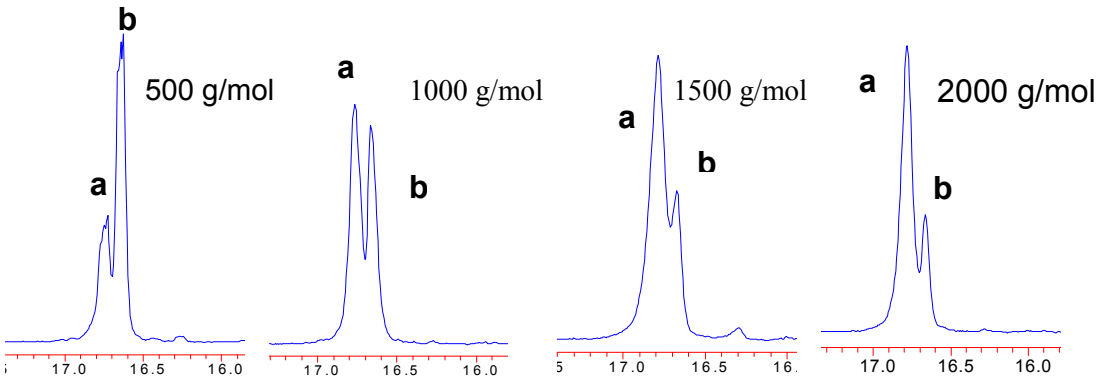

Figure 3. 7. **Expanded ^{13}C NMR spectra of a series of *ortho*-cresol novolac resins with various molecular weights: a) methyl carbons within the repeat units, b) methyl carbons on the endgroups**

The type of methylene linkages (*ortho-ortho*, *ortho-para*, and *para-para*) and the amount in which they form can be calculated using ^{13}C NMR. Since the endgroups formed only *para* methylene linkages, the number of *para* linked species was higher for low molecular weight oligomers (Table 3. 4). As the molecular weight was increased, the *para-para*, *ortho-para*, and *ortho-ortho* linked methylenes approached the expected 1:2:1 statistical distribution.

Table 3. 4. **Percentage isomers formed in *ortho*-cresol novolac resins**

M_n (g/mol)	*p-p* (%)	*o-p* (%)	*o-o* (%)
500	45.2	47.8	7.0
1000	31.2	49.7	19.1
1500	30.0	49.8	20.1
2000	29.2	49.3	21.5

Para-cresol novolacs syntheses, monitored by ^{13}C NMR, showed similar reaction progress as the *ortho*-cresol novolac reactions (Figure 3. 8). Formations of *para*-cresol novolacs were accompanied by the downfield shift of hydroxyl substituted aromatic carbon peaks, increases in both the *ortho-ortho* (36.5 ppm) and the *ortho-para* (40.5 ppm) methylene carbon peaks, and upfield shifts of methyl carbon peaks. The DMSO solvent peak overlapped with the *para-para* methylene carbon peak. However, this was not as important for monitoring the syntheses of *para*-cresol novolac resins since *para-para* methylene linkages only formed when two 2,6-dimethylphenol units dimerized and this was assumed to form in small amounts (especially at low 2,6-dimethylphenol concentrations).

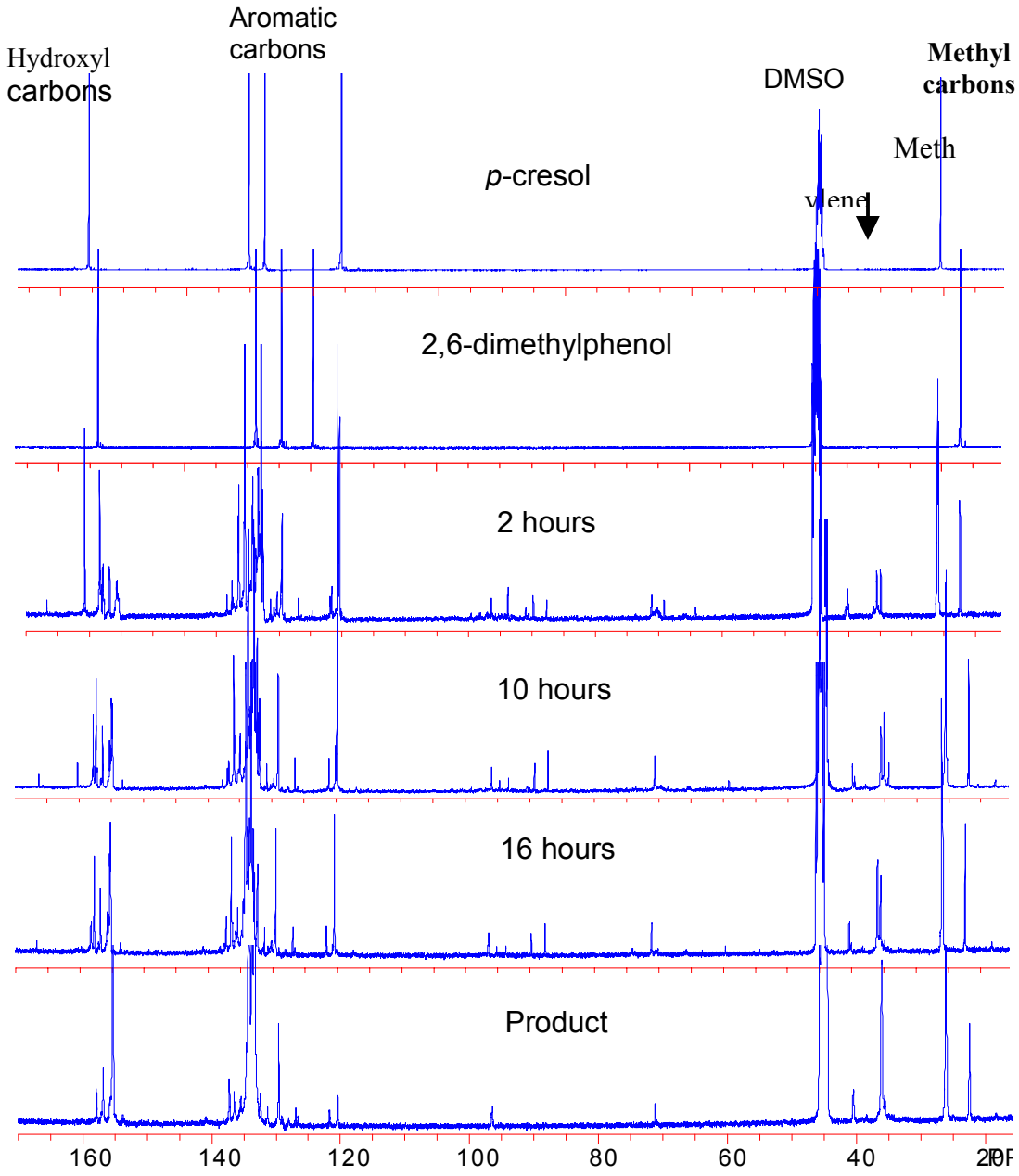

Figure 3. 8. **^{13}C NMR spectra of a 2000g/mol *para*-cresol novolac resin synthesis monitored as a function of reaction time**

Two types of methyl groups were observed for the *para*-cresol novolacs (Figure 3. 9). The *para* methyl carbons within the repeat units resonate at 26.2 ppm, and the *ortho* methyl carbons on the endcapping reagent resonate at 22.4 ppm. The formation of *ortho-para* and *ortho-ortho* methylene linkages was also monitored. Several peaks in the

ortho-ortho methylene region were observed early in the reaction which were attributed to reaction intermediates. At the end of the reaction, only one sharp peak was present in this region.

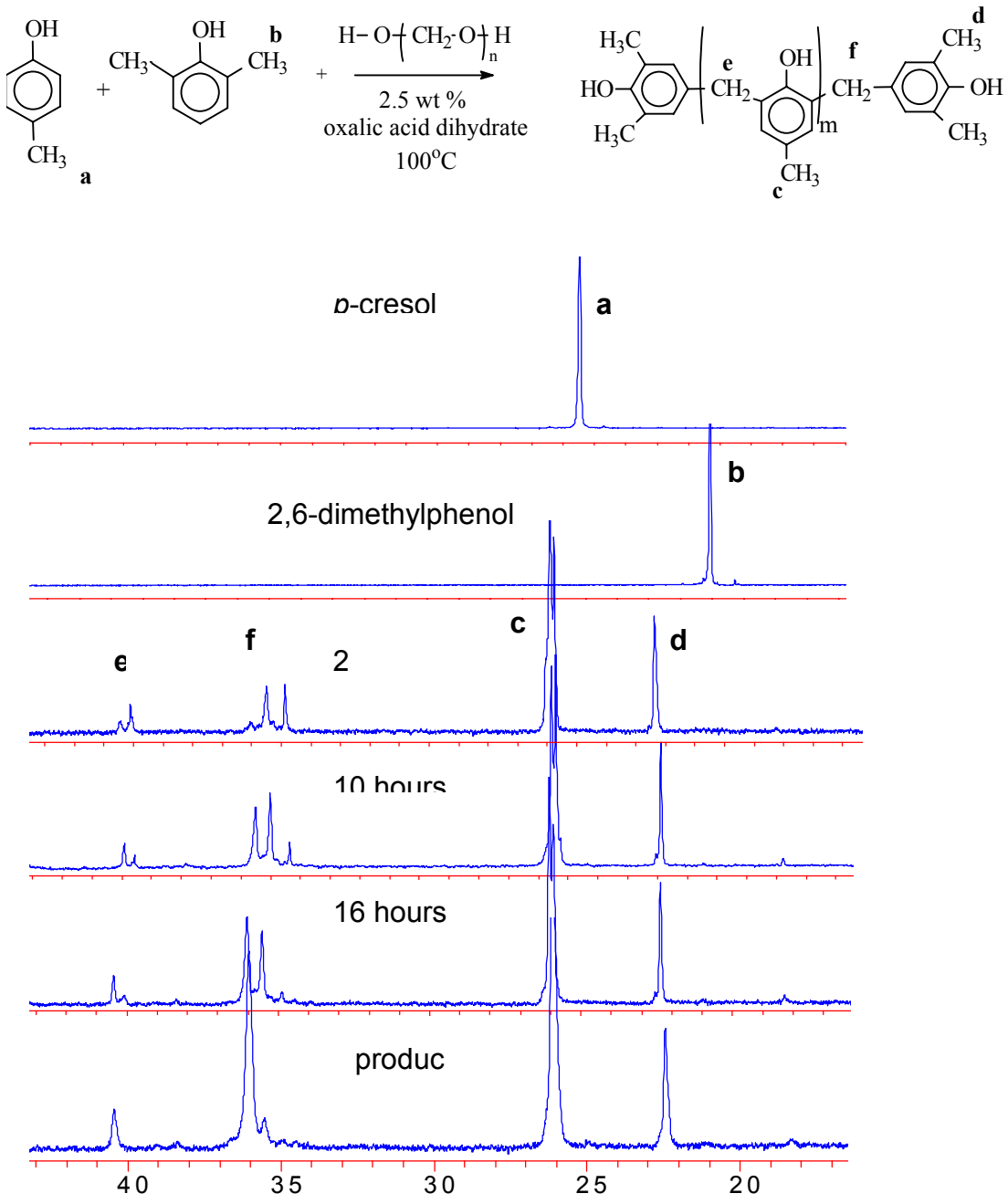

Figure 3. 9. Expanded ^{13}C NMR spectra monitoring the synthesis of a 2000g/mol *para*-cresol novolac resin

^{1}H NMR was used to analyze the monomers and the novolac oligomers to confirm their expected structures (Figure 3. 10 and Figure 3. 11). Six distinct sets of peaks were in the *ortho*-cresol spectrum (Figure 3. 10a). The ^{1}H NMR spectrum of a 2000 g/mol *ortho*-cresol novolac resin (Figure 3. 10b) had broader peaks than the monomer due to the different isomer sequences present. The methyl protons resonated between 1.9 and 2.2 ppm and three sets of peaks between 3.5 and 3.9 ppm were from protons on the methylene linkages. These corresponded to *ortho-ortho* (3.5ppm), *ortho-para* (3.6ppm), and *para-para* (3.7ppm) methylene units. Small amounts of dimethylene ether also formed which resonated at 4.8 ppm.

Similar peaks were observed for *para*-cresol novolacs (Figure 3. 11). Fours sets of peaks were observed for the *para*-cresol monomer. The main difference between the chain structures of *ortho*-cresol versus *para*-cresol novolac resins was the type of methylene linkages. Only *ortho-ortho* linkages are possible between the repeat units for *para*-cresol novolac resins. Therefore, protons on the methylene linkages resonated closer together and were well resolved from any residual water. The hydroxyl proton peaks were also sharper for the *para*-cresol novolacs.

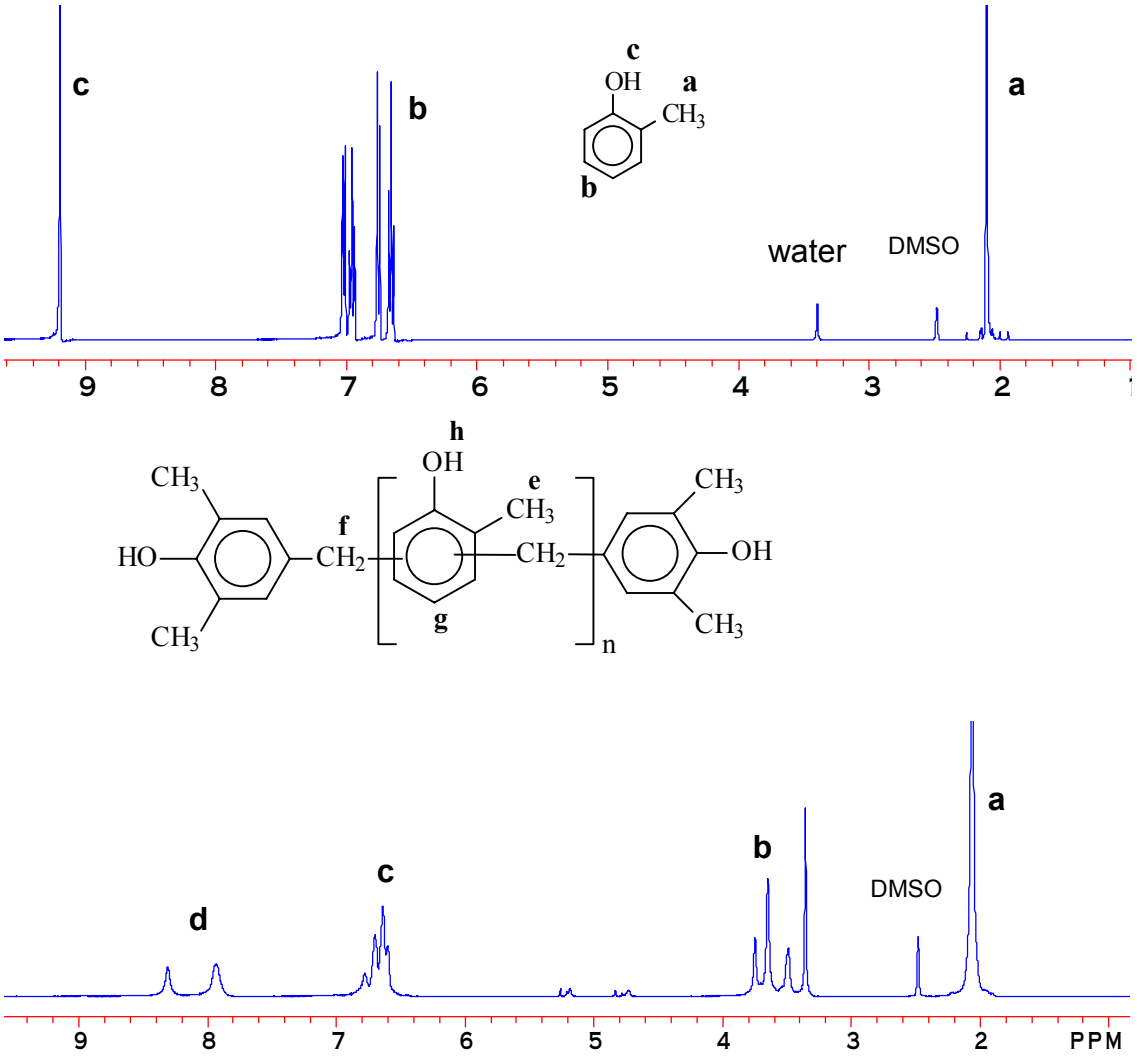

Figure 3. 10. [1]**H NMR spectra of a)** ***ortho*****-cresol, and b) a 2000 g/mol** ***ortho*****-cresol novolac**

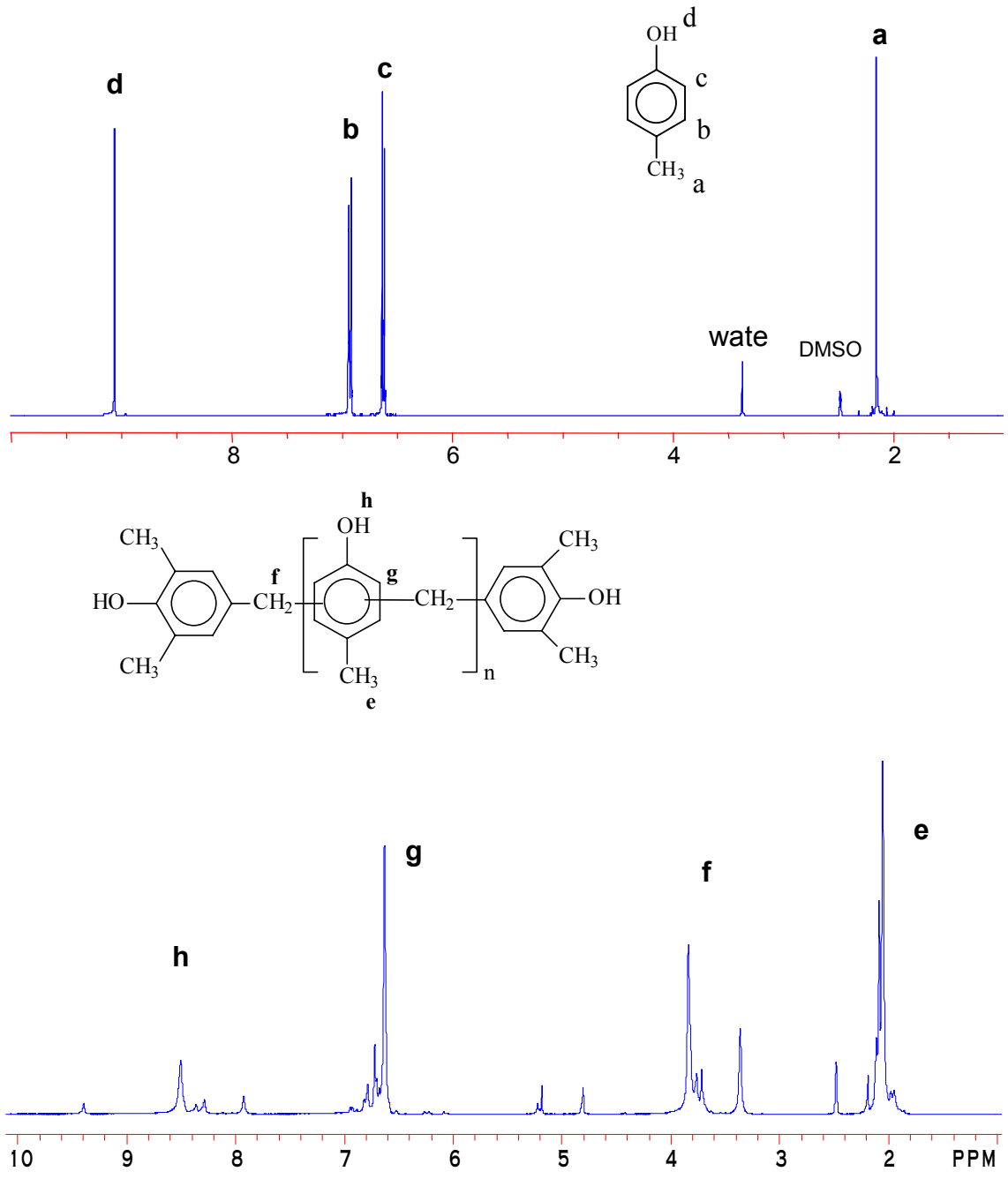

Figure 3. 11. ^{1}**H NMR spectra of a)** ***para*****-cresol, and b) a 2000 g/mol** ***para*****-cresol novolac**

3.3.4. Molecular Weight and Molecular Weight Distributions Determined via GPC

The growth of molecular weight with time for both *ortho*- and *para*-cresol novolac synthesis was monitored using gel permeation chromatography (Figure 3. 12). In gel permeation chromatography, the higher molecular weight oligomers bypass the smaller pores in the packing column and elute faster, and therefore, appear at lower retention volumes. As the reactions progressed, the GPC peaks shifted to lower elution volumes and the area in the region where monomers and low molecular weight oligomers eluted (retention volume 32.6–36 ml) decreased. The final products were comprised of mostly higher molecular weight oligomers eluting between 27 and 32.6 ml.

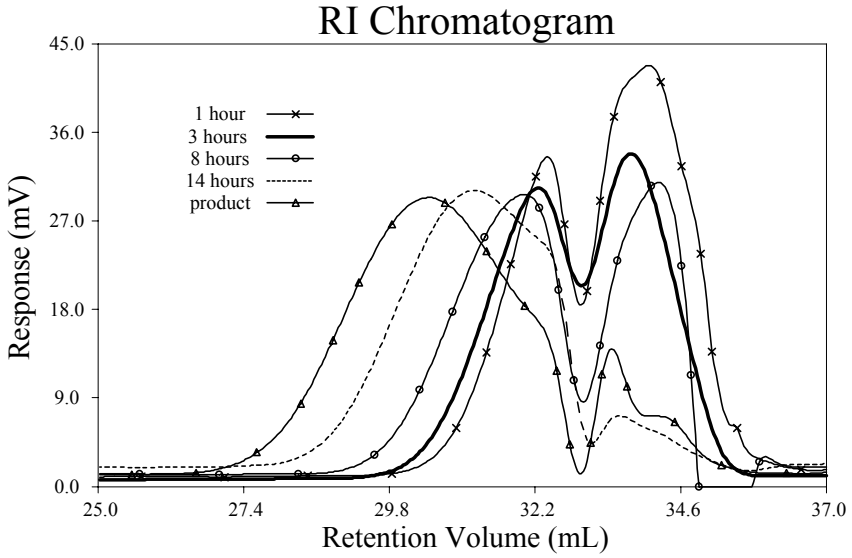

Figure 3. 12. GPC monitoring the synthesis of a 2000 g/mol *ortho*-cresol novolac resin as a function of reaction time

GPC traces of *ortho*- and *para*-cresol novolacs with approximate molecular weights of 500 g/mol, 1000 g/mol, 1500 g/mol, and 2000 g/mol were measured (Figure 3. 13). For both series, the peaks shifted toward lower elution volumes as the average molecular weights increased.

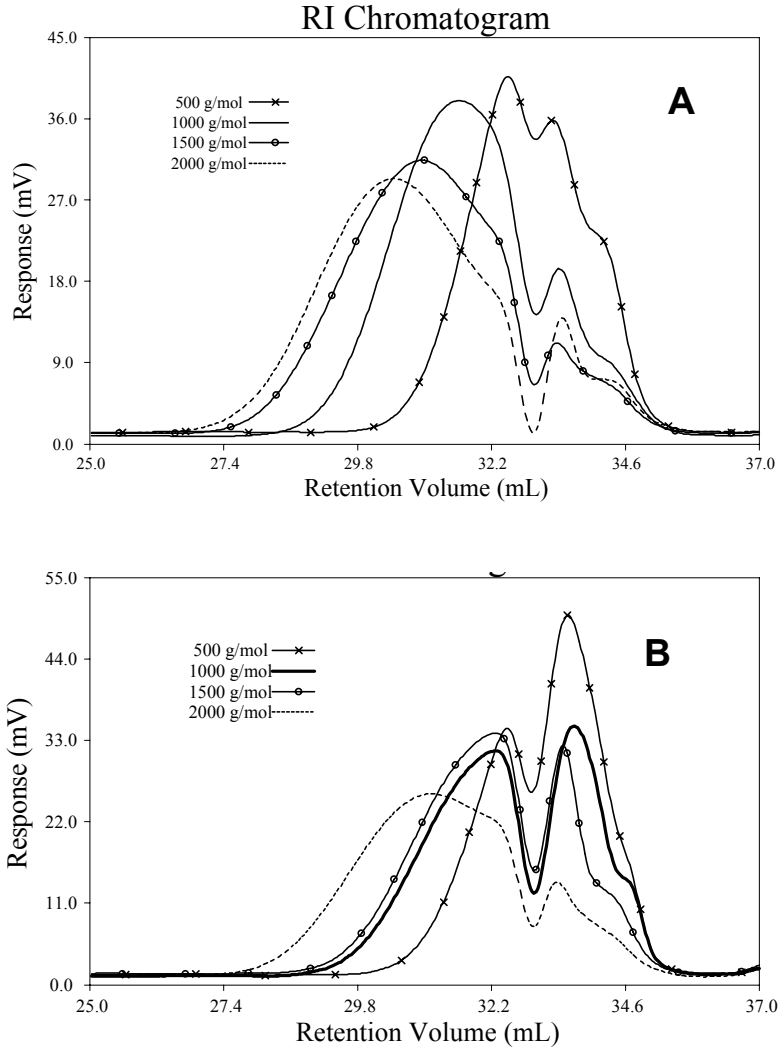

Figure 3. 13. GPC of cresol novolac resins with various molecular weights: a)*ortho*-cresol novolac, b)*para*-cresol novolac

GPC was used to qualitatively compare the molecular weights. Absolute molecular weights could not be derived from GPC using the viscosity detector due to their low molecular weights and correspondingly low solution viscosities. Thus, only the polydispersities of these oligomers and their intrinsic viscosities were evaluated (Table 3. 5). Since cresol novolac resin syntheses are condensation polymerizations, the polydispersity should approach 2 as the molecular weight increases. Low molecular

weight oligomers (500-1000 g/mol) had low polydispersities, but the polydispersity increased as the molecular weight was increased.

As expected, the intrinsic viscosities increased as the molecular weight increased. However, when comparing *ortho*-cresol novolacs to *para*-cresol novolacs with similar number average molecular weights, *ortho*-cresol novolacs consistently had higher intrinsic viscosities (Table 3. 5). This suggested that *ortho*-cresol novolacs have higher hydrodynamic volumes in the NMP chromatography solvent. It was previously reported that different novolac isomers have different elution behaviors.[142,143] The difference in hydrodynamic volumes from isomer structures of *ortho-ortho*, *ortho-para*, and *para-para* was due to varying degrees of solvation. Oligomers with high compositions of *ortho-ortho* linkages (i.e. *para*-cresol novolac resins) may have a higher degree of intramolecular hydrogen bonding, resulting in less solvation and lower hydrodynamic volumes. The propensity for hydrogen bonding may be disrupted for *ortho*-cresol novolacs since three types of methylene linkages are available and were distributed randomly.

---

[142] T. R. Dargaville, F. N. Guerzoni, M. G. Looney, D. A. Shipp, D. H. Solomon, and X. Zhang, "Determination of Molecular Weight Distribution of Novolac Resins by Gel Permeation Chromatography," *Journal of Polymer Science. Part A: Polymer Chemistry* **35**(8), 1399-1407 (1997).

[143] T. Yoshikawa, K. Kimura and S. Fujimura, "The Gel Permeation Chromatography of Phenolic Compound," *Journal of Applied Polymer Science* **15**, 2513-2520 (1971).

Table 3. 5. Polydispersities and intrinsic viscosities of cresol novolac resins

Cresol	M_n (g/mol)	Polydispersity	Intrinsic Viscosity* (dL/g)
ortho	500	1.41	0.037
	1000	1.33	0.049
	1500	1.73	0.066
	2000	1.61	0.075
para	500	1.25	0.031
	1000	1.62	0.046
	1500	1.62	0.052
	2000	2.08	0.067

* in NMP solvent at 60°C

Glass transition temperatures for both the *ortho*- and *para*-cresol novolacs increased as the molecular weight increased (Table 3. 6). The T_gs ranged from approximately 40°C for 500 g/mol resins to 105-110°C for oligomers with number average molecular weights of 2000 g/mol. No significant differences were observed between the T_gs of *ortho* and *para*-cresol novolacs with similar molecular weights.

Table 3. 6. T_g of cresol novolac resins as a function of molecular weight

Ortho Series		*Para* Series	
M_n* (g/mol)	T_g (°C)	M_n* (g/mol)	T_g (°C)
490	40	510	43
930	76	1010	76
1380	92	1460	99
2250	104	2150	110

* Calculated using ^{13}C NMR

3.3.5. Dynamic Viscosities of Cresol Novolac Resins

Efficient melt composite fabrication procedures require low viscosity resins to wet out the fiber. The viscosity profiles of a typical phenolic novolac resin with a molecular weight of ~700 g/mol (M_n) and a series of cresol novolacs were examined as a function of temperature at a heating rate of 2.5°C/minute (Figure 3. 14). All samples were vacuum stripped at 165°C for 2 hours prior to the measurements to remove residual water. As molecular weights were increased, the temperatures required for the viscosity to fall to 10 Pa*s increased for both series of cresol novolac materials. *Ortho*-cresol novolacs (Figure 3. 14. a) had similar viscosities to the *para*-cresol novolacs (Figure 3. 14. b) with similar molecular weights at any given temperature. The viscosity of the 2000 g/mol *para*-cresol oligomer decreased with increased temperature until ~180°C, then gradually increased upon further heating. The reason for this increase in viscosity at high temperatures is presumed to be attributable to degradative crosslinking, but this is as yet unclear. It is possible that the increase in viscosity is due to *o',o'*-dimethylene ether oxidation to *o',o'*-dimethylene ether hydroperoxide followed by degradative crosslinking. The viscosity of the phenolic control reached 10 Pa*s at ~165°C, a higher temperature than that required by a 1500 g/mol cresol novolacs to reach the same viscosity. This suggested that the cresol oligomers may be significantly more amenable to melt processing relative to phenol derived oligomers due to a wider processing window. The phenolic novolac control material behaved similarly to the 2000 g/mol *para*-cresol novolac resin where the viscosity showed a minimum at ~180°C.

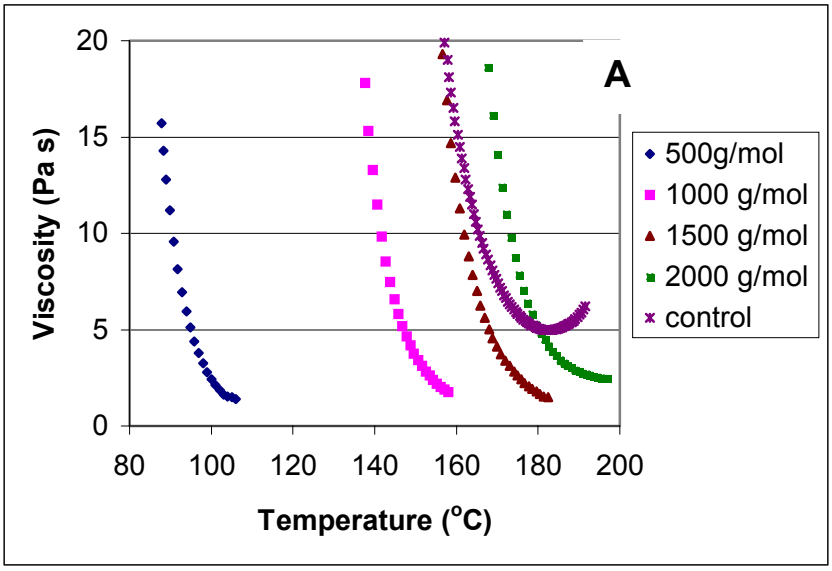

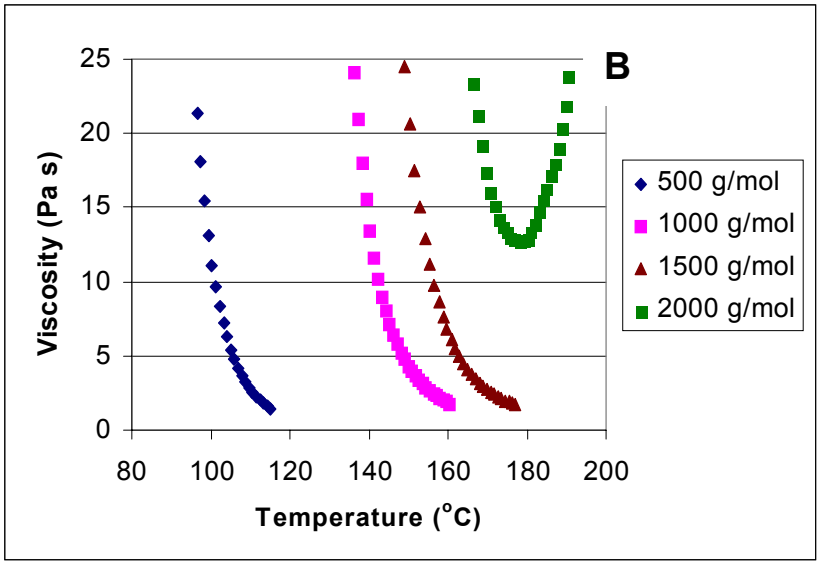

Figure 3. 14. Dynamic viscosity of cresol novolacs measured as a function of molecular weight a) *ortho*-cresol novolac resins, and b) *para*-cresol novolac resins

3.4. Conclusions

A series of controlled molecular weight, 2,6-dimethylphenol endcapped cresol novolac resins have been synthesized. An excess of formaldehyde was required to achieve the targeted molecular weights. The number average molecular weights, determined from ^{13}C NMR spectra, showed good agreement with the targeted number

average molecular weights for both *ortho*- and *para*-cresol novolacs. The amount of *ortho-ortho*, *ortho-para* and *para-para* methylene linkages for the *ortho*-cresol novolac resins, also determined from ^{13}C NMR, approached the statistical distribution as the molecular weights were increased and the contributions from endgroups were less significant. The polydispersities obtained from GPC suggested that molecular weight distributions were reasonably narrow (< 2). The glass transition temperatures increased from ~40°C to 110°C as the molecular weights were increased from 500g/mol to 2000g/mol, but there were no significant differences between the *ortho* and *para*-cresol novolacs with similar molecular weights.

In general, the viscosities of *ortho*- and *para*-cresol novolacs with similar molecular weights were almost identical, but were significantly lower than phenol based oligomers. These cresol novolac resins will be crosslinked with various epoxy resins to form void-free flame retardant networks. Network properties such as toughness, flame retardance, and water uptake, as well as processability will be investigated.

Chapter 4. Structure-Property Relationships of Cresol Novolac/Epoxy Networks

4.1. Introduction

A 2000 g/mol linear *ortho*-cresol novolac resin was crosslinked with various epoxies at defined compositions for use as tough and flame retardant matrix resins. The cresol novolac/epoxy network mechanical and flame properties were compared to a phenolic control, an epoxy control, and a phenolic novolac/epoxy network. Undoubtedly the network properties depended on both the chemical and the network structures, thus this research focused on determining the influences of network structures on properties. The processability of cresol novolac/epoxy mixtures was also evaluated.

4.1.1. Crosslink density and its affects on network properties

Crosslink density (ν) or degree of crosslinking is a measure of the total links between chains in a given mass of materials. It is frequently represented in terms of the molecular weight between crosslinks (M_c) where higher crosslink densities correspond to lower M_c values and vice versa.[144] The portion of crosslinked networks that remains soluble and has finite molecular weights is referred to as the sol fraction. The insoluble crosslinked portion is termed the gel fraction.

Two general types of experimental methods widely used to determine the degree of crosslinking are based on swelling and mechanical testing. However, the observed molecular weight between crosslinks frequently deviates from the theoretically calculated M_c value due to over-simplified assumptions relating swelling or mechanical properties to crosslink densities. For example, trapped physical entanglements should improve the mechanical properties and therefore lead to higher apparent crosslink densities. The presence of dangling chain ends, on the other hand, does not contribute mechanically, and therefore is expected to reduce the apparent crosslink densities. It is also argued that not

[144] *Encyclopedia of Polymer Science and Engineering*, Vol 4. J. I. Kroschwitz, Ed. John Wiley & Sons, New York, 1986.

all crosslink points are mechanically effective which may also introduce errors in the calculations.

For a perfect network with no elastically inactive chains or dangling ends, the swelling by a good solvent at equilibrium is given by

$$1/\nu = M_c = - V_1 \rho_P \frac{\phi^{1/3} - \phi/2}{\ln(1-\phi) + \phi + \chi_1 \phi^2} \qquad \textbf{(4. 1)}$$

where V_1 = molar volume of the solvent

ρ_P = density of the polymer

ϕ = volume fraction of the polymer in the swollen state

χ_1 = polymer solvent (Flory-Huggins) interaction parameter

The elastically inactive chains in the networks may be accounted for by dividing the M_c values by a correction factor, $1\text{-}2M_c/M_n$, where M_n is the number average molecular weight of the polymer before crosslinking. This procedure is most accurate for calculating crosslink densities of typical vulcanized rubbers ($M_c \sim 5000$ g/mol). Although the general trend of increasing M_c with increasing swelling still holds true for more highly crosslinked networks, this method is no longer effective at these lower M_c values.[145]

Crosslink densities can also be derived from mechanical testing such as stress-strain or stress-relaxation experiments for polymers at temperatures well above their T_gs. According to the theory of rubber elasticity, the shear modulus (G) of an ideal rubber is given by

$$G = \nu RT = \nu RT/M_c \qquad \textbf{(4. 2)}$$

where ν = density,

R = gas constant,

T = absolute temperature (K)

[145] L. E. Nielsen, "Crosslinking-Effects on Physical Properties of Polymers," *Journal of Macromolecular Science-Reviews Macromolecular Chemistry* **C3**(1), 69-103 (1969).

The correction factor described previously is sometimes incorporated equation (4.2) to account for dangling polymer chain ends

$$G = \nu RT/M_c\ (1\text{-}2M_c/M_n) \qquad \textbf{(4. 3)}$$

The Young's modulus (E) is approximated by

$$E = 3G \qquad \textbf{(4. 4)}$$

Four major assumptions are made in developing the statistical theory of rubber elasticity: 1) the internal energy of the system is independent of the conformation of the individual chains, 2) the network chains obey Gaussian statistics, 3) the total number of conformations of an isotropic network is the sum of the number of conformations of the individual network chains, and 4) crosslinked junctions in the network are fixed at their mean position; an affine transformation occurs upon deformation.[146]

Crosslinking and the crosslink density greatly influence material properties especially above T_g. Unlike linear polymer chains, which undergo viscous flow above T_g and are incapable of sustaining a constant load, crosslinked networks show elastic characteristics above their T_gs. Crosslinking generally improves physical properties especially above the glass transition temperature. For example, network glassy moduli generally vary slightly as a function of crosslink density, whereas the rubbery moduli increase significantly with increasing degrees of crosslinking. The glass transition temperatures increase with higher degrees of crosslinking. The extent of T_g increase as a function of crosslink density has been approximated by

$$\Delta T_g = A\nu \qquad \textbf{(4. 5)}$$

[146] J. J. Aklonis and W. J. MacKnight, *Introduction to Polymer Viscoelasticity*, Second Edition, John Wiley and Sons, New York, 1983.

where ν is the moles of crosslinks per gram of polymer, and A is a constant on the order of 10^4-10^5 depending on the material.[147] The dependence of T_g may be more pronounced in more highly crosslinked networks than in lightly crosslinked networks.[144] Crosslinking generally decreases creep, compression set, and stress relaxation, and increases tensile strength; it increases refractive index, and lowers thermal expansion and heat capacity.

Fracture toughness is also strongly dependent on the network crosslink density. Highly crosslinked networks are generally brittle and their toughness increases as the crosslink density decreases until the network becomes too loose. Tyberg et al.[148,149] investigated the effects of crosslink density on network properties, including fracture toughness, for phenolic novolac/epoxy networks. The network crosslink density was adjusted by controlling the stoichiometric ratio of phenolic hydroxyl to epoxy groups. A phenolic novolac with a functionality of approximately 7 (determined via ^{1}H NMR) was used.

A schematic representing an idealized crosslinking reaction between phenolic novolac (f=7) and a diepoxide is depicted in Figure 4. 1. If equimolar amounts of phenolic hydroxyl and epoxy groups are used, and assuming 100 % conversion, highly crosslinked materials are expected to form. As the stoichiometric ratio is offset to increase the amount of phenolic hydroxyl groups (or epoxy groups), the network crosslink density decreases. This trend continues until the amount of epoxy (or novolac) present is insufficient to generate fully crosslinked networks.

---

[147] T. G. Fox and S. Loshaek, "Influence of Molecular Weight and Degree of Crosslink on the Specific Volume and Glass Temperature of Polymers," *Journal of Polymer Science* **15**(80), 371-390 (1955).

[148] C. S. Tyberg, M. Sankarapandian, K. Bears, P. Shih, A. C. Loos, D. Dillard, J. E. McGrath, and J. S. Riffle, "Tough, Void-Free, Flame Retardant Phenolic Matrix Materials," *Construction and Building Materials* **13**, 343-353 (1999).

[149] C. S. Tyberg, K. Bergeron, M. Sankarapandian, P. Shih, A. C. Loos, D. A. Dillard, J. E. McGrath, and J. S. Riffle, "Structure-Property Relationships of Void-Free Phenolic-Epoxy Matrix Materials," *Polymer* **41**(13), 5053-5062 (2000).

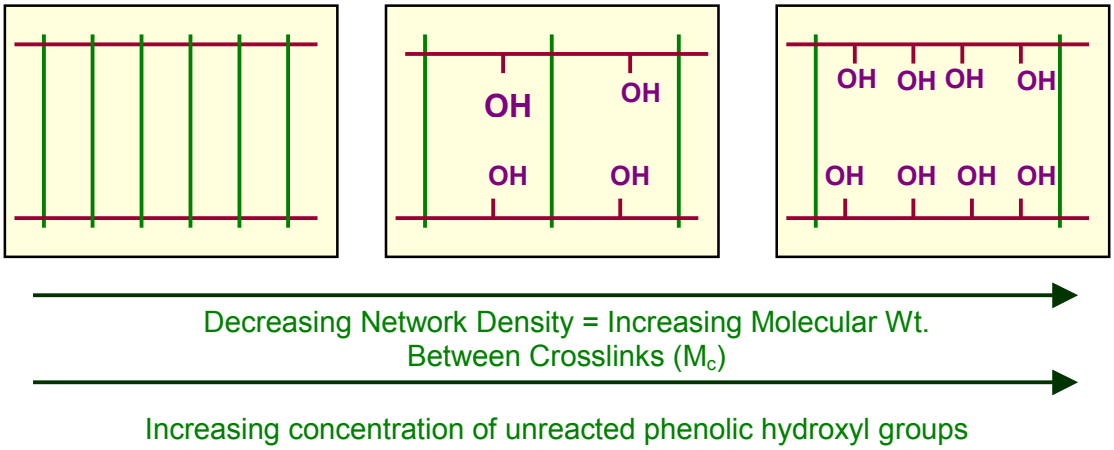

Figure 4. 1. Idealized phenolic/epoxy networks

The critical stress intensity factors, K_{IC}, of phenolic novolac/bisphenol-A epoxy networks were measured as a function of network composition (Table 4. 1).[148] The fracture toughness increased as the phenolic hydroxyl to epoxy ratio was offset from 1/1 to 5/1 where the fracture toughness appeared to reach a maximum. Further stoichiometric imbalance reduced the fracture toughness due to a lack of epoxy component necessary to form well-connected networks.

Table 4. 1. Fracture toughness of phenolic novolac/epoxy networks[150]

Phenol/Epoxy (eq/eq)	Novolac/Epoxy (wt/wt)	K_{IC} (MPa*m$^{1/2}$)
1/1	36/64	0.57
2/1	53/47	0.64
3/1	63/37	0.87
5/1	74/26	1.03
7/1	80/20	0.70

[150] C. S. Tyberg, "Void-Free Flame Retardant Phenolic Network: Properties and Processability, " Dissertation, Virginia Tech, 2000.

The toughnesses of neat and rubber toughened diglycidyl ether based epoxy networks were measured as a function of crosslink density.[151] Slow speed fracture toughness (G_{IC}) test and notched high-speed tensile toughness (G_h) tests revealed that increased toughness occurred with increased M_x for both rubber toughened and unmodified networks. Studies on polyurethane networks derived from triisocyanate reacted with well defined diols,[152] and DGEBA cured with 4,4'-diamino-3,3'dimethyldicyclohexylmethane (3DCM)[153] also correlated increased toughness with increased M_xs.

4.1.2. Cooperativity

Polymers exhibit viscoelastic behaviors in which the combined characteristics of elastic solids and viscous fluids are shown. Two simple transient viscoelastic experimental methods are stress relaxation and creep tests. A stress relaxation test is performed under constant strain and the stress rises initially and decays with time due to dissipation by its fluid like component (Figure 4. 2.a). A creep test involves applying a constant stress to samples and observing the strain increases with time (Figure 4. 2.b).

---

[151] M.C. M. van der Sanden and H. E. H. Meijer, "Deformation and Toughness of Polymeric Systems: 3. Influence of Crosslink Density," *Polymer* **34**(24), 5063-5072 (1993).

[152] H. L. Bos and J. J. H. Nusselder, "Toughness of Model Polymeric Networks in the Glassy State: Effect of Crosslink Density," *Polymer* **35**(13), 2793-2799 (1994).

[153] E. Espuche, J. Galy, F. F. Gerard, J. P. Pascault, and H. Sautereau, "Influence of Crosslink Density and Chain Flexibility on Mechanical Properties of Model Epoxy Networks," *Macromolecular Symposia* **93**, 107-115 (1995).

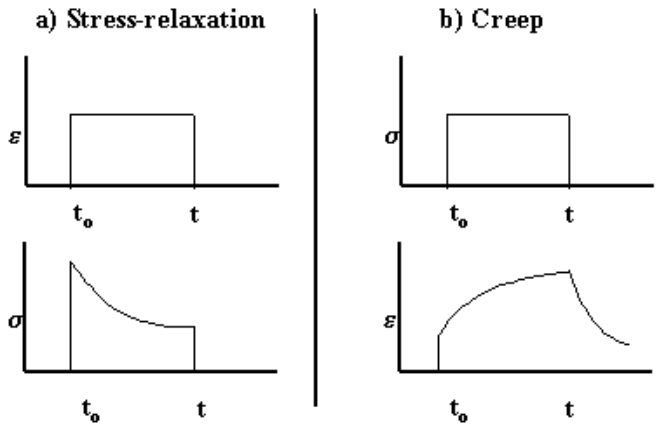

Figure 4. 2. a) Stress-relaxation experiment, and b) creep experiments

When an external force is applied to polymer chains in their equilibrium state, a relaxation process occurs to redistribute the chain conformations until equilibrium is reached. The relaxation of the smallest units in polymer chain requires the shortest relaxation time. Polymer chains composed of many relaxation units can cooperatively relax as a larger unit, which requires a longer relaxation time. A polymer relaxation process, which consists of several mechanisms, can be described using a distribution of relaxation times, or a relaxation spectrum

$$G(t) = \sum_i G_i \exp\left(-\frac{t}{\tau_t}\right) \qquad \textbf{(4. 6)}$$

where G(t), the relaxation modulus at time t, is the sum of individual relaxing elements each with a relaxation time τ_i and a relative intensity G_i.

In a continuum relaxation process, the smallest unit should exhibit the shortest relaxation time. A deformation study on polypropylene showed that the rotation of main chain bonds, most likely between trans and gauche conformations, represents the smallest domain and therefore is the predominate mode of deformation.[154] The rate of rotation from one stable conformation to another is controlled by the number of bonds exceeding

[154] D. N. Theodorou and U. W. Suter, "Shape of Unperturbed Linear Polymer: Polypropylene," *Macromolecules* **18**(6), 1206-1214 (1985).

the highest energy state encountered in the rotation process. The classical rate constant (k) can be used to estimate the kinetics of relaxation

$$k = -\frac{1}{N}\frac{dN}{dt} = k^{*} \exp\left(-\frac{\Delta\mu}{kT}\right) \qquad \textbf{(4. 7)}$$

where N is the number of those conformers in the ground state, Δμ is the energy difference between the activated and ground state, k^{*} is the efficiency term that depends on the intensity of the liberation of the bonds in question, k is the Boltzmann constant, and T is the absolute temperature.

The relaxation of a small unit crowded in a dense polymer domain requires its neighbors to move together. This simultaneous relaxation of one unit along with its neighbors is termed cooperativity. The probability of relaxation becomes smaller in a denser environment, and therefore the cooperative domain size increases. The cooperative domain size (z) therefore affects the activation energy for the relaxation of a single segment (Figure 4. 3).

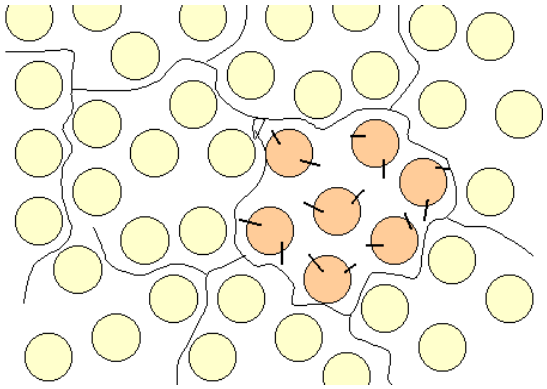

Figure 4. 3. Illustration of cooperativity domain size where z = 7

The temperature dependence of the transition region and non-equilibrium glassy state of a polymer can be investigated by determining its intermolecular cooperativity. Polymers with low cooperativity follow Arrhenius behaviors when they are cooled below their T_g and exhibit narrow relaxation time distributions. For example, in the absence of

neighbor interference, the following Arrhenius equation can be used to describe the relaxation time, τ

$$\ln \tau = \ln \tau^* + \Delta\mu\left(\frac{1}{RT} - \frac{1}{RT^*}\right) \qquad \textbf{(4. 8)}$$

where $\Delta\mu$ = activation energy of conformer rotation (or change)

R = gas constant

T = absolute temperature

T^* = temperature at which the conformer can rotate freely without any neighbor interference

τ^* = relaxation time at which the conformer can rotate freely without any neighbor interference

For cooperative relaxation, the domain size (z) must be introduced. The relaxation time of polymers that consist of larger sterically hindered units must be described using a non-Arrhenius equation

$$\ln \tau = \ln \tau^* + \Delta\mu\left(\frac{z}{RT} - \frac{1}{RT^*}\right) \qquad \textbf{(4. 9)}$$

The above equation is non-Arrhenius since z is temperature dependent.

Materials with Arrhenius behaviors are described as "strong"; on the other hand, materials with non-Arrhenius behaviors are referred to as "fragile". Fragility therefore is a measure of the temperature dependence of the most probable segmental relaxation time near T_g where more fragile corresponds to higher temperature dependence and vice versa. Connolly and Karasz[155] have correlated fragility to the degree of cooperativity. A fragility plot, or cooperativity plot, can be generated by plotting the time temperature shift factor versus (T_g/T). The slope of the line at T = T_g is termed fragility (m) and is proportional to the apparent activation energies normalized by T_g.

[155] M. Connolly and F. Karasz, "Viscoelastic and Dielectric Relaxation Behavior of Substituted Poly(p-Phenylenes) ," *Macromolecules* **28**, 1872-1881 (1995).

$$m = \Delta E/2.303\ R\ T_g \qquad \textbf{(4. 10)}$$

A higher m value corresponds to a more fragile material with a greater degree of intermolecular cooperativity which therefore exhibits a higher temperature sensitivity.

Hydrogen bonding plays an important role in cooperativity for both low molecular weight materials and polymers. The cooperativity of a series of disubstituted benzenes with various potentials for hydrogen bonding, investigated by Angell,[156] showed that materials that can form stronger hydrogen bonding were more fragile. Bohmer et al.[157] and Roland and Ngai[158] observed the same trends. Phenolic novolac/bisphenol-A epoxy networks, showed that both the crosslink density and hydrogen bonding affected the glass formation processes.[150] On the contrary, relatively non-polar polymers such as polyethylene and polytetrahydrofuran showed low fragility values which corresponded to weak intermolecular interactions.

4.1.3. Thermal and thermo-oxidative stability of novolac/epoxy networks

Phenolic networks are well known for their excellent thermal and thermo-oxidative stabilities. A detailed review on the decomposition pathways can be found in chapter 1.8. The present work focuses on characterizing novolac/epoxy networks using cone calorimetry.

The cone calorimetry, so called because of the geometric arrangement of the electric heater, measures the heat release rate, total heat released, ignitability, effective heat of combustion, specific extinction area (a measure of the smoke production), soot yield, mass loss rate, and the evolution of carbon monoxide, carbon dioxide, and other

---

[156] C. A. Angell, "Transport Processes, Relaxation, and Glass Formation in Hydrogen-Bonded Liquids," *Hydrogen Bonded liquids*, J. C. Dore and J. Teixeira, Eds., Vol. **329**, pp59-79, 1991.

[157] R. Bohmer, K. L. Ngai, C. A. Angel, and D. J. Plazek, "Nonexponential Relaxations in Strong and Fragile Glass Formers," *Journal of Chemistry and Physics* **99**(5), 4201-4209 (1993).

[158] C. M. Roland and K. L. Ngai, "Normalization of the Temperature Dependence of Segmental Relaxation Times," *Macromolecules* **25**(21), 5765-5768 (1992).

combustion products. The results obtained using cone calorimetry, specifically ignitability, surface flame spread rate and available surface area, and heat release rate per unit area can be used to predict the behaviors of materials in a full-scale fire. Ignitability and flame spread effects have been shown to be insignificant for most materials. Heat release rate therefore is generally considered the most important material parameter in fire studies and is calculated based on the oxygen consumption principle. The principle uses the basic assumption that the heat of combustion per unit mass of oxygen consumed is essentially constant and has an average value of 13.1 KJ/kg for most organic materials. The heat rate, q, is related to the difference of the initial inflow and the total mass flow of oxygen in the combustion products,[159]

$$q = \left(\frac{\Delta h_c}{r_o} \right) \left(m_{o_2,\infty} - m_{o_2} \right) \qquad \textbf{(4. 11)}$$

where q = heat rate (kW)

Δh_c = net heat of combustion (kJ/kg)

r_o = stoichiometric oxygen to fuel mass ratio

$m_{O2,\infty}$ = initial mass flow of oxygen (kg/s)

m_{O2} = total mass flow of oxygen in combustion products (kg/s)

A primary advantage of this principle is that the instrument does not need to be thermally insulated, allowing for design of an accurate yet simple instrument (Figure 4. 4). Samples can be tested in a horizontal or vertical orientation and can be irradiated with a heat flux from zero to over 100 kW/m^2 with good uniformity. The only limitations are that the sample should not swell sufficiently to interfere with the spark plug operation or with the heater, and the specimens should not show explosive spalling or delamination.[159] Samples that melt and flow upon heating must be tested in the horizontal orientation. The mass loss rate is measured using a load cell; the specific extinction area is

[159] V. Babrauskas, "Development of the Cone Calorimeter – A Bench-Scale Heat Release Rate Apparatus Based on Oxygen Consumption," *Fire and Materials* **8**(2), 81-95 (1984).

determined using a helium-neon laser; and the CO and CO_2 yield during combustion is obtained using a CO/CO_2 analyzer.

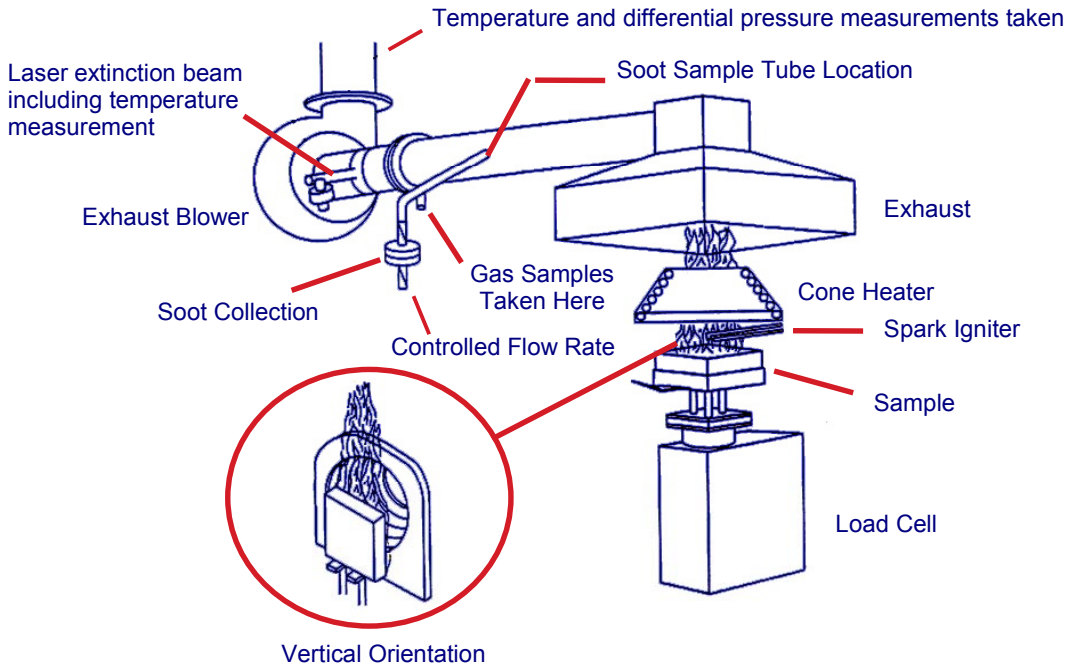

Figure 4. 4. Schematic of a cone calorimeter

Most materials exhibit a single peak heat release rate (PHRR) or maximum in the heat release rate curves. However, in some char forming materials, there may be an initial peak followed by a gradual increase to a second peak. The heat release rate drop after the first peak is attributed to the formation of an isolating char layer and the second peak is suggested to occur when the specimen was "heated through to the rear face and no longer behaves as if thermally thick".[159] An alternative explanation for the observed initial spike is the rapid burning of volatiles that build up prior to ignition. It is possible that both char layer and rapid burning of volatiles contribute to the initial spike. However, to date, there is no concrete evidence for the char layer while intense burning masks the burning of volatiles in non-char yielding materials.

The flame retardance of phenolic novolac/epoxy networks cured with various diepoxides has been measured (Table 4. 2).[148,149] The heat release rate curves for all

networks investigated exhibited an initial spike in addition to the peak heat release rate. The brominated bisphenol-A epoxy cured networks had the lowest peak heat release rates, but produced large amounts of toxic CO gas (high CO/CO_2 ratio). In addition, bromine incorporation released HBr and other carcinogenic by-products during burning. Phenolic novolac cured with siloxane based epoxy yielded networks with low peak heat release rates and the lowest toxicity. Surprisingly, curing networks with bisphenol-F epoxy, fluorinated epoxy, or stilbene epoxy did not alter the peak heat release rates in comparison with the bisphenol-A epoxy cured networks. Networks cured with bisphenol-F epoxy gave rise to higher smoke toxicity compared to the bisphenol-A cured networks.

Table 4. 2. Cone calorimetry results on phenolic novolac/epoxy networks (65:35 wt:wt ratio)

Epoxy	PHRR (kW/m^2)	Char Yield (wt %)	Smoke Toxicity (CO/CO_2) ($x10^{-3}$)
Phenolic Control (Resole)	116	65	11
Epoxy Control	1230	5	44
Bisphenol-A	357	29	34
Brominated bisphenol-A	165	8	189
Bisphenol-F	397	17	76
Disiloxane	325	22	24
Fluorinated	353	--	--
Stilbene	407	--	--

As expected, compositions containing larger amounts of phenolic component showed lower peak heat release rates, higher char yield, and lower smoke toxicity. The same trend in char yield was observed using thermogravimetric analysis.[148,149]

Cone calorimetry was used to evaluate the flame properties of brominated epoxy composites and phenolic composites reinforced with fiberglass, aramid, or graphite fiber under controlled oxygen atmospheres.[160] The time to ignition (TTI) was essentially

[160] F. Hshieh and H. D. Beeson, "Flammability Testing of Flame-Retarded Epoxy Composites and Phenolic Composites," *Fire and Materials* **21**, 41-49 (1997).

identical for all of the epoxy composites under normal oxygen atmosphere. The epoxy/graphite composite showed higher TTI under oxygen-depleted environments, probably due to the higher thermal conductivity of the graphite fiber. The TTI of phenolic composites were proportional to their thermal conductivities at all oxygen levels. Using the TTI to PHRR ratio as an indication of the propensity to flashover, increased oxygen concentration reduced the flame resistance for both epoxy composites and phenolic composites. As expected, phenolic composites showed more resistance to flame and had much lower smoke productions than epoxy composites.

4.2. Experimental

4.2.1. Materials

The 2000 g/mol cresol novolac resin was prepared according to procedures described in chapter 3. Triphenylphosphine (TPP) was purchased from Aldrich. The commercial phenolic novolac resin used in the control experiments was provided by Georgia Pacific (Product #GP-2073). Epon 828 epoxy resin was obtained from Shell Chemical. D.E.N. 438 epoxy was supplied by the Dow Chemicals Co. All reagents were used as received.

4.2.2. Methods

4.2.2.1. Preparation of ortho-cresol novolac networks cured with epoxies

A 2000 g/mol *ortho*-cresol novolac resin was cured with a difunctional or a multifunctional epoxy using triphenylphosphine as the catalyst. To a three neck round bottom flask equipped with a vacuum tight mechanical stirrer and a vacuum adapter was added cresol novolac and ~85 weight % of the required epoxy. The flask was heated in an oil bath to 170°C. When the novolac began to soften at ~170°C, mechanical stirring was begun. Vacuum was applied incrementally to prevent the material from foaming into the vacuum line. Once full vacuum was achieved (2-5 Torr) the solution was stirred for about 10 minutes to degas the blend. During this time the remaining epoxy, with the

catalyst (0.1 mol % based on the total weight of epoxy) dissolved in it, was degassed in a vacuum oven at ~80°C. The vacuum was temporarily released to add the remaining epoxy with catalyst. This was stirred for about 3 minutes to fully degas the samples. The melt was then poured into a mold and placed in a preheated oven. The samples were cured at 200°C for 2 hours and then 220°C for 2 hours.

4.2.2.2. Sample preparation for viscosity determinations

Ortho-cresol novolac/epoxy mixtures were melt mixed at 165°C. The exposure time to heat was maintained for less than 3 minutes to prevent premature curing. The mixed samples were quenched in dry ice/isopropanol chilled aluminum pans. The samples were ground into powder prior to use.

4.2.2.3. Network formation of phenolic control

A resole resin was cured thermally to form a typical phenolic network (phenolic control). The cure cycle consisted of 70°C for 4 days, 130°C for 24 hours, and then 200°C for 24 hours.

4.2.3. Characterization

4.2.3.1. Resin glass transition temperatures

The glass transition temperatures of neat resins were obtained via a Perkin-Elmer differential scanning calorimetry (DSC-7 Instrument). The DSC was calibrated with indium and zinc standards, and ice water was used as the coolant. Samples in aluminum pans were heated from 25 to 180°C at 10°C/min. The glass transition temperatures were calculated as the midpoints of the curves obtained from the second temperature scan.

4.2.3.2. Network glass transition temperatures

A Perkin-Elmer dynamic mechanical analyzer (model DMA-7), in a three-point bending mode, was used to determine the glass transition temperatures of cured networks. The T_gs were calculated from the peaks of the tan delta curves. The static force was set to 200 mN and the dynamic force was set to 175 mN. Samples were heated at 5°C/min

from 25 to 200°C. Two samples of each material were measured and the results were averaged.

4.2.3.3. Critical stress intensity factor, K_{IC}

The critical stress intensity factor, K_{1C}, was used to evaluate the fracture toughness of the phenolic/epoxy networks. The K_{1C} values were obtained from a three-point bend test using an Instron instrument, according to ASTM standard D5045-91.[161] The specimens had a thickness (b; ~3.1mm) and a width (w; ~6.3mm). The single edge notched bending method was used. An eccentric compressive load was utilized to aid the pre-cracking of the specimens.[162] First, a sharp notch was created in the sample by sawing. The sample was placed in a vise where it was subjected to tension and compression (Figure 4. 5), a cold razor blade (which had been immersed in liquid nitrogen) was inserted into the notch and force was applied to initiate a natural crack. The depth of the crack (a) was between 40 and 60 percent of the width (w). The pre-cracked notched specimen was loaded crack down into a three-point bend fixture and tested using an Instron model 4204 instrument. The single edge notched bending rig had moving rollers to avoid excessive plastic indentation. The three-point bend fixture was set up so that the line of action of applied load passed midway between the support roll centers within 1% of the distance between these centers. The crosshead speed was 1.27 mm/minute, and the testing was conducted at room temperature.

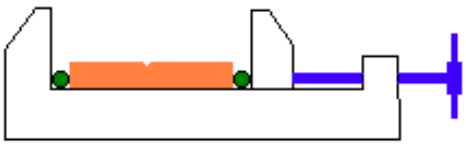

Figure 4. 5. Experimental implementation of the eccentric axial load technique

[161] ASTM D 5045-91 "Standard test methods for plane-strain fracture toughness and strain energy release rate of plastic materials," 1991.

[162] D. A. Dillard, P. R. McDaniels, and J. A. Hinkley, "The Use of an Eccentric Compressive Load to Aid in Precracking Single Edge Notch Bend Specimens," *Journal of Materials Science letters* **12**, 1258-1260 (1993).

The critical stress intensity factor, K_{IC}, was calculated using the following equation.

$$K_{IC} = \frac{P\,S}{B\,W^{3/2}} \frac{3\,(x)^{1/2}\,[1.99 - x\,(1-x)\,(2.15 - 3.93x + 2.7x^2)]}{2\,(1+2x)\,(1-x)^{3/2}} \qquad \textbf{(4. 12)}$$

where P = maximum load (kN)

S = span (cm)

B = specimen thickness (cm)

W = specimen depth or width (cm)

a = crack length

x = the ratio of crack length to width of the specimen, (a/W)

4.2.3.4. Sol/gel fraction separation

The sol/gel fractions of the networks were determined as follows. Samples of approximately 0.6g were submerged at room temperature in ~15 ml acetone for 3 days. The sol fractions were soluble and the gel fractions stayed intact. The gel fractions were separated from the sol fractions by filtering the solids from the solutions. The gel fractions were dried in a vacuum oven at 180°C for 24 hours and compared to their initial weights. The acetone in the sol fractions was evaporated at room temperature in a vacuum oven. The sol fractions were also analyzed by ^{1}H NMR in order to determine their chemical contents.

4.2.3.5. ^{1}H NMR sol fraction characterization

^{1}H NMR spectra were obtained on a Varian Unity 400 NMR spectrometer. 5 mm tubes containing approximately 20 mg sample dissolved in DMSO-d6 or acetone-d6 were analyzed under ambient conditions. The experiment's parameters include 1.000 second relaxation delay, 23.6 degrees pulse, and 6744.9 Hz widths. Thirty-two repetitions were performed for each sample.

4.2.3.6. Room temperature density measurements

Room temperature density measurements were conducted using a Mettler-Toledo AG204 balance adapted with a Mettler-Toledo density determination kit for AT/AG and PG/PR balance. Samples with dimensions of approximately 19 mm x 6.4 mm x 3.2 mm were sanded, then polished, to prevent any trapping of air bubbles. Deionized water was degassed in a vacuum oven at room temperature for 30 min prior to use. Using this setup, the weight of the solid in air (A) and the weight of the solid in water (B) were measured. The temperature of the water was recorded to within 0.1°C and the density of distilled water at that temperature ($\rho(H_2O)$) was obtained from a density table. Room temperature densities were calculated using the following equation

$$\rho = [A/(A-B)]\ \rho(H_2O) \qquad \textbf{(4. 13)}$$

The densities at T_g+50°C were calculated using the densities at room temperature and the coefficients of thermal expansion (CTE) below and above the T_g.

4.2.3.7. Determination of coefficient of thermal expansion (α)

One dimension thermal expansion was measured using a thermomechanical analyzer equipped with a large quartz parallel plate. The specimen height was monitored as the sample was heated from 25°C to 200°C at 5°C/min. The coefficients of thermal expansion (CTE) were determined by calculating the slope above and below the T_g of the material.

4.2.4.8. Rubbery moduli determination via creep tests

The rubbery moduli (E) of networks at 50°C above the glass transition temperatures were determined using a stress-strain test via a Dynastat instrument. Samples with dimensions of approximately 19mm x 6.3mm x 3.1mm were placed in a three-point bend fixture and heated to 50°C above the T_g. A small load (0.01kg) was placed on the sample and the displacements at equilibrium were measured. Equilibrium was reached within 5 seconds. The load was increased by increments of 0.01 kg up to about 0.08 kg while the equilibrium displacement was recorded at each load. The

rubbery moduli were determined from the slopes of load versus displacement curves. The displacement values measured from the Dynastat are accurate to within 0.05 mm.

$$E = g\left(\frac{P}{\Delta}\right)\left(\frac{L^3}{48\,I}\right) \qquad \textbf{(4. 14)}$$

where g = gravitational constant = 9.81 m/s^2

P/Δ = slope of load versus displacement

L = length between supports = 2.54 cm

and

$$I = (1/12)wb^3 \qquad \textbf{(4. 15)}$$

where w = width of the sample

b = height of the sample

According to the theory of rubber elasticity, the number average molecular weight between crosslinks (M_x) is inversely proportional to the rubbery modulus,

$$M_x = 3RT\rho/E \qquad \textbf{(4. 16)}$$

where R = gas constant,

T = experimental temperature (K)

ρ = density of the sample at the experimental temperature; calculated from the room temperature density and CTE values of the samples,

E = elastic modulus obtained from the Dynastat measurements.

4.2.3.9. 10sec relaxation moduli determination via stress relaxation tests

Stress relaxation experiments were also conducted on the Dynastat instrument in the three-point bend mode. The samples were initially heated to 70°C below the T_g (T_g determined from the peak of the DMA tan delta curve). The upper beam was set to a position just above the sample with no contact or applied forces, and the instrument was equilibrated for at least 3 minutes. To begin testing, the upper beam was lowered by 0.1

mm. The load was measured and recorded as a function of time as the sample relaxed for 1000 seconds. The displacement was then removed and the samples were allowed to recover for 2000 seconds. This test was repeated at each temperature interval from T_g-70°C to T_g+30°C at 5°C increments. In addition to the applied displacement, the displacement increased with temperature increases due to thermal expansion by the instrument and the sample. The CTE of instrument was approximately 0.0033 mm/°C and the CTE of the samples was determined using TMA. The sample expansion can be ignored since it is insignificant compared to the instrument expansion and applied displacement. The modulus at each temperature for each displacement was calculated using equation (4.14). The modulus calculated after 10 seconds relaxation was plotted as a function of temperature.

Master curves were constructed from these stress relaxation results according to the time-temperature superposition principle. After a reference spectrum was assigned (generally at the T_g of the network), other spectra, determined at various temperatures, were shifted horizontally until a single continuous curve was generated.

4.2.3.10. Flame retardance measured via cone calorimeter

Cone calorimetry was used to measure the flame retardance of novolac/epoxy networks. Sample panels of approximately 6.3 mm thickness and surface dimensions of 10x10 cm were tested at a 50.0 kW/m^2 incident heat flux in a controlled atmosphere cone calorimeter. The ignitability, peak heat release rate, the evolution of CO and CO_2, and the time to sustained ignition are among some of the parameters measured.

4.2.3.11. Thermal and thermo-oxidative degradation

A Perkin-Elmer TGA-7 thermogravimetric analyzer was used to determine the thermal and thermo-oxidative stabilities of cresol novolac/epoxy networks. Samples of approximately 5-8 mg were placed in a platinum sample pan and heated in a furnace at 10°C/min from 30 to 900°C. Air or nitrogen was used as the carrier gas. The sample weight loss was monitored as a function of temperature.

4.2.3.12. Viscosity measurements

Dynamic complex viscosities were obtained from a Bohlin VOC Rheometer operating in continuous oscillation mode with a frequency of 1 Hz. Temperature control was accomplished with a Bohlin HTC. The auto-strain was set to maintain the torque at 25% of the maximum torque allowed. The maximum strain for the instrument was 0.25. Approximately 0.7g of dry powder sample were pressed into pellets, then placed between the preheated 25 mm diameter parallel plates of the rheometer. The gap was closed to approximately 1mm and the sides were scraped to remove excess sample before the run was started.

A Brookfield DV-III Programmable Rheometer was used to determine the isothermal viscosities of novolac/epoxy mixtures. Approximately 10g of powder samples were placed in disposable sample tubes and heated to the test temperatures. A spindle, which was driven through a calibrated spring, was immersed in the test fluid. The viscous drag of the fluid against the spindle was measured by the spring deflection. The torque was used to calculate the viscosities.

$$\eta\ (cp) = (100/rpm) \times T_k \times SMC \times torque \qquad \textbf{(4. 17)}$$

where rpm = 10

T_k = a constant, equal to 1.0 in these experiments

SMC = a constant which depends on the spindle diameter = 25

4.2.3.13. Equilibrium moisture uptake

To investigate moisture uptake, samples with dimensions of approximately 19 mm x 6.35mm x 1 mm were dried in a vacuum oven for 12 hours at 150°C. The initial weight of each sample was recorded. The samples were then placed in vials containing deionized water. The weights of each sample were measured as a function of time until a constant weight was reached. Water absorption at room temperature and at 62°C was determined. The sample thickness, the dimension in which water penetrates most rapidly, was normalized as the results were plotted as percent water uptake versus $t^{1/2}$/thickness.

4.2.3.14. Kinetic studies via DSC

Arrhenius activation energies, pre-exponential factors, and first order rate constants for novolac/epoxy cure reactions were determined using differential scanning calorimetry according to ASTM E 698–79.[163] Samples were heated at various heating rates and the exothermic reaction peaks were recorded. The temperatures at which the exotherm peaks occurred were plotted as a function of their respective heating rates. Kinetic parameters were calculated from the slope of this plot. The time that was required to reach 50% conversion, or the half-life time, can be predicted. A sample was aged to reach 50% conversion according to the predicted time at the selected temperature and compared to an unaged sample to confirm the validity of this method.

4.2.3.15. Flexural strength and moduli of composites

Transverse flexural tests were performed according to ASTM standard D 790–98. Composite samples with dimensions of 127 mm x 12.7 mm x 2.4 mm were measured in a three-point bend set up. The rate of crosshead motion (R) used was 7.11 mm/min which was calculated based on the following equation,

$$R = ZL^2/6d \qquad \textbf{(4. 18)}$$

where L = support span length (101.6 mm),
d = depth of the beam (2.4 mm),
Z = rate of straining of the outer fiber (0.01).

Flexural strength (σ_f) and modulus (E) were calculated as follows,

$$\sigma_f = 3PL/2bd^2 \qquad \textbf{(4. 19)}$$

$$E = L^3m/4bd^3 \qquad \textbf{(4. 20)}$$

where P = load
b = width of beam tested (12.7 mm)

[163] ASTM E 698-79 (reapproved 1993) "Standard test method for Arrhenius kinetic constant for thermally unstable materials," 1993.

L = support span length (101.6 mm),

d = depth of the beam (2.4 mm),

m = slope of the tangent to the initial straight-line portion of the load-deflection curve.

4.3. Results and Discussion

4.3.1. Properties of *ortho*-cresol novolac/epoxy networks

4.3.1.1. Network formation and characterization

Network structures in crosslinked systems generally have an enormous influence over the mechanical properties. For example, high crosslink densities generally correlate with high strengths but low fracture toughnesses. Typical phenolic novolac networks crosslinked with hexamethylenetetramine (HMTA) are brittle because they are highly crosslinked and filled with voids. Tough, void-free, networks have been prepared by curing phenolic novolacs with epoxies. In addition, if the phenolic novolac was used in excess, the resulting networks exhibited excellent flame retardance properties.[148]

The fracture toughness of crosslinked networks is related to the molecular weight between crosslinks. Increased molecular weight between crosslinks (M_c), or decreased crosslink densities, generally gave rise to tougher networks up to some point where dangling chain ends begin to dominate properties.

A primary objective of this research was to improve the fracture toughness of novolac/epoxy networks while retaining excellent flame retardance. The approach utilizes the known direct correlation between molecular weight between crosslinks and fracture toughness by using higher molecular weight oligomers in the network formation. However, increasing the molecular weight of the phenolic novolac is impractical since branching occurs once the molecular weight reaches 900-1000 g/mol.[164] Branching may lead to higher viscosities and reduce the processability. Branching sites on oligomers

[164] Knopp, A.; Pilato, L. A., *Phenolic Resins: Chemistry, Application and Performance-Future Directions*; Springer-Verlag, New York, 1985.

translate to crosslink points in the cured networks, which effectively increase the crosslink densities. Cresol novolac resins, on the other hand, are linear. Moreover, the molecular weight was strategically controlled with an endcapping reagent.

Table 4. 3. Phenolic materials and their properties

Sample	M_n (g/mol)	T_g (°C)
Phenolic novolac	~ 700	78
Ortho-cresol novolac	~ 2000	104

In this study, a controlled molecular weight 2000g/mol *ortho*-cresol novolac resin was crosslinked with two epoxies, a difunctional bisphenol-A epoxy (Epon 828) and a multifunctional epoxidized novolac (D.E.N. 438) in systematically controlled weight ratios (Figure 4. 6). The used of Epon 828 epoxy was expected to offer better processabilities since it significantly reduced the melt viscosities of novolac/epoxy mixtures. Networks crosslinked with DEN 438 were anticipated to be more flame retardant. The properties of these cresol novolac networks were evaluated and compared to an epoxy control (Epon 828 crosslinked with a stoichiometrical amount of p,p'-diaminodiphenylsulfone [4,4-DDS]), a phenolic control (heat cured resole network), and a phenolic novolac/Epon 828 network (65:35 wt:wt ratio).

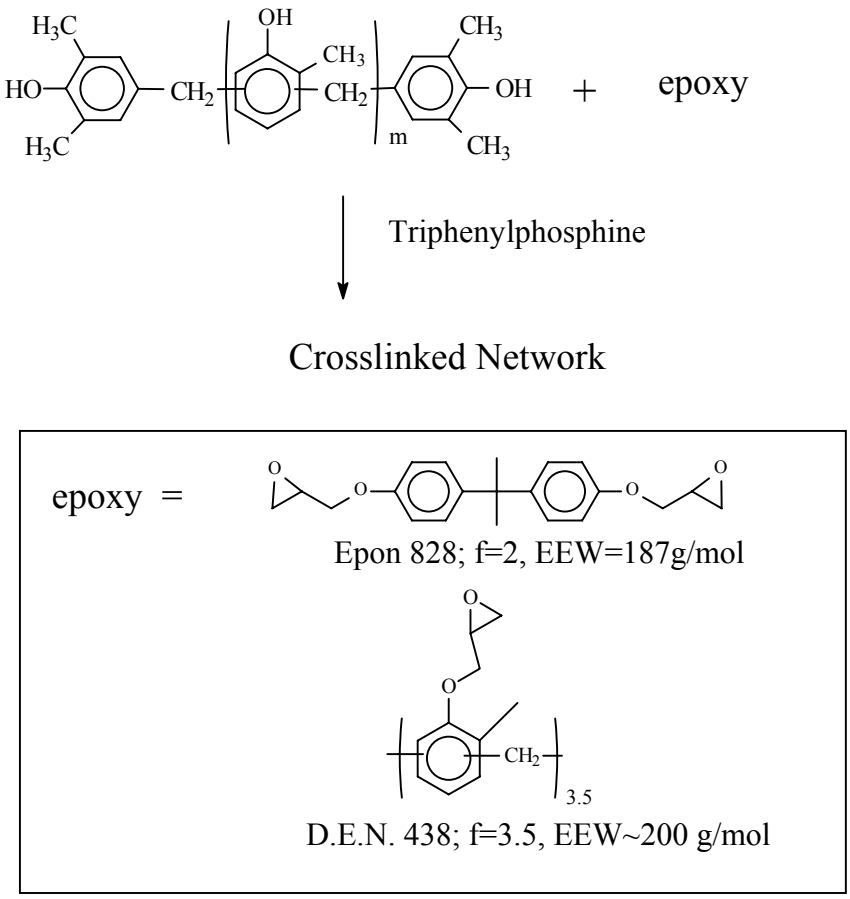

Figure 4. 6. Crosslinking reaction of *ortho*-cresol novolac and epoxy (Epon 828 or D.E.N. 438) using triphenylphosphine as the catalyst

The network properties including fracture toughness, T_g, and weight percentage of sol fractions were determined for Epon 828 and D.E.N. 438 epoxy cured cresol novolac networks (Table 4. 4). Network fracture toughness was determined by measuring the plane-strain stress intensity factor, K_{IC}. Higher K_{IC} values correspond to improved resistance to crack propagation or increased toughness. For both series, the 60:40 wt:wt cresol novolac/epoxy networks exhibited the highest fracture toughness and this remained relatively high as the novolac composition was increased to 70 wt. %. The toughness decreased drastically when the novolac contents were increased to 80 wt. %. The 70:30 and 60:40 wt:wt cresol novolac/epoxy networks had higher toughness values than the phenolic control, the 65:35 wt:wt phenolic novolac/Epon 828 network, and the epoxy

control. The 70:30 compositions had the highest T_gs and lowest sol fractions. The T_g and the sol fraction increased when the novolac composition was increased or decreased.

Table 4. 4. Network properties of *ortho*-cresol novolac/epoxy networks

Epoxy	Novolac Wt %	OH:epoxy	K_{1C} (MPa/m$^{1/2}$)	T_g (^oC)	Sol fraction (%)
Epoxy Control	--	--	0.62	127	--
Phenolic control	--	--	0.16	--	--
Epon 828*	63	3.0:1	0.85	137	12.5
Epon 828**	80	6.2:1	0.65±0.06	144	16.7
	70	3.6:1	1.06±0.04	154	5.4
	60	2.3:1	1.20±0.12	133	7.1
D.E.N. 438**	80	5.0:1	0.46±0.04	145	15.6
	70	2.9:1	1.05±0.09	152	4.3
	60	1.9:1	1.08±0.10	142	11.7

* Phenolic novolac/epoxy networks

** *Ortho*-cresol novolac/epoxy networks

To understand these unexpected network properties, network structures were investigated in an attempt to relate the structures with properties.

A simple approach that determined the chemical compositions of the sol fractions is ^{1}H NMR (Figure 4. 7). Since epoxides show five distinct sets of peaks, the presence of epoxy functionality can be detected with ease. ^{1}H NMR of sol fractions showed traces of epoxy for the network compositions higher in novolac (80:20 and 70:30 wt:wt cresol novolac/epoxy networks). The sol fractions of the 60:40 wt:wt cresol novolac/epoxy network, on the other hand, consisted of large amounts of unreacted epoxies, even though these had a stoichiometric excess of phenol. This suggests that the networks at 60:40 compositions became too dense for further phenolic hydroxyl/epoxy reactions to occur since post-curing well above T_g did not promote any further reactions. This may also explain why the fracture toughness reached a certain maximum limit above which an increase in epoxy content did not increase the toughness.

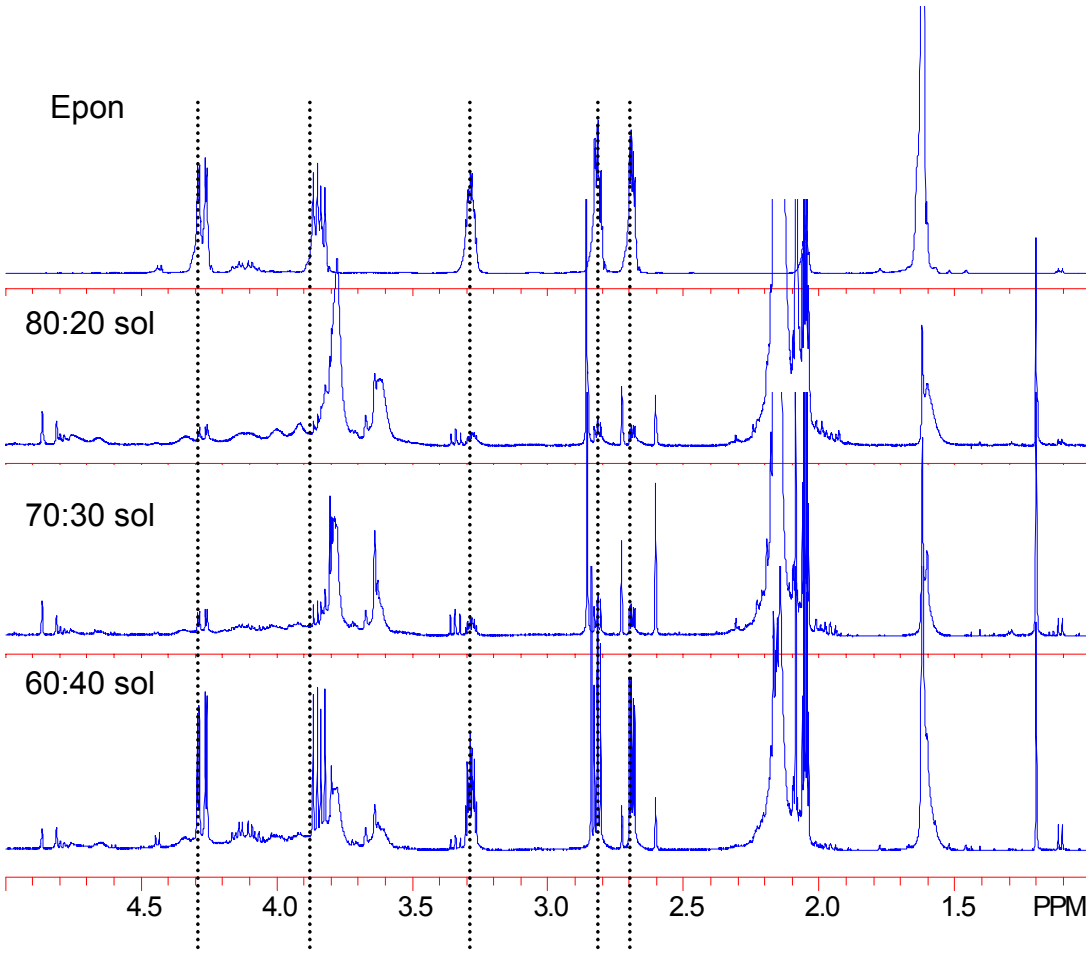

Figure 4. 7. **^{1}H NMR of the sol fraction of cresol novolac/Epon 828 networks**

The effect of network structures on T_g was also explored (Table 4. 4). For both series, the T_g was highest for the 70:30 wt:wt cresol novolac/epoxy networks. This is consistent with the low sol fractions in these compositions suggesting that the chains in these networks are well connected. By contrast, the 60:40 wt:wt cresol novolac/epoxy networks which contained a significant amount of unreacted epoxy groups had lower T_gs. The 80:20 composition also exhibited lower T_gs due to their low crosslink densities and high sol fractions. T_g is a function of crosslink density and the amount of sol fraction/dangling ends in the networks.

To further understand the network structures, the molecular weights between crosslinks were calculated (Table 4. 5). The theory of rubbery elasticity was used to

estimate the molecular weight between crosslinks for the cresol novolac/epoxy networks. According to this theory, network rubbery moduli are inversely proportional to the molecular weights between crosslinks. The rubbery moduli were measured using a stress-strain test in a three-point bend set up at T_g+50°C, a temperature well above the material glass transition temperature. The network glass transition temperatures and densities at the measurement temperature (T_g+50°C) were determined prior to calculation. It should be noted that the rubbery moduli should be measured for networks containing only the gel fraction. However, the rubbery moduli were measured on unextracted networks in these experiments.

Table 4. 5. Crosslink densities of cresol novolac/epoxy networks

Epoxy	Novolac Wt %	T_g (ºC)	ρ (25ºC)	ρ (T_g+50ºC)	Modulus T_g+50ºC	M_x (g/mol)
Epon828*	65	127	1.23	1.18	9.35×10^6	1413
Epon 828**	80	144	1.178	1.163	1.82×10^6	6650
	70	154	1.183	1.168	8.25×10^6	1510
	60	133	1.181	1.168	3.20×10^6	3730
D.E.N. 438**	80	145	1.199	1.184	2.63×10^6	4700
	70	152	1.191	1.173	9.12×10^6	1360
	60	142	1.191	1.174	8.02×10^6	1510

* Phenolic novolac/epoxy networks

** *o*-Cresol novolac/epoxy networks

For cresol novolac/Epon 828 networks, the 70:30 composition exhibited the highest rubbery modulus and therefore the lowest apparent M_x. The calculated M_x (1510 g/mol) is a reasonable value for well connected networks prepared with a 2000 g/mol oligomer. The rubbery modulus decreased and the M_x increased significantly at the 60:40 composition. According to the ^{1}H NMR analysis on sol fractions, a large amount of epoxy remained unreacted at this composition. The low molecular weight fraction, along with dangling chain ends, probably did not contribute mechanically, and therefore reduced the rubber modulus and increased the apparent molecular weight between crosslinks. When the cresol novolac content was increased to 80 weight percent, the

rubbery modulus again decreased. The high molecular weight between crosslinks was attributed to a looser network formed with less epoxy. The same trends were observed for the D.E.N. 438 epoxy cured cresol novolac networks.

Surprisingly, these results indicated that the networks comprised of 80:20 wt:wt cresol novolac/epoxy (or 6.2 hydroxyl per 1 epoxy) did not form sufficiently well connected networks. The stoichiometric ratio was optimized at 70:30 wt:wt cresol novolac/epoxy compositions (or 3.6 hydroxyl per 1 epoxy) where all the epoxies were reacted into the networks and the apparent M_x was most reasonable. At this composition, networks with superior properties, i.e. high fracture toughness, high T_gs, low sol fractions, and sufficiently high crosslink densities were generated. At the 60:40 composition (2.3 hydroxyl per 1 epoxy), the networks became too dense. The lack of molecular mobility probably prevented further phenolic hydroxyl/epoxy reactions, thereby leaving unreacted epoxies in the sol fractions.

Both the glassy and the rubbery moduli were evaluated from a plot of 10-second stress relaxation moduli verses temperature. As described earlier, these moduli were evaluated for unextreacted cresol novolac/epoxy networks. As expected, the rubbery moduli for cresol novolac/Epon 828 networks (Figure 4. 8), phenolic novolac/Epon 828 networks (Figure 4. 9), and cresol novolac/DEN 438 networks (Figure 4. 10) increased as the network crosslink density increased. For most materials, the same trends are observed for glassy moduli where higher crosslink densities lead to slightly higher glassy moduli. However, for Epon 828 cured cresol novolac and phenolic novolac networks, the glassy moduli for the 80:20 composition was significantly higher than for the 70:30 and 60:40 compositions. This increase in the glassy modulus for the 80:20 composition was most likely due to its ability to form strong hydrogen bonding between unreacted phenolic hydroxyl groups. Since the sol fractions were not removed prior to measurement, an antiplasticization effect could also led to the increased glassy moduli. The hydrogen bonding interactions did not play an as important role in the 70:30 and the 60:40 compositions since more hydroxyl groups were reacted with epoxies at these compositions.

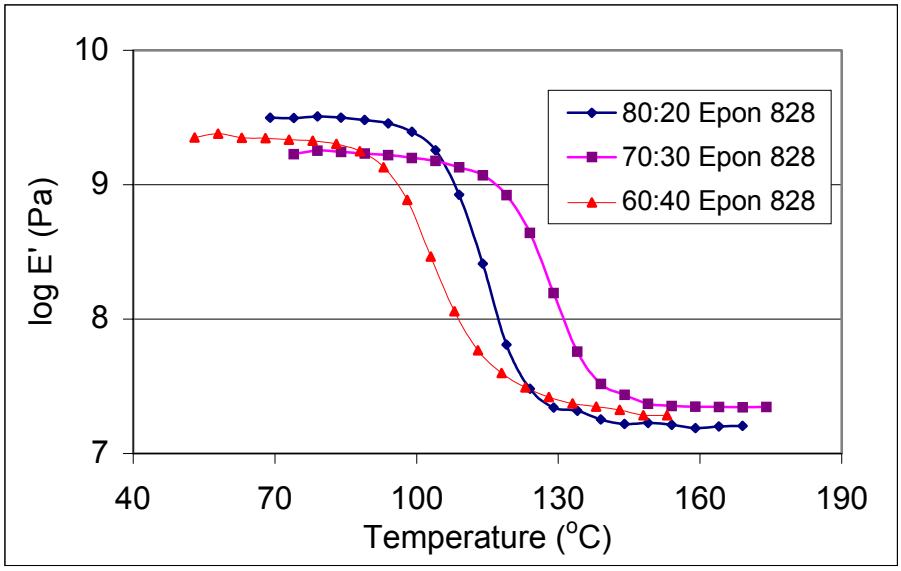

Figure 4. 8. **10s Relaxation moduli as functions of temperatures for cresol novolac/Epon 828 networks**

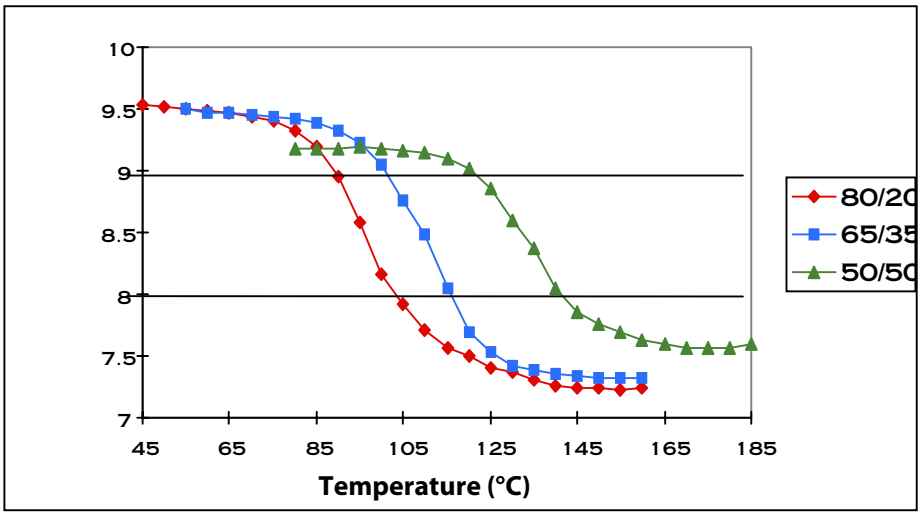

Figure 4. 9. **10s Relaxation moduli as functions of temperatures for phenolic novolac/Epon 828 networks**

The hydrogen bonding interaction, which affects the glassy moduli, was not observed for the D.E.N. 438 cured cresol novolac networks. The glassy moduli for all compositions were comparable (Figure 4. 10). Both the rubbery and the glassy moduli follow the expected trends.

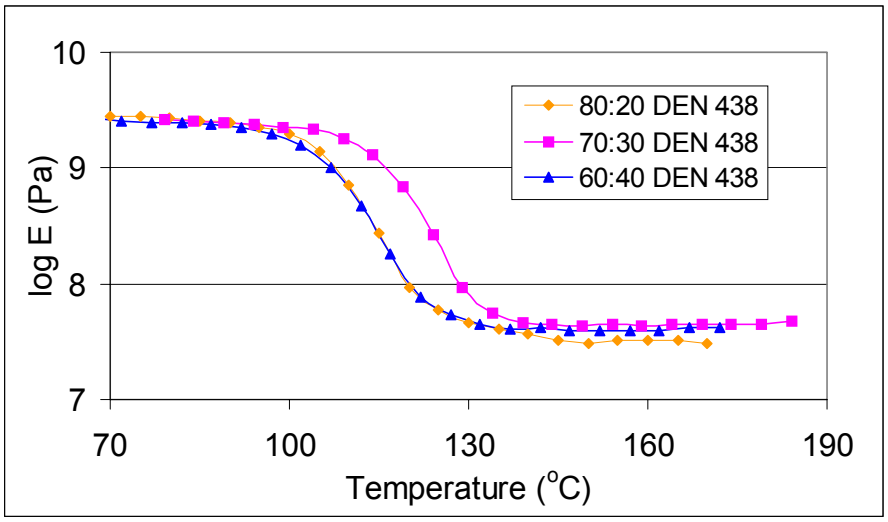

Figure 4. 10. 10s Stress relaxation moduli as functions of temperatures for cresol novolac crosslinked with D.E.N. 438 epoxy

4.3.1.2. Master curves and cooperativity

Network crosslink densities and chemical compositions play important roles in the glass formation processes. The behaviors of cresol novolac/epoxy networks during cooling toward the glass transition region were investigated by the cooperativity theory. The temperature dependence of stress relaxation moduli over a 1000-second period were determined for cresol novolac/epoxy networks near the glass transition regions (T_g-70 to T_g+30ºC) (Figure 4. 11). The relaxation spectrum measured near the glass transition temperature was assigned as the reference. Using the time-temperature superposition principle, horizontal superposition was performed on the log time scale until a single continuous master curve was generated. The shifting involved multiplication of the original time by a temperature shift factor (a_T). The stress relaxation behaviors over a wide range of time or frequency are depicted in these master curves.

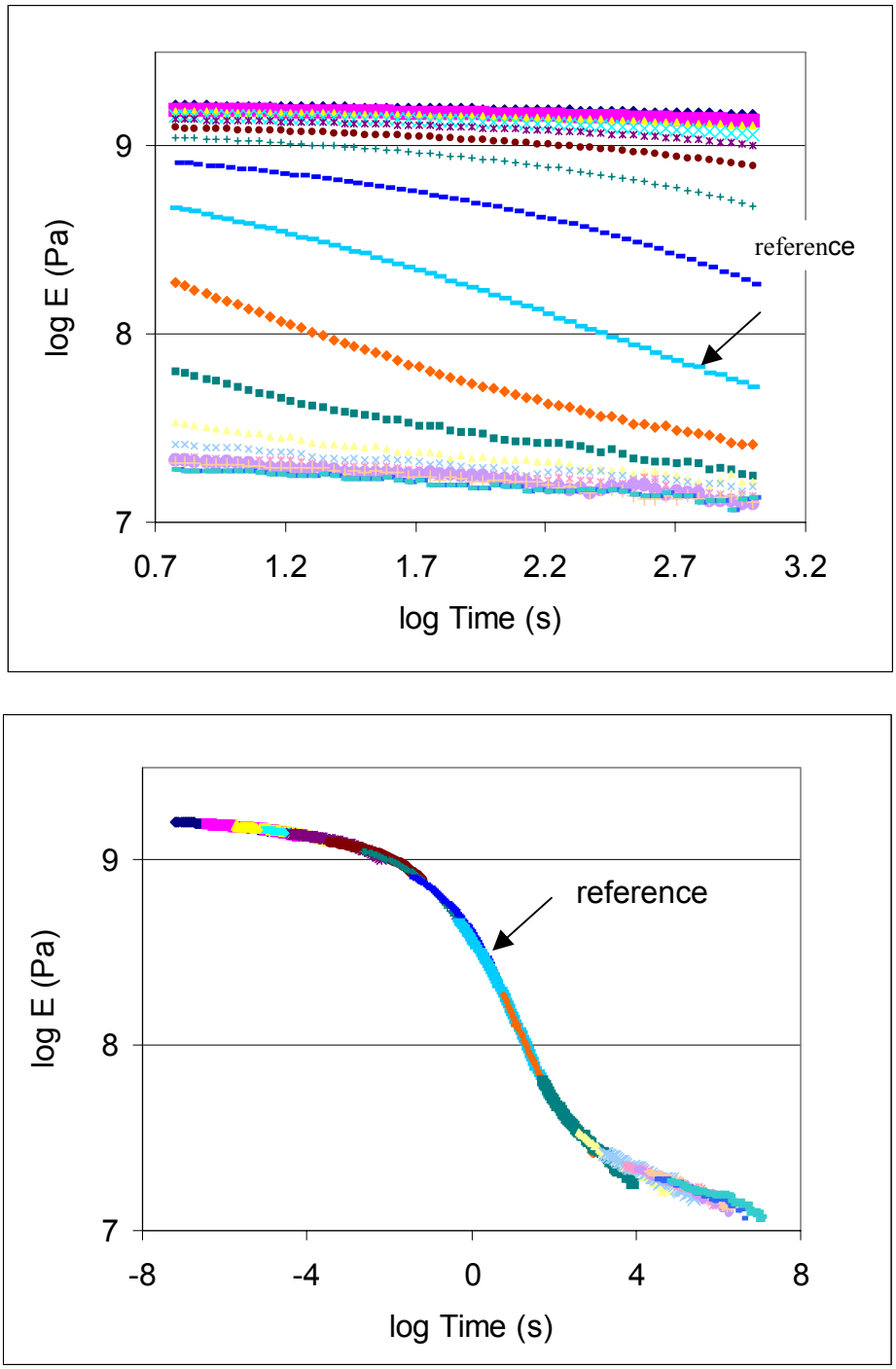

Figure 4. 11. **Master curve constructions for a typical cresol novolac/epoxy network: a) stress relaxation moduli of a cresol novolac/epoxy network measured from T_g-60°C to T_g+40°C at 5°C intervals, and b) the master curve**

The log of the shift factors were plotted against $T-T_g$ (Figure 4. 12). Both the master curve and the shift factor plot must be continuous and show a reasonable shape for this approach to be valid.

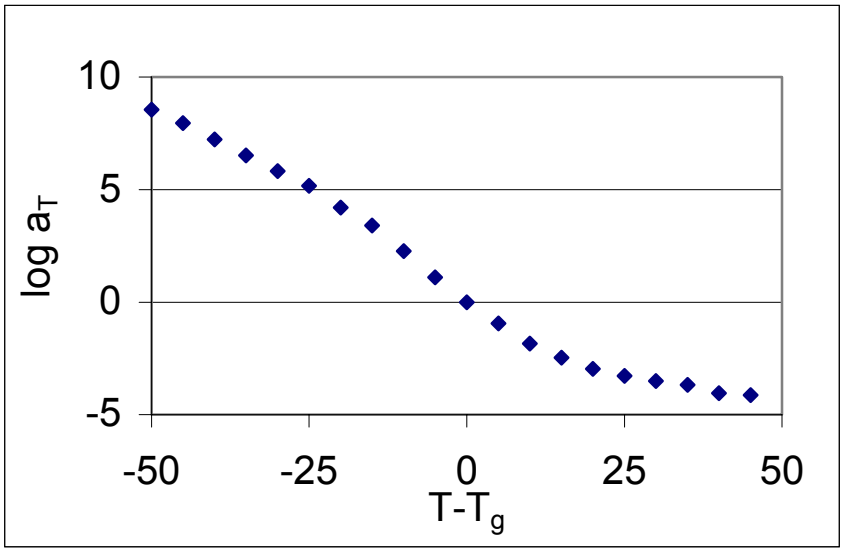

Figure 4. 12. The shift factor plot

The nature of segmental motions from glass to rubber transition was investigated using cooperativity plots (or fragility plots), which are generated by plotting log a_T versus T_g/T (Figure 4. 13 and Figure 4. 14). Data were fitted to a 3rd degree polynomial curve. The slope of the curve where T_g/T equals 1 is described as its fragility (m). As a material is heated from its glassy state through the T_g into its rubbery region, the chains begin to relax. Due to crowding, the relaxation of a single chain requires its neighboring chains to relax simultaneously. The larger the volume of neighboring chains, the more cooperative the material becomes. The fragility (m) therefore depends on the local friction coefficient, inter- and intra-molecular hydrogen bonding, and when applicable, the stiffness of the chain, the morphology, and low molecular weight additives.

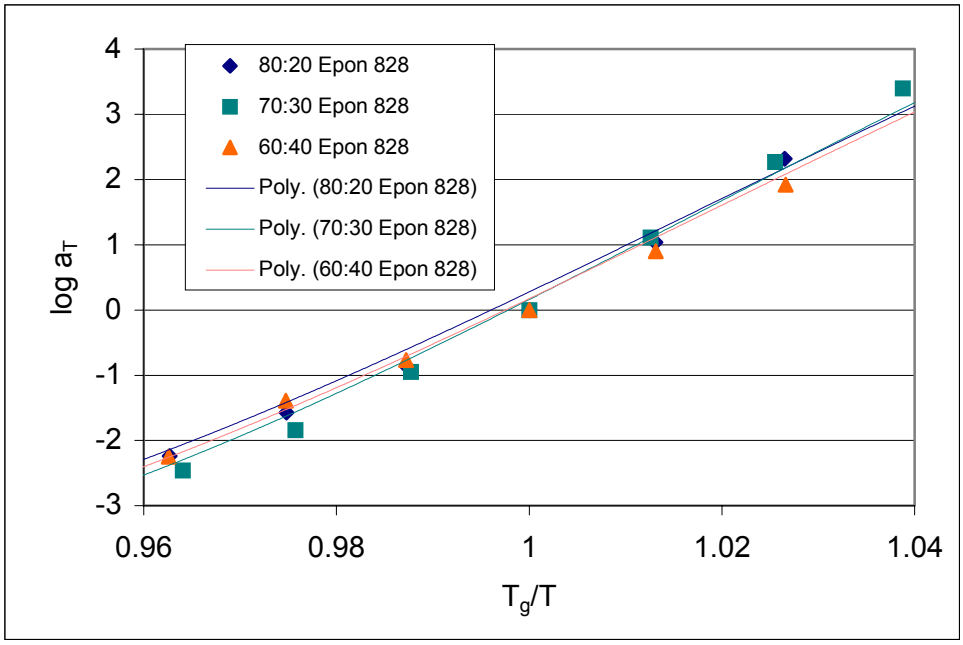

Figure 4. 13. Cooperativity plots of cresol novolac/Epon 828 networks

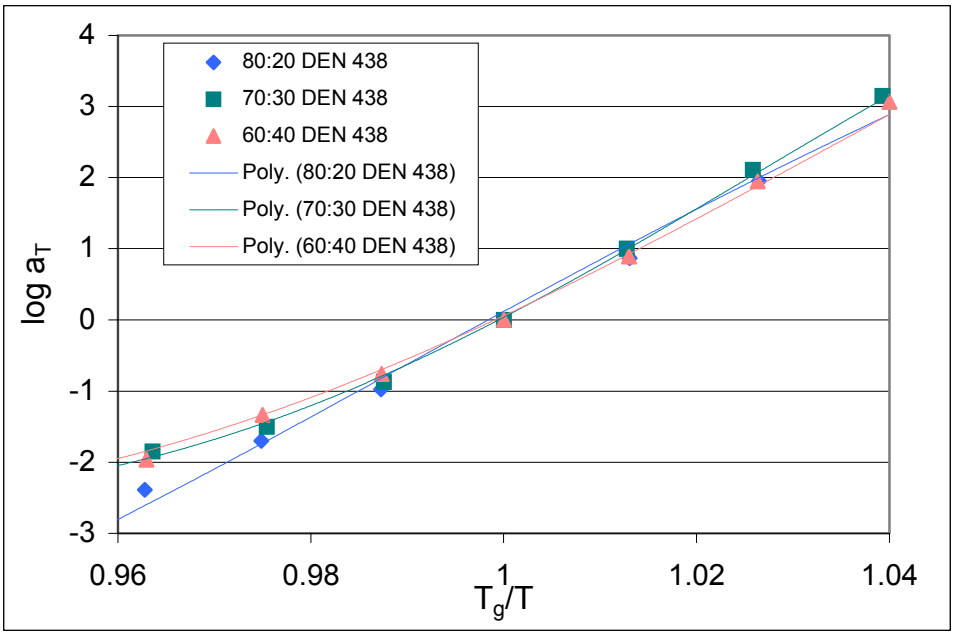

Figure 4. 14. Cooperativity plots of cresol novolac/D.E.N. 438 networks

For cresol novolac/Epon 828 networks, the fragility was highest for 70:30 composition due to its high crosslink density (Table 4. 6). A higher fragility value was observed for the 80:20 composition although it had a lower crosslink density than the 60:40 composition. This was attributed to the presence of large amounts of free phenolic hydroxyl groups which formed strong inter- and intramolecular hydrogen bonding. The 60:40 composition exhibited the lowest fragility value due to its relatively low crosslink density and low propensity for hydrogen bonding. Cresol novolac/Epon 828 networks (70:30 composition) exhibited a significantly higher fragility value than the phenolic novolac/Epon 828 networks with similar phenolic compositions (65:35 composition). Since a pendent methyl substituent was present on each cresol novolac repeat unit, it was anticipated that these bulkier groups reduced the free volume and, therefore, increased the fragility.

Table 4. 6. Fragility measuring the crosslink densities and degree of hydrogen boning interaction for cresol novolac/epoxy networks

Epoxy	Novolac/Epoxy (wt:wt)	M_x (g/mol)	Fragility (m)
Epon 828*	65:35	1410	67
Epon 828**	80:20	7260	75
	70:30	1640	84
	60:40	4110	64
DEN 438**	80:20	5130	71
	70:30	1480	74
	60:40	1650	77

* Phenolic novolac/epoxy networks

** *Ortho*-cresol novolac/epoxy networks

Fragility results indicated that inter- and intramolecular hydrogen bonding was not an important factor in cresol novolac/ D.E.N. 438 networks (Table 4. 6). The 80:20 composition had the lowest crosslink density and therefore the lowest fragility. The 70:30 and the 60:40 compositions had slightly higher fragility values due to higher crosslink densities.

4.3.1.3. Thermal and thermo-oxidative stability

The thermal and thermo-oxidative stabilities of cresol novolac networks were investigated using a thermogravimetric analyzer; the weight loss profiles were recorded as functions of temperature. Samples analyzed in air measured thermo-oxidative stability (Figure 4. 15a). All cresol novolac/Epon 828 epoxy networks were stable up to 400°C, above which the materials began to degrade. A two-step degradation was observed for all samples and the weight loss profiles were similar for all compositions. The 80:20 composition showed a slightly higher thermo-oxidative stability than the 70:30 and the 60:40 compositions. The networks completely degraded at approximately 630°C in air as the weight loss approached 100 percent.

The thermal stabilities were investigated by examining the same samples under nitrogen (Figure 4. 15b). The weight loss began at a lower temperature in nitrogen than in air. The weight loss occurred mainly between 400°C and 500°C where the weight dropped from greater than 90% to ~ 35%. The 80:20 composition again showed only slightly higher heat resistance and had a slightly higher char yield at 900°C. Cresol novolac/D.E.N. 438 networks showed almost identical results as the cresol novolac/Epon 828 networks. Approximately 20 to 30 weight percent char remained for all cresol novolac networks examined in nitrogen.

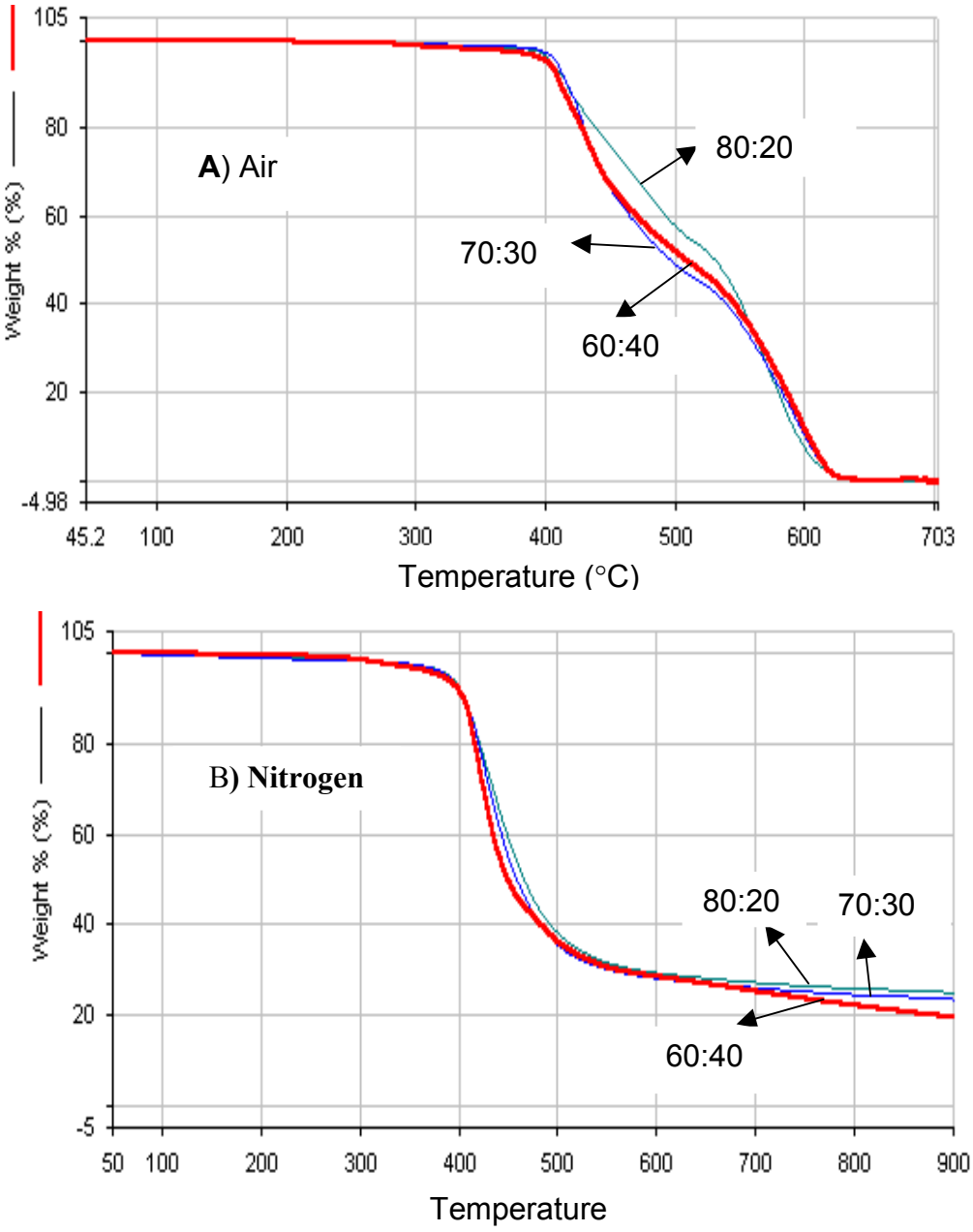

Figure 4. 15. Weight loss measured as a function of temperature for cresol novolac/Epon 828 networks A) in air, and B) in nitrogen

4.3.1.4. Flame results

The flame retardance of these cresol novolac/epoxy networks were measured using a cone calorimeter with a heat flux of 50 kW/m^2 and 20.9% O_2 (atmospheric oxygen). The heat release rate curves, measured as a function of time, showed different burning behaviors for the Epon 828 than those of the D.E.N. 438 epoxy cured networks (Figure 4. 16). The shapes of the curves are representative of the type of epoxy used in the networks. The peak heat release rate (PHRR) occurred at the ignition for networks cured with Epon 828 epoxy. The heat release rate then decreased rapidly as a function of time. The networks cured with D.E.N. 438 epoxy showed an initial spike at ignition. The heat release rate then gradually increased to a maximum followed by a rapid decline. For these networks, the maximum for the bulk heat release rate was assigned as the peak heat release rate. The heat release rate curves of cresol novolac/D.E.N. 438 networks were more desirable since longer times were required to reach the peak heat release rate, and this was more representative of flame retardant char forming materials.

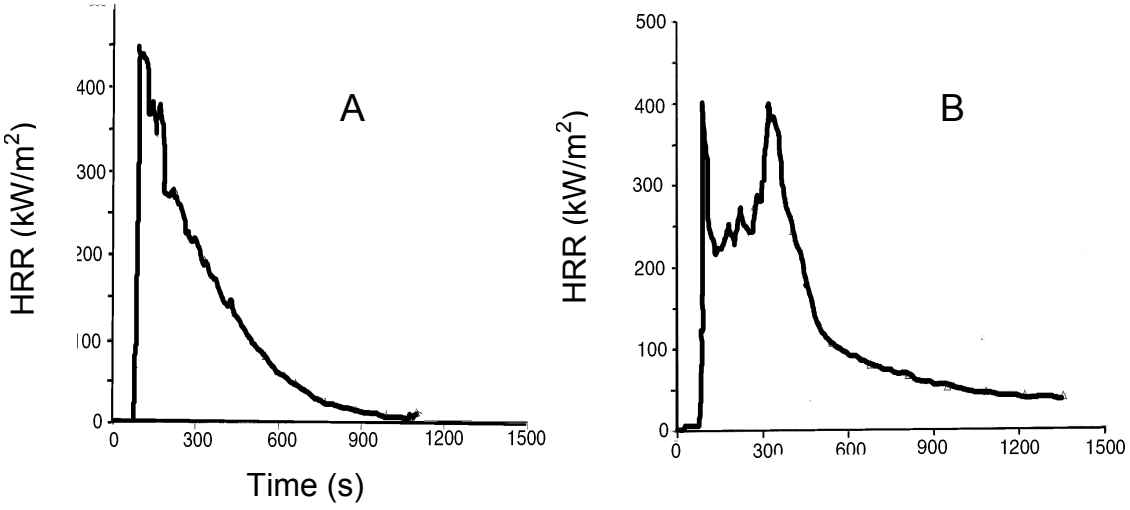

Figure 4. 16. Cone calorimetry results of A) cresol novolac/Epon 828 (70:30 wt:wt ratio), and B) cresol novolac/D.E.N. 438 (70:30 wt:wt ratio)

As expected, networks containing higher novolac contents showed lower peak heat release rates since novolac contributes to the flame retardance (Table 4. 7). Lower

peak heat release rates were observed for networks cured with D.E.N. 438 epoxy probably because D.E.N. 438, an epoxidized novolac, resembles the novolac structure and therefore contributes to the flame retardance. The peak heat release rates of cresol novolac/Epon 828 epoxy networks were higher than for the phenolic novolac/Epon 828 epoxy networks at similar compositions. The extra methyl groups on the cresols may have contributed to the higher peak heat release rate. However, the peak heat release rates of all cresol novolac/epoxy networks (300-450 kW/m^2) were significantly lower than that of the epoxy control (1230 kW/m^2).

Table 4. 7. Flame retardance of cresol novolac/epoxy networks

Networks	Phenolic/Epoxy (wt/wt)	PHRR (kW/m^2)	Char Yield (wt.%)
Epoxy control	--	1230	5
Phenolic control	--	116	63
Phenolic Novo/Epon 828	35/65	357	29
Cresol Novolac/Epon 828	70/30	448	16
	80/20	391	15
Cresol Novolac/D.E.N. 438	60/40	380	17
	70/30	404	18
	80/20	310	18

Higher char yields are desirable since char forms an isolation layer which generally improves flame retardance. According to cone calorimetric results, there were no significant differences in the char yield among the various cresol novolac/epoxy networks. Networks with different compositions prepared with either Epon 828 or D.E.N. 438 epoxy formed 15 to 18 percent char. The char yields were lower for cresol novolac/Epon 828 networks (~16 wt %) than for phenolic novolac/Epon 828 networks (~ 29 wt %) with similar network compositions, but significantly higher than for the epoxy control (~5 wt %). All novolac/epoxy networks exhibited reduced char formation compared to that of the phenolic control network (~63 wt %).

4.3.1.5. Water absorption and diffusion efficient

Water has a T_g of –130°C. Polymers that absorb water are also plasticized by water. Therefore, water generally has a negative effect on the T_g's of polymers and reduces the upper temperature limit for the polymers' applications. Typical phenolic materials are fairly hydrophilic because each phenolic repeat unit contains a free hydroxyl group. By adding a hydrocarbon substituent, such as a methyl group, in close proximity of the hydroxyl groups, such as in the case of cresol novolac, the polymer chains should become less polar and absorb less water.

Equilibrium moisture uptake was studied at both room temperature and 62°C for a series of cresol novolac/epoxy networks. The 62°C water uptake test was designed as an accelerated protocol, but these networks also absorb more water at higher temperatures. Three samples of each specimen were measured at room temperature and the results were extremely reproducible (Figure 4. 17).

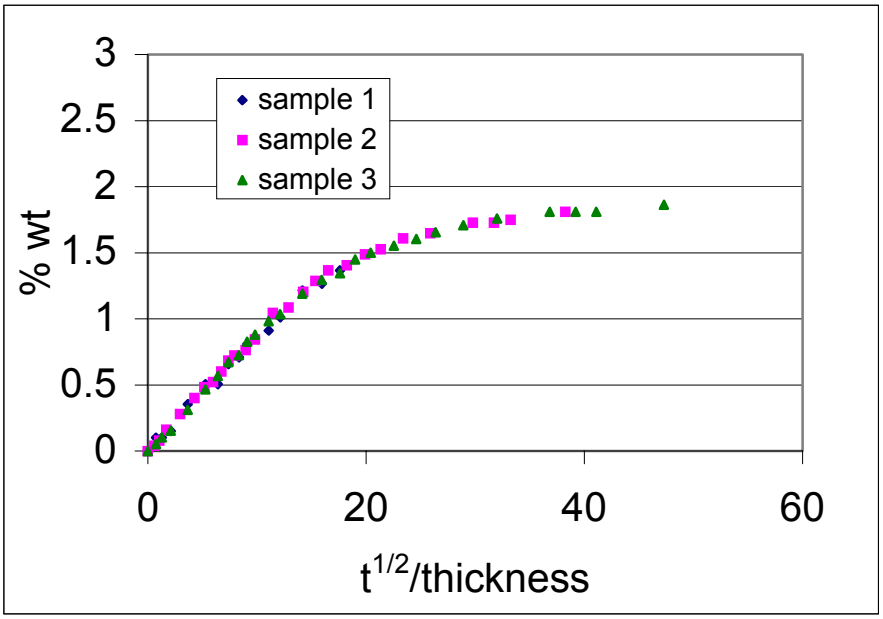

Figure 4. 17. Room temperature weight percent water uptake for cresol novolac/Epon 828 networks (70:30 wt:wt ratio)

The water absorption levels for cresol novolac/epoxy networks were relatively unaffected by the structures of the epoxies (Figure 4. 18). The 80:20 cresol

novolac/epoxy network absorbed slightly more water than the 70:30 and 60:40 cresol novolac/epoxy networks, probably as a result of having more polar phenolic hydroxyl groups in the higher novolac compositions. All of the cresol novolac networks (1.8-2.2 wt %) showed low equilibrium water uptake comparable to that of the epoxy control (2 wt %). Cresol novolac networks absorb significantly lower amounts of water than do their phenolic novolac counterparts. For example, at room temperature the 65:35 wt:wt phenolic novolac/Epon 828 epoxy networks absorbed 3.5 wt. % water whereas the 70:30 wt:wt cresol novolac/Epon 828 networks absorbed only 1.9 wt. % water.

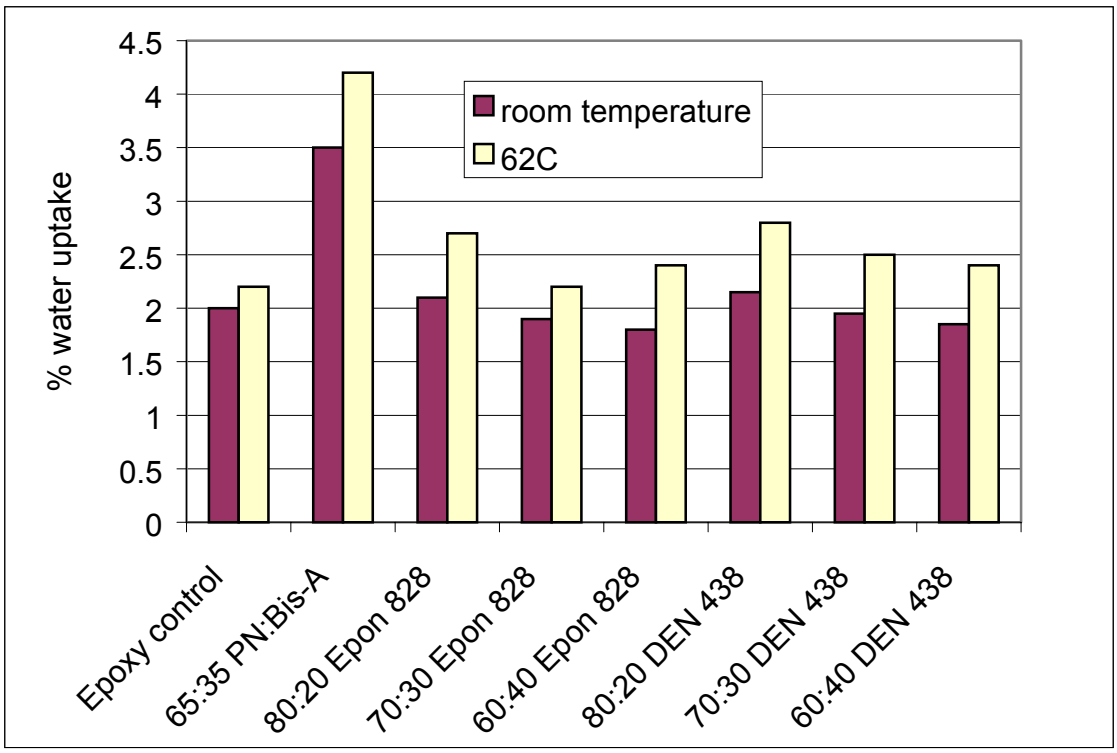

Figure 4. 18. Water uptake results for cresol novolac networks at room temperature and 62ºC

The diffusion coefficient (D) for cresol novolac/epoxy networks were calculated using the weight percent room temperature water uptake measured as a function of time according to the following equation.

$$D = \pi (sb/4M_{\infty})^2 \qquad \textbf{(4. 21)}$$

Where s is the initial slope of the plot wt % water uptake vs. time$^{1/2}$

b is the sample thickness

M_∞ is the equilibrium weight percent water uptake

This calculation assumes that the sample thickness is significantly less than the sample width and height. The network crosslink densities and chemical structures as well as the interactions between the small molecular (water) and the polymer matrix affect the diffusion coefficient.

Table 4. 8. Diffusion efficient of cresol novolac/epoxy networks

Epoxy	Cresol novolac/Epoxy (wt:wt)	D (cm^2/sec)
Epon 828	80:20	1.02×10^{-9}
	70:30	1.27×10^{-9}
	60:40	1.71×10^{-9}
DEN 438	80:20	1.23×10^{-9}
	70:30	1.94×10^{-9}
	60:40	1.56×10^{-9}

4.3.1.6. Reaction kinetics

A differential scanning calorimeter was used to determine the kinetic parameters for the cresol novolac/epoxy reactions. This procedure allowed for the calculation of reaction activation energy and the rate constants as a function temperature. The time that was required to achieve a full conversion at any given temperature thus can be predicted using these kinetic parameters.

Samples were heated from 50°C to 250°C at several heating rates (β) and the temperature at which the exothermic reaction peak occurred (T) was recorded at each heating rate. The activation energy (E) was approximated from the slope of the plot of log β versus 1/T (Figure 4. 19).

$$E \cong -2.19\, R \left[d \log_{10} \beta / d(1/T) \right] \qquad \textbf{(4. 22)}$$

where R is the gas constant (8.3145 J K^{-1} mol^{-1}).

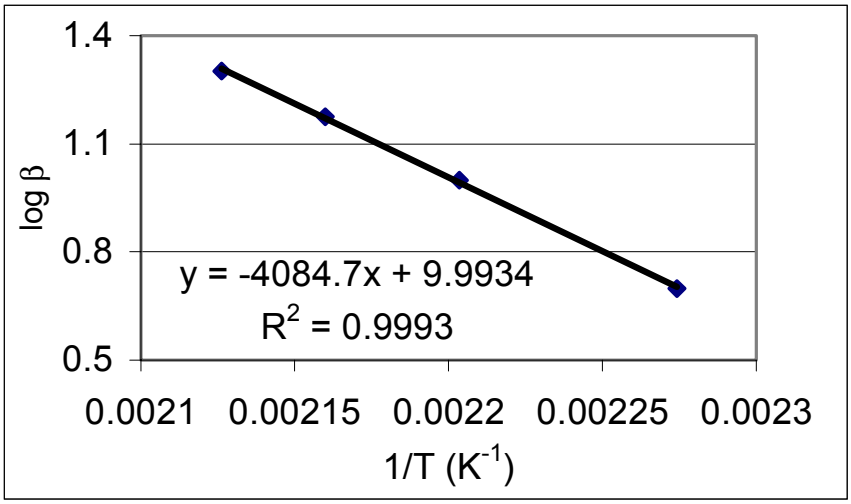

Figure 4. 19. Log heating rate versus 1/T for cresol novolac/epoxy mixture (70:30 wt:wt ratio) with 1 mole % TPP catalyst

The activation energy was refined according to the procedures described in ASTM E 698 until self-consistent. For cresol novolac/epoxy reactions, the activation energy was found to be ~69 KJ/mol, which is comparable to those cited in literature for epoxy ring opening reactions.

The Arrhenius pre-exponential factor (Z) was calculated as follows

$$Z = \frac{\beta \, \mathrm{E} \, e^{(\mathrm{E/RT})}}{\mathrm{RT}^2} \qquad \textbf{(4. 23)}$$

where β is a heating rate (taken from the middle of the range tested) and T is the temperature (K) in the middle of the range.

The kinetic rate constant, *k*, was calculated using the activation energy of the reaction and the pre-exponential factor

$$k = \mathrm{Z} \exp\left(-\frac{\mathrm{E}}{\mathrm{RT}}\right) \qquad \textbf{(4. 24)}$$

The rate constant was plotted as a function of temperature (Figure 4. 20). As expected, the rate constant increased with increased temperatures.

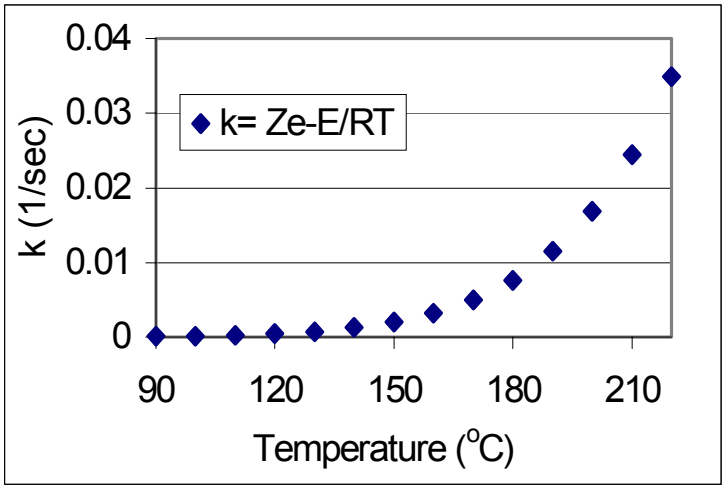

Figure 4. 20. Rate constant (k) versus temperature for a cresol novolac/epoxy mixture (70:30 wt:wt ratio) with 1 mole % TPP catalyst

To confirm the rate constant by an isothermal test, a time (t) was calculated to treat the sample at a chosen temperature (150°C) to achieve 50 % cure,

$$t_{1/2} = 0.693/k \qquad \textbf{(4. 25)}$$

The aged sample and an unaged sample were run in a dynamic scan and compared (Figure 4. 21). The reaction kinetics was confirmed if on an equal weight basis, the peak area or displacement from baselines of the aged sample is approximately one half of that of the unaged sample.

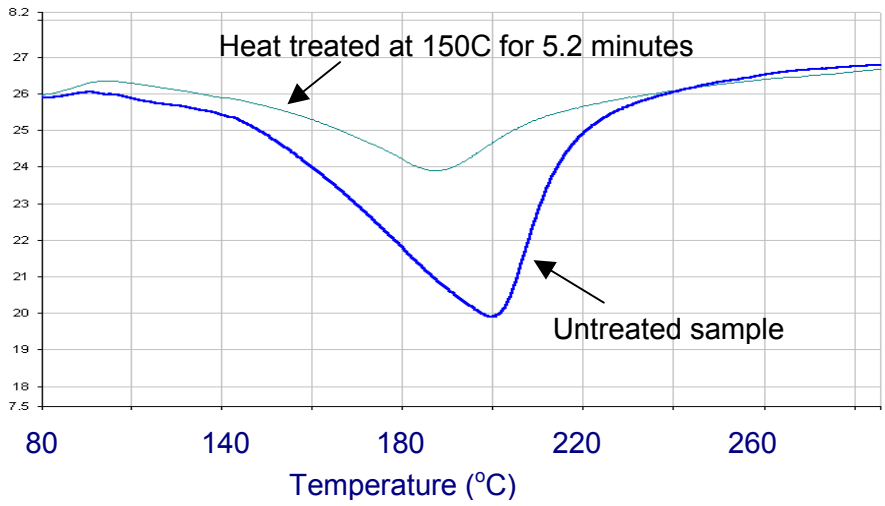

Figure 4. 21. Dynamic DSC scans of an untreated sample versus a heat treated sample

4.3.1.7. Processability

The novolac/epoxy networks studied in this research were evaluated for their potential use in tough, flame retardant composites. Regardless of the fabrication method, the novolac/epoxy resin mixtures must be heated to obtain sufficiently low viscosities for processing (2-10 Pa*s). However, novolacs react with epoxies at elevated temperatures even in the absence of an added catalyst. Even a small amount of reaction greatly increases the viscosity. Therefore, it was essential to determine the processing window in which the novolac/epoxy mixtures remain below a given viscosity at the processing temperatures.

The complex viscosity, measured as a function of temperature, (Figure 4. 22) showed that relatively high temperatures (>185°C) were required for a neat 2000 g/mol *ortho*-cresol novolac resin to reach ~2 Pa*s.

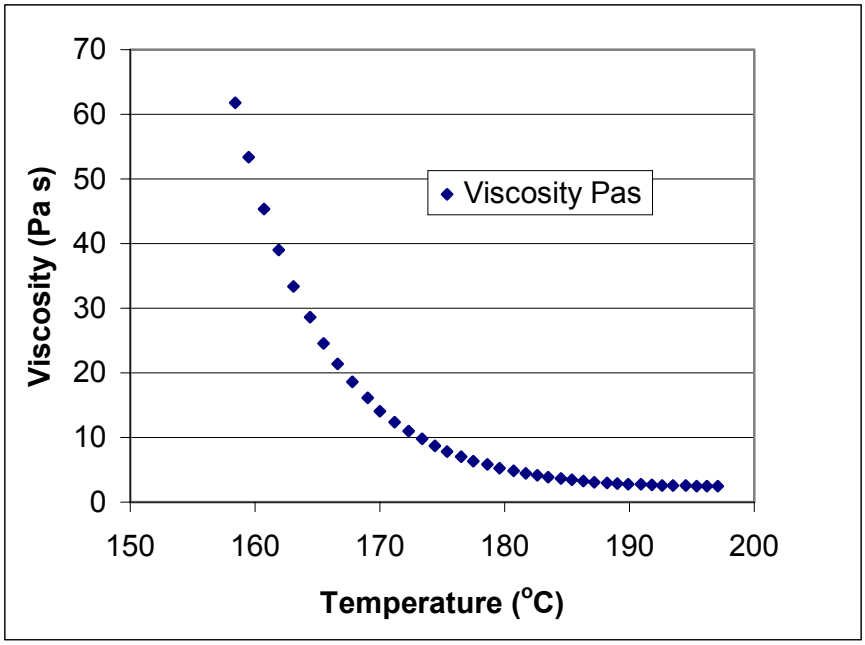

Figure 4. 22. Complex viscosity of a 2000 g/mol neat cresol novolac resin measured as a function of temperature

It was of interest to investigate the viscosity behaviors of the neat phenolic novolac resin used in the control experiments for comparison purposes. Since a significant amount of phenol and other low molecular weight volatile components were present in the typical novolac resin, the complex viscosities of the neat phenolic novolac resin (untreated) and the complex viscosity of this resin heated for 2 hours at 160°C were examined. Phenol and other low molecular weight components clearly reduced the viscosities of the resin (Figure 4. 23). It is important to note that these resins were melt mixed under vacuum at > 140°C, a condition that removed phenol, which should affect the viscosities of the novolac/epoxy mixtures during the prepreg process in composite fabrications.

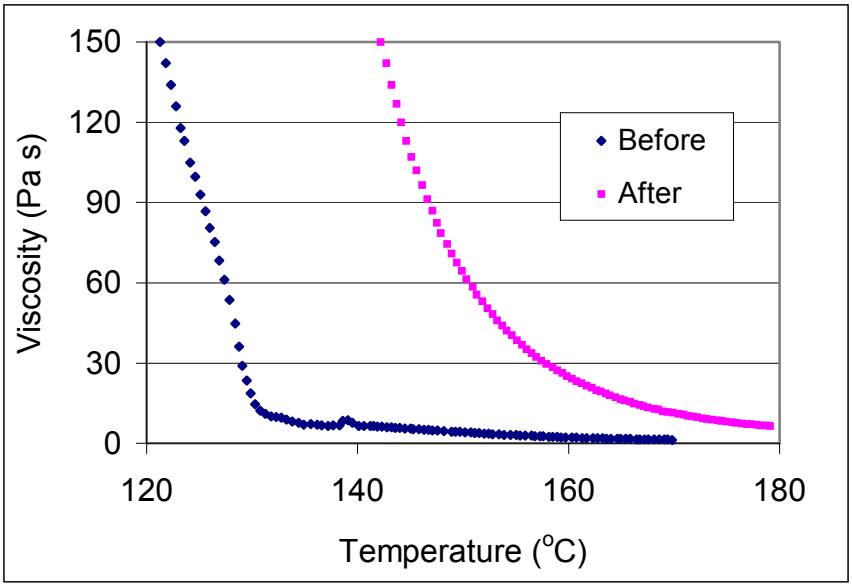

Figure 4. 23. Complex viscosity of a phenolic novolac resin before and after heat treatment (2 hours at 160°C)

Dynamic viscosity measurements for cresol novolac/Epon 828 mixtures showed that increased epoxy content reduced the melt viscosities (Figure 4. 24 a), and therefore, the processability was enhanced as the amount of low molecular weight epoxy increased. From dynamic viscosity measurements, the temperature at which the viscosity reached approximately 2 Pa*s was chosen as the processing temperature. Higher processing temperatures were necessary for compositions with lower amounts of epoxies. The isothermal viscosities were then evaluated at the processing temperatures of each composition to determine the processing windows (Figure 4. 24 b and c). The 70:30 and 60:40 compositions both exhibited great stabilities at their processing temperatures (140°C and 120°C respectively) with very little viscosity increase over 150 minutes.

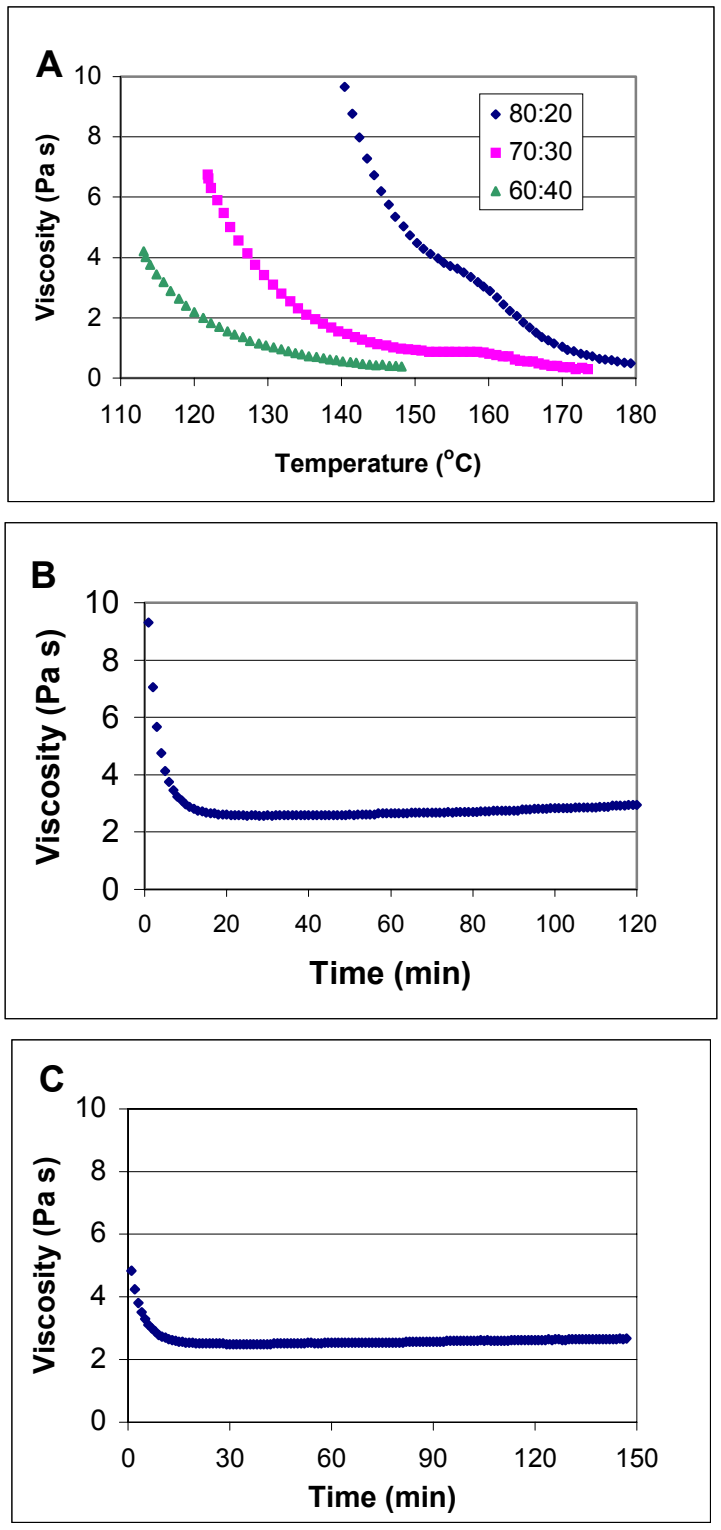

Figure 4. 24. **Viscosity measurements of cresol novolac/Epon 828 mixtures A) dynamic scans for various compositions, B) isothermal scan of the 70:30 composition at 145°C, and C) isothermal scan of the 60:40 composition at 120°C**

Isothermal viscosities were measured for the 65:35 wt:wt phenolic novolac/Epon 828 mixture (140°C) and compared with those of the 70:30 cresol novolac/Epon 828 mixture (145°C) (Figure 4. 25). The cresol novolac/epoxy mixture showed only a slight viscosity increase (from 2.5 to 3 Pa*s) over a 2-hour period, whereas the viscosity of the phenolic novolac/epoxy mixture increased substantially over the same period (3 to 12 Pa*s). Thus, the processing window for the cresol novolac/epoxy mixtures is significantly more desirable than for the phenolic novolac/epoxy mixtures. This increase in the processing window was attributed to the lower reactivity of the cresol novolac with epoxy groups. The methyl group *ortho* to the hydroxyl group probably caused extra steric hindrance to the phenolic hydroxyl/epoxy reactions.

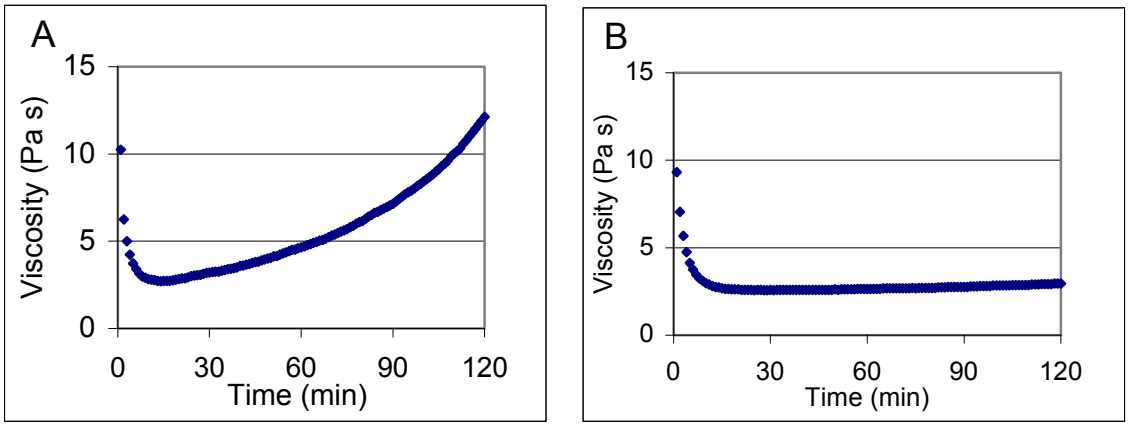

Figure 4. 25. Isothermal viscosity measurements: A) 65:35 wt:wt phenolic novolac/Epon 828 mixture measured at 140°C, and B) 70:30 wt:wt cresol novolac/Epon 828 mixture measured at 145°C

D.E.N. 438 epoxy was not as effective as Epon 828 epoxy in reducing the melt viscosities of cresol novolac/epoxy mixtures (Figure 4. 26A). At the same compositions, higher temperatures were needed to obtain similar viscosities when D.E.N. 438 epoxy was used. All cresol novolac/D.E.N. 438 mixtures required at least 160°C to reach the processable viscosities. At these temperatures, the inherent reaction between cresol novolac and epoxies became apparent as the viscosities increased from approximately 1.5 Pa*s to approximately 3 Pa*s over 100 minutes (Figure 4. 26B).

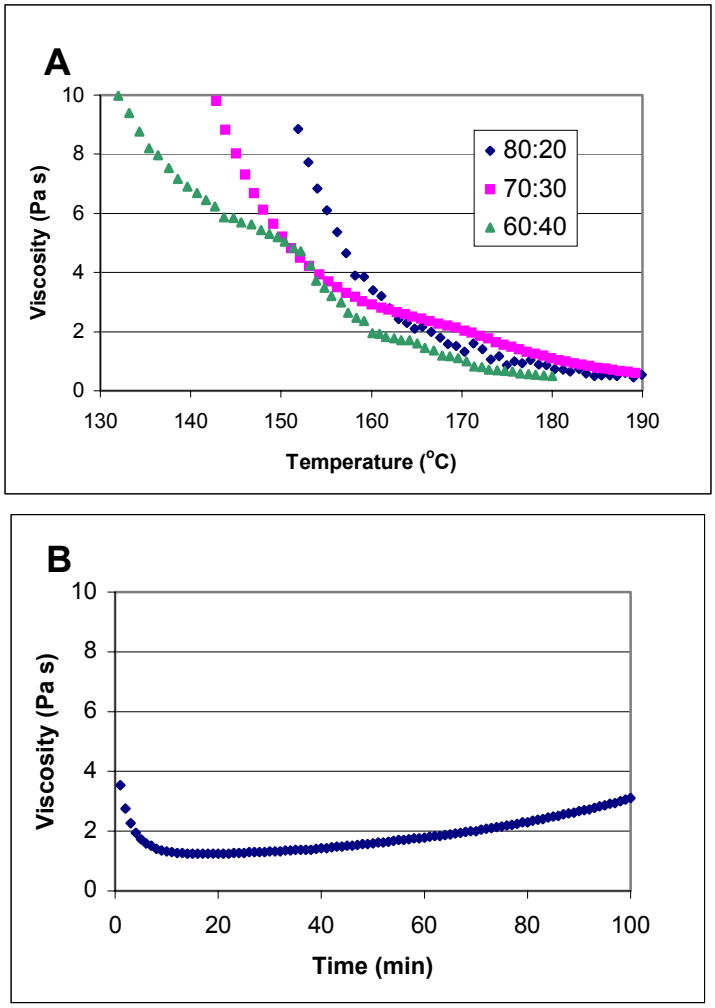

Figure 4. 26. Viscosity measurements for cresol novolac/D.E.N. 438 mixtures: A) dynamic measurements, B) isothermal scan for the 60:40 composition at 160°C

4.3.2. Composites properties

Flexural properties were examined for cresol novolac/Epon 828 composites. The 70:30 composition was chosen since it had the best overall properties, i.e. high K_{IC} and T_g, low sol fractions, good flame retardance, and excellent processability. The composites were reinforced with phenoxy-sized carbon fiber. No catalysts were used for the cresol novolac/epoxy cure reaction. To determine the cure conditions necessary to achieve a cured network, the glass transition temperature was measured as a function of cure time (Table 4. 9). The cresol novolac/epoxy reaction processed very slowly, even at

220°C, in the absence of a catalyst. A sample cured at 220°C for over 10 hours had a T_g that was significantly lower than that of a fully cured (TPP catalyzed) network.

Table 4. 9. Cure condition determination for *ortho*-cresol novolac/Epon 828 network (70:30 wt:wt %), no catalyst

sample	Cure conditions	T_g (°C)
1	1 hr @ 180°C, 4 hrs @ 220°C	Soluble
2	1 hr @ 180°C, 6.5 hrs @ 220°C	Partially soluble
3	1 hr @ 180°C, 8.5 hrs @ 220°C	120
4	1 hr @ 180°C, 10.5 hrs @ 220°C	135
5	TPP cured sample*	154

* cured using 0.1 mole % TPP at 200°C for 2 hours and 220°C for 2 hours

Composite properties were evaluated for the cresol novolac/Epon 828 networks cured under condition 4, i.e. the network was not fully cured. The flexural properties were superior to those of the control epoxy, but they were not as high as the fully cured phenolic novolac/Epon 828 composites (Table 4. 10). The properties of composites with fully cured cresol novolac/epoxy matrix resin should exhibit comparable to those properties of the phenolic novolac/epoxy based composites.

Table 4. 10. Flexural strength and moduli of composites

Sample	σ_{max} (MPa)	E_b (GPa)
Control epoxy	29	8.9
Phenolic novolac/Epon 828 (65:35)	66	11.3
Cresol novolac/Epon 828 (70:30)	46	10.1

4.3.3. *Para*-cresol based networks and their properties

The networks prepared using a 2000 g/mol *para*-cresol novolac and their properties were somewhat explored (Figure 4. 27).

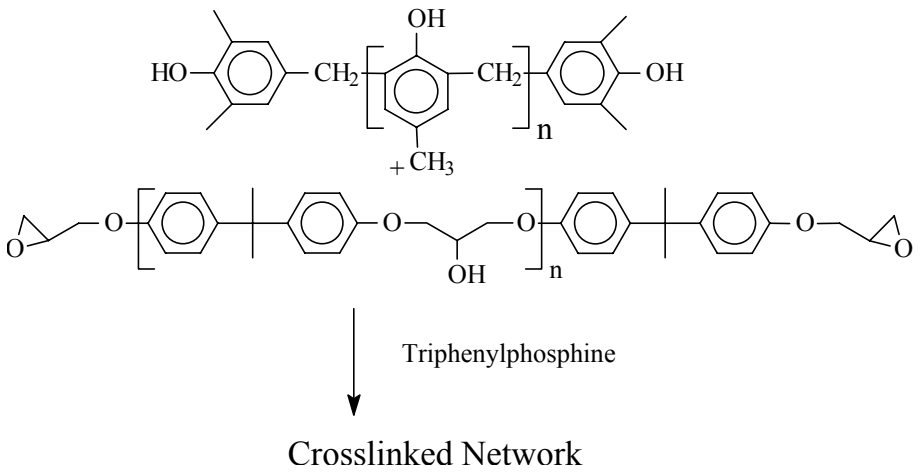

Figure 4. 27. 2000 g/mol *para*-cresol novolac cured with Epon 828

The viscosity profile of a neat 2000 g/mol *para*-cresol novolac resin showed an unexpected increase at higher temperatures (>175°C) (Figure 4. 28). *Para*-cresol novolac oligomers are highly stereo-regular, and therefore may form ordered structures at higher temperatures. In sample preparations, high temperatures were required to obtain low viscosities for proper degassing; however, increasing the temperature to ~ 170°C increased the viscosity when *para*-cresol novolac resin was used. Therefore, sample preparations for these *para*-cresol novolac/epoxy networks became more challenging especially at high novolac compositions (80:20 wt:wt ratio). The 70:30 and 60:40 compositions were successfully prepared.

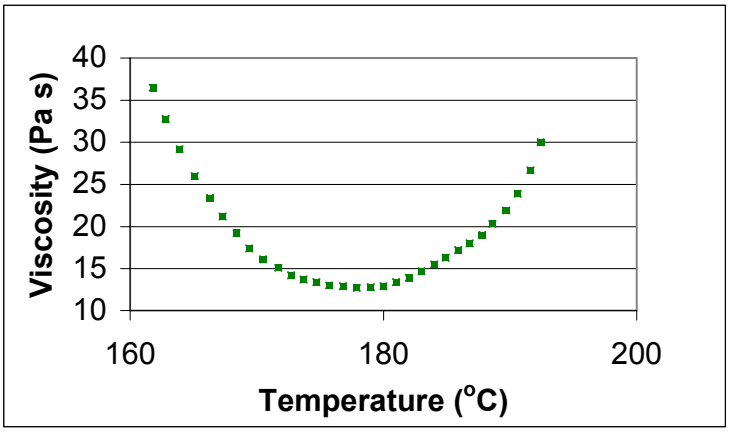

Figure 4. 28. Viscosity of a 2000g/mol *para*-cresol novolac resin (heat rate = 2.5°C /min)

Para-cresol novolac/Epon 828 epoxy network properties did not seem to follow any trend (Table 4. 11). The 70:30 composition showed a lower toughness but a higher T_g than the 60:40 composition. The 70:30 wt:wt *para*-cresol novolac/epoxy networks showed a similar T_g but a significantly lower K_{IC} compared to the *ortho*-cresol novolac/epoxy networks with the same novolac content. These network properties were not only a result of the crosslink density but were complicated by the packing order of *para*-cresol novolac chains. At higher *para*-cresol novolac contents, a higher degree of sterioregularity may lead to the observed higher T_g yet lower K_{IC} values.

Table 4. 11. K_{IC} and T_g of *para*-cresol novolac/Epon 828 networks

Cresol	Sample	K_{IC} (MPa*m$^{1/2}$)	T_g (^oC)
ortho	70:30	1.06	154
para	70:30	0.78	155
para	60:40	0.89	140

4.4. Conclusions

Cresol novolac/epoxy networks were prepared using a controlled molecular weight 2,6-dimethylphenol endcapped *ortho*-cresol novolac resin and the network properties were compared to those of an epoxy control, a phenolic control and a phenolic novolac/epoxy control. The 70:30 and 60:40 compositions exhibited relatively high toughness (> 1 MPa/m$^{1/2}$) and high glass transition temperatures (>140°C). These properties were superior to these of the epoxy control, the phenolic control and the phenolic novolac/epoxy networks (65:35 wt:wt ratio). The molecular weight between crosslinks (~1500 g/mol), determined using the theory of rubber elasticity, showed that the network density was optimized at the 70:30 composition. This M_x was most desirable for networks cured with 2000 g/mol oligomers. Compositions high in novolac content (80:20 wt:wt ratio) had reduced crosslink densities due to insufficient network connectivity; compositions high in epoxy content (60:40 wt:wt ratio) also had reduced

apparent crosslink densities because a lack of mobility prohibited further phenolic/epoxy reactions, which led to increased epoxy sol fractions.

Master curves and cooperativity plots were generated for cresol novolac/epoxy networks. The fragility was used to investigate the temperature dependence of segmental relaxation through the transition region. Both crosslink density and hydrogen bonding affected the properties of Epon 828 epoxy cured cresol novolac networks. Crosslink density seemed to be the dominating factor in the D.E.N. 438 epoxy cured cresol novolac networks.

Cresol novolac/epoxy networks exhibited comparable, relatively low, equilibrium water absorptions similar to that of the epoxy control (~ 2 wt % at room temperature). Their equilibrium water uptake were relatively unaffected by the network compositions. The methyl group on each novolac repeat unit probably reduced water absorption.

The peak heat release rates of *ortho*-cresol novolac/epoxy networks were between 300-450 kW/m^2. The presence of a methyl group on each repeat unit slightly increased the peak heat release rates and reduced the char yields of cresol novolac networks relative to those of phenol novolac networks. The flame retardance of all the novolac/epoxy networks were significantly superior to that of the epoxy control, but inferior to that of the phenolic control.

The kinetic parameters were determined for the cresol novolac/epoxy reactions. The activation energy for these reactions was approximately 69 KJ/mol, which was comparable to the literature values for phenolic hydroxyl/epoxy ring opening reactions. The kinetic parameters allowed for prediction of the cure time required to achieve 99% conversion.

Cresol novolac resins gave rise to longer processing window times when mixed with epoxies at elevated temperatures. This was again attributed to the methyl group in close proximity to the hydroxyl group which sterically hindered the phenolic hydroxyl/epoxy reaction.

5. Maleimide Containing Cresol Novolac Networks and Their Properties

5.1. Introduction

Maleimides are a relatively new class of materials used in high performance structural composite and adhesive applications. Major advantages of maleimide networks include excellent stabilities at elevated temperatures and in hot-wet conditions, low moisture absorptions, and excellent chemical stabilities. The thermal and mechanical properties of maleimide networks are superior to those of most epoxies.[165]

Typical maleimide oligomers are difunctional (bismaleimides) obtained by reacting diamines with maleic anhydride (Figure 5. 1).

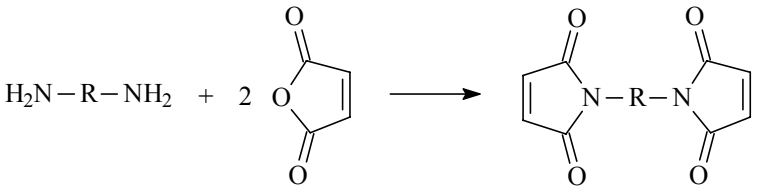

Figure 5. 1. Preparation of bismaleimide from a diamine and maleic anhydride

Bismaleimides can be crosslinked alone or in the presence of a curing agent. Curing bismaleimides alone generally requires high temperatures to initiate reactions and achieve high conversions. Introducing an initiator effectively reduces the cure

[165] K. N. Ninan, K. Krishnan, and J. Mathew, "Addition Polyimide: 1. Kinetics of Cure Reaction and Thermal Decomposition of Bismaleimide," *Journal of Applied Polymer Science* **32**(7), 6033-6042 (1986).

temperatures. Adding peroxide initiators[166] results in free-radical initiations while adding tertiary amines or imidazole[167] leads to anionic initiations.

The thermal cure of bismaleimides such as 4,4'-bismaleimidodiphenylmethane in the absence of initiator was suggested to proceed via a free radical process.[168] This was supported by the increased activation energies observed in the presence of a small amount of impurities, which was proposed to interfere with the free radical reaction. Thermally initiated polymerization of maleimide was also suggested to occur in a heterogeneous manner.[169] Gelation was reached rapidly in the form of microgels, which were attributed to slow initiation rates but fast propagation rates. Macrogelation occurred much later in the reactions.

Anionically initiated maleimide polymerizations proceeded via a more homogeneous mechanism.[169] Both initiation and propagation occurred more rapidly. As expected, maleimide polymerization rates decreased significantly after vitrification due to slow diffusion.

Bismaleimides have been cured with amines to increase the toughness by reducing the network crosslink densities. Curing bismaleimides with diamines involves both a lower temperature primary amine addition to maleimide double bonds (Figure 5. 2a) and a higher temperature homopolymerization of maleimide double bonds (Figure 5.

---

[166] M. Acevedo, J. de Abajo, and J. G. de la Campa, "Kinetic Study of the Cross-linking Reaction of Flexible Bismaleimide," *Polymer* **31**, 1955, (1990).

[167] H. D. Stenzenberger, M. Herzog, W. Romer, R. Scherblich, S. Pierce, and M. Canning, "Compimides: A Family of High Performance Bismaleimide Resins," *30th Nat. SAMPL Symp*. **30**, 1568-1586 (1985).

[168] I. M. Brown and T. C. Sandreczki, "Crosslinking Reactions in Maleimide and Bis(maleimide) Polymers-an ESR Study," *Macromolecules* **23**(1), 94-100, (1990).

[169] A. Seris, M. Feve, F. Mechin, and J. P. Pascault, "Thermally and Anionically Initiated Cure of Bismaleimide Monomers," *Journal of Applied Polymer Science* **48**, 257-269 (1993).

2b).[170] The cure reaction of 1,1-(methylenedi-4,1-phenylene) bismaleimide and 4,4'-methylenedianiline, monitored by FTIR and DSC, showed that the nucleophilic addition of amine to the maleimide double bond, which resulted in extension of network chains, occurred via a second-order reaction. The homopolymerization, which led to crosslinking, proceeded at a rate at least two orders of magnitude lower than did the amine addition. The homopolymerization involved thermal initiations and chain propagations. Lower cure temperatures or increased diamine contents therefore favored the chain extension reactions over the crosslinking reactions.[171]

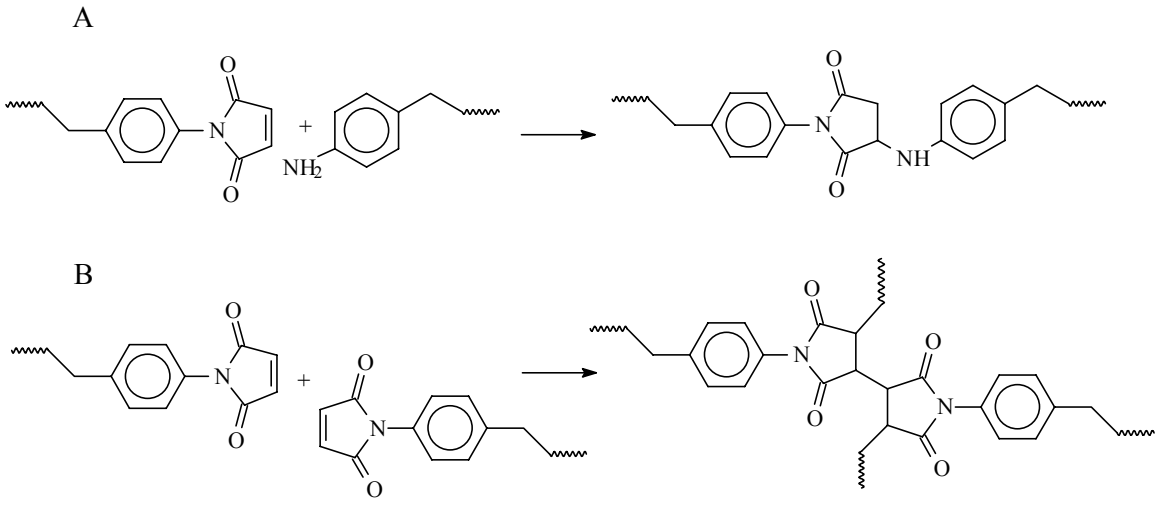

Figure 5. 2. Reactions of bismaleimide in the presence of a diamine: A) chain extension due to an amine addition, and B) crosslinking obtained by maleimide homopolymerization reactions

According to DSC measurements, the temperature of exothermic transition due to bismaleimide/amine reactions decreased as the basicity of the amines increased. It was suggested that faster reactions could be achieved if more basic amines were used in the

[170] A. V. Tungare and G. C. Martin, "Analysis of the Curing Behavior of Bismaleimide Resins," *Journal of Applied Polymer Science* **46**, 1125-1135 (1992).

[171] T. M. Donnellan and D. Roylance, "Relationships in Bismaleimide Resin System. Part I: Cure Mechanisms," *Polymer Engineering and Science* **32**(6), 409-414 (1992).

reactions. However, post-curing above 200°C was necessary for all maleimide/amine reactions to achieve high conversions.[172]

The structures of maleimide and amine affect the network thermal stabilities and flame retardance. For example, higher char yields were obtained for bismaleimides cured with phosphorus based amines.[172]

Several mechanisms were proposed to be involved in the bismaleimide/diallylbisphenol cure. They include 1) homopolymerization of maleimide groups, 2) homopolymerization of allyl groups, 3) reactions between maleimide double bonds and allyl groups via a Diels-Alder reaction, 4) reactions of maleimide with the allyl component and/or another maleimide via a free radical site,[173] and 5) crosslinking reactions via dehydration of the allylbisphenol hydroxyl groups (self-condensation).[174] Cure reaction of 4,4'-methylenebis-(maleimidobenzene) and 2,2'-diallylbisphenol A, monitored using near-IR spectroscopy, showed that the principal reaction pathway involved alternating copolymerization of maleimide and allyl double bonds.[175] Maleimide homopolymerization was found to be significant only during the initial stage of the reaction when heated above 200°C. The self-condensation reactions (pathway 5), which released water as the by-product, were observed over the entire temperature range investigated (140°C to 250°C).

---

[172] I.K. Varma and D.S. Varma "Addition Polyimides. III. Thermal Behavior of Bismaleimide," *Journal of Polymer Science: Polymer Chemistry Ed.* **22**, 1419-1483 (1984).

[173] I. M. Brown and T. C. Sandreczki, "Characterization of Bismaleimide Cure Reaction by Electron-Spin Resonance Techniques," *Abstract Paper to American Chemical Society, S, Polymer Material Science and Engineering*-**128**, 169 (1988).

[174] R. J. Morgan, R. J. Jurek, A, Yen, and T Donnellan, "Toughening Procedures, Processing and Performance of Bismaleimide Carbon Fiber Composites," *Polymer* **34**(4), 835-843 (1993)

[175] J. Mijovic and S. Andjelic "Study of the Mechanism and Rate of Bismaleimide Cure by Remote in-situ Real Time Fiber Optic Near-Infrared Spectroscopy," *Macromolecules* **29**, 239-246 (1996).

Addition curable novolac resins containing maleimide functionalities were prepared by co-reacting phenol and *N*-4-hydroxylphenylmaleimide with formaldehyde (Figure 5. 3). The oligomers were thermally crosslinked or cured with epoxy resins for structural adhesive applications.[176] Network adhesion properties depended on the cure conditions and the test temperatures. Self-cured networks had low lap shear strength and low T-peel strength under ambient conditions, but these properties improved at higher temperatures. The enhanced adhesion at higher temperatures was attributed to thermally induced molecular relaxations in the tightly crosslinked networks. Maleimide-novolac oligomers cured with epoxies showed improved adhesions and higher thermal stabilities compared to novolac/epoxy networks without maleimide. Improved adhesions were attributed to secondary forces of attraction induced by the polar imide groups through their partial polymerization.

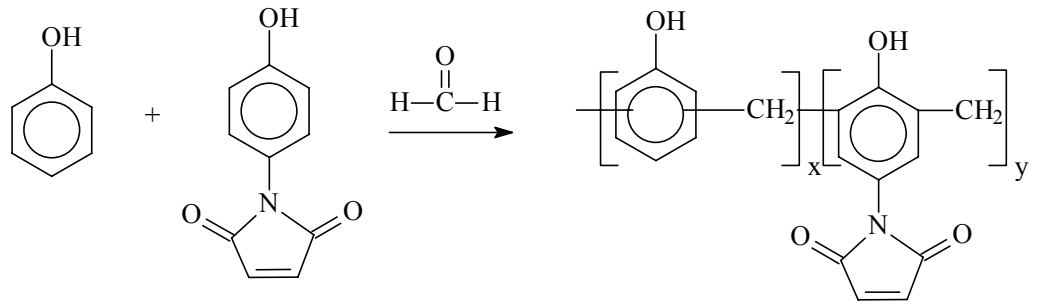

Figure 5. 3. Synthesis of novolac resins containing maleimide functionalities

The goal of this part of the research was to incorporate the maleimide moiety into cresol novolac/epoxy networks and determine the network properties. Cresol novolac oligomers containing maleimide groups (cresol-co-HPM novolac) were first synthesized, followed by crosslinking with bisphenol-A epoxy to form networks. Maleimide groups were expected to behave as latent crosslink sites since the self-cure occurs only at higher temperatures. Adding maleimide groups into networks therefore should improve thermal stabilities and may enhance flame retardance.

---

[176] C. Gouri, C. P. Reghunadhan Nair, and R. Ramaswamy, "Adhesive and Thermal Characteristics of Maleimide-Functional Novolac Resins," *Journal of Applied Polymer Science* **73**, 695-705 (1999).

5.2. Experimental

5.2.1. Reagents

2-Amino-*p*-cresol, 4-aminophenol, *ortho*-cresol, 2,6-dimethylphenol, formaldehyde (37 wt% solution in water), maleic anhydride, oxalic acid dihydrate, paraformaldehyde (powder, 95%), phosphorus pentoxide, and triphenylphosphine were purchased from Aldrich. *N,N*-dimethylformamide, hexane, and diethyl ether were obtained from EM Science. Isopropanol was purchased from Allied Signal, and sulfuric acid was obtained from Fisher Chemical. All reagents were used as received.

5.2.2. Synthetic Methods

5.2.2.1. Synthesis of 4-Hydroxyphenylmaleimide (4-HPM)

To a 2000 ml 3-neck round bottom flask equipped with a mechanical stirrer and an addition funnel was added maleic anhydride (grounded into small pieces) (180g, 1.1mol) and DMF (250 ml) (Figure 5. 4). Once the maleic anhydride completely dissolved, 4-aminophenol (109g, 1mol) was added gradually to the reaction flask through a powder funnel. The mixture was allowed to react at room temperature for 2 hours. In a separate 1000 ml one-neck round bottom flask, P_2O_5 (57 g) and DMF (350 ml) were added. While stirring, H_2SO_4 (25 g) was added drop wise. The H_2SO_4/P_2O_5/DMF mixture was stirred until a homogenous solution was obtained; it was then added drop wise to the reaction through the addition funnel. The reaction mixture was heated to 70°C and held at this temperature for 2 hours to achieve full imidization. To work up the reaction product, approximately 250 ml DMF was removed via vacuum distillation. The reaction mixture was precipitated in ice water, filtered through a Buchner funnel, and then rinsed with deionized water 5 times or until the product was neutral. It was recrystallized in isopropanol, then washed with hexane. The 4-HPM product was dried at 70°C for 2 hours under vacuum prior to use.

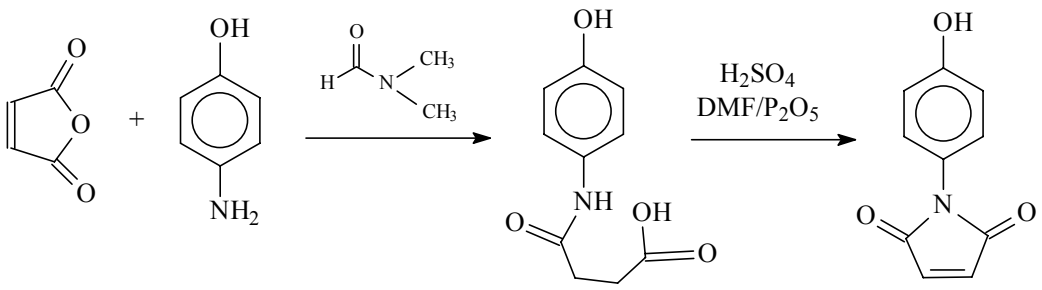

Figure 5. 4. Synthesis of 4-hydroxyphenylmaleimide

5.2.2.2. Synthesis of 2-hydroxy-5-methylphenylmaleimide

The procedure used to prepare 4-HPM was also used to prepare 2-hydroxy-5-methylphenylmaleimide. To work up the reaction, a vacuum distillation was used to remove ~ 250 ml DMF. The reaction mixture was precipitated in ice water and filtered through a Buchner funnel. The precipitated product was dissolved in an 85/15 vol/vol ether/isopropanol mixture and washed with deionized water in a separatory funnel until neutral. A rotovap apparatus was used to remove most of the organic solvent. The product was recrystallized in the remaining solvent with the addition of a small amount of hexane. It was washed with hexane and dried at 70°C for 2 hours under vacuum.

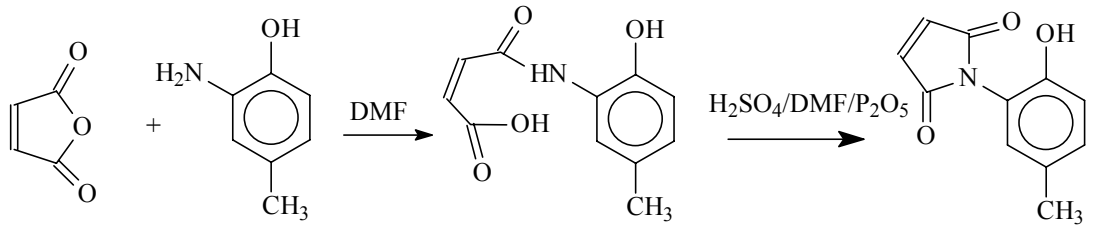

Figure 5. 5. Synthesis of 2-hydroxyl-5-methylphenylmaleimide

5.2.2.3. Synthesis of 2,6-dimethylphenol endcapped *o*-cresol-co-HPM novolac oligomers

Controlled molecular weight, 2,6-dimethylphenol endcapped cresol-co-HMP oligomers were prepared via electrophilic aromatic substitution (Figure 5. 6). The pre-determined amount of reagents, *ortho*-cresol (180.0g), 2,6-dimethylphenol (50.9g), 4-HPM (55.6g), formaldehyde (71.9g), and oxalic acid dihydrate (7.4g) were added to a resin kettle and reacted at 80°C for 48 hours. The product was dissolved in acetone,

precipitated into ice water, then filtered on a Buchner funnel. It was washed with deionized water until neutral and then dried drying at 60°C under vacuum for 5 hours.

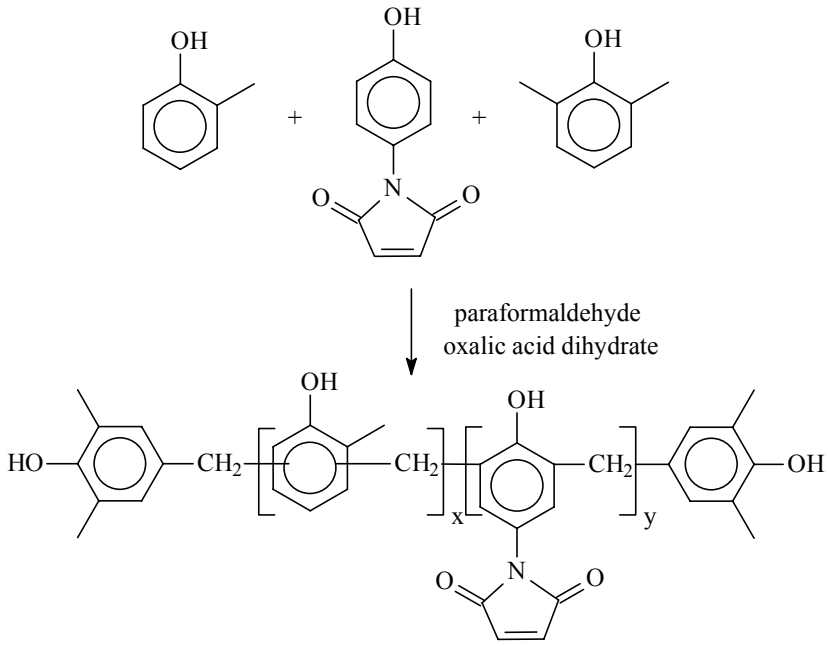

Figure 5. 6. Synthesis of 2,6-dimethylphenol endcapped cresol-co-HMP novolac resin

A sample calculation for the amount of reagent needed to obtain a 1500g/mol oligomer with 15 wt% internal maleimide is as follows. The combined molecular weight of the repeat units per chain (M_u) is obtained by subtracting the combined end group molecular weight (M_e) from the targeted molecular weight (M_n)

$$M_u = 1500 - M_e = 1500 - (121+121+14) = 1244 \quad \textbf{(5. 1)}$$

A normalized molecular weight per repeat unit is calculated for oligomers containing 85 weight percent cresol (repeat unit x) and 15 weight percent 4-HPM (repeat unit y)

$$\text{Normalized } M_n = 0.85 * M_n(x) + 0.15 * M_n(y)$$

$$= 0.85(120)+0.15(201) = 132.2 \quad \textbf{(5. 2)}$$

The number of internal units was calculated by dividing the normalized M_n per repeat unit into M_u

$$(x+y) = M_u/\text{normalized } M_n = 1244/132.2 = 9.41 \quad \textbf{(5. 3)}$$

The number of cresol containing repeat units is 85 percent of (x+y), and the number of 4-HPM containing repeat units is 15 percent of (x+y). There are 2 moles of 2,6-dimethylphenol per chain, and (x+y)+1 or 10.41 moles of formaldehyde.

5.2.2.4. Synthesis of cresol novolacs with 2-Hydroxy-5-methylphenylmaleimide endgroups

2-Hydroxy-5-methylphenylmaleimide was used as opposed to 2,6-dimethylphenol as the endcapper for the synthesis of controlled molecular weight cresol novolac oligomers (Figure 5. 7). The procedures for these reactions were the same as those described in section 5.2.2.3.

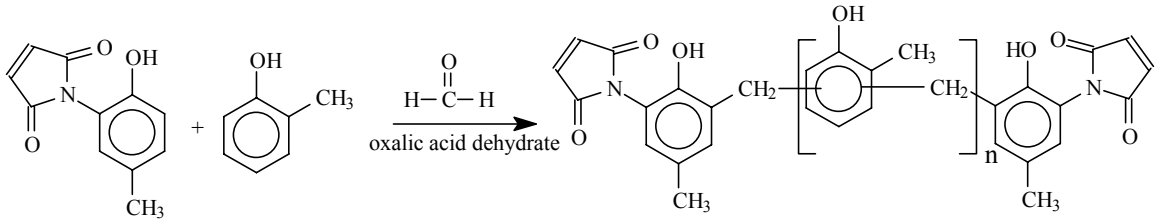

Figure 5. 7. Synthesis of 2-hydroxy-5-methylphenylmaleimide terminated cresol novolac resins

5.2.3. Characterization

The characterization methods used in these experiments, including ^{1}H NMR, DSC, TGA, fracture toughness, gel fraction, and cone calorimetry are described in detail in Chapter 4.2.3.

5.3. Results and Discussion

5.3.1. 4-Hydroxyphenylmaleimide synthesis and characterization

4-HPM monomer was prepared by reacting 4-aminophenol with maleic anhydride.[177] ^{1}H NMR verified the chemical structures and the purity of the monomer

[177] J. O. Park and S H. Jang, "Synthesis and Characterization of Bismaleimides from Epoxy Resins," *Journal of Polymer Science. Part A: Polymer Chemistry* **30**, 723-729 (1992).

(Figure 5. 8). As expected, four sets of peaks were observed for 4-HPM. Protons on imide double bonds (a) resonate at 7.1 ppm; two types of aromatic protons (b and c) are observed at 6.8 and 7.06 ppm, respectively. Phenolic hydroxyl protons resonate at 9.8 ppm. Water and DMSO were found at 3.4 and 2.5 ppm respectively. A clean ^{1}H NMR spectrum of 4-HMP showed that the monomer was relatively pure

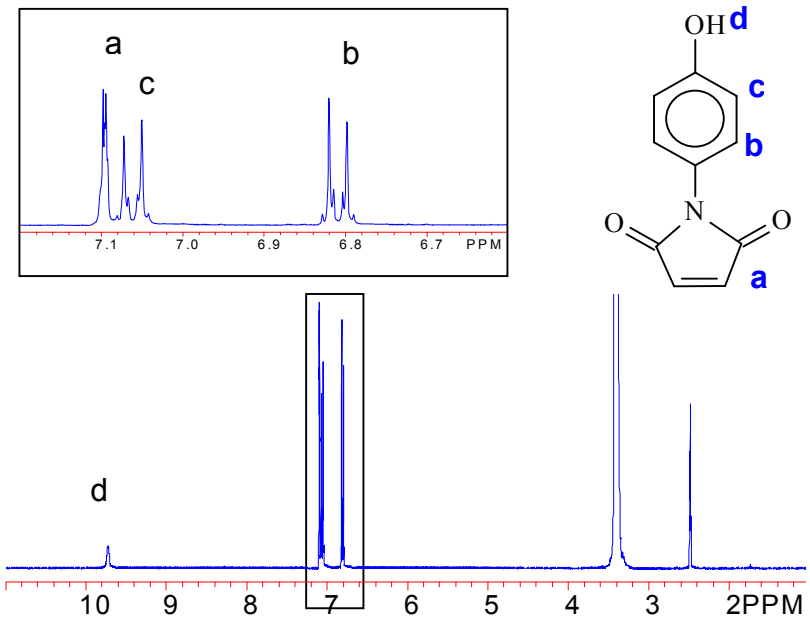

Figure 5. 8. ^{1}H NMR spectrum of 4-hydroxyphenylmaleimide monomer

The melting point of 4-HPM was measured using differential scanning calorimetry (Figure 5. 9). The observed melting point (191°C) was comparable to that cited in the literature.[177] Further heating above the melting point led to an exotherm which was attributed to the crosslinking reactions.

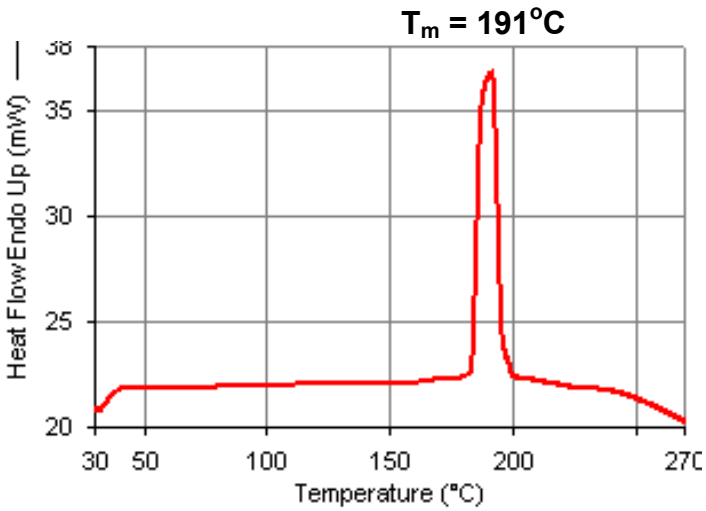

Figure 5. 9. Melting point of 4-HPM determined via DSC

The thermal stability of 4-HMP was investigated using thermogravimetric analysis (Figure 5. 10). No weight loss was observed up to 160°C. Upon further heating, thermal degradation may have led to the observed weight loss. Surprisingly, the onset of weight loss for 4-hydroxyphenylmaleimide occurred below its melting point.

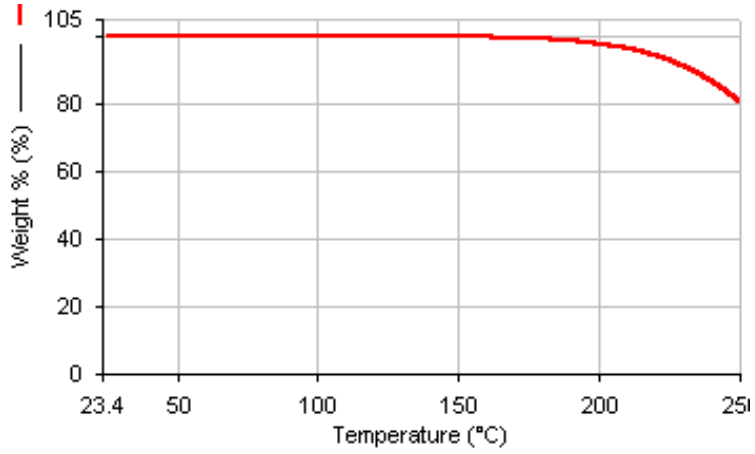

Figure 5. 10. Thermal stability of 4-HPM monomer measured via TGA (10°C/min, N_2)

5.3.2. Cresol-co-HPM novolac oligomers and their properties

Maleimide functionalities were incorporated into cresol novolac oligomers via electrophilic aromatic substitution reactions of cresol and 4-HPM with formaldehyde. The hydroxyl group on 4-HPM should dominate in electron donating compared to the imide group, therefore the monomer was assumed to be difunctional in formaldehyde substitution reactions. The molecular weight of presumed linear cresol-co-HPM novolac oligomers was controlled by adjusting the stoichiometric ratio of monomers (cresol and 4-HPM) to endgroups (2,6-dimethylphenol) (as discussed in Chapter 2).

Cresol-co-HPM novolac oligomers were prepared in three molecular weights. The 1500 and 1250 g/mol oligomers contained 15 mole % maleimide. At this composition, there was at least one maleimide group per chain statistically. A higher maleimide composition was necessary to maintain one maleimide site per chain (statistically) at lower oligomer molecular weights (such as 1000g/mol).

The molecular weights of cresol-co-HMP novolac could not be calculated quantitatively using ^{1}H NMR or ^{13}C NMR spectroscopy due to the complexity of the spectra and extensive peak overlapping. ^{1}H NMR spectra confirmed the presence of maleimide groups which were clearly distinguishable from the other aromatic peaks (Figure 5. 11). Methylene linkages are also evident between 3.4 and 3.9 ppm.

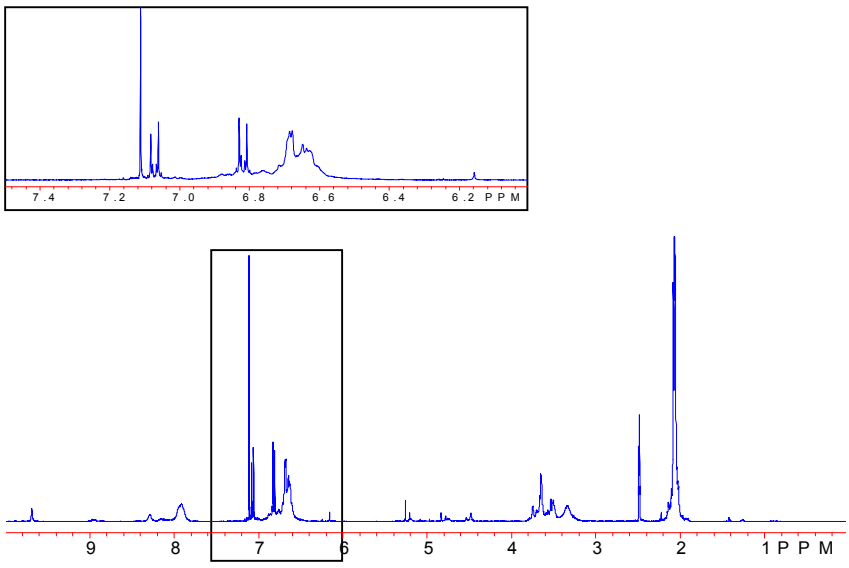

Figure 5. 11. ^{1}H NMR of a typical cresol-co-HPM novolac resin

The glass transition temperatures of cresol-co-HPM novolac oligomers were measured as a function of targeted molecular weight. As expected, increased molecular weights led to higher glass transition temperatures (Table 5. 1). The oligomer molecular weights were particularly important in terms of processability considerations. Higher molecular weight oligomers required more elevated processing temperatures. However, the presence of thermally labile maleimide groups limited the upper processing temperature range. Therefore, the number average molecular weights of cresol-co-HPM novolac oligomers were kept reasonably low. The glass transition temperatures correlated with oligomer processability.

Table 5. 1. T_g of cresol-co-HMP oligomer as a function of M_n

Target M_n (g/mol)	4-HPM content* (Mole %)	T_g (^oC)
1500	15	87
1250	15	54
1000	20	35

* Mole % of internal repeat units bearing maleimide groups

5.3.3. Cresol-co-HPM novolac/epoxy network properties

The fracture toughness, T_g, and sol fractions of cresol-co-HPM novolac/Epon 828 networks cured at various compositions were measured (Table 5. 2). The network properties were affected by the molecular weight of cresol-co-HMP novolac as well as the novolac/epoxy composition. When higher molecular weight cresol-co-HPM novolac oligomers were used (1500g/mol and 1250 g/mol), the 70:30 and the 60:40 compositions showed relatively high T_gs and K_{IC}s and low sol fractions. As the oligomer molecular weight decreased, a larger amount of epoxy was necessary to form well-connected networks. Therefore, only the 60:40 composition exhibited good network properties when the 1000 g/mol oligomer was used. For the well connected networks, the network properties were comparable to those of a 2000g/mol *ortho*-cresol novolac/Epon 828 epoxy network (70:30 wt:wt ratio).

Table 5. 2. Properties of *ortho*-cresol-co-HPM/Epon 828 networks

M_n (g/mol)	Novolac/Epoxy (wt:wt)	T_g (°C)	K_{IC} (MPa*$m^{1/2}$)	Sol fraction (wt. %)
2000*	70:30	154	1.06±0.04	5
1500	80:20	129	0.47	12
	70:30	129	1.18±0.08	3
	60:40	113	0.90±0.10	13
1250	80:20	--	--	25
	70:30	131	0.95±0.05	9
	60:40	156	0.97±0.05	5
1000	80:20	121	--	43
	70:30	125	0.24±0.03	15
	60:40	122	0.87±0.10	7

* cresol novolac/epoxy networks

The thermal stabilities of cresol-co-HPM novolac/epoxy networks were evaluated using thermogravimetric analysis in nitrogen (Table 5. 3). No weight loss occurred below 300°C and all networks were relatively stable up to 400°C. Interestingly, the char yield and the temperature for 5 percent weight loss seemed relatively unaffected by the network composition but was somewhat affected by the molecular weight of the cresol-co-HPM novolac oligomer. In general, slightly higher char yields and temparatures for 5 percent weight loss were observed for networks prepared with higher molecular weight oligomers. For all network compositions, the char yield was between 21 and 27 weight percent and the temperature where 5 percent weight loss occurred ranged from 340°C to 390°C.

Table 5. 3. Thermal stability of cresol-co-HMP novolac/epoxy networks measured using thermogravimetric analysis

M_n (g/mol)	Novolac/Epoxy (wt:wt)	Char yield (Wt. %)	Temperature (5 wt% loss)
1500	80:20	25	388
	70:30	26	370
	60:40	27	376
1250	80:20	26	358
	70:30	27	362
	60:40	23	357
1000	80:20	23	348
	70:30	25	340
	60:40	21	369

Cresol-co-HPM novolac/epoxy networks (80/20 composition) derived from higher molecular weight novolac oligomers showed slightly higher initial degradation temperatures (Figure 5. 12). The char yields at 800°C were similar for these networks.

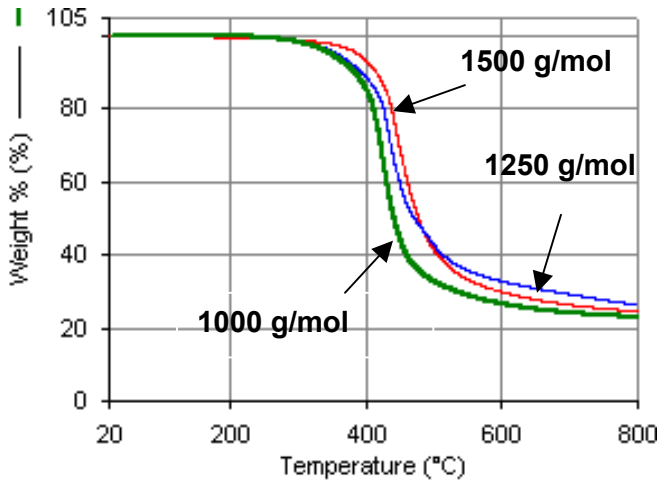

Figure 5. 12. Percent weight loss for cresol-co-HPM novolac/epoxy networks (80:20 wt:wt ratio) prepared with different oligomer molecular weights, monitored using thermogravimetric analysis

Cone calorimetry was used to evaluate the flame retardance of cresol-co-HPM novolac epoxy networks. Samples were ignited at 50 kW/m^2 radiant heat flux under atmospheric air conditions. The effects of network composition were investigated using networks prepared with 1250 g/mol cresol-co-HPM novolac oligomers (Table 5. 4). The 80:20 and 70:30 compositions showed comparable relatively low peak heat release rates (~400 kW/m^2). The char yield for the 80:20 composition was slightly higher than for the 70:30 composition. As expected, the composition with the highest epoxy content (60:40 wt:wt ratio) exhibited the highest peak heat release rate and the lowest char yield.

Table 5. 4. Cone calorimetry measuring the peak heat release rate (PHRR) and the char yield of 1250 g/mol cresol-co-HPM/epoxy networks

Novolac:Epoxy (wt:wt)	PHRR (kW/m^2)	Char yield (°C)
80:20	407	16
70:30	396	15
60:40	572	12

The heat release rate curves of the 1250 g/mol cresol-co-HPM novolac/epoxy networks showed a two stage burning for the 80:20 and the 70:30 compositions (Figure 5. 13). The burning intensified to a single peak heat release for the 60:40 composition. Although the 80:20 and the 70:30 compositions had similar peak heat release rates, the heat released at both stages was significantly lower for the 80:20 composition. Therefore, the 80:20 composition showed superior flame resistance compared to the 70:30 composition.

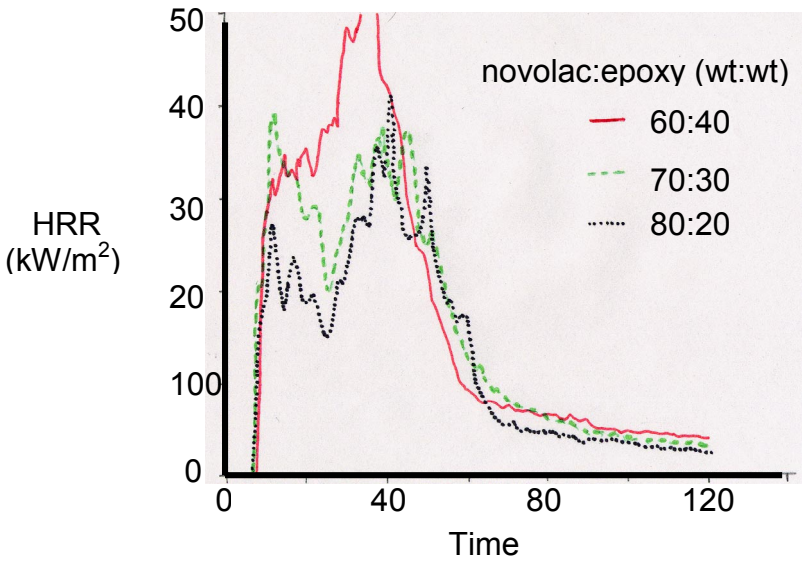

Figure 5. 13. Heat release rate curves for cresol-co-HPM novolac/Epon 828 networks

The effects of novolac oligomer molecular weight on the flame retardance were also explored (Table 5. 5). The peak heat release rates and the char yields were obtained for cresol-co-HPM novolac/epoxy networks (60:40 wt:wt ratio) prepared with different molecular weight novolacs . The networks prepared with the highest oligomer molecular weight (1500 g/mol) exhibited the lowest peak heat release rate and the highest char yield. The flame retardance decreased slightly as the oligomer molecular weight decreased. Networks containing higher molecular weight novolacs may improve flame retardance by favoring the phenolic type degradation pathways, which leads to higher thermal and thermo-oxidative stabilities.

Table 5. 5. Cone calorimetry results for 60:40 wt:wt cresol-co-HPM/epoxy networks prepared with different molecular weight oligomers

M_n (g/mol)	PHRR (kW/m^2)	Char yield (°C)
1500	514	15
1250	572	12
1000	543	10

5.3.4. Characterization of 2-Hydroxy-5-methylphenylmaleimide

2-Hydroxy-5-methylphenylmaleimide was prepared using the same method as the 4-HPM syntheses. This monomer was intended for use as an endcapper in the cresol novolac synthesis. The most reactive site for electrophilic aromatic substitution was expected to be the free *ortho* position with respect to the hydroxyl group.

^{1}H NMR indicated that 2-hydroxy-5-methylphenylmaleimide monomer was successfully prepared. The correct peak integrations in a clean NMR spectrum identified the pure compound (Figure 5. 14).

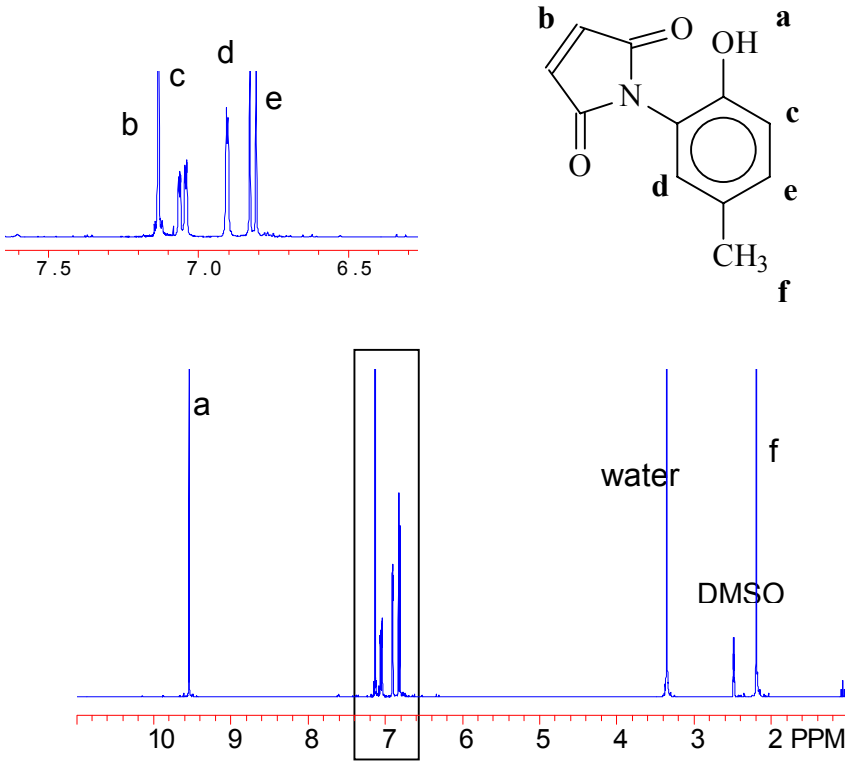

Figure 5. 14. ^{1}H NMR of 2-hydroxy-4-methylphenylmaleimide

Successive dynamic DSC scans were used to monitor the thermal crosslinking reactions of 2-hydroxy-4-methylphenylmaleimide (Figure 5. 15). The first dynamic DSC scan showed a melting point at 160.8°C followed by an exotherm. Successive heatings

showed increased T_gs with each heating cycle which was indicative of increases in molecular weight. The amount of exotherm decreased with each heating cycle.

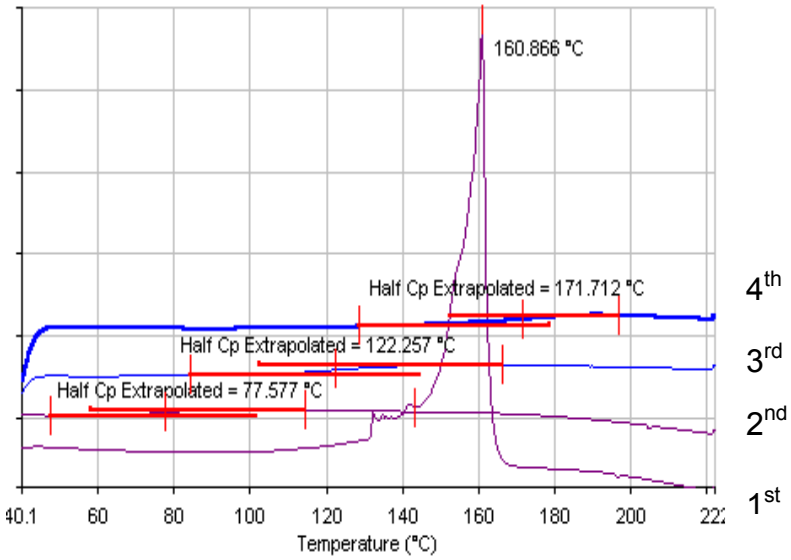

Figure 5. 15. Successive dynamic DSC scans of 2-hydorxy-4-methylphenylmaleimide

The thermal stabilities of 2-hydroxy-4-methylphenylmaleimide, investigated using TGA, indicated that the monomer was thermally unstable even below its melting point. The degradation initiated at approximately 110°C (Figure 5. 16). Only 20 weight percent remained at 250°C for 2-hydroxy-4-methylphenylmaleimide as opposed to 80 weight percent for 4-HPM (Figure 5. 10). The major difference between 2-hydroxy-4-methylphenylmaleimide and 4-HPM is the position of the imide group relative to the hydroxyl group. The two functionalities are *para* to each other on 4-HPM, which eliminates the possibility for interactions. The imide and hydroxyl group are *ortho* to each other on the 2-hydroxy-4-methylphenylmaleimide. The observed ease for 2-hydroxy-4-methylphenylmaleimide degradation may be facilitated by the interaction between the hydroxyl and carbonyl oxygen on the imide group. This degradation, which produced volatile materials, prohibited the use of 2-hydroxy-4-methylphenylmaleimide monomer in void free networks.

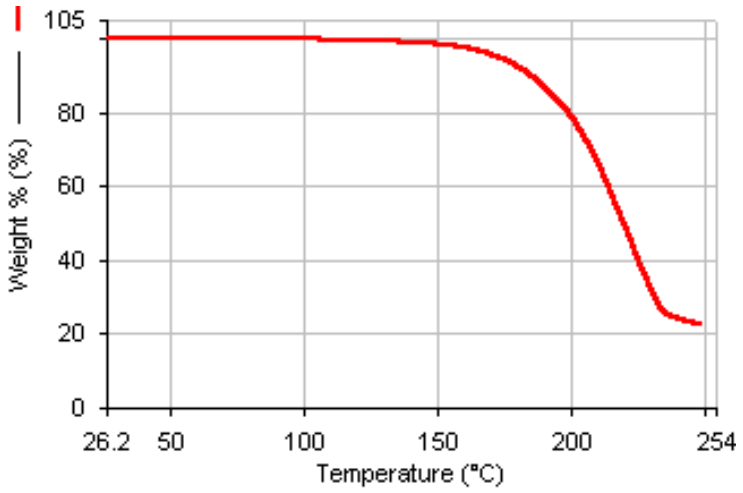

Figure 5. 16. TGA monitoring the weight loss of 2-hydroxy-4-methylphenylmaleimide monomer as a function of temperature (10°C/min, N_2)

5.4. Conclusions

4-hydroxyphenylmaleimide and 2-hydroxy-4-methylphenylmaleimde were synthesized and characterized. 4-HPM was significantly more thermally stable than 2-hydroxy-4-methylphenylmaleimide which begin to degrade even at 110°C. 4-HPM was incorporated into 2,6-dimethylphenol endcapped cresol novolac oligomers. Cresol-co-HPM oligomers prepared in different molecular weights were subsequently crosslinked with Epon 828 epoxy. The network properties and processability depended on the molecular weight of the cresol-co-HPM novolac oligomers and the novolac to epoxy ratios. Lower molecular weight novolac oligomers favored processability, whereas higher molecular weight novolac oligomers led to superior network properties. Network composition also played an important role since compositions high in novolac exhibited enhanced flame retardance, but a sufficient amount of epoxy was required to form fully crosslinked networks with good physical integrity. The 1250 g/mol cresol-co-HPM novolac/Epon 828 network (70:30 wt:wt ratio) presented a good compromise by which networks with excellent properties could be processed easily.

6. Latent Initiators for Novolac/Epoxy Cure Reactions

6.1. Introduction

Composites are becoming increasingly more important in replacing metals and concrete in structural applications due to their excellent oxidative stability and freeze thaw durability. One factor governing the feasibility of mass production is processability, which may comprise up to 80 percent of the final cost. Therefore, efficient processing is essential in producing cost effective composites.

Novolac/epoxy networks are investigated in this research as matrix materials for tough, flame retardant composites. The mechanism for triphenylphosphine (TPP) catalyzed phenolic novolac/epoxy cure reactions was proposed to consist of two steps (Figure 6. 1).[178] The reaction initiates with a triphenylphosphine attack on an epoxy ring to form a zwitterion (A). In the presence of phenolic hydroxyl groups, the zwitterion undergoes rapid proton transfer to generate a phenolate anion and an alcohol (B). The propagation step consists of phenolate anion attacking another epoxy group (C) or an electrophilic carbon next to the triphenylphosphine to form a linkage and regenerate the catalyst. These steps are repeated until a crosslinked network is formed.

[178] R. W. Biernath and D. S. Soane, "Cure Kinetics of Epoxy Cresol Novolac Encapsulants for Microelectronics Packaging," *Contemporary Topics in Polymer Science*, J. C. Salamone and J. S. Riffle Eds., 7, 130-159 (1992).

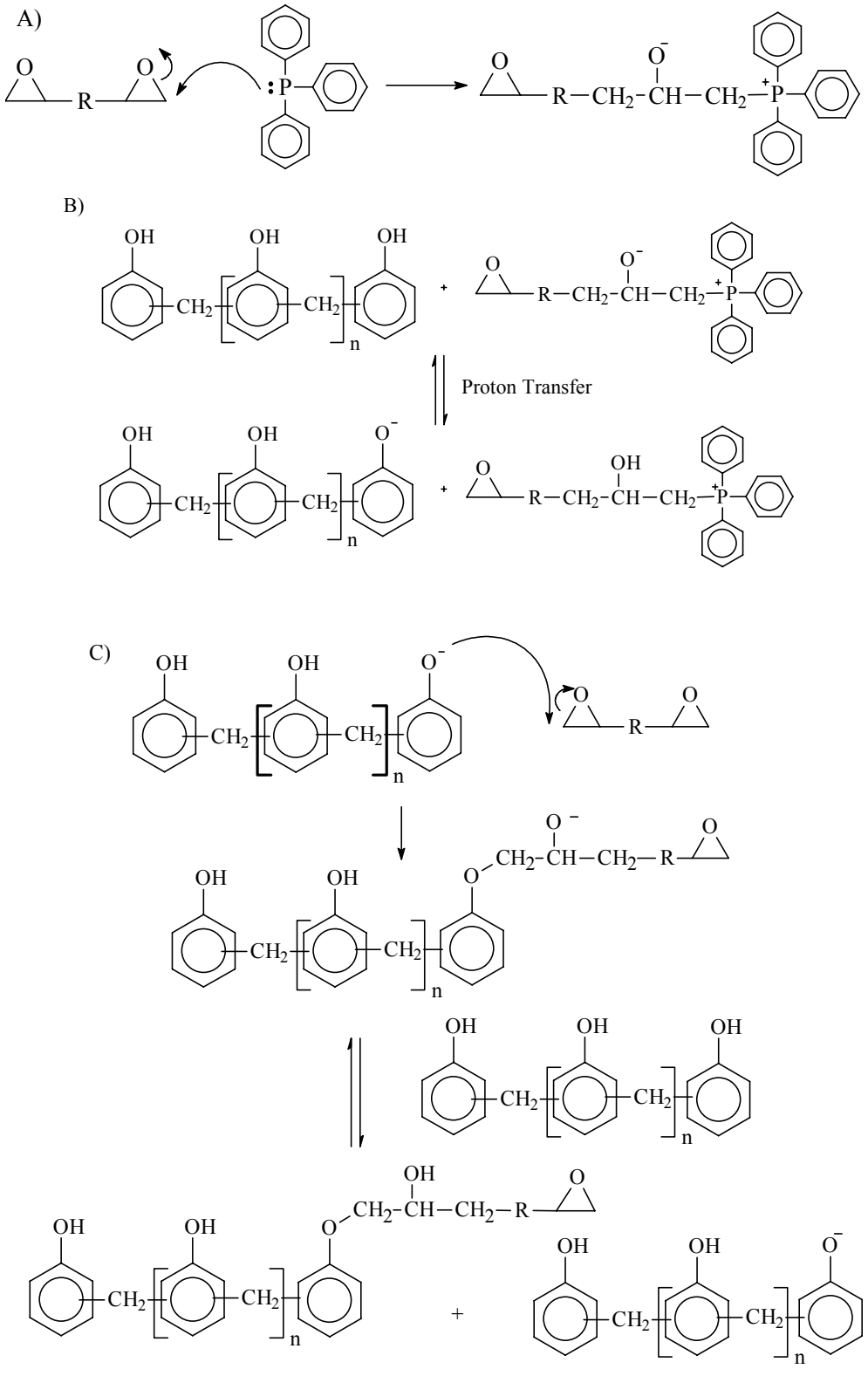

Figure 6. 1. Mechanism of TPP catalyzed phenolic novolac/epoxy reaction

One method for composite fabrication is pultrusion (Figure 6. 3) where spools of carbon fiber are pulled through a bath containing a low viscosity resin or the resin is poured onto the fibers. The fiber embedded in resin then enters a heated metal mold where rapid cure proceeds. Regardless of the fabrication method, a low viscosity resin (< 10 Pa*s) is a requisite for the wetting of the fibers. Once the resin reaches the heated metal mold, fast cure (99% conversion within 5 to 10 minutes) is ideal.

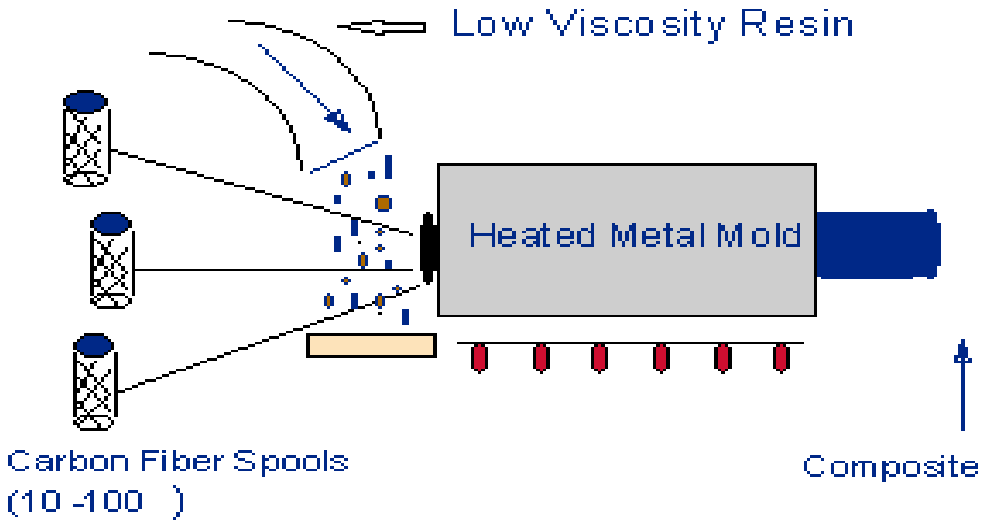

Figure 6. 3. Diagram of pultrusion processing

The major setback thus far with these phenolic novolac/epoxy systems has been optimizing the processing conditions such that long processing time windows and short cure times are obtained. Phenolic novolac/epoxy mixtures (65:35 wt:wt ratio) must be heated to approximately 140°C to reduce the viscosity to the processable range (2-10 Pa*s). At this temperature, the resin mixture reacts slowly and remains processable for approximately 100 minutes. However, curing uninitiated phenolic novolac/epoxy mixtures requires one hour at 240ºC. The cure rates can be greatly accelerated at reduced temperatures with the addition of an initiator such as TPP. However, adding as little as

0.07 mole % TPP (based on moles of epoxy) reduces the processing window to approximately 10 minutes 140ºC while the cure still required 2 hours at 180ºC.[179]

One approach to overcome this problem is to place the catalyst directly onto the fiber so that the resin is not exposed to the catalyst until just prior to cure. An advantage for this approach is that high concentrations of catalyst can be loaded onto the fiber. A salt of Ultem® type poly(amic acid) and tris(2,4,6-trimethoxylphenylphosphine) (TTMPP) has been used as sizing materials for carbon fiber (Figure 6. 4).[180] TTMPP was used as opposed to TPP since the more basic TTMPP was necessary for the salt formation. The salt is stable under ambient conditions but imidizes rapidly at elevated temperatures to release the tertiary phosphine catalyst. Studies have shown that rapid cure rates can be achieved using this approach. However, the high cost associated with this process and raw materials limit its feasibility. Therefore, the key issue remains that a latent catalyst, which can be added directly into the resin mixtures, must be developed to efficiently process these composites.

[179] C. S. Tyberg, K. Bergeron, M. Sankarapandian, P. Shih, A. C. Loos, D. A. Dillard, J. E. McGrath, and J. S. Riffle, "Structure Property Relationships of Void Free Phenolic Epoxy Matrix Materials," *Polymer* **41**(13), 5053-5062 (2000).

[180] C. S. Tyberg, P. Shih, K. N. E. Verghese, A. C. Loos, J. J. Lesko, and J. S. Riffle, "Latent Nucleophilic Initiator for Melt Processing Phenolic-Epoxy Matrix Composites," *Polymer* **41**(26), 9033-9048 (2000).

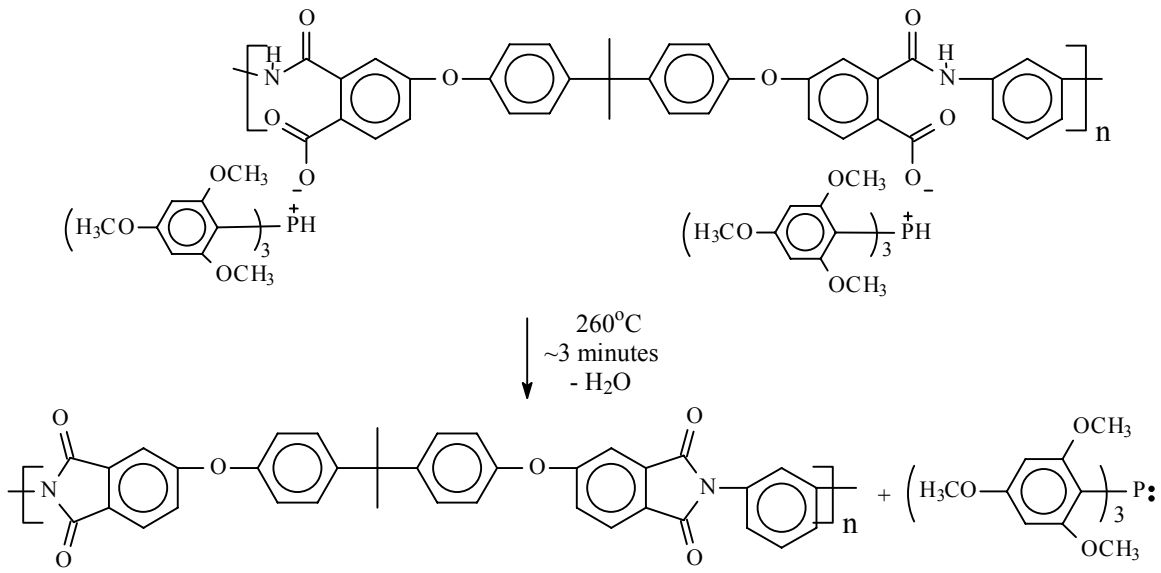

Figure 6. 4. High temperature imidization of PAAS to release TTMPP catalyst

The use of latent catalysts or initiators have been somewhat explored. Latent catalysts, which form active species by external stimulation such as heating or photo-irradiation to catalyze or initiate the polymerization or curing, enhance the pot life and the handling of the thermosetting resins, or increase the processability of the resins.

Latent catalysts comprised of primary or secondary amine salts of a strong acid have been added to phenolic resole resins to extend storage stabilities while retaining rapid cure characteristics of typical acid catalyzed resole resins.[181] These resins can be cured in the presence of a strong acid to enhance the reaction rate without heating to excessively high temperatures. However, the pot life of such compositions suffers in the presence of strong acid catalysts. Strong acids, especially sulfonic acids, were therefore mixed with amines to form latent catalysts which dissociate at elevated temperature to regenerate the acids. The cure rates in the presence of an amine salt of a strong acid were found to be comparable to those of the free strong acid catalyzed resole reactions; the pot life, on the other hand, was extended relative to that of the free strong acid catalyzed resoles.

[181] U.S. Patent 5,344,909 to D. A. Jutching, T. M. McVay, and R. F. Pennock "Latent Catalyzed Phenolic Resole Resin Composition," Sep. 6, 1994.

A cationic salt, *N*-benzylpyrazinium hexafluoroantimonate (BPH) (Figure 6. 5), was investigated as a latent thermal catalyst for epoxy/phenolic novolac reactions.[182] BPH was considered as a latent catalyst since no appreciable amount of reaction occurred below 100°C in its presence. An autocatalytic reaction kinetic mechanism was proposed to occur for the epoxy/phenolic novolac/BPH cure. Dynamic differential scanning calorimetry showed that an increased phenolic novolac content resulted in decreased initial cure temperatures and therefore reduced the cure times.

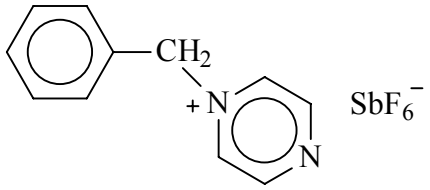

Figure 6. 5. The chemical structure of *N*-benyzlpyrazinium hexafluoroantimonate

Microencapsulated reactant and/or platinum or tin catalysts were utilized in storage stable hydrosilation reactions.[183] Mixtures of organohydrogensiloxane reactants and catalyst are only stable under ambient conditions for a few hours. Encapsulating the reactant or the catalyst in a thermoplastic organic polymer, which has a T_g higher than room temperature but lower than the cure temperature, effectively isolates the two under storage conditions. The reagents are liberated to allow rapid mixing at the desired cure temperatures.

Microencapsulated catalysts can be prepared using chemical, physico-chemical, or physical methods. The chemical methods[184,185] generally involve *in-situ* free radical or

---

[182] S. Park, M. Seo, and J. Lee, "Isothermal Cure Kinetics of Epoxy/Phenol-Novolac Resin Blend System Initiated by Cationic Latent Thermal Catalyst," *Journal of Polymer Science: Part A: Polymer Chemistry* **38**, 2945-2956 (2000).

[183] U.S. Patent Re. 33,749 to C. Lee, D.R. Juen, J. C. Saam, and R. L. Willis, Jr., "Storage Stable Heat Curable Organosiloxane Compositions Containing Microencapsulated Platinum-Containing Catalysts," Reissued Date: Nov. 19, 1991.

[184] US. Patent 3,859,228 to M. Morishita, Y. Inaba, S. Kobari, M. Fukushima, and J. Abe, "Method of microcapsule preparation," Jan. 7, 1975.

condensation polymerization of polymers on the surface of finely divided catalyst in the form of solid particles or droplets. An example of a physico-chemical method involves emulsifying or dispersion in the continuous phase 1) the finely divided particles or droplets, and 2) a solution of the encapsulant in a liquid that is immiscible with the continuous phase. The encapsulant solvent is evaporated, and the emulsion/dispersion is then precipitated, and dried. The physical method involves direct mixing of catalyst and polymer via physical means such as dissolving in a common solvent followed by evaporation of the solvent.

Special care must be taken to isolate the catalyst within the encapsulated particles and away from the exterior surface. For example, in the hydrosilation reactions, even trace amounts of catalyst on the surface lead to premature curing of organosiloxane compositions.[183] Encapsulated particles were often washed with a solvent to remove the excess reagents collected on the surface of the capsules. The shell of microencapsulation must also be sufficiently thick to prevent diffusion of reagents from the interior to the surface.

Salicyclic acid salts have been used as thermal latent catalysts for the preparation of linear polycarbonates from cyclic oligomers.[186] Salicyclic acids salts have carboxylate groups which are stable up to 220°C and are not sufficiently nucleophilic to initiate reactions. At higher temperatures (>220°C), salicyclic acid salts were suggested to undergo a decarboxylation reaction to form phenolates (Figure 6. 6). The decomposition reaction occurred slowly between 220°C and 240°C and more rapidly at higher temperatures. Phenolates were significantly more nucleophilic and catalyzed the polymerization of the carbonate cyclics. The addition of such catalysts allowed the cyclic oligomers to be heated to low viscosities in composite fabrications and promoted rapid cure at higher temperatures.

---

[185] U.S. Patent 4,462,982 to M. Samejina, G. Hirata, Y. Koida, Y. Kobayashi, A. Kida, "Microcapsules and method of preparing same," July 31, 1984.

[186] U.S. Patent 5,087,692 to K. R. Steward and A. J. Salem, "Preparation of Linear Polycarbonates from Cyclic Oligomer Compositions With Salicylic Acid Salt as Catalyst," Feb. 11, 1992.

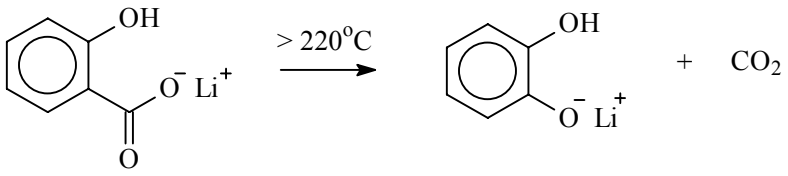

Figure 6. 6. Decarboxylation reaction of salicylic acid salt to form phenolate

Several onium salts, such as iodonium,[187] sulfonium,[188] ammonium,[189] pyridinium,[190] and phosphonium salts,[191] have been reported as excellent thermally latent cationic catalysts. However, drawbacks for these cationic catalysts include poor solubility in monomers and organic solvents, and the residual salts in cured resins may lead to undesirable properties. Recently, phosphonium ylides were introduced as non-salt thermally latent catalysts.[192] Phosphonium ylides were prepared by reacting

---

[187] J.V. Crivello, "The Discovery and Development of Onium Salt Cationic Photoinitiators," *Journal of Polymer Science. Part A: Polymer Chemistry* **37**(23), 4241-4254, (1999).

[188] F. Hamazu, S. Akashi, T. Koizumi, T. Takata, and T. Endo, "Novel Benzyl Sulfonium Salt Having an Aromatic Group on Sulfur Atom as a Latent Thermal Initiator," *Journal of Polymer Science. Part A: Polymer Chemistry* **29**(11), 1675-1680 (1991).

[189] S. Nakano and T. Endo, "Cationic Polymerization of Glycidyl Phenyl Ether by Benzylammonium salts," *Journal of polymer Science. Part A. Polymer Chemistry* **33**(3), 505-512 (1995).

[190] S. B. Lee, T. Takata, and T. Endo, "(*para*-Methoxybenzyl)-*p*-Cyanopyridinium and (*alpha*-Methylbenzyl)-*p*-Cyanopyridinium Hexafluoroantimonates-Activated Latent Thermal Catalysts," *Macromolecules* **23**(2), 431-434 (1990).

[191] K. Takuma, T. Takata, and T. Endo, "Cationic Polymerization of Epoxide with Benzyl Phosphonium Salts as the Latent Thermal Initiators," *Macromolecules* **26**(4), 862-863 (1993).

[192] M. Kobayashi, F. Sanda, and T. Endo, "Application of Phosphonium Ylides to Latent Catalysts for Polyaddition of Bisphenol A Diglycidyl Ether with Bisphenol A: Model System of Epoxy-Novolac Resin," *Macromolecules* **32**(15), 4751-4756 (1999).

triphenylphosphine with an alkyl bromide, followed by dehydrobrominating with Na_2CO_3 (Figure 6. 7). The catalytic activities were found to increase with increased electron-accepting character of the acyl group and the active species were suggested to be the phosphonium cation.

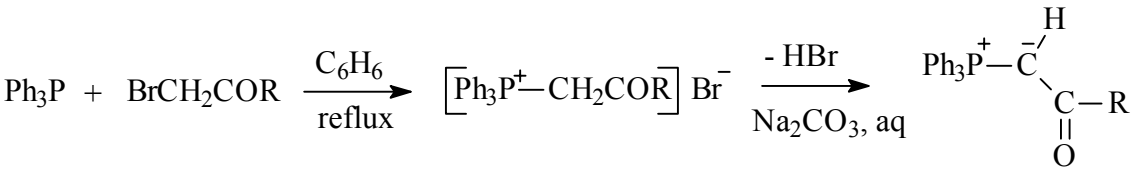

Figure 6. 7. Preparation of phosphonium ylides

Several approaches were investigated in this research for preparing thermally latent catalysts for novolac/epoxy network formation reactions. One approach involves developing sequestered catalyst particles that can be dispersed in the novolac/epoxy mixtures. Ideal sequestered catalyst particles should show minimal activity at the processing temperatures (~140°C) yet promote fast reactions at the cure temperatures (200-240°C). All approaches used an organic thermoplastic polymer matrix to sequester a tertiary amine or phosphine catalyst. The control of the glass transition temperature of the sequestered catalyst particles, which governed catalyst release, was key in successful preparation of appropriate latent catalysts. Sequestered catalysts investigated include miscible and immiscible polymer/catalyst blends, polymeric catalysts, and salts of poly(amic acid)s and tertiary amines.

The second approach utilizes a poly(amic acid)-trihexylamine salt as a sizing material. The kinetics and composite properties were evaluated for samples cured with this sizing.

6.2. Experimental

6.2.1. Materials

Acetic acid (Glacial)

Supplier: Aldrich FW: 60.06

CH_3COOH

Used as received

1,2,4,5-Benzenetetracarboxylic dianhyride (pyromellitic dianhydride or PMDA)

Supplier: Aldrich FW: 218.12 m.p., °C 283-286

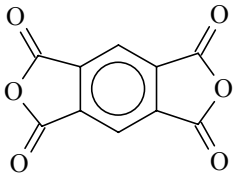

Purification: PMDA was obtained in polymer grade purity and was dried at ~180°C under vacuum for at least 12 hours prior to use.

3,4,3',4'-Biphenyltetracarboxylic dianhydride (BPDA)

Supplier: Aldrich FW: 294.224 m.p., °C 300

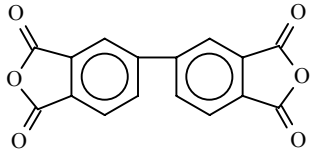

Purification: BPDA was obtained in polymer grade purity and was dried at ~180°C under vacuum for at least 12 hours prior to use.

***N,N*-Dimethylacetamide (DMAc)**

Supplier: Aldrich FW: 87.12 m.p., °C 164.5-166

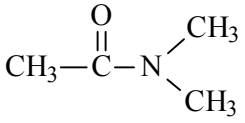

Purification: DMAc was dried using activated molecular sieves prior to use.

Bisphenol-A

Supplier: Aldrich FW: 228.29 m.p., °C 158-159

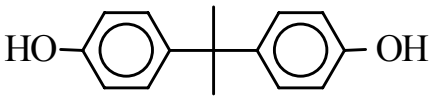

Used as received

Bis[4-(3,4-dicarboxyphenoxy)phenyl]propane dianhydride (Bisphenol-A dianhydride)

Supplier: General Electric

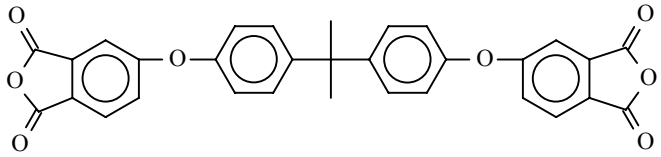

Purification: Bisphenol-A dianhydride was recystallized from toluene and acetic anhydride four times, then washed with toluene and n-heptane. The recrystallized bisphenol-A dianhydride was dried in a vacuum oven at 140°C overnight immediately prior to use.

Carbazole

Supplier: Aldrich FW: 167.21 m.p., °C 243-246

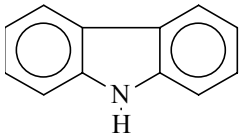

Used as received

Chlorobenzene

Supplier: Aldrich FW: 112.56 b.p., °C 132

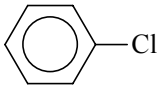

Purification: Chlorobenzene was vacuum distilled prior to use.

Chloroform

Supplier: Aldrich FW: 119.38 b.p., °C 61

$CHCl_3$

Used as received

Epon 828

Supplier: Shell chemicals EEW: 187

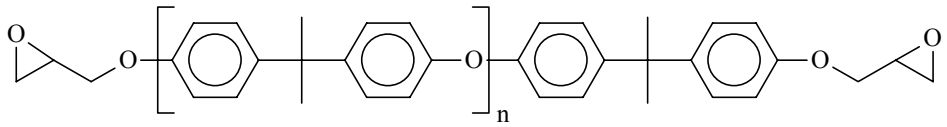

Used as received

4,4'-(9-Fluorenylidene)dianiline (FDA)

Supplier: Aldrich FW: 348.45 m.p., °C 237-239

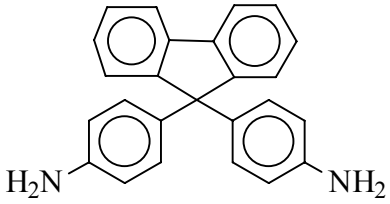

Purification: FDA was obtained in polymer grade purity and was dried at ~180°C under vacuum for at least 12 hours prior to use.

Imidazole

Supplier: Aldrich FW: 68.08 m.p., °C 89-91

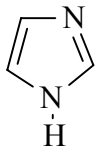

Used as received

Phthalic anhydride (PA)

Supplier: Acros Organics FW: 148.117 m.p., °C 134

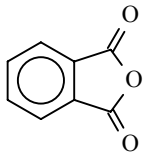

Purification: PA was sublimed under vacuum at ~ 120°C prior to use.

Matrimid

Supplier: Ciba Chemicals T_g, °C 300

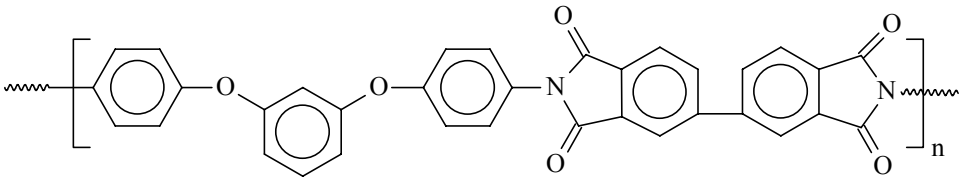

Used as received

Methyl alcohol (methanol, CH_3OH)

Supplier: Aldrich FW: 32.04 b.p., °C 64.7

Methanol was obtained in HPLC grade and used as received

1-Methyl-2-pyrroilidinone (NMP)

Supplier: Fisher Scientific FW: 99.13 b.p., °C 202 (81-82°/10mm)

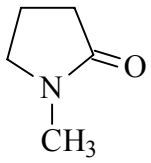

Purification: NMP was purified for use in poly(amic acid) synthesis by drying over calcium hydride for at least 12 hours, followed by distillation under reduced pressure.

Phenolic novolac

Supplier: Georgia-Pacific (Product # GP-2073) n=5

Supplier: Occidental (Product # 29-619) n=2.4

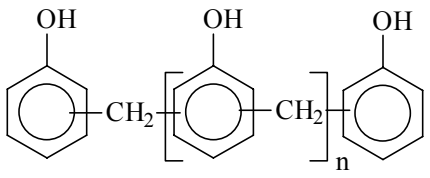

Used as received

***meta*-Phenylenediamine (*m*-PDA)**

Supplier: Aldrich FW: 108.14 m.p., °C 66

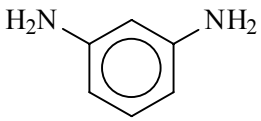

Purification: *m*-PDA was sublimed under vacuum at ~65°C. This monomer oxidizes readily in air and was used soon after sublimation. It was stored in a dark brown bottle to prevent oxidation.

***para*-Phenylenediamine (*p*-PDA)**

Supplier: Aldrich FW: 108.14 m.p., °C 145

Purification: *p*-PDA was sublimed under vacuum at ~140°C, successively two times. This monomer oxidizes readily in air and was used soon after sublimation. It was stored in a dark brown bottle to prevent oxidation.

Phenylsilane

Supplier: Aldrich FW: 108.22 b.p., °C 120

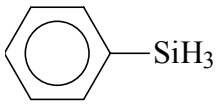

Used as received

2-Propanol (isopropanol)

Supplier: Aldrich FW: 60.10 b.p., °C 97

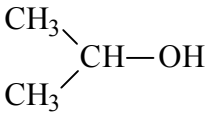

Isopropanol was obtained in the HPLC grade and used as received

Potassium carbonate (K_2CO_3)

Supplier: Aldrich FW: 138.21 m.p., °C 891

Used as received

Tetrahydrofuran (THF)

Supplier: EM Science FW: 72.11 b.p., °C 65-67

Purification: In the poly(amic acid) synthesis, THF was refluxed over sodium with a small amount of bezophenone as an indicator for dryness and distilled immediately prior to use.

Toluene

Supplier: Aldrich FW: 92.14 b.p., °C 110.6

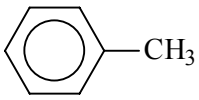

THP was obtained in the HPLC grade and used as received

Trihexylamine

Supplier: Aldrich FW: 269.52 b.p., °C 263-265

$:N((CH_2)_5CH_3)_3$

Used as received

Triphenylphosphine (TPP)

Supplier: Aldrich FW: 262.29 m.p., °C 79-81

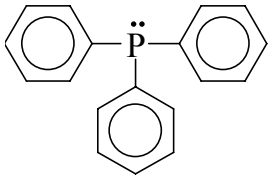

Used as received

Udel

Supplier: Amoco Tg: 187 °C

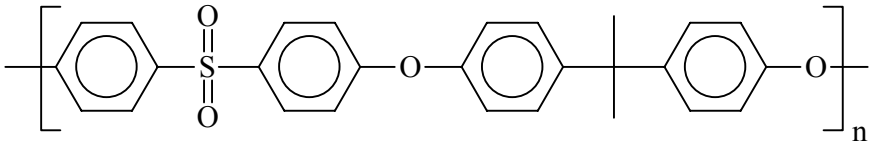

Used as received

Ultem

Supplier: GE

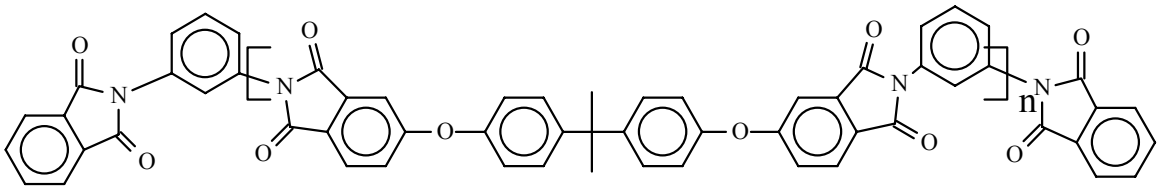

Used as received

6.2.2. Methods

6.2.2.1. Melt mixing of phenolic novolac/epoxy resins

Kinetic studies were evaluated for phenolic novolac/Epon 828 epoxy mixtures prepared with novolac (n=5 or n=2.4). A 65/35 composition was used for the novolac having n=5 and a 60/40 composition was used for the novolac having n=2.4. Unless otherwise stated, the novolac resin having n=5 was used in the Results and Discussion section. Novolac (65 g) was charged to a 500 ml three-necked round bottom flask

equipped with a mechanical stirrer and heated to 160°C until a viscous fluid was formed. Epon 828 epoxy (35 g) was then added. The phenolic novolac/epoxy mixture was stirred vigorously for 3-5 minutes until a homogenous mixture was obtained. The mixture was poured into aluminum pans chilled over an isopropanol/dry ice bath, then ground into a fine powder and stored for later use.

6.2.2.2. Preparation of polymer/TPP sequestered catalysts

Polyimides (Ultem or Matrimid) or polysulfone (Udel) and triphenylphosphine (up to 50 wt %) were dissolved in a minimal amount of chloroform. The homogeneous solution was dried in a hood until a viscous material was formed. The mixture was then chilled under liquid nitrogen and the solidified material was ground into a powder using a mortar and pestle. The powder was separated using a sieve (mesh size 60). The larger particles were reground until a fine powder was obtained. This reground powder was then combined with the original fine powder fraction. The particles were dried under vacuum for 8 hours at room temperature, then 2 hours at 80°C. Only the "small" particles which passed through the sieve were used in the kinetic studies described herein.

To remove residual catalyst on the surface of the particles, a thin layer of the sequestered catalyst particles was placed on a piece of filter paper in a Buchner funnel and washed with acetone or warm methanol (~30°C). The total exposure time of the particles in the solvent was limited to approximately 3 minutes.

6.2.2.3. Synthesis of Poly(arylene ether phosphine oxide)

Poly(arylene ether phosphine oxide) [P(AEPO)] was synthesized using the procedures described in literature.[193] The Carother's equation was used to determine the amount of reagents needed to obtain a targeted number average molecular weight. A typical reaction procedure for the synthesis of a 20,000 g/mol P(AEPO) is as follows

[193] C. D. Smith, H. Grubbs, H.F. Webster, J. P. Wightman, and J. E. McGrath, "Poly(Arylene Ether Phosphine Oxide)s. 1. Overview of Chemistry, Thermal-Stability and Oxygen Plasma Resistance," *Abstract of Papers of the American Chemical Society*, *PMSE* **52**(part 2), 202, (1991).

(Figure 6. 8). Into a 4-necked round bottom flask equipped with an overhead stirrer, a N_2 inlet, a Dean Stark trap connected to a condenser and N_2 outlet, and a thermometer was charged bisphenol-A (31.01g, 0.136 mol), BFPPO (43.91 g, 0.140 mol), and phenol endcapper (0.331g, 0.00351 mol). DMAc (~ 300 ml) was added to make a 20 wt. % solution. Then a 15 % excess of K_2CO_3 (22.21g, 0.161mol) and toluene (~125 ml) were added to the solution. The mixture was azeotroped at 145°C for four hours. Then the temperature was raised to 160°C and the reaction was continued for an additional 12 hours. The viscous product mixture was cooled to room temperature, diluted with chloroform, and filtered through a Buchner funnel to remove inorganic salts. Glacial acetic acid was used to neutralize the solution which was then precipitated in an 80:20 methanol:water mixture in a high-speed blender. The product was vacuum dried at 100°C for ~12 hours. The purification process was repeated when necessary.

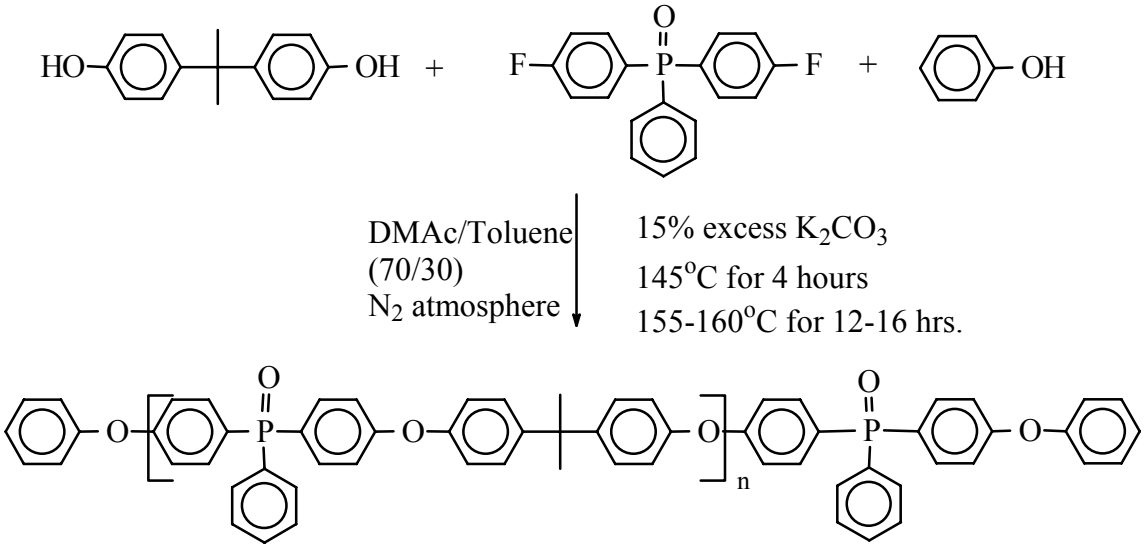

Figure 6. 8. Synthesis of poly(arylene ether phosphine oxide)

6.2.2.4. Reduction of Poly(arylene ether phosphine oxide)

Phenylsilane was used to reduce the poly(arylene ether phosphine oxide)s to their corresponding phosphines.[194] The amount of reduction depended on the phosphine oxide to phenylsilane ratio, reaction temperature and pressure, and reaction time. The ratio of P=O group to phenylsilane was set at 1.5 in these experiments. In a dry three-necked flask equipped with a mechanical stirrer, a N_2 inlet and outlet, P(AEPO) (8.74 g, 0.0173 mol P=O) was dissolved in distilled chlorobenzene (~78.7ml, 10 wt % solution). Then phenylsilane (2.86g, 3.20ml, 0.0261 mol) was added dropwise to the solution over a 5 minute period. The solution was heated slowly to 110°C and reacted until the desired amount of reduction was achieved. The extent of reduction was monitored via ^{31}P NMR.

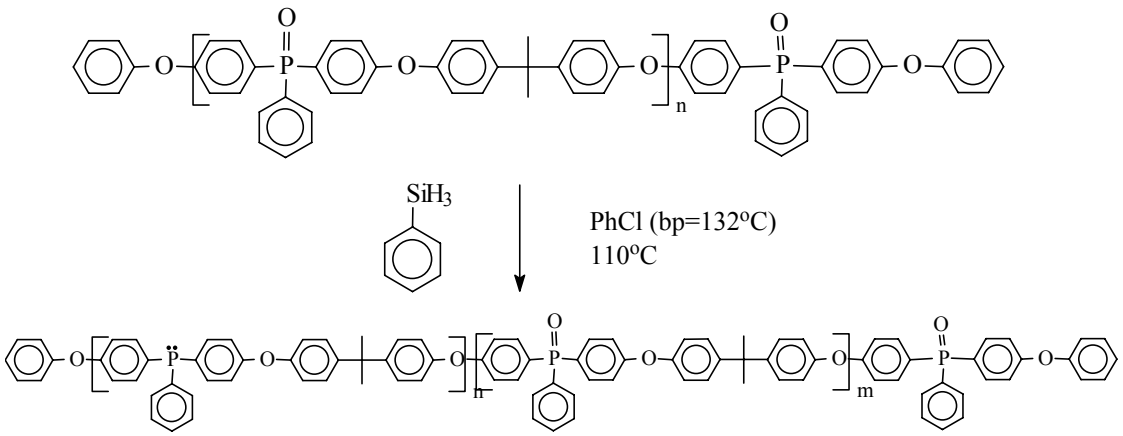

Figure 6. 9. Reduction of phosphine oxide to phosphine using phenylsilane

6.2.2.5. Synthesis of Ultem type poly(amic acid)

The stoichiometry was controlled by the Carother's equation to achieve controlled molecular weight poly(amic acid)s. Bisphenol-A dianhydride (51.3g, 0.0986 mol) was weighed into a dry 500 ml round bottom flask have a magnetic stir bar. The flask was sealed with a rubber septum and purged with nitrogen. Dry THF (250 ml) was added to the flask via a cannula. Phthalic anhydride (0.7524g, 0.0051mol) and *m*-phenylene

[194] E. Bonaplata, H. Ding, B.E. Hanson, and J. E. McGrath, "Hydroformylation of Octene-1 with a Poly(Arylene Ether Triarylphosphine) Rhodium Complex," *Polymer* 36(15), 3035-3039 (1995).

diamine (10.9313g, 0.1011 mol) was placed in a separate 100ml round bottom flask, sealed with a rubber septum and purged with nitrogen. Dry THF (50ml) was added to the 100 ml flask by cannula and the mixture was stirred for approximately 10 minutes until all monomers dissolved. The solution was then added to the heterogeneous bisphenol-A dianhydride/THF mixture by cannula. The 100 ml flask was rinsed twice with approximately 25 ml dry THF, and the wash solution was added to the reaction flask by cannula. After 24 hours, the polymer solution was poured into a Teflon dish, placed inside a covered glass container equipped with a nitrogen sweep, and was exposed to a brisk nitrogen flow at room temperature for ~ 48 hours to evaporate the solvent. The poly(amic acid) was then placed in a vacuum oven at room temperature to further remove the solvent. The poly(amic acid) contained approximately 20 weight percent THF according to ^{1}H NMR determinations. This was used to obtain an accurate weight of the poly(amic acid) for salt formation. The number average molecular weight of the polyimide determined by GPC was 22,000g/mol.

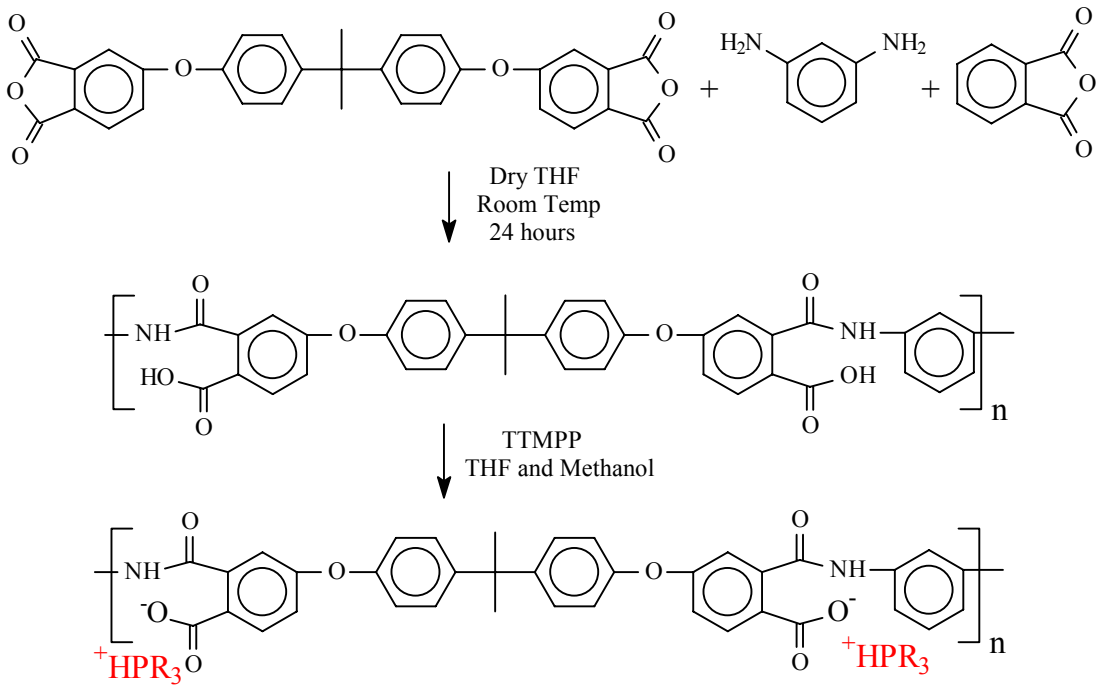

Figure 6. 10. Synthesis of Ultem type poly(amic acid) salt with TTMPP

6.2.2.6. Preparation of Ultem type poly(amic acid) salt with TTMPP

To a 2000 ml beaker with a magnetic stir bar was added THF (1000ml), methanol (500 ml), and TTMPP (52.3 g, 0.098 mol, a 10 % excess relative to carboxylic acid groups). Once the TTMPP had dissolved, the poly(amic acid) (28.1 g, 0.089 mol) was added. The solution was stirred for 6 hours until all of the poly(amic acid) had dissolved, then poured into a Teflon boat to evaporate the solvent.

6.2.2.7. Synthesis of FDA/BPDA based poly(amic acid) salts

Tertiary amine salts of FDA/BPDA poly(amic acid)s were prepared using the following general approach. In a flame dried 100 ml round bottom flask containing a magnetic stir bar, BPDA (2.51 g, 0.008475 mol) and FDA (3 g, 0.008460 mol) were dissolved in distilled DMAc (20 ml) and reacted at room temperature for 2-3 hours to form poly(amic acid). Tertiary amine, trihexylamine or imidazole (0.00888 mol), predissolved in isopropanol was added dropwise to the poly(amic acid) solution while stirring vigorously. The stirring was continued until a homogenous solution was obtained. The poly(amic acid) salt solution was vacuum distilled at ~70°C to remove most of the solvent and then placed in a vacuum oven at ~80°C overnight.

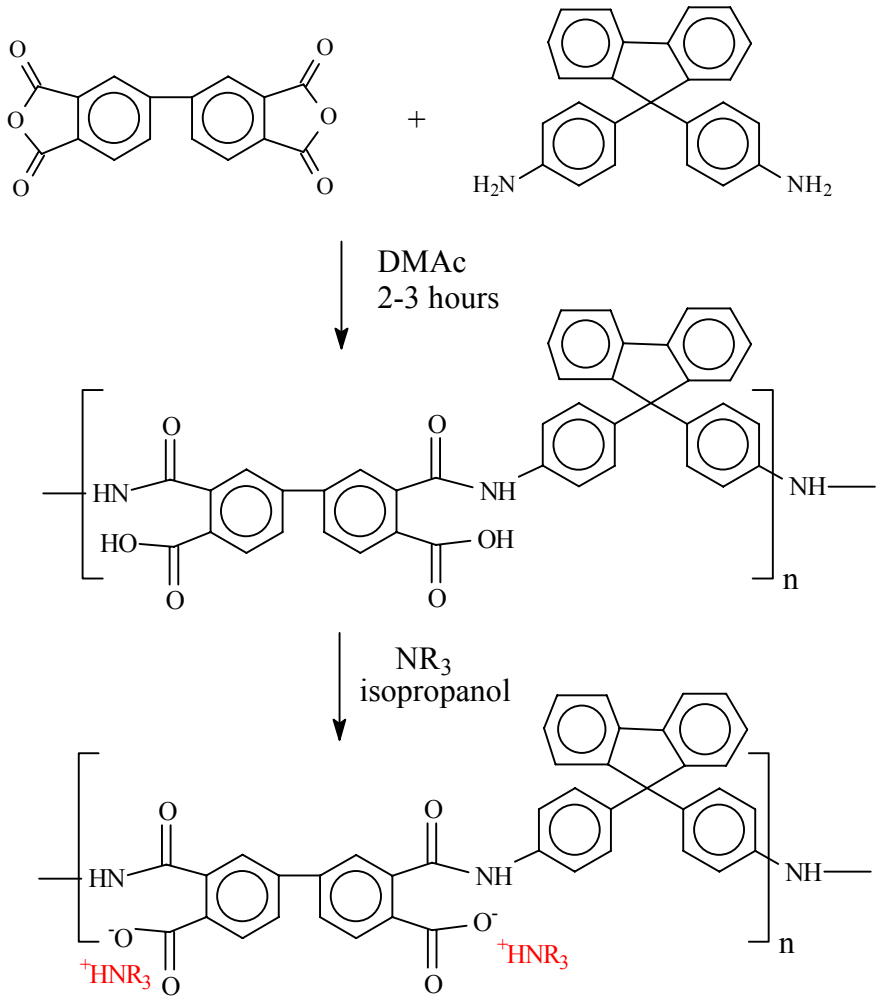

Figure 6. 11. Synthesis of biphenyl dianhydride and FDA based poly(amic acid) and poly(amic acid) salt

6.2.3. Characterization

6.2.3.1. Differential scanning calorimetry (DSC)

A Perkin-Elmer DSC-7 was used for differential scanning calorimetric measurements. The DSC was calibrated using indium and zinc standards, and ice water was used as the coolant. The novolac/epoxy mixture, ground previously, was hand mixed with the appropriate amount of sequestered catalyst particles until a uniform mixture was obtained. Samples of 5-7 mg were sealed in aluminum pans and heated from 25 to 180°C

at 10°C/min. The glass transition temperatures were calculated as the midpoint of the curves.

For isothermal analysis, samples were heated from room temperature to the chosen processing or reaction temperature at 200ºC/min, followed by monitoring the heat capacity as a function of time. The time to 99 % conversion was calculated by using the partial peak area from the exotherm of isothermal DSC analyses.

6.2.3.2. Viscosity measurements

A Brookfield DV-III Programmable Rheometer was used to determine the isothermal viscosities of novolac/epoxy mixtures at processing temperatures. Approximately 10 g of powder samples were placed in disposable sample tubes and heated to the test temperatures. A spindle, which was driven through a calibrated spring, was immersed in the test fluid. The viscous drag of the fluid against the spindle was measured by the spring deflection. The torque was used to calculate the viscosities.

6.2.3.4. ^{1}H NMR

^{1}H NMR and ^{13}C NMR spectra were obtained on a Varian Unity 400 NMR spectrometer. For ^{1}H NMR, 5 mm tubes containing approximately 20 mg sample dissolved in chloroform-d, acetone-d_6, or DMSO-d_6 were analyzed under ambient conditions. The experimental parameters included a 1.0 second relaxation delay, 23.6 degree pulse, and 6744.9 Hz spectral width. Thirty-two repetitions were performed for each sample.

6.2.3.5. ^{31}P NMR

Solution Phosphorus (^{31}P) NMR spectra were also obtained on a Varian 400 MHz instrument, corresponding to a phosphorus frequency of 161.9 MHz. All spectra were referenced to 85% H_3PO_4 at 0 ppm, and dichlorophenyl phosphine sulfide was used as a standard (76.05 ppm).

6.2.3.6. Scanning electron microscopy

SEM was used to investigate the surface structures as well as the cross-sections of particles. For particle surface analysis, particles were adhered to the plate. For cross-section analysis, particles were potted in epoxy resin and microtomed until a smooth cross-section was obtained.

6.2.3.7. Thermogravimetric analysis

A Perkin-Elmer TGA-7 Thermogravimetric analyzer was used to determine the thermal and thermo-oxidative stabilities of the cresol novolac/epoxy networks. Samples of approximately 5-8 mg were placed in a platinum sample pan and heated in a furnace from 30 to 900°C at 10°C/min. Air or nitrogen was used as the carrier gas. The sample weight loss was monitored as a function of temperature or time.

6.2.4. Composite preparation and testing methods

6.2.4.1. Synthesis of Ultem type poly(amic acid) salt with trihexylamine

An Ultem type poly(amic acid) salt was obtained by first reacting Bisphenol-A dianhydride with *meta*-phenylene diamine to form poly(amic acid); it was then mixed with trihexylamine to form the poly(amic acid) salt (Figure 6. 12). Bisphenol-A dianhydride (22.97 g, 0.04415 mol) was dissolved in dry THF (150 ml) in a flame-dried 500 ml round bottom flask with a stir bar. In a separate 100 ml flame dried flask, *meta*-phenylene diamine (4.877g, 0.04512 mol) was dissolved in dry THF (25 ml). The m*eta*-phenylene diamine solution was added to the Bisphenol-A solution via a cannula. The 100 ml flask was rinsed twice with ~ 25 ml dried THF, and the wash solution was added to the reaction flask. The mixture was allowed to react at room temperature for 24 hours. Trihexylamine (25g, 0.101 mol, 5 % excess over the acid groups), dissolved in methanol (60 ml), was added dropwise to the poly(amic acid) solution. The mixture was stirred for 2 hours. The solution containing the poly(amic acid) acid salt was poured into a Teflon dish, air dried at room temperature overnight, then placed in a vacuum oven to further remove the solvent.

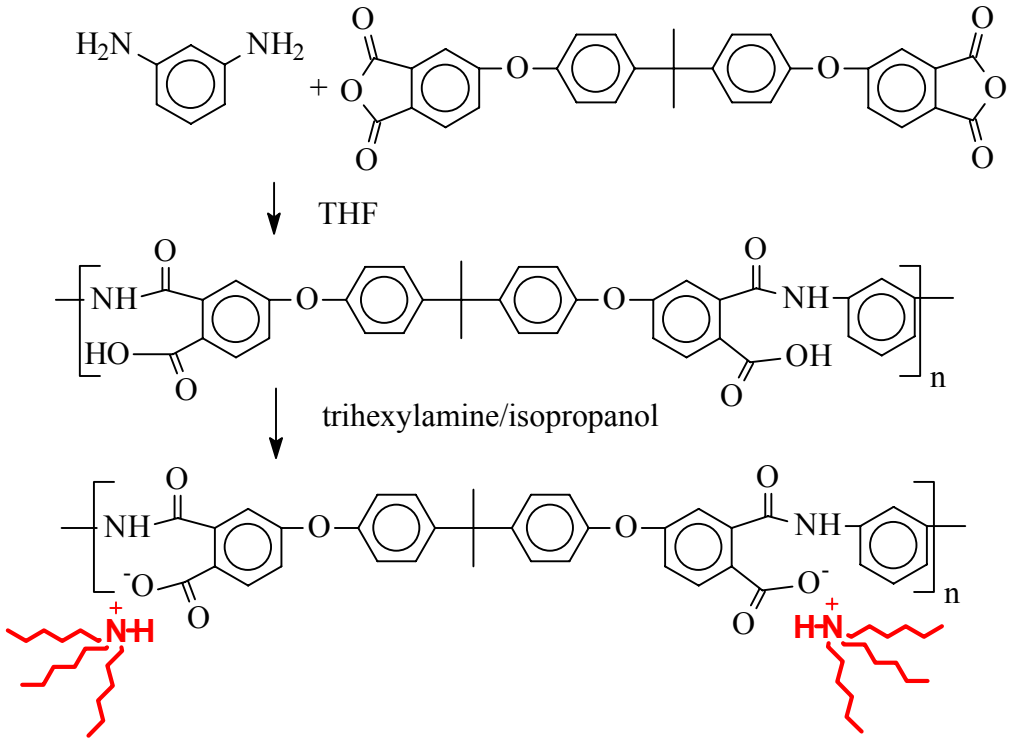

Figure 6. 12. Preparation of Ultem type poly(amic acid) salt with trihexylamine

6.2.4.2. Sizing of carbon fiber

Fiber tows were sized on a small-scale custom made sizing line (Figure 6. 13) from 1.5 weight percent PAAS/trihexylamine solutions in methanol. The tows passed through the sizing bath and were first air dried in the vented tower at room temperature. Then the tows were passed through the same vented tower at 150°C for approximately 3-5 minutes to imidize the poly(amic acid) salt and release the trihexylamine.

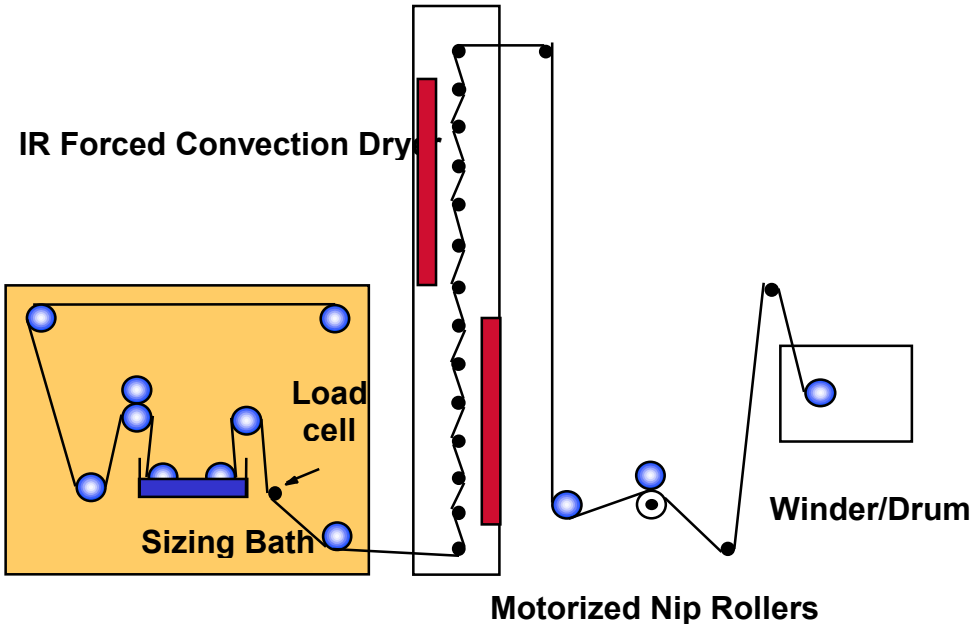

Figure 6. 13. Schematic of a sizing line

6.2.4.3. Hot-melt prepregging and composite fabrication

A lab scale Model 30 prepregger manufactured by Research Tools Corporation, Ovid, Michigan was used in the composite preparation (Figure 6. 14). In this apparatus, a PAAS/trihexylamine sized AS-4 carbon fiber tow was pulled through a resin pot containing a novolac/epoxy resin mixture heated to a low viscosity, then through a wedge-slit die at the bottom of the heated resin pot. The wetted tow was then passed between a pair of flattening pins and around a guide roller before being wound on a drum. The flattening pins and the guide rollers were independently heated. The set-point temperatures of the resin pot, flattening pin, and roller were determined by viscosity data. The set-point temperature was 140°C for the 65/35 wt/wt phenolic novolac (n=5)/epoxy mixtures. Low melt viscosities were critical to permit good wet-out of the reinforcing fiber tows and yield uniform resin content. The prepregs were then cut into 6”x6” plies, laid in a metal mold and cured under pressure to form composite panels. The weight percent of fibers in the composite was 71-75 %. Panels for mechanical testing were prepared in unidirectional and in cross-plies with various numbers of plies depending on the test.

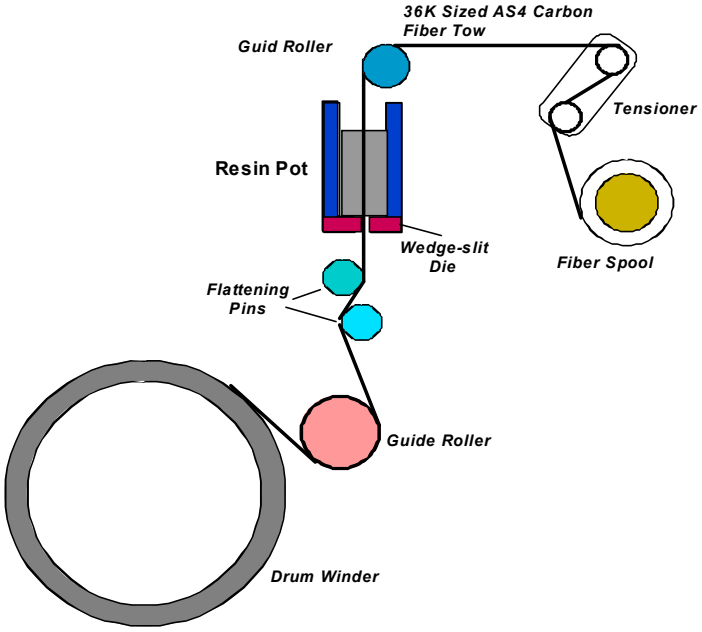

Figure 6. 14. Schematic representation of the hot melt prepregging process

6.2.4.4. Composite fiber volume fraction

The fiber volume fractions of the composites were calculated by first determining the density of the composite using Archimedes' principle. The weight of a composite specimen was measured in air and in water. The density of the composite can be calculated using the following equation.

$$\rho_c = W_{air}/(W_{air}-W_{water}) * \rho_{water} \quad \textbf{(6. 1)}$$

where ρ_c is the density of the composite, ρ_{water} is the density of water, W_{air} is the weight of the sample in air, and W_{water} is weight of the sample in water. The fiber volume fraction was then calculated using the rule of mixtures

$$\nu = (\rho_c-\rho_{resin})/(\rho_{fiber}-\rho_{resin}) \quad \textbf{(6. 2)}$$

where ν is the fiber volume fraction, ρ_{fiber} is the density of the carbon fiber = 1.8 g/cc, ρ_{resin} is the density of the resin = 1.23 g/cc, and ρ_c is the composite density calculated from equation (6.1).

6.2.4.5. Kinetic studies of novolac/epoxy reaction with trihexylamine

Arrhenius activation energies, pre-exponential factors, and first order rate constants for novolac/epoxy cure reactions were determined using a differential scanning calorimetry according to ASTM E 698–79.[195] Samples were heated at various heating rates and the exothermic reaction peaks were recorded. The temperatures at which the peak of exotherm occurred were plotted versus their respective heating rates. Kinetic parameters were calculated from the slope of this plot. The time that was required to reach 50% conversion, or the half-life time, was calculated for a selected temperature. A sample was aged to reach 50% conversion according to the predicted time at the selected temperature and the residual reaction heat was compared to heat of an unaged sample to confirm the validity of this method.

6.2.4.6. Flexural properties

Transverse flexural tests were performed according to ASTM standard D 790–98 to evaluate the composite properties. Composite samples with dimensions of 127 mm x 12.7 mm x 2.4 mm were measured in a three-point bend fixture. The rate of crosshead motion (R) was 7.11 mm/min, which was calculated use the following equation,

$$R = ZL2/6d \qquad \textbf{(6. 3)}$$

where L is the support span length (101.6 mm), d is the depth of the beam (2.4 mm), and Z is the rate of straining of the outer fibers (0.01).

Flexural strength and modulus were calculated as follows,

$$\sigma_f = 3PL/2bd^2 \qquad \textbf{(6. 4)}$$

$$E = L^3m/4bd^3 \qquad \textbf{(6. 5)}$$

where P is the load, b is the width of beam tested (12.7 mm) and m is the slope of the initial straight-line portion of the load-deflection curve.

[195] ASTM E 698-79 (reapproved 1993) "Standard test method for Arrhenius kinetic constant for thermally unstable materials," 1993.

6.2.4.7. Tensile testing

Tensile properties were evaluated for both cross-ply and unidirectional composites. The cross-ply consisted of four plies of 0°,90°,90°,0° directions, and the unidirectional panel consisted of 3 plies in the zero direction. Composite panels were cut and ground to ¾" x 6" samples.

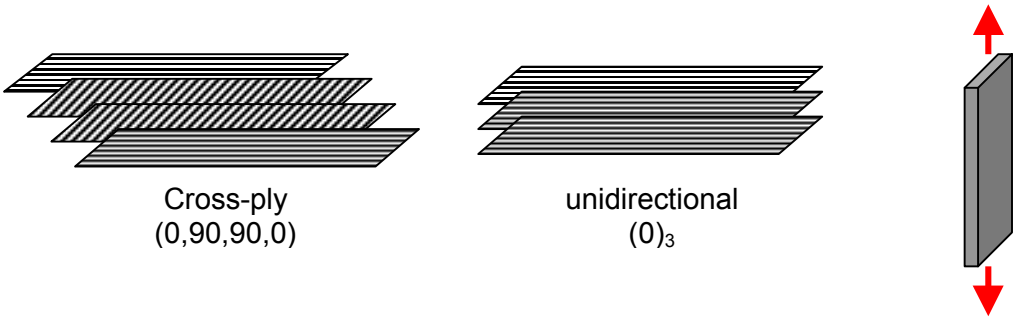

Figure 6. 15. Composite ply lay up to form crossply or unidirectional specimen for tensile testing

To mount 1½" long epoxy/fiber glass tabs onto the end of each sample, specimens were measured and marked on each side. The mid-section of the tested specimen was covered. The exposed ends were grip blasted on both sided to create rough surfaces. One side of the epoxy/glass fiber tab was also grip blasted. The epoxy/glass fiber tabs were chemically bonded to the sample specimens via a two part epoxy adhesive (Figure 6. 16). The sample specimens adhered to the epoxy tabs were placed in a mold with spacers and cured in an oven at 50°C for two hours. A fifteen-pound weight was placed on top of the mold to squeeze excess adhesives between the bond layers during the oven cure.

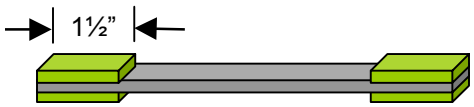

Figure 6. 16. Tensile test specimen with epoxy/glass fiber tabs

Two strain gages (precision strain gages, CEA-06-125UW-350, from Measurement Groups, Inc) were adhered to the sample; one on each side and

perpendicular to each other. The transverse strain and the axial strain can thus be measured by monitoring the changes in voltages due to expansion or contraction of the test specimen. Wires were soldered onto the strain gages.

Tests were performed on a servo-hydraulic MTS test frame in load control mode. A loading rate of 100 pounds per second was applied. The loading cycle was programmed into the Microprofiler^{TM}, which controlled the instrument once a test was begun. A pair of MTS Model 647 hydraulic wedge grips, a 448.82 test controller, a 418.91 Microprofiler^{TM}, a 413.81 master controller and a 464.80 data display unit were used. The signals from the extensometers were amplified using a 2310 Vishay Measurement group amplifier box. LabView® software was used to monitor the load, stroke and strain signals during the tests.

The ultimate tensile strength (F^{tu}) was determined using

$$F^{tu} = P^{max}/A \qquad \textbf{(6. 6)}$$

where P^{max} is the maximum load prior to failure and A is the average cross-sectional area of the specimen. The tensile strain (ε_i) was calculated from the extensometer displacement (δ_i) and the extensometer gage length (L_g)

$$\varepsilon_i = \delta_i/L_g \qquad \textbf{(6. 7)}$$

The Poissons ratio (ν) relates transverse strain ($\Delta\varepsilon_t$) and axial strain ($\Delta\varepsilon_l$)

$$\nu = - \Delta\varepsilon_t/\Delta\varepsilon_l \qquad \textbf{(6. 8)}$$

6.2.4.8. Mode II Toughness (G_{IIC})

Ten plies of unidirectional fiber with 0.05 mm thick delamination tab placed midway through the laminate were cured. The delamination tab was 2" (50.8 mm) from the outside edge of the panel. The panel was cut and ground to 12.5x2.0 cm (5"x0.79") sample size with approximately 1½" tab remaining in the composite. A natural initial crack approximately 1 mm past the delamination tab was generated by placing a thin wedge in the crack and tapping lightly with a hammer.

The compliance (C') of the uncracked portion of the sample was tested using an end notched flexural specimen geometry in a three-point bend loading (Figure 6. 17).

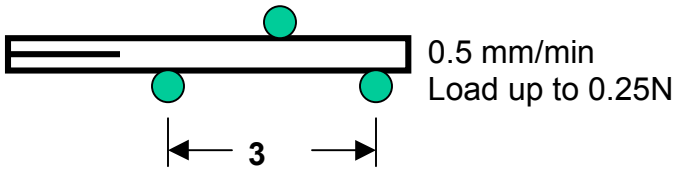

Figure 6. 17. Compliance determination of the uncracked sample

The flexural modulus (E_f) can be calculated using

$$E_f = \frac{L^3}{4\,b\,C'\,h^3} \qquad \textbf{(6. 9)}$$

where L = half the span,

b = specimen width,

C' = compliance of the uncracked sample

h = half of the specimen height.

The sample was then loaded in a 4" (101.1 mm) span in a three point bend fixture. The sample was placed such that a/I ~ 0.5. The sample was tested at 0.5 mm/min deflection rate until the crack propagated to the center of the sample.

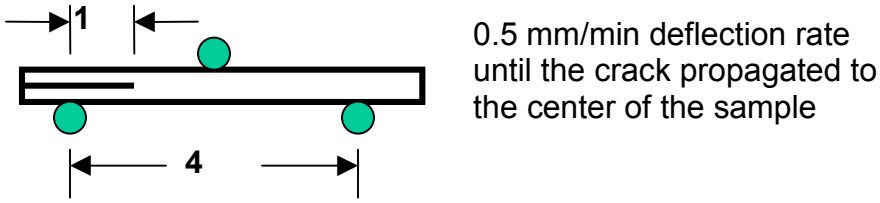

Figure 6. 18. Compliance determination of cracked samples

A corrected crack length (a_{corr}) was calculated using the flexural modulus and the compliance of the pre-crack sample.

$$a_{corr} = \left[\frac{8\,E_f\,Cbh^3}{3}\right]^{1/3} \qquad \textbf{(6. 10)}$$

where C is the compliance of the pre-crack sample.

The G_{IIC} can then be calculated from the load and displacement at failure (P and Δ) and the corrected crack length.

$$G_{2C} = \frac{9 \Delta a_c^{\,2} P}{2 b (2 L^3 + 3 a_c^{\,3})} \qquad \textbf{(6. 11)}$$

The failure was assigned as the onset of the crack. The specimen did not break when the crack reached the midpoint.

6.3. Results and Discussion

The phenolic novolac (n=5) /epoxy resin system investigated in this research must be heated to approximately 140°C to achieve the low viscosities necessary to wet-out the reinforcing fiber in composite preparations. The addition of a small amount of tertiary amine or phosphine catalyst in novolac/epoxy mixtures at this temperature causes premature reactions and reduces the processing window to minutes or even seconds. Curing novolac/epoxy mixtures in the absence of a catalyst requires long cure times at high temperatures and is unpractical. Therefore, a latent catalyst is needed for the novolac/epoxy reaction to achieve both good processability at 140°C and reasonably fast cure rates between 200-240°C. The ideal catalyst would be inert at processing temperatures, yet would cause reactivity at cure temperatures.

Several approaches for preparing thermally latent catalysts were examined in this research. The basic principle involves encapsulating or sequestering a tertiary amine or phosphine in a thermoplastic polymer where the T_g of the sequestered catalyst fall between the processing temperature and the cure temperature. Ideally, the amine or phosphine catalyst will be immobilized in the glassy material at the processing temperature, but is released at the cure temperature to catalyze the novolac/epoxy reaction.

6.3.1. Miscible polyimide/TPP sequestered catalysts

6.3.1.1. Effect of TPP on the glass transition temperatures of the blends

Two commercially available polyimides, Ultem® and Matrimid®, were examined. The miscibility of the polyimide with TPP was established by measuring the glass transition temperatures of the blends as a function of blend composition. A single glass transition temperature between those of the two pure components is indicative of a miscible blend. As expected, TPP plasticized both polyimides as shown by the decreased glass transition temperatures with increased TPP content (Figure 6. 19).

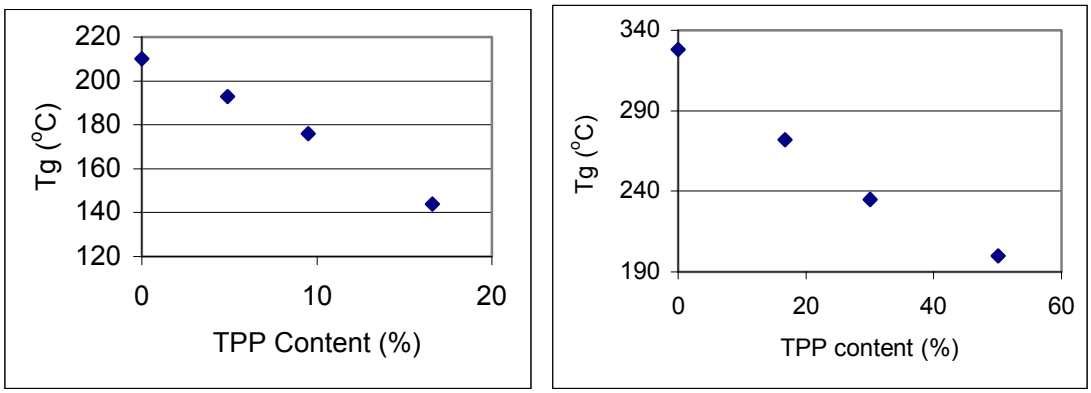

Figure 6. 19. Glass transition temperature of polyimide/ TPP blend measured as a function of TPP content a) Ultem® /TPP blend b) Matrimid® /TPP blend

Only small amounts of TPP (3-9 wt %) can be added to Ultem while maintaining the preferred blend glass transition temperatures (between the processing temperature and cure temperature, preferably between 180 and 200°C). For these blends to be used as catalysts, large loadings would be required to achieve high reaction rates since the TPP contents are low in these particles. Udel/TPP catalysts are thus impractical for catalyzing the novolac/epoxy reactions. Matrimid, on the other hand, possesses a much higher glass transition temperature. Therefore significantly more TPP can be mixed with Matrimid while maintaining the desirable T_gs. The 50/50 Matrimid/TPP blend composition had a glass transition temperature (~200°C) which lay in the targeted range.

Thermogravimetric analysis was used to evaluate the weight loss as a function of temperature for Matrimid/TPP blends. The weight loss of the blends was compared to that of the Matrimid. More rapid weight loss was observed for blends containing higher TPP contents. The initial weight loss temperature decreased substantially as the TPP content increased. This was important since the initial weight loss temperature was reduced to approximately 150°C for the 50/50 blend composition, which was only 10°C above the processing temperature.

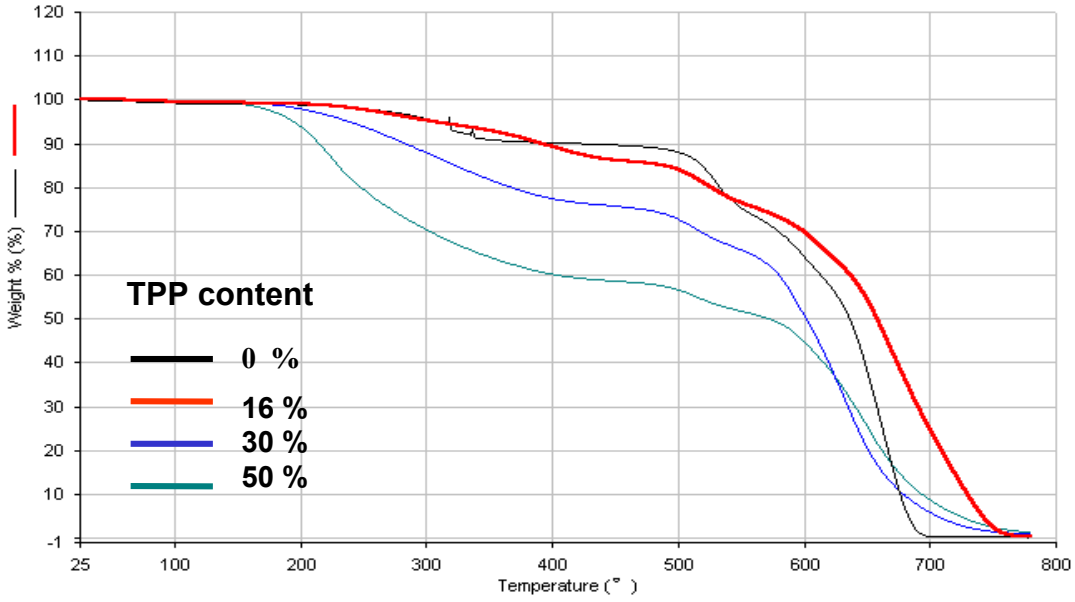

Figure 6. 20. Percent weight loss of Matrimid/TPP blend as a function of temperature

Interestingly, the addition of TPP to Matrimid seemed to enhance the thermal stability, especially at the 16 weight percent TPP loading. Higher temperatures were also required to degrade Matrimid/TPP blends completely. TPP is known to improve the thermal stability and flame retardance at relatively high concentrations.

6.3.1.2. Particle formation and characterization

Sequestered catalyst particles were prepared in the manner described in Section 6.2.2.2. A variety of particle sizes and shapes resulted from this grinding (Figure 6. 21

A). To obtain particles with a more uniform size distribution, a sieve was used to separate the smaller particles (Figure 6. 21 B) from the larger ones (Figure 6. 21 C).

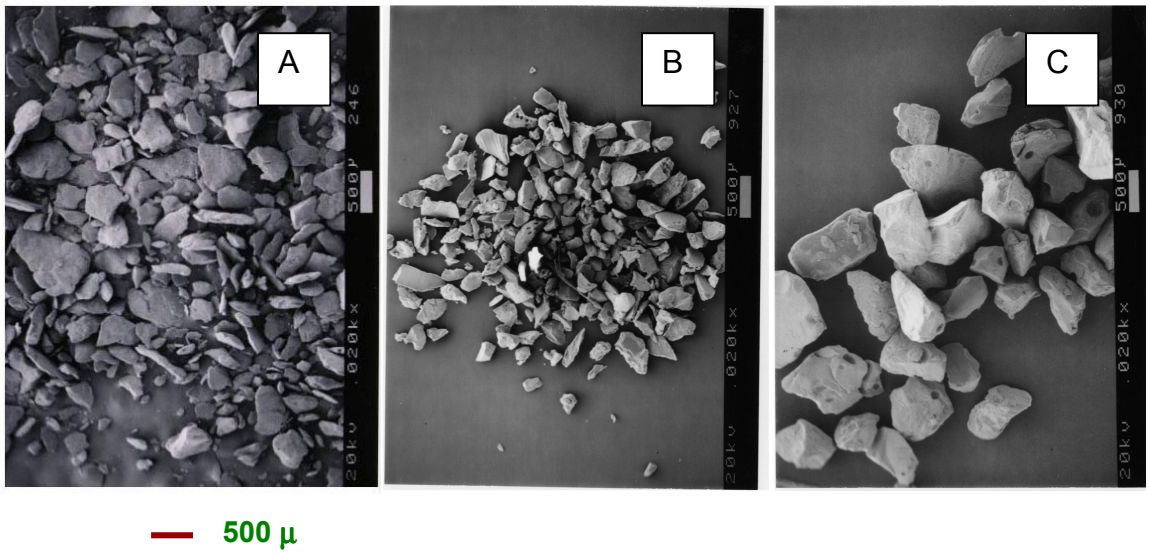

Figure 6. 21. SEM of Matrimid/TPP particles a) before separation, b) fine particles that passed through the sieve, and c) larger particles that did not pass through the sieves

6.3.1.3. Processing windows and cure times

The catalytic activity of Matrimid/TPP sequestered catalysts (unwashed) at both processing and cure temperatures were measured using isothermal differential scanning calorimetry. It should be noted that the ground particles might not be fine enough to be mixed in the novolac/epoxy mixtures to assure that 5-7 mg samples are truly representative of the bulk concentrations. The exotherms of the novolac/epoxy reactions were monitored at 135°C, 200°C and 220°C for the novolac/epoxy mixtures without catalyst, with 1 mole % sequestered Matrimid/TPP catalyst, with 2.5 mole % sequestered Matrimid/TPP catalyst, or with 1 mole % free TPP catalyst. At 135°C, no significant exotherm was observed for the novolac/epoxy mixtures without catalyst or in the presence of sequestered Matrimid/TPP catalysts (Figure 6. 22). A large exotherm was observed, however, for the novolac/epoxy mixture containing one mole percent free TPP catalyst. These results indicated that the novolac/epoxy reaction rate was significantly

decreased or eliminated at the 135°C processing temperature in the presence of sequestered catalysts.

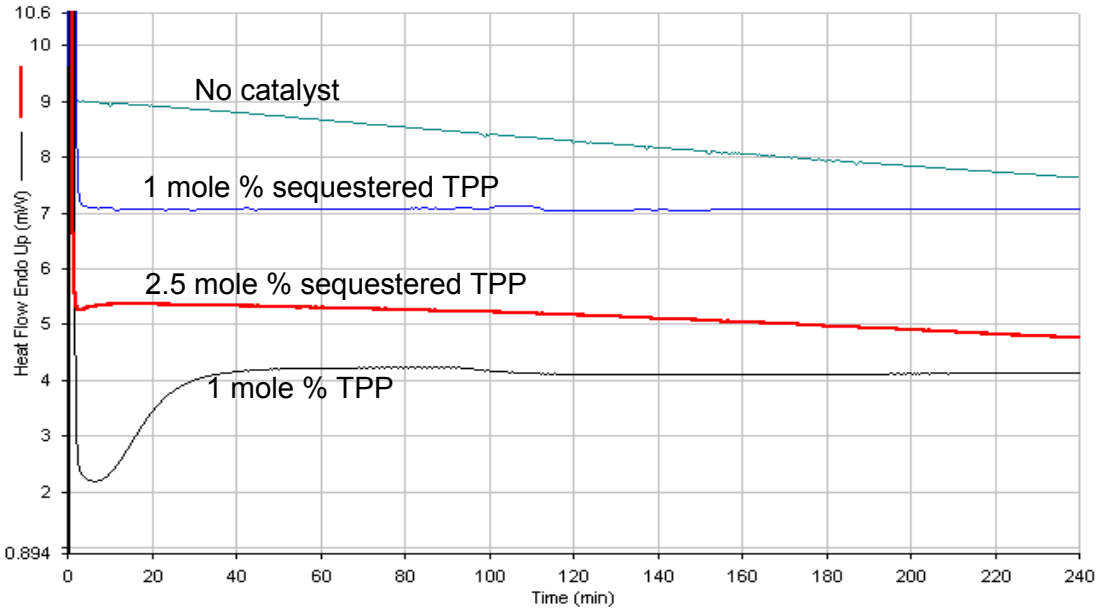

Figure 6. 22. Isothermal DSC at 135ºC for phenolic novolac/Epon 828 epoxy mixtures with no catalyst, with a Matrimid/TPP (50:50) sequestered catalyst, or with free triphenylphosphine catalyst (arbitrary vertical placements of curves)

At 200°C (of Figure 6. 23), enhanced reaction rates were observed for novolac/epoxy mixtures containing the sequestered catalyst compared to the rate of the uncatalyzed mixture. Since the cure temperature was similar to the glass transition temperature of the catalyst, low chain mobility may have restricted the diffusion of TPP catalyst into the novolac/epoxy resin mixture, which led to longer cure times. As expected, novolac/epoxy mixtures containing higher catalyst concentrations yielded higher reaction rates. Novolac/epoxy mixtures containing free TPP catalyst exhibited rapid fast reaction at 200°C (essentially complete reaction in less than 10 minutes).

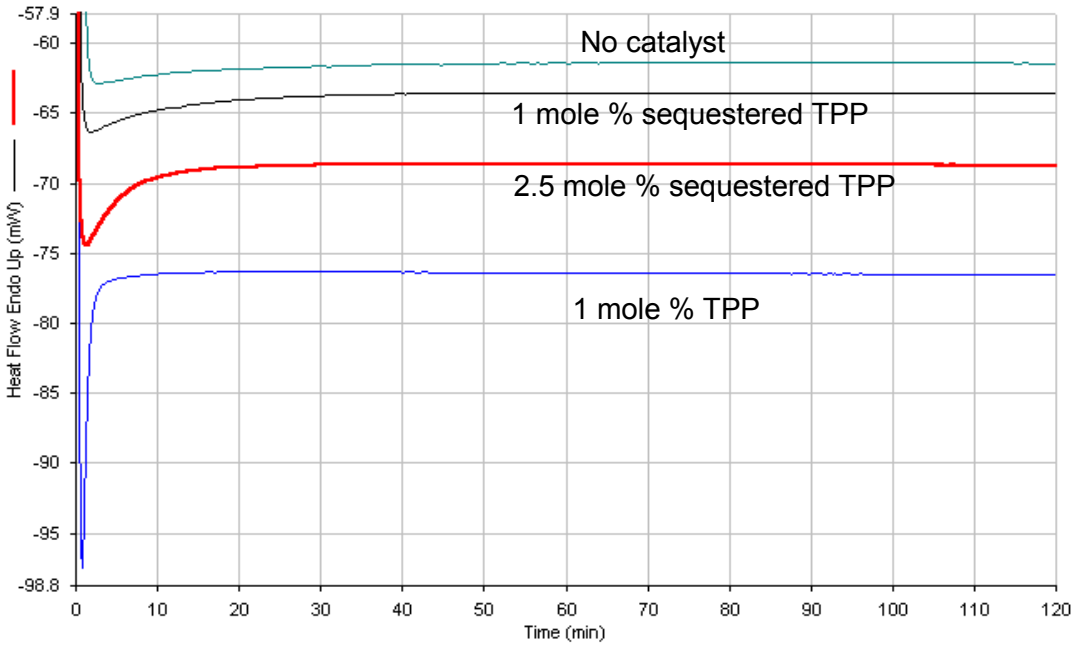

Figure 6. 23. Isothermal DSC at 200ºC for phenolic novolac/Epon 828 epoxy mixtures with no catalyst, with a Matrimid/TPP (50:50) sequestered catalyst, or with free triphenylphosphine catalyst

The novolac/epoxy reaction rate of mixtures containing sequestered catalysts increased substantially at 220°C (Figure 6. 23) compared to those reacted at 200°C. This was expected since higher temperatures lead to faster reaction rates. The enhanced rate observed at this temperature was probably also due to faster TPP release rates by the polymer matrix at a temperature that is higher than the initial glass transition temperature. As TPP diffuses from the Matrimid/TPP particles, the concentration of TPP in the particle decreases. If the diffusion of TPP is assumed to be nearly zero when the Matrimid/TPP becomes a glass, only that amount of TPP which exists between the original TPP concentration in the sequestered catalyst mixture and the TPP concentration in the glass at the reaction temperature can be released into the novolac/epoxy mixture. The amount of TPP released at a given reaction temperature can in theory be calculated. However, other factors such as diffusion of Matrimid in novolac/epoxy mixtures may also affect TPP release.

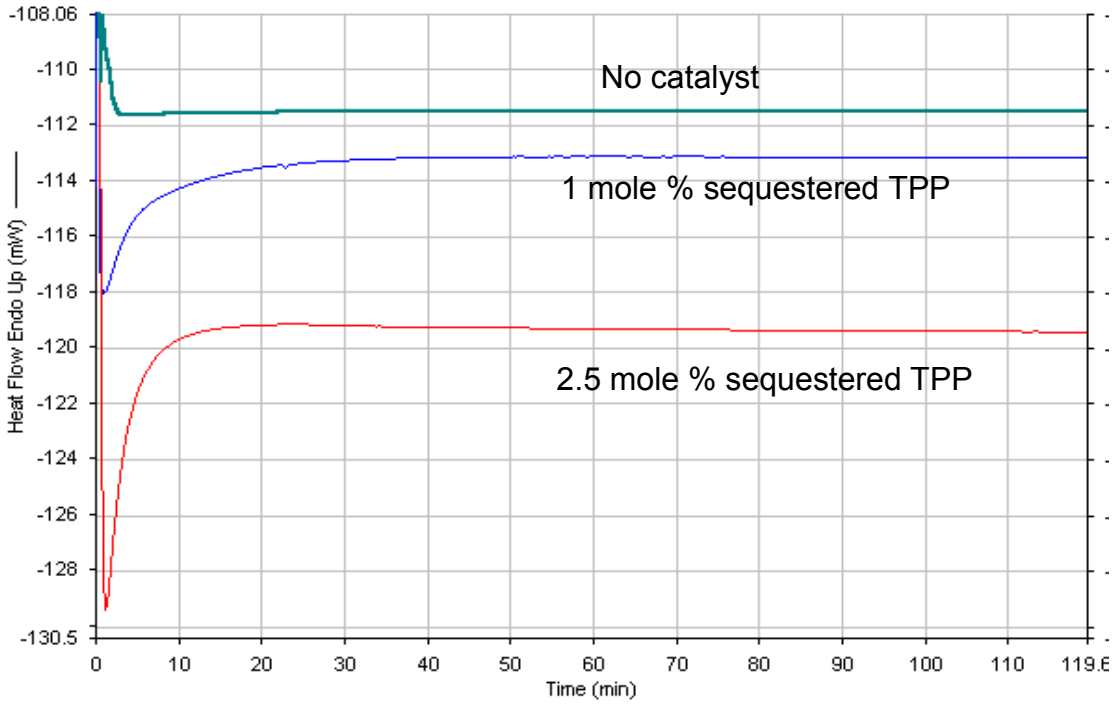

Figure 6. 24. Isothermal DSC at 220ºC for phenolic novolac/Epon 828 epoxy mixtures with no catalyst, with a Matrimid/TPP (50:50) sequestered catalyst, or with free triphenylphosphine catalyst

A small amount of TPP was expected to be collected on the surface of sequestered particles due to the processing procedures. The reaction rates between phenolic hydroxyl and epoxies could be greatly enhanced even in the presence of a small amount of catalyst. Therefore, the Matrimid/TPP particles were washed with acetone or warm methanol in an attempt to remove residual TPP on the particle surfaces.

Isothermal viscosity measurements, conducted at 140°C, were used to assess the processability of phenolic novolac/Epon 828 epoxy containing 1 or 2.5 mole percent Matrimid/TPP sequestered catalyst, acetone washed Matrimid/TPP catalyst, or warm methanol washed Matrimid/TPP catalyst (Figure 6. 25). The processing windows were extended significantly for all phenolic novolac/epoxy mixtures containing sequestered catalysts relative to those mixtures containing free TPP. Viscosity curves of free TPP catalyzed novolac/epoxy mixtures are not shown since they cured too rapidly. The processing time windows of novolac/epoxy mixtures in the presence of sequestered

catalysts were reduced relative to those of the uncatalyzed mixtures. Mixtures containing larger amounts of catalyst not only led to reduced processing windows but also to higher initial viscosities (5-6 Pa*s) than those having lower concentrations (3-4 Pa*s). The processing windows improved for novolac/epoxy mixtures containing washed Matrimid/TPP sequestered catalysts.

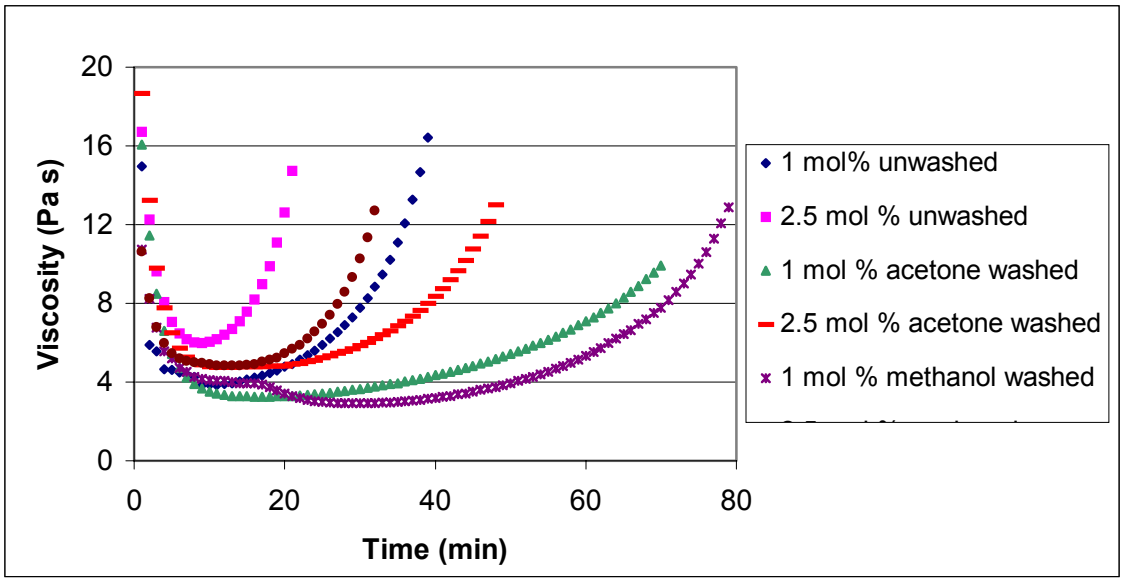

Figure 6. 25. Isothermal viscosity at 140°C for phenolic novolac /Epon 828 epoxy mixtures with Matrimid/TPP sequestered catalysts (50:50), unwashed, acetone washed and methanol washed.

The processing windows and the cure times for phenolic novolac/epoxy mixtures containing sequestered catalysts are summarized in Table 6. 1. The cure times were estimated from isothermal differential scanning calorimetry measurements as the times at which the exotherm curves returned to the baseline. Longer cure times were required for novolac/epoxy mixtures containing Matrimid/TPP sequestered catalysts compared to mixtures containing the free catalyst. The slower rates in mixtures containing sequestered catalysts were attributed to the diffusion of the catalysts. There may be a time lag due to the kinetics of TPP diffusion from Matrimid into the novolac/epoxy mixtures. Moreover, as described previously, the glass transition temperatures of Matrimid/TPP particles depended on the blend composition. As TPP diffused into the

novolac/epoxy mixture, the glass transition temperature of the particles rose accordingly, and eventually reached that of the cure temperature. A certain amount of TPP remained in the Matrimid due to a lack of mobility at these compositions. The mixtures containing free TPP catalyst were solvent mixed and the catalyst was homogeneously dispersed in the novolac/epoxy mixtures prior to cure. As expected, faster rates or shorter cure times resulted with increased catalyst concentrations. Longer cure times were observed for novolac/epoxy containing washed catalyst particles. The reduced rate was attributed to a lesser amount of catalyst in the washed particles.

Table 6. 1. Processing windows and cure times of phenolic novolac/epoxy and Matrimid sequestered catalysts

Sample	TPP content (mol %)	Processing window* (min)	Cure time** (min)
Free TPP	1.0	< 1	15
Unwashed	1.0	30	40
	2.5	15	20
Acetone washed	1.0	65	60
	2.5	40	40
Methanol washed	1.0	70	50
	2.5	30	35

* Time to reach 10 Pa*s at 140°C

** Time to 99% conversion at 220°C

6.3.1.4. Surface and cross-section morphologies of the catalyst particles

SEM was used to study the outer surfaces and cross-section surfaces of the unwashed sequestered catalyst particles. The outer surfaces of Matrimid/TPP sequestered catalyst particles were rough and porous (Figure 6. 26). This was expected since these particles were prepared by grinding the Matrimid/TPP mixture that contained a small amount of chloroform. Chloroform evaporation upon drying was expected to create porosity as well as the observed surface roughness.

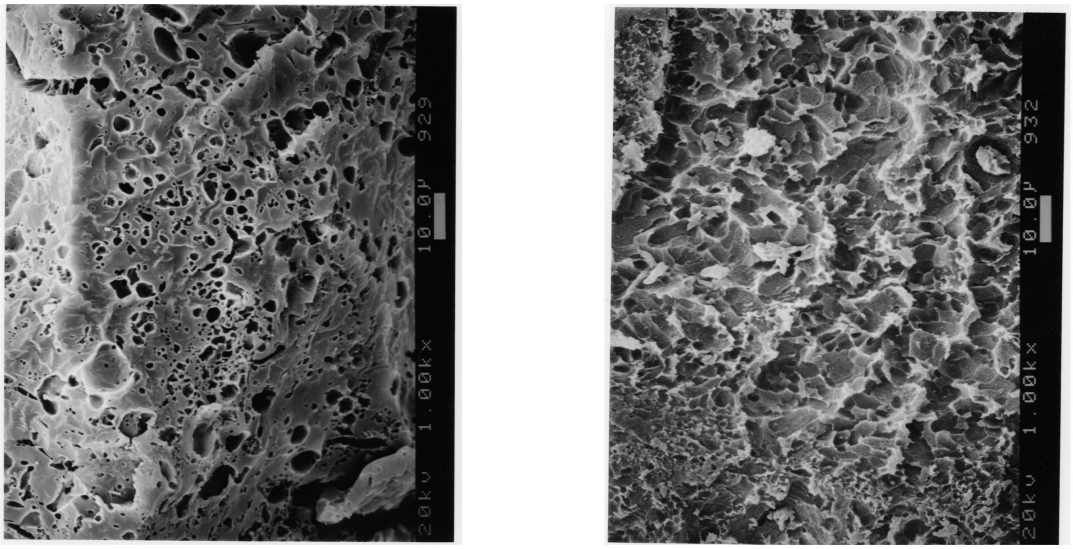

Figure 6. 26. SEM of Matrimid/TPP particle surfaces

To determine the bulk structures of the particles, the cross-section of an unwashed particle was examined using SEM (Figure 6. 27). A considerable amount of voids were observed. The distribution of the void diameters seemed to be bimodal with the majority of voids having an average diameter of ~0.2□m. There were also some larger voids with average diameter of ~0.4-0.5 □m.

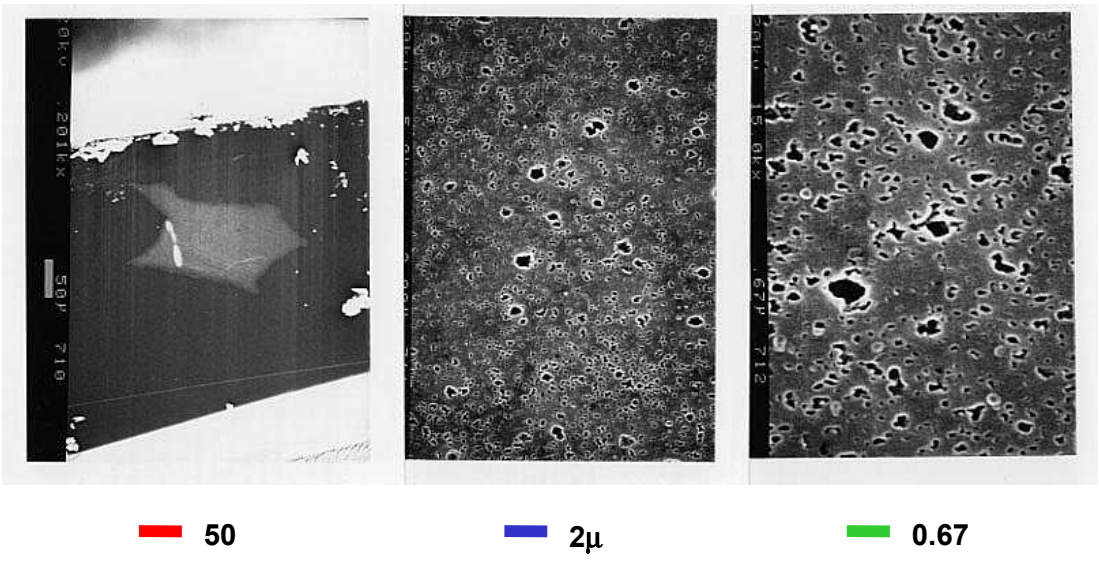

Figure 6. 27. SEM of a cross-section of a Matrimid/TPP particle

6.3.2. Udel®/TPP sequestered catalysts

6.3.2.1. Blend Composition

Immiscible catalyst blends prepared by sequestering TPP in Udel polymer were also examined. These particles had a melting point and a glass transition temperature due to TPP and Udel respectively. One advantage of using immiscible sequestered catalysts is that the diffusion of TPP occurs above the glass transition temperature of the polymer matrix and is independent of the blend composition.

The TPP concentration in the particles was calculated using ^{1}H NMR integration ratios (Figure 6. 28). A single set of aromatic peaks between 7.28-7.35 ppm was observed for the TPP, and four sets of aromatic peaks were observed for the Udel polymer. The TPP/Udel peak integration ratio decreased significantly for warm methanol washed particles indicating that a significant amount of TPP was removed during washing (Table 6. 2).

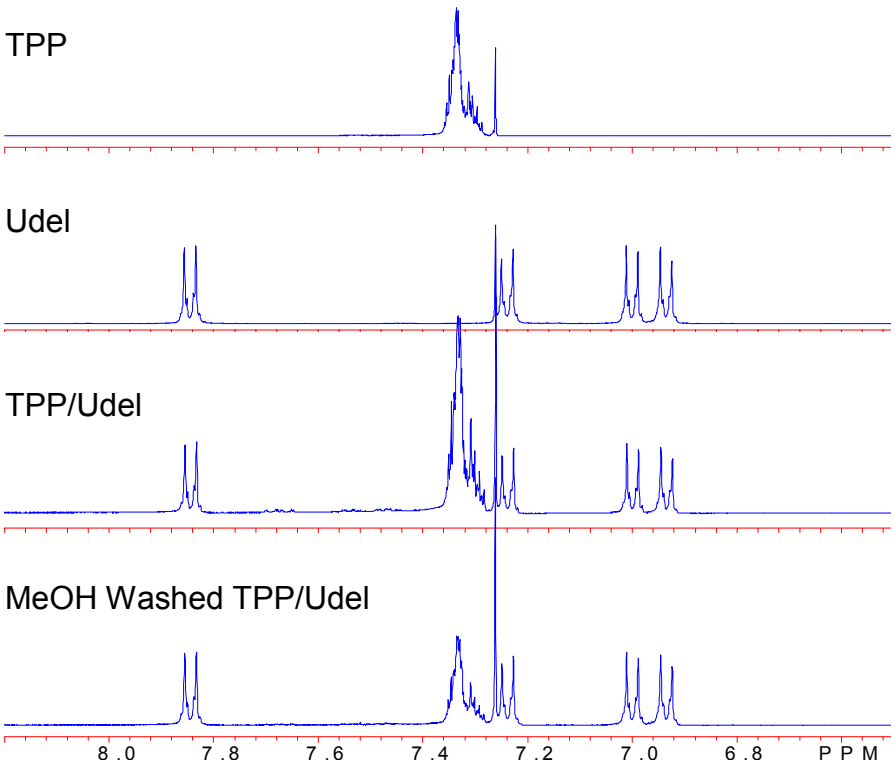

Figure 6. 28. ^{1}H NMR of TPP, Udel, Udel/TPP, and methanol washed Udel/TPP

Table 6. 2. Particle compositions of unwashed and methanol washed Udel/TPP particles

Sample	TPP (wt %)	Udel (wt %)
Unwashed	49	51
Warm methanol washed	36	64

6.3.2.2. Processing windows and cure times

Phenolic novolac/epoxy reactions in the presence of unwashed Udel/TPP sequestered catalyst were monitored using isothermal differential scanning calorimetry at 140°C and at 200°C (Figure 6. 29). No exotherm was detected at the processing temperature (140°C) for novolac/epoxy mixtures containing 0.65 or 1.6 mole % Udel/TPP sequestered catalyst. At 200°C, the sequestered catalysts catalyzed the mixtures. The reaction appeared to reach completion in 15 minutes when 1.6 mol % catalyst was used.

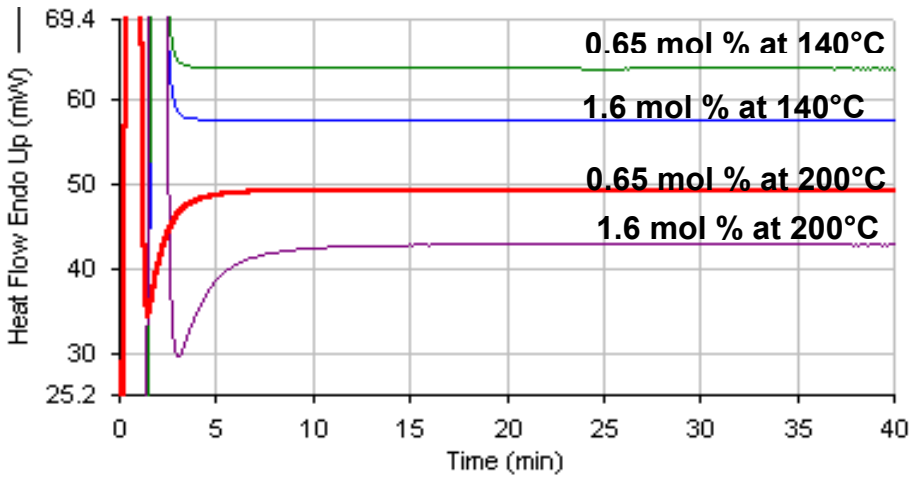

Figure 6. 29. DSC scans of phenolic novolac/epoxy mixtures containing Udel/TPP catalyst

Isothermal viscosity measurements, determined at 140°C, were used to evaluate the processabilities of the phenolic novolac/epoxy mixtures containing unwashed Udel/TPP sequestered catalyst particles (Figure 6. 30). The processing time window increased significantly for novolac/epoxy mixtures containing Udel/TPP sequestered

catalyst compared to mixtures containing free TPP catalyst. However, the processing time window decreased relative to the uncatalyzed mixtures. Furthermore, the time for processing was reduced as the concentration of the sequestered catalyst was increased. The premature reaction was attributed to TPP catalyst on the particle surface, which catalyzed these reactions. A small amount of TPP probably also diffused from the sequestered particle into the novolac/epoxy mixture.

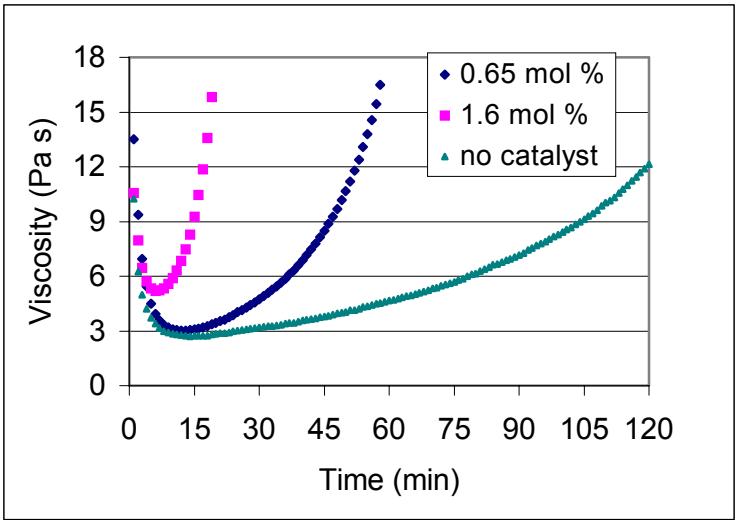

Figure 6. 30. Isothermal viscosity determination of phenolic novolac/epoxy mixtures at 140°C without catalyst, with 0.65 mol % catalyst, and with 1.6 mol % catalyst.

6.3.2.3. SEM of Udel/TPP Sequestered catalysts

Cross-sections of Udel/TPP sequestered catalyst particles were examined using SEM (Figure 6. 31). Unlike the Matrimid/TPP particles where small voids were evenly distributed throughout the particle, Udel/TPP particles consisted of smooth surfaces with larger voids. At higher magnifications, TPP crystals embedded in Udel polymer matrix were observed. The crystals could form from homogeneous mixtures at temperatures below the melting pointing of TPP (79-81°C) if they non-glassy. This condition could be satisfied if the crystallization occurred while solvent was still present or if the T_g of the solvent-free Udel/TPP mixture was below 79-81°C. Since the sequestered catalyst had a T_g slightly lower than that of the pure Udel (according to DSC measurements), the crystallization probably occurred in the presence of solvent.

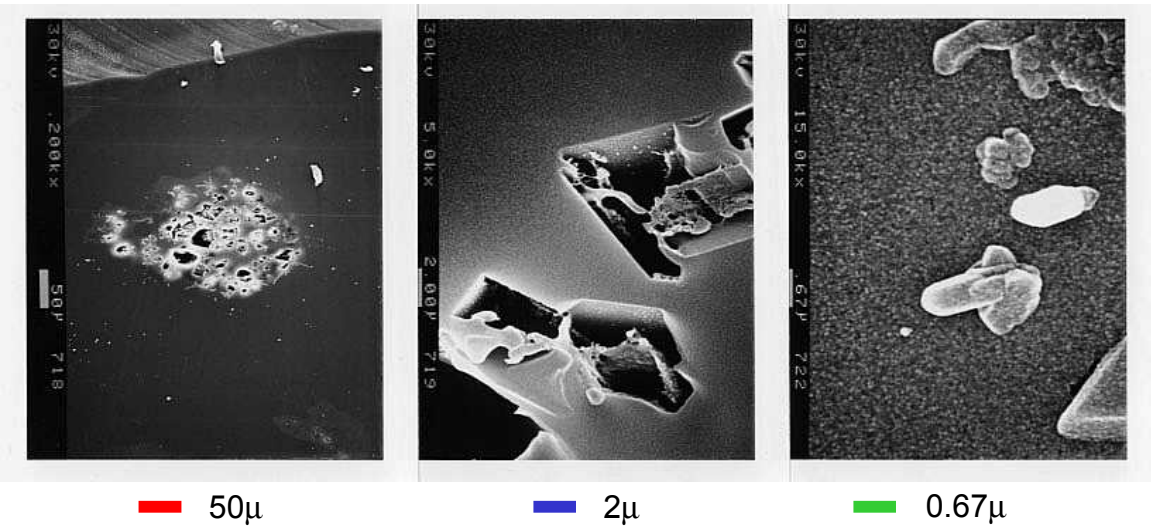

Figure 6. 31. SEM of a cross-section of an Udel/TPP particle

6.3.3. Partially reduced poly(arylene ether phosphine oxide)s

Poly(arylene ether phosphine oxide)s were prepared via nucleophilic aromatic substitutions. The molecular weights were controlled using the Carother's equation to dictate the feed compositions. A fraction of the phosphine oxide groups was reduced to phosphine groups to yield a statistical copolymer containing both phosphine oxide and phosphine groups. The phosphine groups were expected to catalyze novolac/epoxy reactions when the copolymer was added to a novolac/epoxy mixtures.

6.3.3.1. Reduction of P(AEPO)

The poly(arylene ether phosphine oxide)s were reduced using phenylsilane as the reducing agent. The reduction rate depended on the time, temperature, pressure, phosphine oxide to phenylsilane ratio, and the amount of solvent used. The reductions were conducted at 110°C at atmospheric pressure and had a phosphine oxide group to phenylsilane molar ratio of 2:3. Since the glass transition temperature of the polymer was affected by the degree of reduction (Figure 6. 32), it was important to determine an optimal degree of reduction of the P(AEPO) for its use as a latent catalyst. The goal,

then, was to achieve the maximum degree of reduction while maintaining the glass transition temperature of the copolymer well above the processing temperatures.

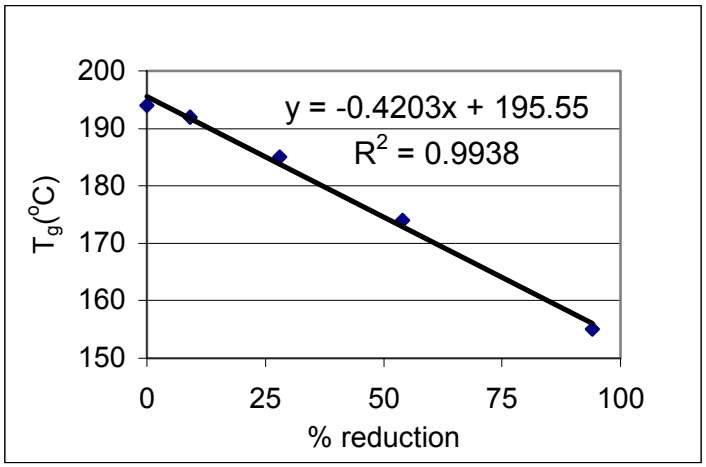

Figure 6. 32. Glass transition temperature vs. percent reduction of P(AEPO

Under the described experimental conditions, samples were periodically taken to determine the amount of reduction as a function of reaction time (Figure 6. 33). The percent of reduction appeared to increase linearly with reaction time during the initial stage (0 to 60 % reduction); the reduction rate then decreased as the reaction proceeded.

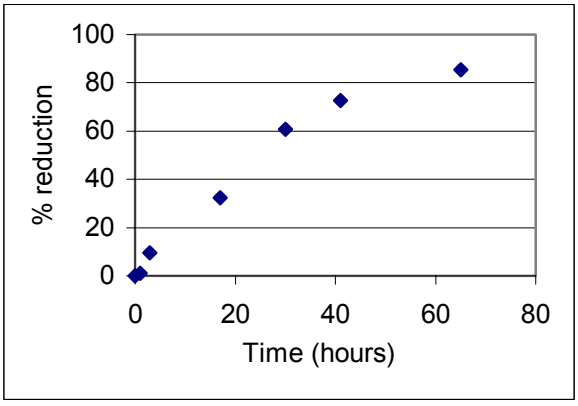

Figure 6. 33. Percent reduction of (P=O) as a function of reaction time for P=O:SiH_3Ph (1:1.5 molar ratio)

Based on the plots generated (Figure 6. 32 and Figure 6. 33), 40 hours reaction time was chosen since a significant amount of reduction had occurred and the glass transition temperature remained reasonably high. The number average molecular weight, percent reduction and glass transition temperature of the partially reduced P(AEPO) were determined (Table 6. 3). This polymer was investigated for its potential use as a latent catalyst for phenolic novolac/epoxy reactions.

Table 6. 3. Properties of partially reduced P(AEPO)

Sample	M_n (g/mol) GPC	% reduction ^{31}P NMR	T_g (°C) DSC
Partially reduced P(AEPO)	16,600	69	163

6.3.3.2. Processing windows and cure times

Isothermal DSC scans, measured at 140°C, showed very little exotherm for phenolic novolac/epoxy mixtures containing 1 mole percent (moles of phosphine units per moles of epoxide rings) reduced P(AEPO) (Figure 6. 34). The cure rate, at 220°C, was accelerated in the presence of the polymeric catalyst. However, the mixture required approximately 30 minutes to reach completion. One explanation for the slower than expected rate was that a time lag may occur for the polymeric catalyst to become homogeneously mixed and active in the novolac/epoxy mixture.

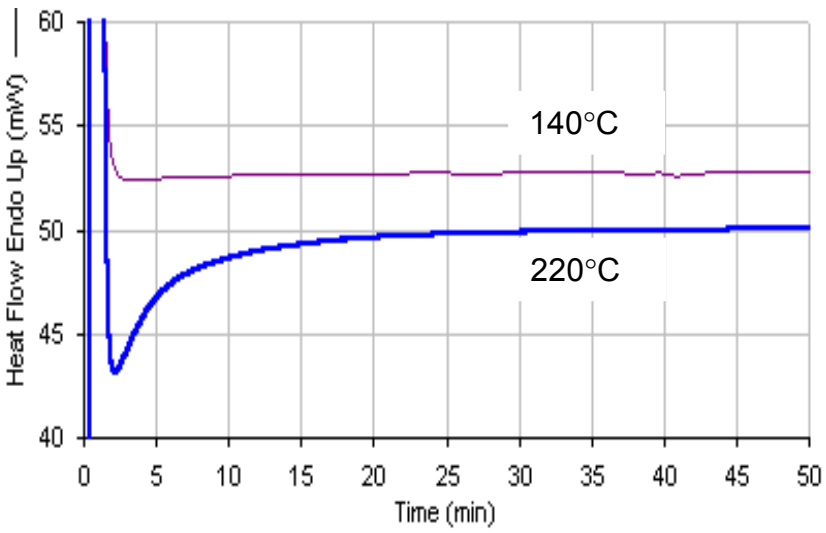

Figure 6. 34. Isothermal DSC of phenolic novolac/Epon 828 with 1 mol % reduced P(AEPO) at 140°C and at 220°C

Isothermal viscosity, measured at 140°C, showed that the phenolic novolac/epoxy mixture containing 1 mol % polymeric catalyst had improved processability compared to the mixtures containing free TPP catalyst, but reduced processability compared to the uncatalyzed mixtures (Figure 6. 35). The processing window decreased from 110 minutes to 45 minutes when the polymeric catalyst was introduced. The immobilized phosphine groups on the surface of the particles may have catalyzed the reaction causing premature cure.

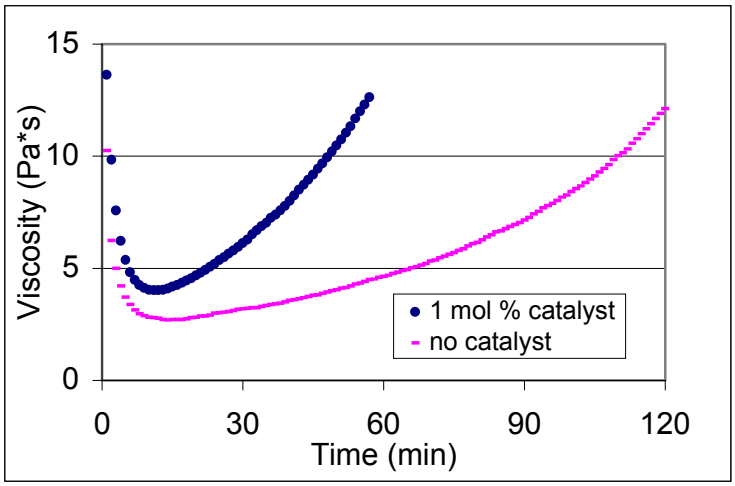

Figure 6. 35. Isothermal viscosity (140°C) of phenolic novolac/Epon 828 epoxy with reduced P(AEPO)

6.3.4. Poly(amic acid) salts

Polyimides are tough engineering thermoplastics used in electronic applications and as high performance structural composites and adhesives.[196] One approach to synthesize high molecular weight polyimides is through the poly(amic acid) route. The initial reaction involves dianhydrides reacting with diamines under strict anhydrous conditions at room temperature to form poly(amic acid)s. To prevent chain scission due to hydrolytic instability, poly(amic acid)s are generally converted to poly(amic acid) salts using a base such as a tertiary amine or phosphine. Poly(amic acid) salts can be stored until they are imidized at high temperatures to release the amines or phosphines and form imide linkages. Tertiary amines or phosphines catalyze the novolac/epoxy reactions; the salts of tertiary amines and phosphines bear positive charges on the nitrogen and phosphorus atoms and are inert. The goal therefore is to develop a thermally latent tertiary amine or phosphine catalyst in which the catalyst is encapsulated in the poly(amic acid) salt at the processing temperature, but is liberated to form free amine or phosphine catalyst at cure temperatures. The imidization temperature, therefore, is key in preparing suitable poly(amic acid) salts for these purposes.

Three poly(amic acid) salts were prepared for use as latent catalysts (Figure 6. 36). PAAS (**1**) was prepared by reacting bisphenol-A dianhydride with *m*-phenylene diamine and complexed with tris(2,4,6-trimethoxyphenyl)phosphine (TTMPP). The slightly more basic TTMPP was used as opposed to TPP, which was necessary to form salts with the weakly acidic carboxylic acid groups on poly(amic acid)s. PAAS (**2**) and (**3**) were prepared by reacting 4,4'-(9-fluorenylidene)dianiline (FDA) with biphenyldianhydride (BPDA) to form the poly(amic acid), and then using imidazole or trihexylamine as counter ions to form the poly(amic acid) salt. Imdazole is a weaker base than trihexylamine due to its aromatic nature. The structure of imidazole is also significantly different from that of the trihexylamine. Trialkylamines, with long alkyl chains, had the high boiling points that were necessary to keep the catalyst in the reaction mixtures at the cure temperatures.

---

[196] G. Odian, *Principle of Polymerization, 3rd Ed.*, John Wiley & Sons, Inc. New York, New York, 1991.

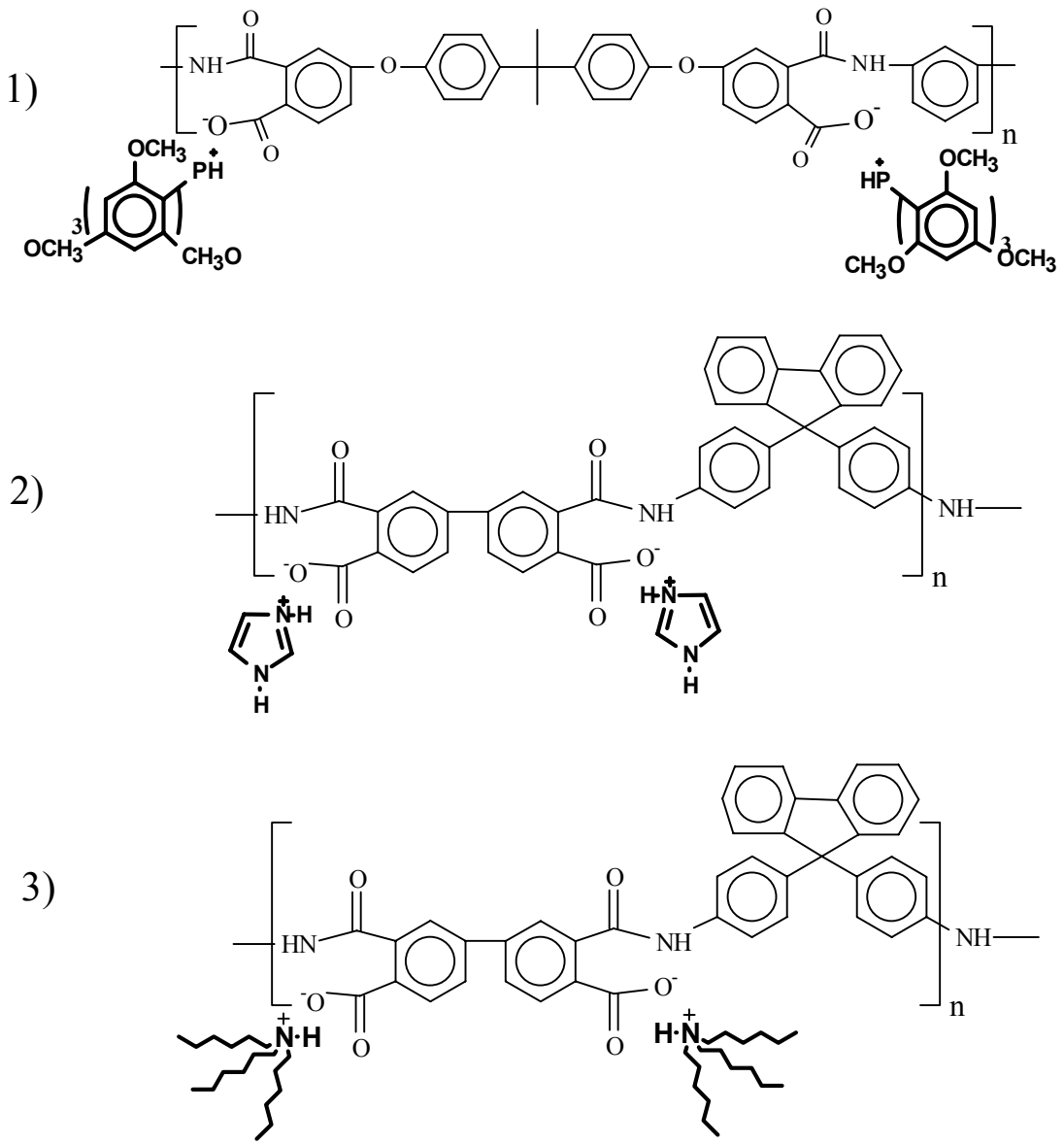

Figure 6. 36. Poly(amic acid) salts 1) Ultem type PAAS/TTMPP, 2) FDA/BPDA based PAAS/imidazole, and 3) FDA/BPDA based PAAS/trihexylamine

The onset and the bulk imidization temperatures of the poly(amic acid) salts were observed by dynamic DSC scans (Figure 6. 37). PAAS (1), which had a low glass transition temperature (~ 55°C), showed the onset of imidization at 110°C. The imidization temperature of PAAS (1) was well below the processing temperatures of the novolac/epoxy resins. PAAS (2) and (3) did not exhibit clear glass transition temperatures, but exhibited endotherms followed by the expected imidization exotherms.

The peak of the endotherm for PAAS (3) (~135°C) occurred at a higher temperature than that for PAAS (2) (~120°C). The endotherm was attributed to the energy required to break apart the salts.

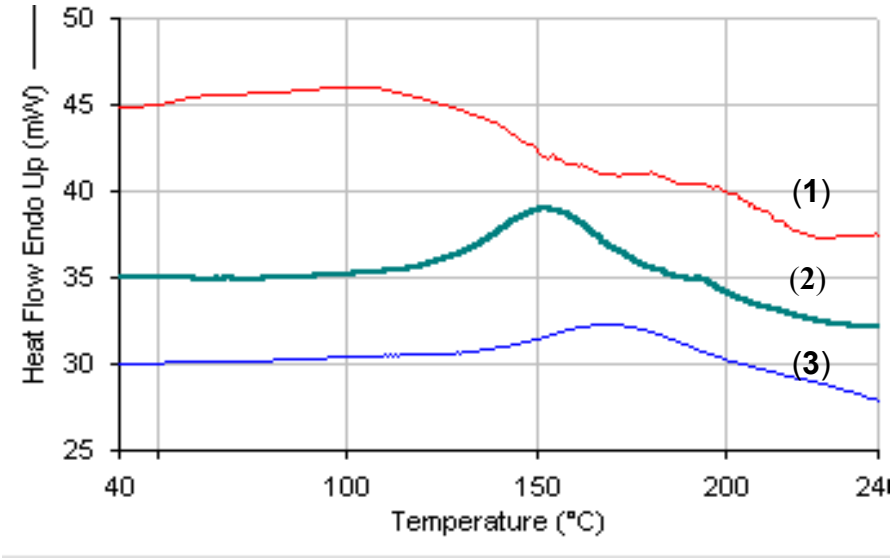

Figure 6. 37. Dynamic DSC scans of (1) Ultem PAAS/TTMPP, (2) FDA/BPDA based PAAS/imidazole, and (3) FDA/BPDA based PAAS/trihexylamine

The onset and the peak of the exotherm were measured using dynamic differential scanning calorimetry for novolac/epoxy reactions in the presence of PAAS catalysts (Figure 6. 38). The glass transition temperature of the novolac/epoxy mixtures was observed at ~60°C. The onset of the phenolic novolac/epoxy reaction in the presence of PAAS (1) occurred at 100°C and the peak of the exotherm was found at 162°C. The onset of the reaction occurred at a significantly lower temperature than the processing temperature indicating that PAAS (1) could not be used as a latent catalyst. Phenolic novolac/epoxy mixtures containing PAAS (2) or (3) showed reaction onset temperatures at approximately 120 and 135°C, respectively. Mixtures containing PAAS (3) also showed a significantly higher peak exotherm temperature compared to mixtures containing PAAS (2). The onset temperatures were lower than the processing temperatures. This suggested a reduced processing time window since even a small amount of reaction will result in a large increase in viscosity.

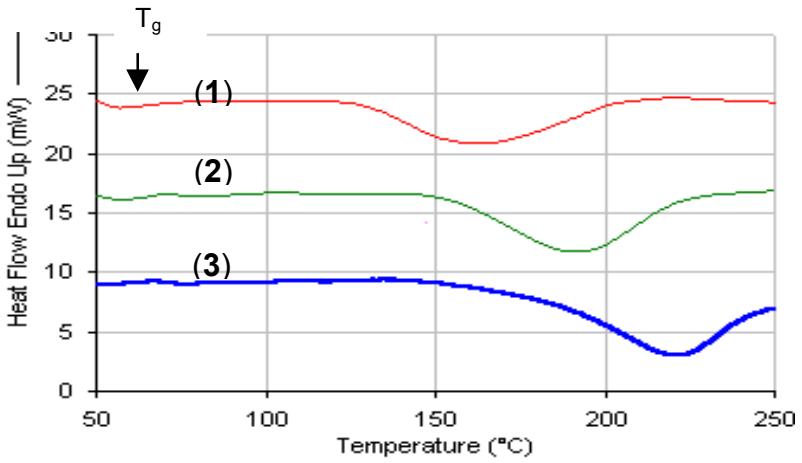

Figure 6. 38. Dynamic DSC scans of novolac/epoxy mixture with 2 mole % PAAS (1) Ultem PAAS/TTMPP, (2) FDA/BPDA PAAS/imidazole, and (3) FDA/BPDA PAAS/trihexylamine

To further investigate the catalytic activities, isothermal DSC scans were used to characterize the reaction of phenolic novolac/epoxy mixtures containing PAAS (**1**), (**2**), or (**3**). The isothermal DSC scans of mixtures containing 2 mole % PAAS (**1**) showed fast reactions at the cure temperature (200°C) but also at the processing temperature (140°C) (Figure 6. 39). This was expected since the imidization process is appreciable at the processing temperature.

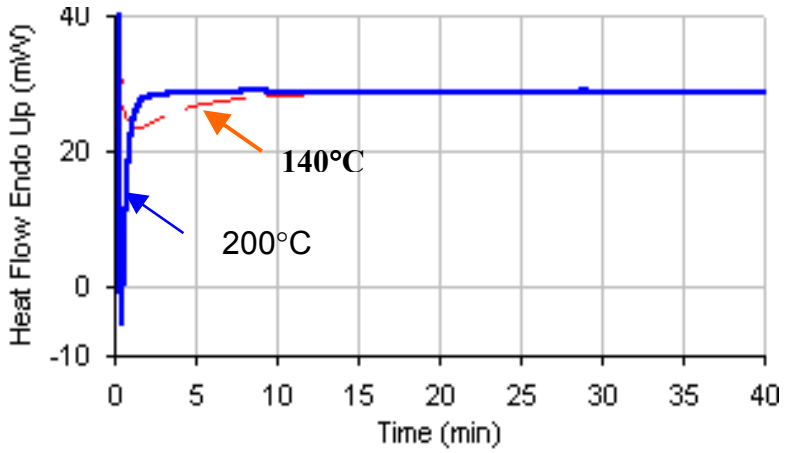

Figure 6. 39. Phenolic novolac/epoxy with 2 mol % Ultem type PAAS/TTMPP

Isothermal DSC indicated that phenolic novolac/epoxy mixtures containing 2 mole % PAAS (2) showed fast reactions at the curing temperature (Figure 6. 40). However, a significant amount of reaction also occurred at the processing temperature.

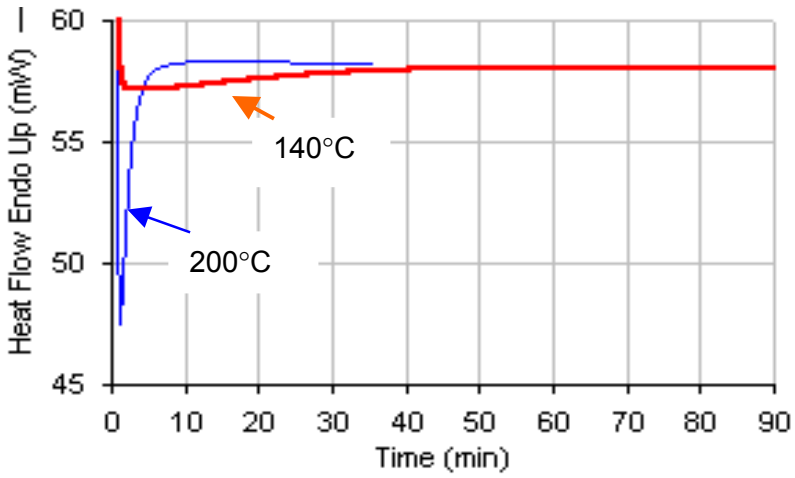

Figure 6. 40. Phenolic novolac/epoxy with 2 mol % PAAS (FDA/BPDA) imidazole

Isothermal DSC scans of phenolic novolac/epoxy mixtures containing PAAS (3) were compared to those of the uncatalyzed mixtures and of the mixtures containing free trihexylamine catalyst at 140°C (Figure 6. 41) and at 200°C (Figure 6. 42). No significant exotherm was detected at 140°C for the uncatalyzed phenolic novolac/epoxy mixture and mixtures containing 2 mole % PAAS (3). Mixtures containing free trihexylamine showed rapid cures even at the processing temperature.

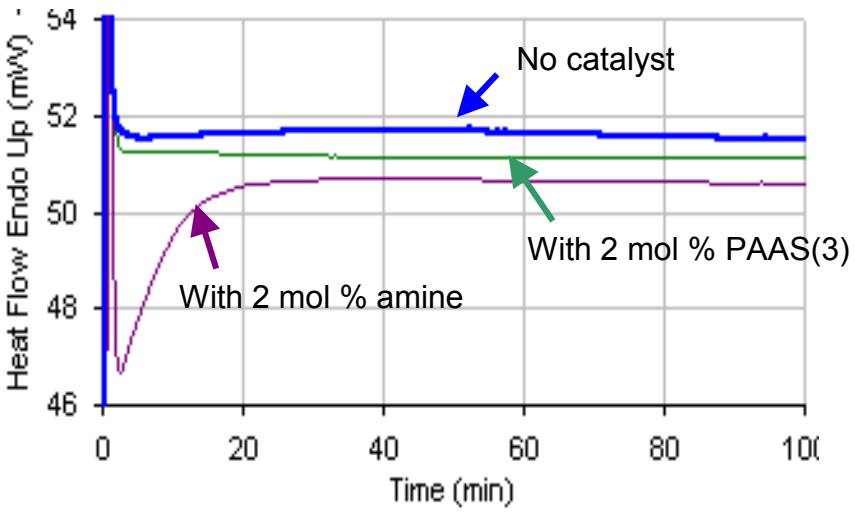

Figure 6. 41. Isothermal DSC at 140°C for novolac/epoxy mixtures: no catalyst, with PAAS (FDP/BPDA/trihexylamine), and with free trihexylamine

The cure rate at 200°C of novolac/epoxy mixtures with 2 mole % PAAS (3) was significantly increased than that of the uncatalyzed mixtures (Figure 6. 42). However, mixtures with sequestered catalysts required a longer cure time (20 minutes) than mixtures containing free TPP catalysts (~ 10 minutes). The reduced cure rate was attributed to imidization time as well as diffusion of the released trihexylamine catalyst into the novolac/epoxy mixtures.

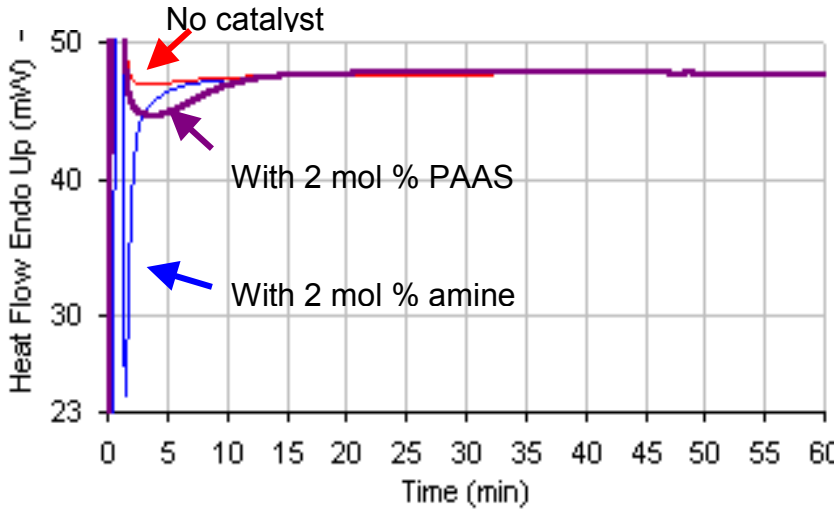

Figure 6. 42. Isothermal DSC at 200°C of phenolic novolac/epoxy without catalyst, with PAAS (FDP/BPDA/trihexylamine), and with free trihexylamine

Comparatively, the PAAS (3) catalyzed system showed the highest thermal stability and the lowest reaction rate of the PAAS catalyzed systems at the novolac/epoxy processing temperature. Isothermal viscosity was determined for phenolic novolac/epoxy mixtures containing 2 mole % PAAS (3) (Figure 6. 43). The mixture was processable for approximately 20 minutes. Although there was a substantial increase in the processing window of this mixture over that of the mixture containing free amine catalyst, the processing window was still significantly reduced compared to that of the uncatalyzed system.

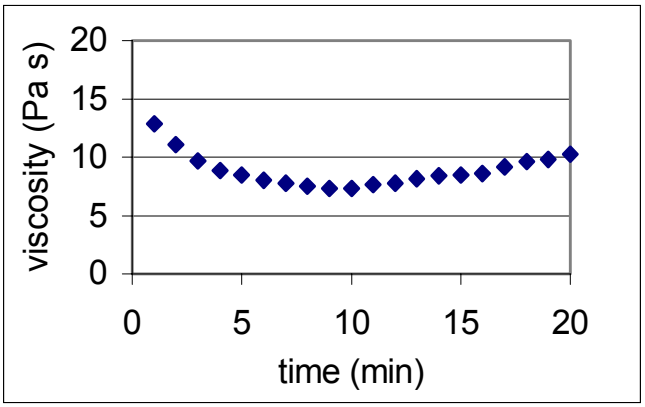

Figure 6. 43. Viscosity during heating and holding at 140°C of phenolic novolac/epoxy with 2 mole % PAAS-3 (FDP/BPDA/trihexylamine),

6.3.5. Processability of a lower molecular weight phenolic novolac mixed with epoxy

The properties and processability of networks prepared using a lower molecular weight phenolic novolac (n=2.4) was also explored. The main advantage of using a lower molecular weight resin is that a lower processing temperature can be used.

The network properties derived from both "high" and "low" molecular weight novolac oligomers were compared (Table 6. 4). The novolac/epoxy composition was slightly different in these networks. The higher molecular weight novolac had a higher resin glass transition temperature but gave rise to a lower network glass transition temperature. On the other hand, the fracture toughness of the network prepared using the higher molecular weight resin was slightly higher.

Table 6. 4. Resin and network properties of novolac resins of different molecular weights

Resins			Networks		
Source	$F_{(OH)}$	T_g (^oC)	Novolac/epoxy	K_{IC}	T_g (^oC)
Georgia Pacific	7.0	78	65:35	0.85	120
Occidental	4.4	63	60:40	0.75	134

$F_{(OH)}$ = number of hydroxyl groups per novolac chain determine using ^1H NMR

Isothermal viscosity measurements showed that a lower temperature (120°C) could be used to process the lower molecular weight novolac/epoxy mixtures and achieve comparable viscosity as the higher molecular weight novolac/epoxy mixture, which must be heated to 140°C. Lower processing temperatures also translate to increased processing windows since the reaction rate of phenolic hydroxyl with the epoxy was reduced at lower temperatures.

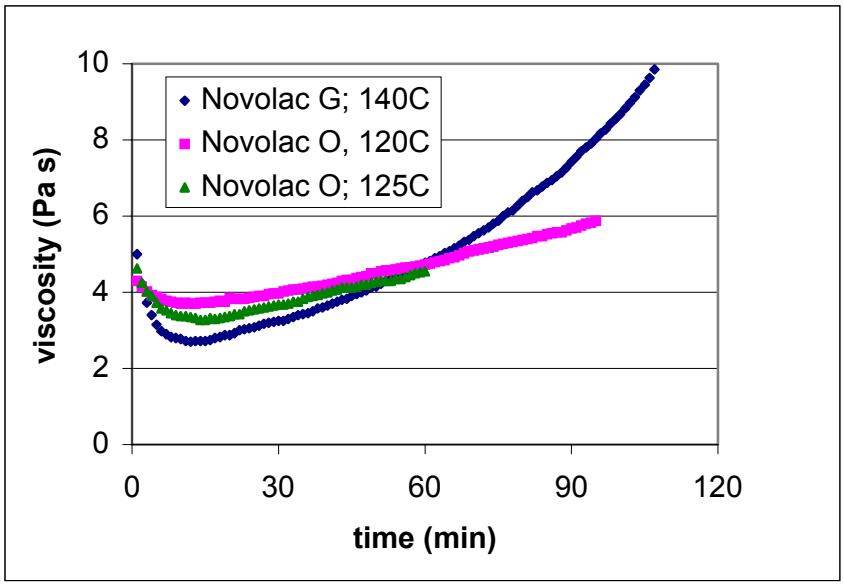

Figure 6. 44: Isothermal viscosities of phenolic novolac/epoxy mixtures, Novolac G (Georgia Pacific resin, $f_{(OH)} = 7$) and Novolac O (Occidental resin, $f_{(OH)} = 4.4$)

Isothermal viscosities of the "low" molecular weight phenolic novolac (Novolac O) mixed with epoxy with and without sequestered catalysts were measured (Figure 6. 45). PAAS (3) [FDA/BPDA/trihexylamine] and methanol washed Udel/TPP sequestered catalysts were investigated. Although the processing temperature was reduced to 120°C, adding the sequestered catalysts reduced the processing time windows. Mixtures containing either catalyst had a processing window between 25 and 30 minutes.

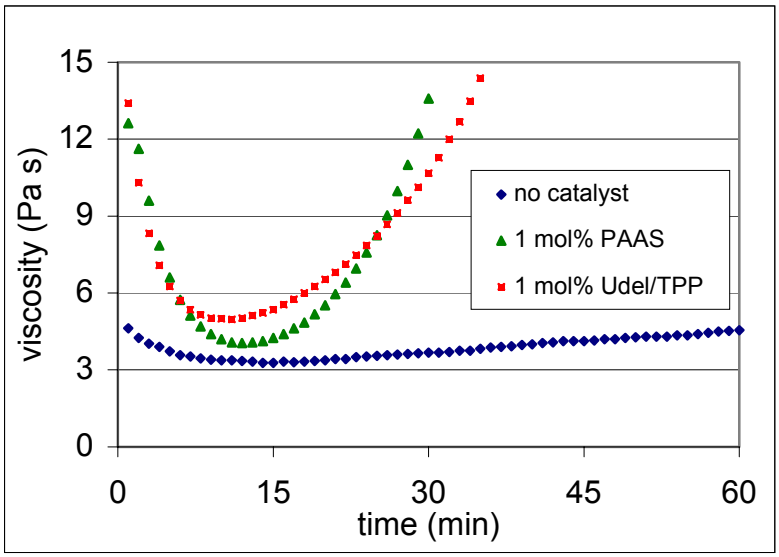

Figure 6. 45: Isothermal viscosity of lower molecular weight phenolic novolac/epoxy mixtures with and without sequestered catalysts

6.3.6. Properties of poly(amic acid)/trihexylamine salt sized carbon fiber reinforced novolac/epoxy composites

6.3.6.1. Reaction Kinetics

A thorough understanding of the reaction kinetics of the novolac/epoxy catalyzed by non-sequestered trihexylamine was necessary for determining the appropriate cure cycles for composites containing latent initiator sizings. The kinetic parameters such as activation energy, pre-exponential factor, and first order rate constants were calculated according to ASTM E 698.

Samples were heated at various heating rates (β), and the exotherm peak temperature shifted correspondingly (Figure 6. 46). A plot of log β versus 1/peak temperature of the exotherm was generated (Figure 6. 47). The activation energy was estimated using the slope of the plot. The rate constant, which was subsequently calculated, was used to predict the time to reach 99% conversion for phenolic novolac/epoxy reactions containing 3 mole % trihexylamine.

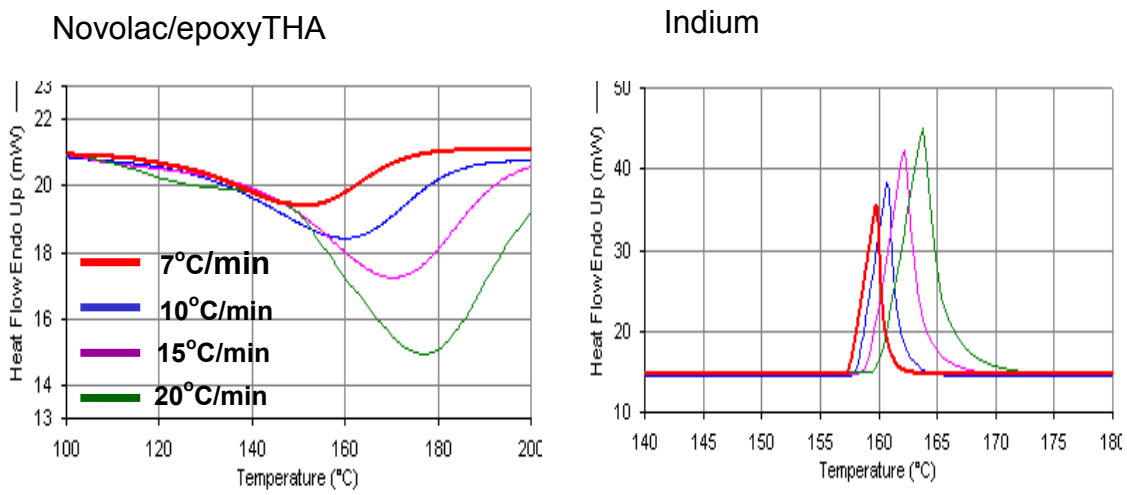

Figure 6. 46. Dynamic DSC scans of a novolac/epoxy/trihexylamine mixture measured at different heating rates. The peak shift due to the instrument response lag was corrected by measuring the indium melting point at these same heating rates.

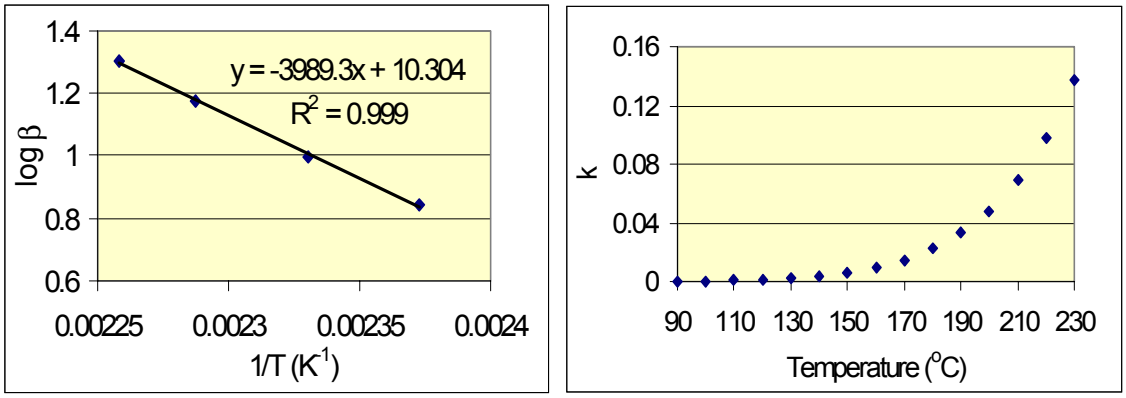

ASTM: E698: β= heating rate (degree C/min) ; Z = pre-exponential factor
Reaction peak maxima are obtained via DSC
$E \sim -2.19R(d \log_{10}\beta / d(1/T))$; $Z=\beta E e^{E/RT}/RT^2$; $k = Z e^{-E/RT}$

Figure 6. 47. a) log heating rate (β) versus 1/peak temperature of the exotherm, and b) rate constant versus temperature for a novolac/epoxy mixture containing 3 mole percent trihexylamine

6.3.6.2. Flexural properties

The transverse flexural properties measure the resin properties in unidirectional composites. Previous work has shown that the type of sizing had no effect on the transverse flexural strength for composites with a fully cured matrix. A composite prepared from G' sized fibers had similar flexural strength to that prepared from poly(amic acid)/TTMPP sized fibers.[197] In this work, composites prepared with poly(amic acid)/trihexylamine sized fibers had similar flexural modulus to and a slightly higher flexural strength than that of the composite prepared with the G' sized fibers. These results indicated that the cure time could be reduced from 4 hours to less than 30 minutes while maintaining or improving the composite's flexural properties. These results also suggested that there were no differences in using poly(amic acid)/TTMPP versus poly(amic acid)/trihexylamine sizing in curing phenolic novolac/epoxy resins.

[197] C. S. Tyberg, "Void-Free Flame Retardant Phenolic Networks: Properties and Processability," Dissertation, Virginia Tech, March 22, 2000.

Table 6. 5. Transverse flexural strength and modulus of unidirectional AS-4 carbon fiber reinforced phenolic novolac/epoxy composites

Sizing	Phenolic/Epoxy wt/wt	Cure Cycle	90° Flexural Strength (MPa)	90° Flexural Modulus (GPa)
G'[197]	70/30	200°C (1hr) 220°C (3hr)	66	11.3
PAAS/THA	65/35	180°C (20min) 200°C (10min)	74±3	11.1±0.2

PAAS/THA= Ultem type poly(amic acid)/trihexylamine salt

6.3.6.2. Mode II toughness

The mode II toughness of composites prepared with the poly(amic acid)/trihexylamine sized fibers appeared to be slightly lower than that of the composites prepared with G' or poly(amic acid)/TTMPP sized fibers. The mode II toughness calculated for composites having poly(amic acid)/trihexylamine salt sized fiber was lower than that calculated for composites having poly(amic acid)/TTMPP salt, but the toughness values were within the standard deviations of each other. The composite prepared with the poly(amic acid)/trihexylamine sizing also had a slightly lower fiber volume fraction. All of these phenolic novolac/epoxy composites exhibited a relatively high mode II toughness, similar to the value of toughened epoxies,[198] and exceeding the toughness of untoughened carbon fiber/epoxy composites.[199]

[198] M. S. Mdahakar and L. T. Drzal, "Fiber-Matrix Adhesion and its Effect on Composite Mechanical Properties: IV. Mode I and Mode II Fracture Toughness of Graphite/Epoxy Composites," *Journal of Composite Materials* **26**(7), 936-968 (1992).

[199] E. M. Woo, and K. L. Mao, "Interlaminar Morphology Effects on Fracture Resistance of Amorphous Polymer-Modified Epoxy/Carbon Fiber Composites," *Composites Part A* 27A, 625-631 (1996).

Table 6. 6. Mode II composite toughness of unidirectional AS-4 carbon fiber reinforced phenolic novolac/epoxy composites

Sizing	Mole % Initiator	Cure Cycle	Fiber Volume Fraction %	G_{IIC} (J/m^2)
G'	0	200°C (1hr) 220°C (3hr)	66.4	1410±302
PAAS/TTMPP	3.2	180°C (20min) 200°C (10min)	69.0	1224±205
PAAS/THA	3.3	180°C (20min) 200°C (10min)	66.4	882±198

6.3.6.3. Quasistatic tensile properties

The static tensile properties were determined for both unidirectional and crossply composites. The ultimate tensile strength for unidirectional AS-4 carbon fiber reinforced composites was significantly higher than the reported tensile strength[200] for glass fiber reinforced novolac cured with hexamethylenetetramine (<700 MPa).

Table 6. 7. Static tensile properties of AS-4 carbon fiber reinforced phenolic novolac/epoxy composites

sample	Fiber Volume Fraction %	F^{tu} (MPa)	ν
Unidirectional (0,0,0)	64.2	1540±143	--
Crossply (0,90,90,0)	65.0	823±29	0.049±0.012

[200] C M. Ma, H. Wu, Y. Su, M. Lee, and Y Wu, "Pultruded Fiber Reinforced Novolac Type Phenolic Composite-Processability, Mechanical Properties and Flame Resistance," *Composite Part A-Applied Science and Manufacturing* **28**(9-10), 895-900 (1997).

The axial and transverse strains were monitored as functions of stress. As expected for stiff composite materials, the axial strain was significantly higher than the transverse strain.

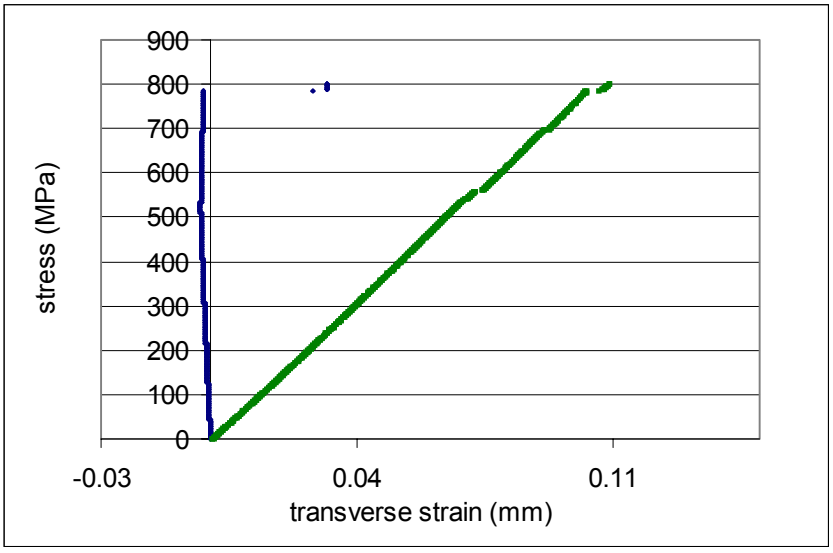

Figure 6. 48. Stress vs. transverse strain for crossply PAAS/trihexylamine sized AS-4 carbon fiber reinforced phenolic novolac/epoxy composites

6.4. Conclusions

Several sequestered catalysts were investigated in this research for use as latent initiators for phenolic novolac/epoxy cure reactions. All approaches used the glass transition temperatures of the particles as means for controlling catalyst release. The use of all sequestered catalysts in novolac/epoxy mixtures significantly increased the processing windows compared to the mixtures containing free catalysts, and the reaction rates were enhanced significantly at the cure temperatures in the presence of sequestered catalysts. However, diffusion of catalyst from sequestered particles to novolac/epoxy mixture led to reduced processing windows compared to the uncatalyzed systems. Even a small amount of catalyst which diffused into the reactant led to premature curing. At cure temperatures, reactions proceeded slower when a sequestered catalyst was used as opposed to when the free catalyst was used. The slower reactions were attributed to the time that was necessary for the catalysts to become uniformly dispersed in the

novolac/epoxy mixtures. The failure to release all of the catalyst when the reaction temperature lag below the T_g of the pure polymer sequestering agent reduced the actual TPP concentration in novolac/epoxy mixtures.

A poly(amic acid)/trihexylamine salt was synthesized for use as a latent initiator sizing for carbon fiber reinforced composites. Reaction kinetics indicated that fast phenolic novolac/epoxy reaction rates could be achieved in the presence of trihexylamine. Composites prepared with poly(amic acid)/trihexylamine sized fiber showed properties comparable to those prepared with the G' sized and poly(amic acid)/TTMPP sized fiber. These results suggested that poly(amic acid)/trihexylamine sizing could be used as a latent initiator for phenolic novolac/epoxy composite fabrications.

7. Conclusions

The ultimate goal of this research was to develop tough, flame-retardant, processable carbon fiber reinforced composites for structural applications. The focus has been on oligomer syntheses, network formation and properties, and latent initiator preparation.

An important aspect of this research was to synthesize linear controlled molecular weight cresol novolac resins. In these reactions, difunctional *ortho*- or *para*-cresol was reacted with monofunctional 2,6-dimethylphenol as an endcapping reagent, paraformaldehyde and oxalic acid dihydrate at 100°C for 24 hours followed by heating gradually to 200°C under mild vacuum. The molecular weights were controlled by the cresol to endcapping reagent ratio and an excess of formaldehyde was necessary to achieve the targeted molecular weights. The need for about 10 mol % excess formaldehyde was unexpected. Some of the excess formaldehyde needed could be attributed to small amounts evolving from the reaction apparatus during synthesis, and also to formaldehyde lost to dimethylene ether linkage formation. However, it was reasoned that a dynamic equilibrium reaction between formaldehyde substitution and elimination must also occur to allow for the desired molecular weights to be generated. This synthetic method consistently produced oligomer molecular weights very close to the targeted values based on endcapper to cresol predicted ratios. An effective method was developed for monitoring the reaction progression and calculation the molecular weight using ^{13}C NMR. Various chemical shifts allowed for confirmation of very high reaction conversions. High conversions of reactive phenolic ring positions were necessary to achieve the targeted molecular weights.

The network structure-property relationships were determined for a linear cresol novolac resin crosslinked with Epon 828 (Bisphenol-A epoxy) or DEN 438 (epoxidized novolac) at defined compositions. Cresol novolac/epoxy networks were prepared using a 2000 g/mol controlled molecular weight 2,6-dimethylphenol endcapped *ortho*-cresol novolac resin and the network properties were compared to an epoxy control, a phenolic control and a phenolic novolac/epoxy network (65:35 wt:wt ratio). The 70:30 and 60:40

compositions exhibited relatively high toughness (K_{IC} > 1 MPa/$m^{1/2}$) and high glass transition temperatures (>144-154°C). It is important to note that the properties of these networks prepared from readily available cresol monomers exceeded those of the epoxy control, the phenolic control and the phenolic novolac/epoxy networks. The increased glass transition temperatures were attributed to the methyl carbon on cresols which hindered chain rotations while the increased toughness was achieved by controlling the network crosslink density.

The molecular weight between crosslinks showed that the network density was optimized at the 70:30 composition (3.6:1 eq:eq ratio) (M_x ~1500 g/mol). These molecular weights between crosslinks were most desirable for networks cured with 2000 g/mol oligomers. Compositions high in novolacs (80:20 wt:wt ratio) had reduced crosslink densities due to insufficient network connectivity; compositions high in epoxies (60:40 wt:wt ratio) also had reduced apparent crosslink densities since the lack of mobility prohibited further phenolic/epoxy reactions, which led to increased epoxy sol fractions.

The molecular relaxation behavior into the glassy region were investigated to assess the network crosslink density and chemical structures in the glassy state. Master curves and cooperativity plots were generated for cresol novolac/epoxy networks. The fragility, which was used to investigate the temperature dependence of segmental relaxation through the transition region, showed that both crosslink density and hydrogen bonding affected the Epon 828 epoxy cured cresol novolac networks. It was possible that an antiplasticizer effect caused by the low molecular weight sol fractions in the network also led to the apparent increased glassy moduli. Crosslink density seemed to be the dominating factor in the D.E.N. 438 epoxy cured cresol novolac networks.

The major chemical difference between phenolic novolac and cresol novolac is the pendent methyl substituent on cresol. In the present work, all methyl groups are *ortho* with respect to the hydroxyl substituent. This provided a steric affect which reduced the equilibrium water uptake by increasing the hydrophobicity. Cresol novolac/epoxy networks exhibited comparable relatively low equilibrium water absorptions as the epoxy control (~ 2 wt. % at room temperature) and were relatively unaffected by the network compositions. The *ortho*-methyl substituent also reduced the

reaction rate of the hydroxyl group with epoxies due to a steric effect. This produced longer processing time windows when the novolac were reacted with epoxies at elevated temperatures.

The presence of the methyl group on each repeat unit slightly increased the peak heat release rates and reduced the char yields for cresol novolac networks. The peak heat release rates of *ortho*-cresol novolac/epoxy networks were between 300-450 kW/m^2. The flame retardance of all of the novolac/epoxy networks were significantly improved compared to that of the epoxy control, but inferior to the flame retardance of phenolic control.

Another important aspect of this research involved developing latent initiators or catalysts for the novolac/epoxy reaction. Several sequestered catalysts were investigated for use as latent initiators to enable melt processing of novolac/epoxy mixtures. Ideal sequestered catalysts are inert at the processing temperature but catalyze reaction efficiently at the cure temperatures. All approaches used the glass transition temperatures of the particles as the means for controlling catalyst release. The use of all sequestered catalysts in novolac/epoxy mixtures significantly increased the processing windows compared to the windows for mixtures containing free catalysts, and the reaction rates were accelerated considerably by the sequestered catalysts at the cure temperature. However, diffusion of catalyst from the sequestered catalyst particles into the novolac/epoxy mixture led to reduced processing windows compared to that of the uncatalyzed systems. At cure temperatures, reactions proceeded slower when a sequestered catalyst was used than when the free catalyst was used. The slower reactions were attributed to slow catalyst diffusion to form uniform dispersions in the novolac/epoxy mixtures.

An alternative method involved placing the catalyst directly onto the carbon fiber as a sizing. A poly(amic acid)/trihexylamine salt was synthesized for use as a latent initiator sizing for carbon fiber reinforced composites which would release trihexylamine upon imidization. Reaction kinetics indicated that fast phenolic novolac/epoxy reaction rates could be achieved in the presence of trihexylamine. Composites prepared with poly(amic acid)/trihexylamine salt sized fiber showed properties comparable to those prepared with the G' sized and poly(amic acid)/tris-(trimethoxyphenylphosphine) salt

sized fiber. These results suggested that the poly(amic acid)/trihexylamine salt sizing could be used as a latent initiator for phenolic novolac/epoxy carbon fiber composite fabrications.

8. Recommendation for Future Work

The properties of cresol novolac/epoxy networks approach those required by the microelectronics industry, i.e. high glass transition temperatures combined with toughness and flame retardance. The toughness of cresol novolac/epoxy networks may be improved by incorporating elastomeric or thermoplastic modifiers. Adding phosphorus or nitrogen based additives may also improve the flame retardance.

The primary need for achieving efficient composite fabrication is to develop latent catalysts which can be added directly into the novolac/epoxy mixtures under melt processing conditions. The present work demonstrated that the sequestered catalysts prepared by the physical blending method were inadequate for obtaining good melt processability in the phenolic novolac/epoxy systems studied. Alternative methods should be explored to obtain fully encapsulated controlled size particles. Fully encapsulated catalyst particles should eliminate pre-mature curing at the processing temperature yet promote fast reactions at the cure temperature. Proposed methods for preparing such particles might include a chem-physical approach in which a layer of polymer is coated onto the catalyst particle surface via co-precipitation or a chemical approach in which monomers are reacted *in-situ* onto the catalyst particle surface to form a protective polymeric layer. These methods should also allow better control over particle size, which is necessary to form uniformly dispersed novolac/epoxy/particle resin mixtures.

It is also recommended that the melt processability of the less reactive cresol novolac/epoxy mixtures be investigated in the presence of sequestered catalysts developed in this research. Longer processing-time windows are expected in this combination. However, this approach will only be effective if the polymer in the sequestered particles is immiscible with the cresol novolac/epoxy mixture.

VITA

Sheng Lin-Gibson was born in Shanghai, China in 1975. She grew up in Shenyang, a northeastern city in the Liaoning province. Sheng came to America when she was 12 years old and lived with her parents and brother in Greenbelt, Maryland. There she attended middle school and high school. Her family moved to Blacksburg, Virginia in 1992, where Sheng finished her high school career at Blacksburg High School. Upon graduation in 1993, Sheng stayed in Blacksburg to attend Virginia Tech and pursue degrees in Biochemistry and Chemistry. While taking Organic Chemistry as a freshman, she was given the opportunity to conduct undergraduate research under the direction of Dr. Judy S. Riffle and the Center for Adhesives and Sealant Science (CASS). Upon graduation in May of 1997, Sheng participated in IBM's summer internship program at the T.J. Watson research laboratory and returned to Virginia Tech in the fall to pursue a Ph.D. in chemistry under the guidance of Dr. Riffle. Sheng defended her dissertation in April 2001. She received a National Research Council Fellowship and will be conducting research related to nanocomposites and nanotubes at the National Institute of Standard and Technology (NIST) in Gaithersburg, Maryland.